ASSESSMENT OF ERTS-1 IMAGERY AS A TOOL FOR REGIONAL GEOLOGICAL ANALYSIS IN NEW YORK STATE

Yngvar W. Isachsen, Robert H. Fakundiny, and Stephen W. Forster, Geological Survey - New York State Museum and Science Service, Albany, N.Y. 12224

May 28, 1974
Type III Report

Prepared for

GODDARD SPACE FLIGHT CENTER
Greenbelt, Maryland 20771

TECHNICAL REPORT STANDARD TITLE PAGE

1. Report No.	2. Government Accession No.	3. Recipient's Catalog No.

4. Title and Subtitle	5. Report Date
Assessment of ERTS-1 Imagery as a Tool for Regional Geological Analysis in New York State	May 28, 1974
	6. Performing Organization Code
7. Author(s) Y.W. Isachsen, R.H. Fakundiny, S.W. Forster	8. Performing Organization Report No.
9. Performing Organization Name and Address	10. Work Unit No.
Geological Survey-New York State Museum and Science Service, Albany, New York 12224	11. Contract or Grant No. NAS5-21764
	13. Type of Report and Period Covered TYPE III REPORT
12. Sponsoring Agency Name and Address Edmund Szajna Goddard Space Flight Center Greenbelt, Maryland 20771	14. Sponsoring Agency Code
15. Supplementary Notes	

16. Abstract

Linear anomalies dominate the new geological information derived from ERTS-1 imagery, total lengths now exceeding 26,500 km. Maxima on rose diagrams for ERTS-1 anomalies correspond well with those for mapped faults and topographic lineaments. Multi-scale analysis of linears show that single topographic linears at 1:2,500,000 may become dashed linears at 1:1,000,000 aligned zones of shorter parallel, en echelon, or conjugate linears at 1:500,000, and shorter linears lacking any conspicuous zonal alignment at 1:250,000. Field work in the Catskills suggests that the prominent new NNE lineaments may be surface manifestations of dip slip faulting in the basement, and that it may become possible to map major joint sets over extensive plateau regions directly on the imagery. Most circular features found were explained away by U-2 airfoto analysis but several remain as anomalies. Visible glacial features include individual drumlins, drumlinoids, eskers, ice-marginal drainage channels, glacial lake shorelines, sand plains, and end moraines.

17. Key Words (Selected by Author(s))	18. Distribution Statement
geology, structure, lineament, linear, ERTS-1 imagery, New York State, circular feature	

19. Security Classif. (of this report)	20. Security Classif. (of this page)	21. No. of Pages	22. Price*
None	None		

*For sale by the Clearinghouse for Federal Scientific and Technical Information, Springfield, Virginia 22151.

PRECEDING PAGE BLANK NOT FILMED

PREFACE

This report summarizes investigative methods and accomplishments on a project to evaluate the usefulness of ERTS-1 imagery as a spectral geological mapping tool. ERTS-1 imagery was found to be particularly well suited to detect topographically-expressed features, including numerous large-scale structures which would probably never have been discovered without a regional synoptic capability such as that provided by ERTS-1. The new structural data derived in this study are being incorporated into a Tectonic Atlas of New York State which is in progress.

TABLE OF CONTENTS

LIST OF ILLUSTRATIONS

LIST OF TABLES

1. INTRODUCTION

1.1 The objective of this investigation has been to extract a maximum amount of new geological information from ERTS-1 imagery over New York State and thus to evaluate its usefulness in regional geological studies. The overriding emphasis has been on bedrock geology, but glacial features have been annotated on selected fall and winter imagery, and one temporal study was made to evaluate the effects of a severe storm on Lake Ontario. The investigation was carried out at three scales: 1:1,000,000, 1:500,000, and 1:250,000, with the bulk of the work having been done on the 1:1,000,000 scale imagery which was received on a regular basis from NASA. Analysis of the imagery was considerably expanded using remote sensor data acquired by high, intermediate, and low-level aircraft, as well as by conventional ground study. Earlier results of our investigation, the main portions of which are incorporated herein, have been reported in previous publications by Isachsen and others (1973, 1974a, 1974b), Isachsen (1973a, 1973b, 1974) and Fakundiny (1974).

1.2 New York State provides a highly varied test area for evaluating ERTS-1 imagery as a source of new geological information not readily seen at conventional mapping scales. The State covers a number of well defined physiographic provinces (Figure 1), and contains lithologic units ranging in age from Proterozoic to Pleistocene (Figure 2). It stretches west-east across five tectonic provinces as follows (Figure 3): 1) a continental platform (Platform I) consisting of Lower and Middle Paleozoic strata resting on a Proterozoic basement, 2) the Adirondack Dome Mountains which are located on the eastern edge of this platform and expose Proterozoic basement of the Grenville Province, 3) the Appalachian Foldbelt with its several subdivisions including the Hudson Highlands (reactivated Proterozoic basement) and the Taconic allocthones, 4) the Triassic Fault Trough (Palisadian Taphrogen) and 5) Cretaceous coastal plain sediments on Paleozoic basement (Platform II).

1.3 For a general description of the geology and physiography of the State the reader is referred to Broughton and others (1966); the tectonic subdivisions are discussed in Fisher and others (1971).

2. DATA HANDLING, INVESTIGATIVE PROCEDURE, AND IMAGERY RECEIVED

2.1 The procedures which finally evolved for data handling and imagery analysis are shown by flow chart in Figure 4. Incoming imagery, consisting of 9 inch positive transparencies and 70 mm positive and negative transparencies of New York State and adjacent areas were logged according to scene designation (Figure 5) and other identifying factors, including delineation of cloud-free areas (Figure 6). Image descriptors for NASA were tabulated at this stage. Diazo paper prints of bands 5 and 7 were then made for the browse file.

2.2 After completion of these "housekeeping duties", the imagery was subjected to analysis in three stages, as expressed by Roman numerals in Figure 4: I. photogeologic identification of suspected geological signatures in ERTS-1 imagery; II. laboratory screening of these signatures; III. field investigation of remaining "ERTS-1 anomalies", IV. preparation of ERTS-enhanced geological maps and V. publication.

2.2.1 Stage I: Identification in the 9 inch film positives of all spectral signatures (points, lines and areas) which might be geologically-linked. These were traced onto clear acetate overlays and color-coded according to the spectral band on which they were best displayed. The overlay data were then assembled to produce a map which was continually updated, using both new imagery as it arrived, and the screening procedures described below. Similar procedures were followed using 1:500,000 and 1:250,000 black and white and color prints of selected ERTS-1 imagery. Multiband color viewing of photographically reprocessed 70 mm positives, utilizing either a Spectral Data Corporation (SDC) Model 64 Viewer-Projector, or sandwiched diazo color film positives on a light table, was used on an experimental basis to corroborate or expand the above spectral signatures. Selected anomalies were investigated further by electronic enhancement techniques through the generous assistance of the Rome Air Development Center, the State University of New York at Albany, NASA/GSFC, and the Jet Propulsion Laboratory.

2.2.2 Stage II: Evaluation of the suspected geological signatures in terms of existing information (geological, cultural, and other maps, airfoto mosaics, and other remote sensor data – particularly that obtained by supportive NASA aircraft) in order to identify them as one of the following:

a. clearly non-geological (e.g. power transmission lines, highway segments, railroads)

b. clearly geological but previously mapped (e.g. faults, topographic lineaments, formational boundaries)

c. other signatures not previously known, which might be geologically linked (e.g. linear valleys, tonal discontinuities or lines, aligned drainage features, straight segments of streams). These were classified as Stage II features or "ERTS anomalies".

2.2.3 Stage III: Field investigation, using small aircraft for initial ground location and identification, followed by conventional ground study of representative anomalies.

2.2.4 Stages IV and V: Compilation of data to produce ERTS-enhanced geological maps which, together with interpretive texts, will be published and made available for inclusion in the State's computerized Land Use Natural Resources Survey (LUNR).

2.3 ERTS-1 imagery received through 8May74 totals 400 frames covering 34 scene areas over New York State and portions of adjacent states and Canada. An inventory of this imagery in terms of geological usefulness is as follows: useful (0-50 percent cloud cover), 73 percent; marginally useful (50-70 percent cloud cover), 10 percent; useless (70-100 percent cloud cover), 17 percent.

2.4 The entire state is now covered by at least one image having greater than 70 percent cloud-free area for summer and fall, and 90 percent cloud-free in winter. Mosaics made from diazo paper prints of the summer-fall and the winter images at 1:1,000,000 are reproduced as Figures 7 and 8.

3. EXPERIMENTATION WITH PHOTOGRAPHIC REPROCESSING AND MULTISPECTRAL VIEWING METHODS

3.1 Early in the study, the 1:1,000,000 film positives of usable imagery which had been received were analyzed in transmitted white light (i.e. Stage I analysis) and the data combined into a statewide "spectral geological map" at 1:1,000,000 (Isachsen and others, 1973, Figure 2). For the late summer and fall imagery, it was found that bands 5 and 7 complemented each other and contained all the spectral signatures which appeared to be geologically-linked; no additional data were found on bands 4 and 6.

3.2 After all the more obvious features of possible geological linkage had been extracted from the standard black and white film positives, it was decided to experiment with various other photogeologic methods in order to work out an optimum set of procedures for the remainder of the study. The following experiments were performed:

1. Investigation to determine what effect photographic reprocessing to produce higher contrast prints might have on the identifiability of linears in ERTS-1, band 5. A cloud-free image of east-central New York, image (1079-15122-5) was chosen for the experiment because it includes a variety of geological provinces, namely: the Adirondack Mountains, consisting of high-grade metamorphic rocks, the Allegheny Plateau (or Appalachian Uplands) comprising horizontal Silurian and Devonian strata, the Mohawk and Hudson Valleys underlain by variably faulted and folded Cambrian and Ordovician sedimentary rocks, and the Taconic Mountains which consist of allocthonous Cambrian and Ordovician sedimentary rocks. The two prints in question are reproduced in Isachsen and others (1973, Figures 10 and 11). The photographic reprocessing method used was as follows: from a 70 mm ERTS-1 negative, a Kodalith film positive was prepared by contact printing. From this positive, a 70 mm high-contrast negative was made with Kodak Professional Copy film. D-72 developer was used. Paper enlargements were then made at 1:1,000,000 of both the reprocessed and unreprocessed 70 mm negatives, and identifiable linears (some 270) were inked on clear mylar overlays. A comparison showed that all linears identifiable on one image were clearly recognizable on the other, although the expression of linears was greater on the high-contrast reprocessed image.

2. Multispectral color-additive viewing of 70 mm positives of bands 4, 5, 6, and 7, as received from NASA, using the SDC Viewer-Projector. Despite considerable experimentation with a variety of scenes, no information was added to that obtained by conventional viewing in transmitted light. Later attempts, using photographically reprocessed imagery, are described under 4 below.

3. Pre-formatting of ERTS-1 70 mm film positives for multispectral viewing, to avoid the time consuming task of separately registering each band in the Viewer every time a scene is to be viewed. After some experimentation, a successful method was devised as follows: on a 9.5 x 12 inch piece of 0.005 inch clear mylar, the positions of the four viewer windows in the 9.5 inch roll film holder are roughly located. Two perfectly parallel horizontal lines are then drawn to guide the placement of the upper edge of the 70 mm film positives. Using these lines, the images are carefully taped in perfect parallelism. This pre-formatted array permits rapid registration, requiring only limited x-y adjustment, the need for rotational adjustment having been eliminated.

4. Multispectral color-additive viewing of photographically reprocessed film positives, using an SDC Model 64 Viewer-Projector (or diazo color film sandwiches). Experimentation with several ERTS scenes using numerous combinations of spectral bands, color filters, and illumination intensity produced a variety of striking effects (Isachsen and others, 1973, Figure 12). Most of the color patterns produced merely accentuate tonal differences which are readily observable in the black and white imagery. Some, however, are subtle and are not visible in the black and white images. An attempt was made to determine the cause of these subtly-colored areas by comparison with numerous different kinds of maps. A cloud-free image of the northern Adirondacks taken 11Oct72 (scene no. 1080-15174) was chosen for the comparison. This image covers the Adirondack Highlands which are dominantly forested, and the St. Lawrence Lowlands which are mainly given over to dairy farming. Kodacolor prints of the SDC image were superimposed on the various maps, using a Bausch and Lomb Zoom Transfer Scope, model ZT-4. The maps used were as follows:

   a. Geologic Map of New York, Adirondack Sheet, reduced from Fisher and others (1971)

   b. Physiographic diagram of New York State (Figure 1)

   c. Pleistocene Geology of the St. Lawrence Lowland (MacClintock and Stewart, 1965)

   d. Map of areas burned by Adirondack forest fires of 1903 (Suter, 1904)

e. Forest-type areas map (Stout, 1958)

f. Economic viability of Farm Areas (Conklin and Linton, 1969)

g. Soil Association map of New York State (Cline, 1961)

h. Ground Water in New York (Heath, 1964)

In only one instance was any correlation noted with the subtle color patterns; comparison with the forest-type map indicated a rough, local delineation (less than 5 percent) of the boundary between areas of aspen-grey birch-paper birch and spruce-fir-northern hardwoods northeast of Cranberry Lake. The virtual lack of correlation with this map was somewhat surprising after noting that Hoppin (1973), in the Bighorn region, found a good correspondence between false-color patterns and dominant forest types.

5. Multidate color-additive analysis of ERTS-1 imagery. An experimental multidate comparison was made of a scene for which there exists imagery for four essentially cloud-free passes, namely the northern Adirondacks for 23Sept72, 11Oct72, 18Nov72, and 9Jan72. Photographically unreprocessed 70 mm film positives of bands 5 and 7 for these dates were projected in registry using the SDC Model 64 Viewer-Projector. The most tonally varied and informative image (11Oct72) was projected in red, and the other images were superimposed, in turn, using first a blue and then a green filter to determine what "color features" were added. The results were as follows:

   a. the September image, which is a rather flat, light grey image, added no new information, but merely produced an overall green wash which was accentuated where the October image is dense and therefore transmitted very little red light.

   b. the November image, in which the Adirondacks have an overall dark grey tone, highlights mines, dry tailings ponds and unforested summits of some of the high peaks. The cause appears to be snow cover which makes the image more transparent in these areas.

   c. the January image, which is very dark grey overall, adds only snow-covered lakes (which have an expectably high albedo).

6. Experiment with Log E dodged prints of ERTS-1 imagery. In the southern Adirondacks, any tendency for the dominant east-west arcuate trend of lithological units to reflect characteristic tonal signatures would be masked by the strong NNE topographic grain (Figure 7) which is accentuated by the low-angle solar

illumination. We were able to subdue this high density contrast through the cooperation of Charles Woodward of Lockwood, Kessler and Bartlett who provided Log E dodged film negatives for all bands of image no. 1080-15174 for study. The technique was successful in subduing density contrast to a limited extent, but no new tonal variations were seen.

3.3 The experiments described above were intended not as rigorous investigations, but rather as relatively rapid tests to help determine which methods, beyond the more conventional approaches, would provide a sufficient yield of new geological information to justify the time involved. From the largely negative results obtained, we conclude that for the region under study the most advantageous method of photogeologically analyzing ERTS-1 imagery is to study bands 7 and 5 separately.

4. EXPERIMENTATION WITH ELECTRONICALLY ENHANCED IMAGERY

4.1 One of the objectives of this project was to experiment with the electronic image-processing equipment generously made available at Rome Air Development Center. An afternoon was therefore spent with Captain James Turinetti, using that part of the Center's "System 800" made by Spatial Data Systems, Inc. which converts the grey scale of black and white film products into a 32-color video display.

4.2 ERTS 9.0 inch film positives of the four spectral bands of the northern Adirondacks (scene no. 1080-15174) were examined using a great variety of color combinations in a search for linear or areal spectral information which had not been detected by conventional photogeologic analysis. Regardless of instrument manipulation, of the 15 shades on the ERTS grey scale, only the 11 darker shades were detectable as separate colors. A mosaic of positive transparencies of the entire Adirondacks was also examined on the color display (1080-15174, 1080-15180, 1079-15115, 1079-15122). By calibrating only to the grey scale it was possible to distinguish 11 of the 15 shades.

4.3 The principal limitation was not that of density spread, however, but the comparatively low resolution of the SDS display. Although the resolution would appear to be adequate for color enhancement of small-area, high-resolution conventional aerial photography, it degrades ERTS imagery to a degree that is not compensated for by the asset of color visualization. In short, geological information was diminished in the color display, and no new potentially geologic information was seen.

4.4 As indicated in the preceding pages, the present investigation has depended almost solely upon conventional photogeological analysis of imagery, coupled with multispectral color-additive viewing using an SDC Viewer-Projector. This approach has been highly successful in extracting linear and curvilinear information from the imagery. Indeed it is apparently the only way in which this task can be performed at the present time. According to A. Gillespie (telephone communication)

the problems connected with direct digital production of a linear map from imagery (as opposed to an operator-produced map) are formidable, due mainly to the difficulty of determining a coherent weighting system.

4.5 Quite another matter, however, is the capability of existing computer image processing techniques to yield greatly-enhanced images for photogeological study (e.g. Goetz and others, 1973; Vincent, 1973).

4.6 In the interest of having a "first look" at the potential of such image processing, an afternoon (24Oct73) was spent at NASA/GSFC with the generous assistance of Ms. Lottie Brown experimenting with computer processing of the 11Oct72 ERTS-1 scene of the northwest Adirondacks. Unfortunately time was too short to explore adequately the potentialities of most of the image processing tasks which can be performed with Goddard's IDAM program. The following limited amount of image processing was accomplished, and 35 mm daylight Ectachrome color transparencies were made of the video screen for study:

1. For the whole scene, density stretching of band 4 (stretched to 30 levels) and the production of a color composite of bands 4, 5, and 7 (bands 5 and 7 had a good density-level spread to begin with) to test for improvement in delineation of linear features.

2. 4x enlargement of the above color composite (assigning 4 TV pixels to one ERTS-1 pixel) of Blue Mountain Lake area to see if any previously undetected linears could be found which might correspond with the northeast-trending fault plane solution for the earthquake swarms that occurred from May 1971 to April 1972 (Sbar and others, 1972) and again during July 1973 (Aggarwal and others, 1973).

3. Similar enlargement of Mt. Whiteface to see if recent landslide scars not visible on routinely-processed Goddard color composite imagery could be seen.

4.7 An evaluation of the color transparencies obtained above produced the following results:

1. No new linears were found in the scene nor were previously observed linears notably enhanced. This is probably because the density level spread on the original imagery of bands 5 and 7 was already favorable for linear detection.

2. No linears were delineated along the trace of the plane of epicenters. In view of the low magnitude of the quakes (3.6) this is not surprising. It was admittedly a "long shot", attempted mainly because field work during the earthquake activity showed that existing fractures in the epicenter area have strikes in the same sector as the 2-3.5 km deep quakes. More will be said about ERTS-1 and seismicity in New York in a later section.

3. The enlargement of the Mt. Whiteface area did facilitate the recognition of landslides, even on the shaded side of the Mountain (Figure 34); the slides were not visible on the unenhanced imagery.

5. ERTS-1 AND BEDROCK GEOLOGY

5.1 Regional Geological Features

5.1.1 The synoptic value of ERTS-1 imagery is readily appreciated from a single satellite image, but perhaps even more from a mosaic of an entire State (Figures 7 and 8) where, despite the loss in resolution due to 2.5x photo-reduction of the original mosaic, major physiographic, geologic, and tectonic provinces can be seen (compare with Figures 1, 2 and 3). Major tectonic provinces visible in the mosaics include the Adirondack Dome Mountains, Platform I, the narrow belt of upturned Silurian-Devonian rocks deformed during the Acadian Orogeny, the Appalachian Foldbelt, the Palisadian Taphrogen, and Platform II. Two physiographic regions which are independent of the tectonic provinces appear prominently in the imagery, namely the Tug Hill Upland, which is defined both topographically and by its forested plateau surface, and the Catskill Mountains. (Both of these, incidentally, are composed of erosionally-resistant deltaic rocks, one Ordovician, the other Devonian).

5.1.2 Outlining the Adirondacks can be seen the major unconformity between the Grenville Basement and the onlapping Paleozoic section which has at its base the Potsdam Sandstone of Upper Cambrian age. The contact is accentuated by a topographically-induced land use boundary, namely forest versus farmland, but it is also well delineated geologically, particularly along the southwestern, southern and eastern Adirondacks, by the abrupt termination of the east-west arcuate pattern in the basement where it meets the Potsdam contact. This pattern results from differential erosion of basement lithologies.

5.1.3 Along its northern, western, and southwestern borders, the crystalline Adirondack basement is expressed on ERTS-1 imagery as a slightly dissected planar surface which dips gently away from the central part of the Adirondack Dome (Figures 7 and 11). This surface is exposed in a belt ranging in width from 10 km in the north to about 20 km along the western perimeter, and corresponds closely to the physiographic section designated as the "Fall Zone Belt" by Buddington and Leonard (1968, p. 8). It is doubtless a tilted erosion surface, from which the Paleozoic units have been stripped by erosion. A striking feature of the paleoplane in the northern Adirondacks is its abrupt termination to the southeast, along a topographic lineament which had not previously been mapped, to produce a pseudo-cuesta. Along the northern border of the Adirondacks, the contact between this erosion surface and the Potsdam Sandstone is well displayed as a boundary between forest and cultivated farmlands. About 10 km to the north, the contact between the Potsdam Sandstone and the Theresa sandy dolostone is also marked by a change in land use influenced by bedrock.

5.1.4 Along the southwestern border of the Adirondacks, the basement-Potsdam contact is accentuated by the Black River. In the intervening section, basement exposures are continuous from the Central Highlands, across the Frontenac Arch of the Northwest Lowlands, into the main Grenville Province of Canada. Potsdam occurrences are here limited to scattered relict patches.

5.1.5 Inside the Adirondacks, many previously-mapped geological structures can be identified. These include the major east-west arcuate folds extending across the southern Adirondacks, a number of domical structures, plunging folds, refolds, and other structures which have topographic expression, as well as major faults most of which trend north-northeast.

5.1.6 Within the Appalachian Foldbelt, major subdivisions can be seen in the ERTS-1 imagery at the original 1:1,000,000 scale, albeit notably better at 1:500,000. In Figures 48 and 60, the Allegheny Plateau with the Catskill Mountains as its eastern projection, is readily identified by its dendritic drainage pattern. The straight eastern edge of the Catskill Mountains, which has long been referred to as the "Wall of Manitou", is prominently displayed. A major insight into its cause has been provided by ERTS-1 imagery, as will be discussed later.

5.1.7 About 20 km south of the Catskills, the Shawangunk Mountains begin, and extend southwestward into New Jersey where they are known as the Kittatinny Mountains. They represent a comparatively narrow belt of upturned Silurian and Devonian rocks, dominated by the Shawangunk conglomerate, which marks the western boundary of the Appalachian Foldbelt.

5.1.8 An angular unconformity between the tilted Shawangunk conglomerate(Silurian) and isoclinally-folded Ordovician shale and graywacke beds of the Hudson Valley is seen on the imagery as the eastern edge of the Shawangunk Mountains. These beveled Ordovician rocks extend eastward to the resistant Proterozoic basement rocks of the Hudson Highlands, north of the wide portion of the Hudson River. Between the southern extension of the Shawangunk Ridge and the Hudson Highlands, a synclinal belt of down-faulted Silurian and Ordovician strata occurs. It is marked by the elongate Greenwood Lake at its southern end, and by the isolated Schunemunk Mountain mass at its northern end about 10 km southeast of the point at which the Hudson River enters the gorge (fiord) through the Hudson Highlands. The Highlands extend northeastward, where they appear to merge, in the 1:1,000,000 imagery, with the more highly-metamorphosed Paleozoic rocks of New England. (In the 1:500,000 imagery, the northern boundary of the Hudson Highlands is better delineated). The elongate Housatonic Highlands, a separate Proterozoic mass, can be seen northeast of the Hudson Highlands. The belt of Taconic allocthones north of the Hudson Highlands are not well defined in the 1:1,000,000 print, but can be seen somewhat better at the 1:500,000 scale.

5.1.9 The Triassic basin borders the Hudson-New Jersey Highlands along the Ramapo fault, and is bounded on the east by the Hudson River. The Palisades diabase sill forms a vertical escarpment along the west shore of the river. It can be seen in the imagery as a faint line parallel to, and within 500 meters of, the shoreline. The Hudson flows along the onlapping contact between the Triassic red beds and the high-grade Appalachian basement rocks to the east. This basement, in turn, forms the substrate for the Cretaceous and Pleistocene formations of Long Island.

6. ERTS-1 LINEAR FEATURES IN NEW YORK STATE

6.1 Introduction and Terminology

6.1.1 Without question, the most significant contribution of ERTS-1 imagery to date in New York State has been the location of more than 400 combined Stage II and Stage III linears in the Adirondacks which had not previously been recognized, and many more Stage I and Stage II linears elsewhere in the State. This linear-detecting capability of ERTS-1 imagery was the most frequently cited geological application at a recent Symposium on Significant Results from the Earth Resources Satellite, ERTS-1 (Short, 1973).

6.1.2 Terminology relating to linear features on aerial photographs and other remotely sensed imagery stands in need of considerable clarification and more strict definition. Terms such as linear, lineament, fracture, and fault have been used in the literature to describe lines on photographs which may not have received any field checking whatever. The importance of avoiding genetic terminology in the presentation of photogeologic data, even for planetary studies, appears to require periodic emphasis (e.g. Schmitt, 1966; Schultz and Ingerson, 1973). We consider it essential, therefore, to define the terms used herein to designate photographic features, as distinct from their identification on the ground. We employ three classes of terminology: 1) a non-genetic term to describe the feature as seen on an aerial photograph or satellite image, 2) another non-genetic term to describe the feature on the ground, and 3) a term to classify the feature genetically. In the first category are terms such as "circular feature", "linear feature" (or simply "linear", a short form of "photolinear"), but not lineament. We use "linear" in the sense proposed in Dennis' (1967) International Tectonic Dictionary, to signify a line on an aerial photograph or image, irrespective of its validity on the ground (e.g. whether it turns out to be a cultural feature, a geological feature, an artifact, or an unexplained line). Linears can be designated as "topographic" or "tonal", depending upon their appearance in the photography or imagery.

6.1.3 We reserve the term "lineament", on the other hand, for a naturally occurring feature, i.e. one which has been confirmed to exist on the ground. This follows the usage of certain earlier workers (e.g. Hobbs, 1904a, Lattman, 1958). Most commonly, lineaments are topographic features ("topographic lineaments") and as such can be described in more specific geomorphic terms, such as "straight stream valley", "elongate lake", "straight lake shoreline", etc. Tonal lineaments are commonly botanical interfaces, such as "natural vegetation border" or "dark vegetation strip".

6.1.4 The application of genetic terminology generally depends upon finding that most elusive feature of lineaments, bedrock exposure. Where such can be found, terms like "fault trace", "shear zone", "en echelon joint set" or "lithological contact" can be applied without equivocation. Where bedrock is not exposed along the lineament, it may, of course, still be possible to infer the geological nature of the lineament in the context of local and regional geology (e.g. Gross, 1951).

6.1.5 In the photogeologic phase of imagery analysis, at least three types of biases are unavoidably introduced. Linear features which parallel trends of lithology or foliation are intentionally omitted, although there are doubtless places where field work would demonstrate the existence of colinear fractures or joint concentrations. A bias also exists against linears which may be perfectly aligned with the multispectral scanner raster lines in the imagery. Still a third bias is introduced by the azimuth of solar illumination, which preferentially highlights linear valleys at high angles to the direction of illumination and diminishes the identifiability of those parallel to it, as demonstrated later.

6.1.6 Stage II studies have been completed in the Adirondacks and are well advanced for southeastern New York. Stage III investigations are furthest advanced in the Adirondacks, although preliminary results have also been obtained from ground studies in the Catskill region which has been selected as a sample area for the geological calibration of ERTS imagery over the Allegheny Plateau. Because of the enormity of the State in terms of ground checking, the evaluation of individual ERTS-1 linear and curvilinear anomalies will doubtless occupy the attention of field geologists well into the future as new geological mapping is undertaken.

6.1.7 In the discussion of ERTS-1 linear features which follows, a general comparison will first be made between linears seen on imagery from the ERTS-1 and NIMBUS-I satellites over New York State. This will be followed by the results of Stage I, Stage II, and Stage III studies on ERTS-1 imagery in the Adirondack region, Stage I analysis for the remainder of the State, and Stage II and Stage III study in the Catskill Mountains.

6.2 ERTS-1 and NIMBUS-I Linears

6.2.1 A map showing linear features observed on ERTS-1 imagery at 1:1,000,000 is shown on Figure 9. In the Adirondacks, and much of southeastern New York, these represent Stage II and Stage III linears. Elsewhere in the State they are unscreened, although the vast majority can be seen on the imagery to be straight stream valleys and valley segments.

6.2.3 The linears in New York State range in length from 1.5 to 200 km, and the majority are straight. The combined lengths of these ERTS-1 linear anomalies exceeds 26,580 km, not including recognized linear portions of the Hudson River and the Finger Lakes.

6.2.4 Prior to the successful launching of ERTS-1, the only orbital imagery available over New York State was that obtained by APT, ITOS, and NIMBUS-I satellites. With the exception of one frame of NIMBUS-I imagery, only the broadest geomorphological features could be seen at the low-resolution involved, i.e. the Adirondacks and the Tug Hill Plateau (e.g. Anderson, 1968).

6.2.3. In our original proposal to NASA we called attention to a long faint linear visible on a NIMBUS-I image of orbit 254, taken September 14, 1964. This image was taken at an altitude of 308 miles above Lake Ontario when the satellite malfunctioned, and instead of going into a circular orbit with a perigee of some 700 miles, went into an elliptical orbit with a perigee of 266 miles.

6.2.4 C.I. Taggart (1965) noted the close correspondence between tonal variations on this imagery and the rock units delineated on the 1:250,000 Geologic Map of Pennsylvania, particularly in the Valley and Ridge Province. Through his generous cooperation, and that of J.R. Kenney of the National Research Council of Canada, both of whom had noted linears in the imagery (written communication), we were able to obtain copies of this image for study (Figure 10). The photograph is a second generation print of a video display of the signal received in Ottawa.

6.2.5 The linears and circular feature shown in the lower part of Figure 10 were seen independently by two of us (Isachsen and Forster). The linear marked with dots at either end was taken from an image of the same transmission as above, but was received and recorded at Frobisher Bay. It must be emphasized that any or all linears may be "electronic anomalies" rather than ground features; the absence of another oribital pass covering the same area precludes a check on this question. Nevertheless, it was decided to compare the NIMBUS-I anomalies with known geology and with anomalies seen in ERTS-1 imagery.

6.2.6 The results are as follows:

1. The circular anomaly located on the NIMBUS image just northwest of the St. Lawrence River near the U.S. - Canadian border has no manifestation whatever on either the ERTS-1 imagery or airphoto mosaics at 1:62,500 made from 1968 aerial photographs, and remains unexplained.

2. The longest NIMBUS-I linear in the Adirondacks passes through Tupper Lake and corresponds with a series of roughly aligned ERTS-1 linears and topographic lineaments, although it is less explicitly defined than the others, especially north of Tupper Lake. It is located parallel to, and 20 km west of, the Long Lake topographic lineament which nearly bisects the Adirondack Dome (Figure 11).

3. The other NIMBUS-I linears in the Adirondacks have as good or better ground identification, except for the two that form an open, west-facing V.

4. Elsewhere in the State, only the long, westernmost, northnortheast linear corresponds with ERTS-1 linears, and that only in the upper part, where it coincides with the Genesee River south of Rochester.

5. Within a range of five degrees or so, the linear maxima plotted from the NIMBUS-I image also appear within the plots of known linear features in the basement rocks of the Adirondack Dome (compare Figures 14 and 15).

6.3 ERTS-1 Linears in the Adirondack Mountains: Stage II Investigation

6.3.1 The most spectacular area of linear display in the State, if not in the whole northeast, is the Adirondack Mountain region (Figures 7 and 9). The linear features seen in the imagery include the majority of known faults and topographic lineaments shown on the Geologic Map of New York at 1:250,000 (Fisher and others, 1971; Isachsen, 1973). Of those not visible in the imagery at 1:1,000,000 (shown by black lines in Figure 12a most are short. The easternmost group occur in the Champlain Valley, an area of low relief, and are therefore less likely to be expressed in the imagery.

6.3.2 A numerical summary of the Adirondack linear information shown in Figures 7 and 11 is tabulated below:

Category	Number	Combined length, km
Previously mapped faults and topographic lineaments seen on ERTS-1 imagery	232	1890
ERTS-1 linear anomalies which have survived Stage II investigation	319	2622
Total of above	551	4512
Previously mapped faults and topographic lineaments not discernible on ERTS-1 imagery	297	1750

6.3.3 The ERTS-1 linear anomaly data for the Adirondack region are summarized in the two rose diagrams of Figure 13a. The upper diagram is an unweighted plot of the total number of linears, whereas the lower diagram takes the lengths of linears into account.

6.3.4 The generally similar appearance of the two diagrams holds up well under closer scrutiny. The maxima appearing in the weighted diagram can also be seen in the unweighted one, namely: N75W, N45W, N-N20W N25E, N40E, N50E, N60-70E, and 90E. This close correspondence indicates that, in general, the lengths of the anomalous linears are proportional to their frequency for any given azimuth.

6.3.5 When the above diagrams are compared with analagous plots of previously mapped faults and topographic lineaments (Figure 13b), both differences and similarities appear. The most notable difference is that the major concentration of ERTS-1 linear anomalies occurs in the 30° sector (N40E to N70E) whereas previously-mapped linear structures fall in the 35° span between N15E and N50E. This may reflect differences in the geological control and expression of these newly discovered linears. More

likely, however, to the extent that they are topographic linears, they are so well expressed in this sector because it is essentially orthogonal to the azimuth of solar illumination in October (153°, 34° elevation). Consistent with this interpretation is the low incidence of linears parallel to the direction of illumination (N20-45W), despite the fact that linears in this direction are fairly abundant on the ground (Figure 13b). Wise (1969) has demonstrated experimentally the critical effect of direction of illumination on the display of linears, although he used considerably lower elevations (5 to 20 degrees). The interpretation presented above is consistent with the conclusions reached by MacDonald and others (1969) from a look-direction study of side-looking radar images.

6.3.6 Despite the difference in relative magnitudes of the maxima, a very close correspondence exists for their directions, except for two. The maxima of Figure 13b, which also appear as prominent directions (within 5 degrees) on the imagery, are as follows: N70W, N45W, N20W, N-S, N40E, N50E, N70E, and N80E. On the ERTS-1 linear diagram, however, a N25E set is prominent rather than the N15E set mapped on the ground. The most prominent ERTS-1 set (N60E) is very subordinate among the known ground linear features. However, its trend is within 3° of being perpendicular to the direction of solar illumination and this probably explains its prominence.

6.3.7 An even stronger correlation would, of course, have been seen if all the topographic lineaments visible in the imagery had been included in Figure 13a, rather than only the new ones. A combined plot of all previously mapped faults and topographic lineaments, together with the new ERTS-1 linears, in the Adirondacks is shown in Figure 15.

6.4 ERTS-1 Linears in the Adirondack Mountains: Stage III Investigation

A major problem associated with field checking of ERTS-1 anomalies is locating them on the ground. As indicated earlier, this is greatly facilitated by visually transferring data from the ERTS-1 photographic product to another photographic product at a more useful field scale, namely airfoto index sheets at 1:62,500. It is then relatively easy to transfer the feature to the approximately correct location on 1:62,500 topographic maps, particularly if it is a topographic one. Following this, the most economical and effective way to locate the feature on the ground was found to be by observation and photography from low level aircraft.

6.4.1 Field studies carried on both by conventional ground methods and by observation and photography from low level aircraft, has permitted further definition and identification of ERTS-1 linear anomalies. The result has been to declassify some, reclassify others, and to add a small additional number which were originally considered too marginally expressed on the imagery to be designated as photogeologic linears. Before giving a tabulation of these changes, photographic

illustrations of both previously-mapped and new lineaments will be discussed in order to show the capabilities and limitations of ERTS-1 imagery for the detection and mapping of topographic lineaments. In the illustrations selected, preference has been given to those occurring within the Marcy Massif, the major body of metanorthosite in the Adirondacks, because of its relative homogeneity and massiveness as compared with surrounding rocks (Isachsen and Moxham, 1968; Isachsen and Fisher, 1971); the scene is normalized in terms of solar illumination, and the bedrock is normalized in terms of rock mechanical properties.

6.4.2 A location map and descriptive information is given in the Appendix for linears still "in good standing", Figure 17 locates figures below.

6.4.3 The longest clearly-defined topographic lineament in the Adirondacks is the previously-mapped feature that extends from the Marcy Massif metanorthosite south-southeast, across nearly every Adirondack rock type, to the southern boundary of the Adirondacks where it passes beneath Paleozoic strata without any apparent offset in the cover rocks (Figure 11). Its length is nearly 120 km. Geomorphically, the most impressive part of this lineament is the Long Lake section (Figure18). It is interesting that this, the longest linear feature, occurs near the western limit of intense lineament development (Figures 7 and 9).

6.4.4 A previously-mapped lineament in the high peaks region, located entirely within the Marcy Massif, is that which passes through Avalanche Lake located in the shadow of Mt. Colden (Figure 19). An orthogonal lineament set crossing Mt. Colden cannot be distinguished on the ERTS-1 imagery owing to a combination of its small scale and its near parallelism to the multispectral scanner raster lines.

6.4.5 A new linear, ERTS-1 anomaly number 291, can be seen in Figures 20 and 21. It is located entirely within the Marcy Massif metanorthosite. The linear, now confirmed as a topographic lineament, turns out to be a 16 km-long southward extension of a previously-mapped lineament. It extends both north and south beyond the portion shown in the photograph.

6.4.6 The contrast in relief between this new lineament and a previously mapped one (which has, of course, a stronger expression in the imagery) can be seen by comparing Figures 20 and 22. The Ausable Lakes lineament is marked photogeologically not only by topography, but, also be a vegetation boundary, i.e. conifers on the east slope, deciduous trees on the west.

6.4.7 A far more subtle topographic lineament found in the ERTS-1 imagery is shown in Figure 23. This broad, relatively short (6 km) linear valley extends west-northwest, transecting at nearly right angles the North River-Mt. Marcy range. The northern edge of the North River Mountains appears in the left middleground. The linear is

terminated to the west by a major north-northeast linear which passes just east of Popple Hill, the dark mountain in the middle of the valley.

6.4.8 Several arms of Cranberry Lake in the east central Adirondacks are broad linear valleys developed in granitic gneiss (Figures 7 and 24). Extensions of these lineaments, first observed from low level aircraft (Figure 24), were found on re-examination to be visible in the imagery (linears 176a and 176b in Appendix II). A view of another arm of Cranberry Lake showing lineament 175 appears in Figure 25. ERTS-1 imagery has been especially useful in this part of the Adirondacks where topographic maps predate stereomapping methods.

6.4.9 A rocky shoreline along Lake Champlain permitted interesting aerial documentation of ERTS-1 lineaments. Shoreline expression includes the formation of coves, discontinuity in the shoreline cliffs, and inclination of joints near the structures suggestive of conjugate shears associated with faulting (Figures 26 and 27).

6.4.10 Another lineament located in metanorthosite is shown in Figure 28 It well illustrates a question that continues to plague us in the identification of photolinears in ERTS imagery, namely, what minimum length is required before a linear feature can be classified as a topographic lineament, and hence assumed to be structurally controlled? The question arises again in considering Figures 34 and 35. In the present illustration, however, the continuation of the linear beyond the head of the valley is judged a valid reason for the classification. A ground check is desirable to ascertain the cause of the lineament.

6.4.11 Figure 29 illustrates a previously-mapped fault in mangerite which, in the imagery, appears to have an eastward extension.

6.4.12 More subtle lineaments are seen in the Seward Range (Figures 30 and 31). These contrast sharply with the strong geomorphic expression of other linears in the same metanorthosite massif farther east (Figures 17 and 19). Indeed, they occur near the western limit of strong lineament development, and deserve ground study and verification.

6.4.13 Figure 32 shows part of topographic lineament 309 which connects two previously-mapped linear elements, and extends one of them, to define a single lineament 50 km long.

6.4.14 An example of the difficulty that can be experienced in identifying a topographic lineament, even from the best vantage point, is shown in Figure 33. The linear feature is faint, at best, in the photograph despite its clarity in the imagery.

6.4.15 Figures 34 and 35 illustrate a linear valley which is tentatively classified as a topographic lineament because it notches the ridge.

Its possible continuation beyond the ridge is obscured in shadow, even on the computer-enhanced image.

6.4.16 A short, straight lineament is illustrated on the east side of Catamount Mountain in the northern Adirondacks (Figure 36). It is quite possible that Taylor Pond should also be classified as a lineament inasmuch as it is developed within a relatively massive charnockite.

6.4.17 A subtle linear valley cutting Follensby Pond in the central Adirondacks (Figure 37) is classified as a topographic lineament because it transects lithologic boundaries at right angles. The apparent cuesta in the photograph reflects eastward dipping foliation in a mangeritic gneiss.

6.4.18 Another subtle linear valley is shown in Figure 38. Although unimpressive in this lighting, the linear is well displayed in the imagery and is tentatively classified as a topographic lineament.

6.4.19 An example of a declassified linear is shown in Figure 39. Although fairly convincing on the imagery, it turns out to be a ridge crest enhanced by a vegetation boundary, but without any apparent geological control; it is located entirely within gabbroic metanorthosite.

6.4.20 In contrast to linear valleys described above which are well defined on the imagery but very subtle in the field, there are other shorter ones which have the opposite characteristics. One example is a newly-discovered lineament trending N42W (Figure 40). Perhaps the reason it is not delineated on ERTS is that it too closely parallels the azimuth of solar illumination. A photograph taken farther south along the side of the MacIntyre Range (Figure 41) shows numerous lineaments cutting the mountainside. The most pronounced of these, that which passes on the right of snow-capped Iroquois Peak, is a new lineament not originally identified on the imagery. It strikes N82W at a high angle (55°) to the azimuth of solar illumination. Another of these lineaments trends N40W, within 13° of the solar illumination direction, and is barely visible on the imagery. The other steeply inclined lineaments are in shadow on the imagery. Note, however, the two lines running from left to right midway across the mountain. One of these shows clearly on the imagery as a new lineament. Each of these lineament sets will be studied in the field to determine and compare their origins. They appear to offer an intriguing prospect for regional basement stress analysis.

6.4.21 Another photograph of the MacIntyre Range, taken south of the preceding illustration, shows the blocky upper surface of the Range produced by intersecting orthogonal and oblique lineaments (Figure 42). Two major previously-mapped lineaments, appearing broadly curved in this view, cross the picture from left to right. At least five other

newly discovered lineaments are shown, but none of these can be mapped with confidence in the imagery. In the left middleground a vertical lineament crosses Cliff Mountain (see also Figure 43). It is not clearly visible in the imagery.

6.4.22 A further example of newly discovered lineaments which are below the detectability of ERTS-1 resolution (either summer or winter) are illustrated in Figure 44. These lineaments were subsequently observed on U-2 photography where they can be seen to be orthogonal to the pronounced north-northeast linear valleys.

6.4.23 An exceptional exposure of a fault surface in the Adirondacks is that exposed in the east-west open pit operation of the Barton Garnet Mine in North Creek, eastern Adirondacks (Figure 45). The fault zone marks the contact between charnockite on the right (south) and the garnetiferous olivine metagabbro which is being mined. The fault zone is about 3 meters wide, is chloritized but not brecciated, and shows both horizontal and vertical slickensiding. It strikes east-west and dips about 75° north in the western (near) end of the pit and swings through the vertical at the eastern end. As can be seen in Figure 45, the fault surface is quite irregular. Also visible are broad rolls in the surface which have subhorizontal axes. Away from the excavation the fault cannot be recognized owing to an absence of outcrops. Brecciation does not characterize this east-west fault, but can be seen in several Adirondack road cuts along the north-northeast and northwest topographic lineaments (e.g. Figure 47).

6.4.24 An example of closely-spaced jointing as a cause for the development of a linear stream channel segment is illustrated in Figure 46. About 50 meters upstream from this photograph a healed plastic shear zone occurs between two facies of metanorthosite, suggesting the possibility of rejuvenated brittle deformation along an old shear zone.

6.5 Status of ERTS-1 Linears in the Adirondack Region

6.5.1 On the Geologic Map of New York, 1961 edition, (Fisher and others, 1961) Isachsen added in the Adirondack region numerous topographic lineaments which could be seen clearly on 1:62,500 topographic maps made by stereophotogrammetric methods. The contour interval of these maps is 20 feet. The linear features were designated "topographic lineaments" to distinquish their status from that of mapped faults. Interestingly, the two are, in most instances, indistinquishable topographically except where mapped faults have only slight topographic expression. To this group can now be added new topographic lineaments found on the ERTS-1 imagery. These will be discussed subsequently.

Table 1. RESULTS OF STAGE II AND STAGE III EVALUATION OF ERTS-1 LINEAR FEATURES IN THE ADIRONDACK REGION

Photogeological Classification	Topographic Expression				
	CTL*	TL	NTL	Totals	Previous Totals
I. Declassified Stage I Linears					
1. Man-caused photolinears which are unrelated to natural features, e.g. highways, transmission lines, railroad beds, canals, etc.			20	20	20
2. Normal lithological contacts and foliation trends	43	2	9	54	51
3. Unverifiable on the ground as linear features				17	
SUBTOTALS	43	2	29	91	71
II. Retained Stage II and Stage III Linears					
1. Straight stream valleys	101	21		122	27
2. Straight segments of stream courses			5	5	96
3. Meandering streams with overall alignment			3	3	7
4. Elongate lakes or straight lake shorelines	2		2	4	7
5. Edge of topographic high or aligned segments of same	6			6	8
6. Dark vegetation strips			8	8	30
7. Natural vegetation borders			6	6	7
8. Combinations of two or more of above, indicating topographic expression which predominates	80	16	33	129	57
9. Unexplained			36	36	125
SUBTOTALS	189	37	93	319	364
TOTALS	232	39	122	410	435**

*CTL = clearly a topographic lineament on imagery and on ground
TL = topographic lineament on ground but not obviously so on imagery
NTL = not a topographic linear feature on imagery, and/or not yet checked on ground

**Present and previous totals are reconciled by subtracting 30 curvilinears from the previous total and adding 5 new linears. Previous totals are from Isachsen, 1973.

6.5.2 The breakdown of ERTS-1 linear features resulting after Stage II and incomplete Stage III investigations in the Adirondack Mountains is shown in table 1. At the head of the table are listed the declassified Stage I linears. These comprise about 20 percent of the original total of unscreened linears, and will not be considered further. Each of the remaining linears was classified both in terms of its photogeologic description (left column) and its topographic expression (CTL, TL, or NTL of table 1, defined in footnote) in order to determine the number of new ERTS-1 topographic lineaments. It can be seen that both the CTL and TL categories are topographic lineaments by definition (postponing for the present the question of possible additional requirements besides straightness and topographic expression, such as minimum length and other geomorphic characteristics). The same applies to those NTL linears in photogeologic classes one through four which must have topographic expression even though they might appear on the imagery as featureless, dark vegetation strips which are determined from airfoto index sheets to occur along straight stream courses. (Such linears would be placed in class 1 under NTL). Summing these topographic lineaments yields a total of 236, or nearly 75 percent of the total number, 319. Trends of NTL linears are not unique (cf. Figures 13a and 16).

6.5.3 Before comparing previous and present totals, it should be noted that the present totals refer only to linear features; 30 curvilinears from the previous list have been omitted. Also omitted is the earlier designation "ridge crests" because the linears involved were not caused by any variations in structure (or lithology), the terrane involved being relatively homogeneous metanorthosite of the Marcy Massif. Rather, they are explainable as residual linear ridges bounded by parallel topographic lineaments. Allowing for these changes, the following are notable reclassifications:

1. Seventeen linears were declassified as unverifiable on the ground as linear features.

2. About 75 percent of the dark vegetation strips were found to coincide with "straight stream valleys" and were hence transferred from a botanical to a geomorphic category.

3. About 65 percent of the "unexplained" linears were reclassified, many as combinations of geomorphic and botanical categories.

4. About 95 percent of the "straight segments of stream courses" were reclassified into other categories, mainly "straight stream valleys".

6.5.4. Although the overwhelming majority of our ERTS-1 imagery analysis was done with the 1:1,000,000 imagery regularly received from NASA, a multi-scale comparison was made of linears as revealed at 1:500,000 and 1:250,000 as well, using EROS paper positive enlargements of band 7 for the same images shown in the Adirondack mosaic of Figure 11, and the winter imagery of 8Jan73, and 9Jan73 (image nos. 1169-15121 and 1170-15175). The comparison was made using all linears seen on the fall and winter imagery, although very few linears were seen on the winter image that did not appear on the fall image.

6.5.5. Results of this comparative analysis were as follows:

1. Surprisingly, all the linears detected at 1:250,000 were also observable at 1:500,000 (Figure 12b).

2. The majority of the linears seen at the above scales had also been seen at 1:1,000,000 except for 433 new short linears, the majority of which are less than 5 km long, but have a combined length of 2155 km.

When this latter group were searched for on the 1:1,000,000 imagery, 87 percent were not observed, 10 percent were observed without reservation, and 3 percent were seen with slight difficulty.

6.6 Geological Identification and Origin of ERTS-1 Topographic Lineaments in the Adirondacks

6.6.1 In determining the origin of topographic lineaments, there is no substitute for data obtained from either natural or man-made bedrock exposures. These may demonstrate that the lineament is an erosional reflection of bedding, other lithological layering, schistosity or foliation, although such a determination can commonly be made in the laboratory using existing geological maps which tend to concentrate on these geological parameters. Such linear features would be termed "lithological linears" and declassified as ERTS-1 linear anomalies. The bulk of ERTS-1 lineaments, however, depend for a genetic classification on outcrop data. Outcrops may reveal a variety of structural features, including closely-spaced jointing, or evidence of faulting such as shearing, brecciation, slickensiding or other cataclasis, stratigraphic offset or drag folding, mineralogical changes such as retrograde metamorphism, intense rock alteration, etc. Unfortunately, however, such processes cause accelerated weathering and erosion, with the result that outcrops are scarce or absent altogether. Buddington and Leonard (1962, p. 130), for example, note in reference to mapping in the Cranberry Lake region of the central Adirondacks that "the inquiring geologist cannot reach out his hand and place it on a fault surface of any one of the major faults in the district". As early as 1894, Kemp commented on the same difficulty in the northeastern Adirondacks. This problem is further magnified in a statewide study

such as this one; the sheer magnitude of the field problem demands the use of statistical approaches to the question of genesis, similar to those suggested by Gross (1951). Our approach has been, and continues to be, as follows:

1. Comparing ERTS-1 lineaments with previously mapped faults or joint controlled valleys, as to azimuth, scale, and other features, and extrapolating origin therefrom.

2. Field reconnaissance in selected representative areas in the hope of "geologically-calibrating" the imagery for extrapolation across broad regions. This approach has greatest potential in the Allegheny Plateau.

6.6.2 The first approach leads us to suspect that the north-northeast lineaments in the Adirondacks are the traces of high angle faults and fracture zones. This is based largely on the experience of Matt Walton, who made detailed bedrock geological maps of four contiguous 15 minute quadrangles in the eastern Adirondacks where these linear fractures are so abundant. Walton (oral communication) found that fault breccias and/or stratigraphic displacement could generally be demonstrated for these lineaments, although they had been earlier interpreted as classic geomorphological examples of joint control. Earlier examples of lineaments controlled by closely-spaced joints and fault zones were given previously but no generalizations can be made from these at present.

6.6.3 The origin of tonal lineaments presents a greater problem. However, an explanation has been found for one outside the Adirondacks which trends east-northeast across a terrane of horizontal limestone in the Helderbergs at the northeastern end of the Allegheny Plateau. We learned from Stephen Egemeier, a geologist-speleologist, that he has mapped the geology in a series of aligned caves which are parallel to and perhaps coincident with the linear in question. He has found that each cave is developed by solution along a fault which has a displacement of only a few feet or less. This provides a new perspective on tonal linears in carbonate terranes, although additional field work will have to precede any generalizations.

6.7 ERTS-1 Linears in New York Exclusive of the Adirondack Region

6.7.1 Introduction

6.7.1.1 Several types and scales of images, aerial photographs and shaded relief maps were used in evaluating ERTS-1 imagery of southeastern New York for linear signatures, and to extend this evaluation regionally into central and western New York. The analyses were compared with existing information and with new field data collected from a test area in the Catskill Mountains and Hudson Lowlands that encompasses thirty 15-minute topographic quadrangles (Figures 3 and 48).

6.7.1.2 Scene C3 was chosen for detailed photogeologic analysis because it permits a comparison of linear characteristics across several physiographic, geologic, and tectonic provinces (Figures 1, 2, 3, and 60). In addition, a portion of the Ramapo fault, one of the few tectonic features in the northeastern United States which is strongly suspected to be seismically active (Page and others, 1968) can be clearly seen (Figure 60).

6.7.2 Multi-scale photogeologic analysis of scene C3, Catskill Mountains and southeastern New York.

6.7.2.1 A Stage I multi-scale photogeologic analysis of linears was made of fall and winter images of scene C3 (Figures 5, 48 and 49). The data sources and scales used were as follows:

1. Mosaics of ERTS-1 imagery at 1:2,500,000 (Figures 7 and 8).

2. Positive transparencies of bands 5 and 7, and false color composite prints of bands 5, 6, and 7 at 1:1,000,000 (Figures 48 and 49).

3. Black and white positive prints of band 7 enlarged to 1:500,000.

In addition, straight valleys were plotted from 1:62,500 topographic maps of the Margaretville and Phoenicia quadrangles in the Catskill Mountains (see Figures 3 and 48 for location) and from an uncontrolled airphoto mosaic index sheet of the same area at the same scale.

6.7.2.2 Linear signatures were recorded on clear acetate overlays for each of the above data sources, and were then compared with each other and with geological maps at various scales, through the use of scale-changing viewers (Bausch and Lomb Zoom Transferscope and overhead viewing projector). The data and results pertaining to these analyses are presented in Figures 50-59, and are discussed below. The justification for drawing the many short linears shown on these diagrams is the fact that comparisons with U-2 photography showed lines as short as 1 -1.5 km on ERTS-1 imagery to be unequivocal photolinears. This is documented in a later section.

6.7.2.3 The multi-scale comparison of ERTS images showed that the shortest lines generally classified as linears at the various scales were: 1:2,500,000, 5 km; 1:1,000,000, 2 km; 1:500,000, 1 km; 1:250,000, ½ km. This expectable inverse linear relationship between scale of imagery and length of linears suggests that a line must be at least 1.5-2 mm long, on any scale image, before an interpreter confidently identifies it as a "straight line". It was also observed that numerous short, aligned segments at the larger scales appear to coalesce into single long linears at the smaller scales. This occurs wherever the smaller segments lie in a straight line or zone, whether they strike parallel to

that line, en echelon to it, or are conjugate sets, no matter what the strike (e.g. Figure 68). For example, the N65E trending set of linear segments near the northeast corner of Figure 51 appears at 1:2,500,000 to be a single linear almost one hundred kilometers long, at 1:1,000,000 a dashed line (Figure 54) and at 1:500,000 as an alignment of two sets of en echelon segments lying in a N65E zone (Figure 81). At 1:250,000 the individual linears are no longer recognizable as part of a through-going structure.

6.7.2.4 Figures 50, 54, 55, and 56 are maps of linears which were observed at various scales on black and white positive prints derived from the same band 7 positive transparency used in making 52a. A comparison of these Figures shows that for southeastern New York, more linears, both topographic and tonal, were observed at the 1:1,000,000 scale than at any other scale. This is in contrast to a similar comparison made in a very different geological province, namely the Adirondacks, which was discussed earlier. Several consistent variations can be seen in going from smaller to larger scales:

1. Continuous topographic linears become zones of discontinuous aligned segments, and the same applies to tonal linears.

2. Many topographic linears become tonal linears.

6.7.3 Comparison of linear content in fall and winter imagery

6.7.3.1 In the course of this analysis, a comparison was made between the linear information revealed in summer-fall versus winter imagery at 1:2,500,000. As can be seen by comparing Figure 50 and 51, much more detail is present in the summer-fall mosaic than in the winter mosaic. This may be due to the higher contrast of the winter print, and in part to a poor image product for the central New York scene. The longest continuous linear measured on any image of the Allegheny Plateau is on the winter image at 1:2,500,000, and appears to extend continuously for more than 90 kilometers.

6.7.3.2 Figures 52a and 52b show the linear analysis for southeastern New York made on band 7 of the 100ct72 image (see also Figure 48). Figure 53 is a subtraction map showing the linears observed on band 7 of the winter image at 1:1,000,000 (i.e. Figure 49) but not on the fall image. It can be seen that the winter image emphasizes the shorter linears more effectively than the fall image does, especially in the Catskill Mountains which are located in the northwestern portion of the scene.

6.7.3.3 Many of the tonal signatures on the fall image are topographically expressed on the winter image, probably due to shadow enhancement occasioned by the lower angle of solar illumination in winter.

6.7.3.4 Figure 54 shows the linears from both the fall and winter images at 1:1,000,000, and combines the data of Figures 52 and 53. This map is used for all subsequent linear analysis of the scene at the 1:1,000,000 scale. It contains the 322 tonal and 977 topographic linears observed on the fall image as well as the 23 tonal and 699 topographic linears seen only on the winter map, making a total of 2021 linears.

6.7.3.5 Field inspection to classify all these linears on the ground would require an inordinate amount of time. Observation from low-flying aircraft can be used advantageously to supplement ground study. As an example, tonal linear number 75, located on the ERTS image of Figure 64, can be instantly identified from small aircraft as a topographic lineament (Figure 64).

6.7.3.6 To test the differences between ERTS-1 image analysis and some traditional map and image products, a linear analysis was made of the Margaretville and Phoenicia 15-minute topographic maps in the Catskill Mountains (Figures 48, inset, and 57) and an airphoto index mosaic of the same area (Figure 58). Figure 59 shows the ERTS-1 linears of this areaenlarged from Figures 52 and 53, with heavy lines representing the fall linears and thin lines the winter linears. Although some of the fine detail observed on the topographic map is not seen on the ERTS-1 linear map, the main valleys all show clearly.

6.7.4 Photogeologic analysis of ERTS-1 linears in southeastern New York

6.7.4.1 The photogeologic characteristics of ERTS-1 linear sets in scene C3 are summarized in Table 2 under the following categories:

1. Relative prominence in the various geologic provinces.

2. Mode of expression (topographic or tonal).

3. Length.

4. Straightness, or direction of concavity.

5. Distribution density: dense where generally less than 5 kilometers apart, moderate where 5 to 10 kilometers apart, sparse where greater than 10 kilometers apart.

6. Regularity of spacing: even where spaced evenly, uneven where clustered in zones or areas.

7. Clarity of expression: poor where difficult to observe on image product, moderate where generally easy to observe, and prominent where the linear set is one of the more dominant sets observed.

Table 2. Chart summarizing the directions and characteristics of Stage I linears for scene C3 in southeastern New York

	ERTS-I IMAGERY									TOPOGRAPHIC MAPS 1:24,000	AIRPHOTO INDEX SHEETS
	1 : 1,000,000						MOSAIC OF N.Y., 1:2,500,000		1:500,000	1:250,000	
DIRECTION	PROVINCE	LINEAR TYPE (minor expression in parentheses)	LENGTH in km	STRAIGHTNESS AND CONCAVITY DIRECTION	DISTRIBUTION	SPACING	FALL	WINTER			
N80W	all except Atlantic Coastal plain	tonal	10-50	slightly curved to N and S	sparse	even	topo in Catskills	tonal in Appalachian Plateau	poorly expressed	All directions expressed. All long linears are tonal, all short are topo. All directions have less dense distribution and all are unevenly spaced.	prominent, 1-20 km	prominent 1-2 km
N60W	west of Hudson River	topo-tonal	10-50	straight	dense in NW sparse in south & east	even or uneven in zones	topo in Catskills; tonal in east	poorly expressed	poorly expressed N60E tonal linear 30-50 km prominent in Hudson Highlands		moderately expressed 2-5 km	1-2 km
N20W	all	tonal (topo)	5-40	straight in Catskills slightly curved in S, to NE, NW	dense	even	topo in west tonal in east	topo in west tonal in east	poorly expressed tonal (topo)		prominent 5-15 km	moderately expressed 2-5 km
N15W	west of Hudson Highlands and Taconics	tonal	10-40	short-straight long-curved to east	sparse	uneven	topo in west	poorly expressed	poorly expressed		poorly expressed 2-5 km	prominent 1-2 km
N-S	Catskills Hudson Highlands Manhattan Prong Atlantic C. P.	topo (tonal) tonal (topo) tonal tonal	10-50 10-50 25 10	slightly curved to east & west	dense	even	topo in Catskills; tonal in south	topo in west tonal in east	short topo in Catskills; all other areas tonal		moderately expressed 2-5 km	poorly shown
N15E	all	topo (tonal) (topo only in Catskills)	5-30	straight	dense in all but Shawangunks	even to uneven	topo in Catskills; topo-tonal in east	topo in west tonal in east	topo in Catskills; all other areas tonal		prominent 2-15 km	prominent 5-15 km
N20E	all	topo-tonal	5-40	straight to slightly curved to west	dense in all but Shawangunks	uneven and in zones	topo in west; topo-tonal in east	topo in NW tonal-topo in east	topo in Hudson Highlands; all other areas tonal		poorly expressed	moderately expressed 2-5 km
N25E	Catskills Shawangunks Hudson Highlands Taconics	topo (tonal)	5-10 10 10 10	straight	sparse	uneven	short topo in south + Catskills	poorly expressed	prominent short topo in Catskills		moderately expressed 5 km	moderately expressed 1-2 km
N45E	Hudson Highlands Manhattan Prong	tonal (topo)	5-15 5-15	straight	sparse	uneven	topo in Hudson Highlands	topo in southeast	short topo in Catskills; long tonal in Hudson Highl.		prominent 15-20 km	moderately expressed 2-5 km
N65E	all	topo-tonal	5-100	straight	dense	even and in zones	long topo in Catskills; short topo in Hudson Highl.	long topo in Catskills	short topo everywhere long tonal in south		moderately expressed 5-10 km	prominent 2-5 km
N85E	Catskills Hudson Highlands Taconics	topo (tonal)	5-20 5-25 5-25	straight	sparse	uneven in zones	short topo in Catskills	poorly expressed	poorly expressed		moderately expressed 5 km	prominent 5 km

6.7.4.2 Early analysis revealed linear and curvilinear sets having average azimuths in the following directions: N80W, N40W, N20W, N15W, N, N15E, N20E, N25E, N45E, N65E, and N85E, and a N60W set that may be curved extensions of the N40W set. In further analysis the curved sets were divided into short segments such that each segment has a small arc with an average azimuth direction lying in one of the 18 ten-degree divisions of the northern semi-circle of a rose diagram. This study revealed a dominance of length-weighted linear segments trending between N5W and N75E. The rose diagram of Figure 67 summarizes these analyses, but does not distinguish topographic from tonal linears.

6.7.4.3 Most topographic linears in scene C3 are straight, while a number of longer tonal linears are slightly curved. The directions of concavity vary, but a consistency exists within some sets.

6.7.4.4 Tonal linears commonly cross both topographic linears and other tonal linears. Topographic linears, on the other hand, generally do not cross each other except in parts of the Taconic and Catskill Mountains. Shorter topographic linears almost nowhere cross other topographic linears, but many abut against larger topographic linears.

6.7.5 Field study of bedrock structures in the Catskill Mountains

6.7.5.1 Because the southeastern New York scene has an area exceeding 10,000 square miles, it was decided to limit new field studies to a test area consisting of thirty 15-minute quadrangles (Figure 61). An index of these topographic maps is given in Figure 62. For this study area one other type of image analysis was performed for linear characteristics; a comparison was made of the differences in expression between the fall and winter images. Figure 63 shows that approximately 60 of the tonal linears observed on the fall image correspond to topographic linears on the winter image. In contrast only four of the tonal linears observed on the winter image correspond to topographic linears on the fall image.

6.7.5.2 The field study included measuring structural elements in outcrops and comparing them with topographic features nearby. Approximately 125 localities were visited. Figure 64 shows 18 of the localities in the northeastern corner of the study area where measurements were taken. Table 3 summarizes the findings at these localities, and shows that a definite correspondence exists between joint set strike directions and the directions of straight valleys. This limited study indicates a possible correspondence between straight valleys and regionally developed joint sets having dips greater than 60 degrees. Some of these sets may be parallel to faults with small offset, but this has yet to be proven in the area, as will be discussed later for the Stony Clove topographic lineament. With this idea in mind joints were measured throughout the 30 quadrangle study area. About 250 measurements were recorded and were divided into two major categories, each with three subdivisions (Figure 65). The symbols with the thicker lines represent "master" joint sets. These are sets that cut all the beds of an outcrop and appear to extend to adjacent outcrops. The symbols with thinner lines

TABLE 3. COMPARISON OF ERTS-1 LINEARS AND GROUND DATA IN THE NORTHERN CATSKILL MOUNTAINS

FIELD LOCATION NUMBER	LINEAR NO. AND AZIMUTH	AZIMUTH OF TOPOGRAPHIC FEATURE	ATTITUDE OF JOINTS MASTER SET UNDERLINED	7½' QUADRANGLE (15' QUADRANGLE)	REMARKS	DEGREE OF CORRESPONDENCE OF LINEAR WITH GROUND DATA
1	*Topo 131 N15E	Valley N15E	N15E, 85E	Leeds (Coxsackie)	Folded Limestone - Jointed, jointing perpendicular to bedding and parallel to fold axes	Perfect with valley and joint set
2	Tonal 36 N40W	Flood Plain Valley N40W	No Outcrop	Leeds (Coxsackie)	Catskill Creek	Perfect with valley, no rock outcrops
3	Summer Tonal 29 curved: east end N60W, west end N75W, winter topo N20E	NE Catskill Front Front trends ≈ N60W	N20E, 80E N60W, 70NE	Freehold (Durham)	Redbed Sandstones and shales, N60W 70NE joint is slightly curved convex upward	Summer tonal perfect with northern front of Catskills and subordinate joint set; winter linear perfect with valley and master joint set
4	Near topo127 N60W	NE Catskill Front Front trends ≈ N60W	N60W, 90 N50E, 90	Freehold (Durham)		Perfect with valley and master joint set
5	Topo 127 N60W Topo 128 N20E	Catskill Front ≈N60W Narrow Valley N30E	N60W, 80NE N35E, 85W	Hensonville (Durham)	N35E 85W joint curved and irregular	Perfect with northern point of Catskills and subordinate joint set Good with valley, fair with master joint set
6	Topo 128 N20E	Narrow Valley N30E	N35E, 90 N60W, 90	Hensonville (Durham)	N35E joints are plumose and planar	Fair with valley; valley parallels master joint set
7	Tonal 31 N20E	Narrow Valley N10E	N50E, 80NW N35W, 80E	Hensonville (Durham)	Tonal linear 28 trends, N10E ∴ geomorph reason for valley not understood	Good with valley, poor with joints
8	Topo 110 Curved, generally N-S Topo 109 N35E	Narrow Valley segment N40W, part of larger valley system trending N15E, Valley side N30E	N40W, 90 N30E, 82NW N85E, 78S (All moderately weak)	Ashland (Gilboa)	In Stone Quarry N40W joint curved N30E joint curved and plumose concave downward N85E curved	One linear poor with valley, and lacks correlation with joints, other linear perfect with valley side and with joints
9	Topo 107 N75E	Major Valley segment west end N75E	N75-80E, 75-90N (weak)	Ashland (Gilboa)	Near Stone Quarry Joint only in sandstone	Perfect with valley, and subordinant joint set
10	Near Topo 104 N15E	Outcrop on hillside near a straight valley-hillside trending N40W	N50W, 90	Ashland (Gilboa)	Poorly jointed outcrop on hillside in sandstone	No correspondence with valley or joint set
11	Topo 123 N15E	Narrow Valley N15E	N15E, outcrop Status uncertain	Ashland (Gilboa)	No outcrops that are definitely in place Hillside boulders have joints ll to valley but not sure how much creep has taken place	Perfect with valley and joint set
12	Small unnumbered topo N75W	Narrow Valley N80W Narrow Valley N5E	N80W, 84N N32W, 80E N5E, 90	Prattsville (Gilboa)		Perfect with valley and master joint set
13	Small unnumbered topo N40W	Two valleys meet: N40W N30E Small Valley N65E	N80W, 80S N25W, 74NE N72E, 90	Prattsville (Gilboa)	N72E joint is curved	Fair with valley and master joint set Small valley perfect with subordinant joints
14	Small unnumbered winter topo N40W	Short, narrow valley Segment N30E	N30E, 90	Prattsville (Gilboa)	Joint is curved only one joint set in outcrop	Perfect with valley and master joint set
15	Topo 92 N45E Small unnumbered winter linear N75W	Short narrow valley generally N45E, nearby short valley ¼ mile to the north N75W	N80W, 90 N10E, 60W	Prattsville (Gilboa)		Perfect with valley, no correspondence with joints; perfect between joints, unnumbered linear and short valley ¼ mile north of outcrop
16	Topo 114? N60E	Narrow Valley N60E	N55E, 76N	Roxbury (Hobart)	Only good joint set in outcrop	Perfect with valley and joint
17	Topo 114? N60E	Narrow Valley end N60E	N50E, 80N N55W, 75SW	Roxbury (Hobart)		Good with valley and master joint
18	Unnumbered linear E-W	Narrow, very straight valley E-W	No outcrops	Roxbury (Hobart)	Very straight valley trending E-W which shows as barely recognizable linear on ERTS image. No outcrops were found.	Perfect with valley, no rock outcrop

*TOPO = TOPOGRAPHIC LINEAR; TONAL REFERS TO NON-TOPOGRAPHIC LINEAR
FIELD LOCATIONS ARE SHOWN ON FIGURE 27

represent joints that occur in only some beds of the outcrops, and do not appear to have very much lateral or vertical extent. Master joint sets having dips greater than 60 degrees are probably the ones that influenced regional erosional processes to produce straight valleys.

6.7.5.3 A comparison of rose diagrams for summed lengths of linears of the Catskill Mountains and summed number of joints in the study area is shown in Figures 66a and 66b. The diagram of linears shows an arc of strong maxima between N15E and N35E, whereas that for joints shows two prominent directions, one generally east-west and the other between N5W and N15E. This discrepancy may well be due to the fact that we are comparing a complete sample of linears with only a small, road-controlled sample of the joints in the region. The east-west joints may correspond to the very short east-west linear sets which pervade the Catskills but add relatively little magnitude to the summed-length diagrams. It is interesting to note that Parker (1942) found far fewer joints trending east-west than northwest-southwest (Figure 79a).

6.7.5.4 A further point must be considered in analyzing rose diagrams of linears in the Catskills and other parts of the Allegheny Plateau. Close inspection of images at scales larger than 1:1,000,000 shows that topographic linears in this region may actually be straight zones of linear segments which are not necessarily aligned parallel to the zone in which they lie, but may have an en echelon orientation within the zone. Alternatively, the linear may consist of a zone of both parallel and en echelon segments. Figure 68 illustrates these three geometric variations. If the short segments were developed in response to local joint set patterns, and the linear zones to a regional density distribution of these local joint sets, the maxima on rose diagrams of joints would not correspond with those for linears. Where linear segments have the same strike as the valley they occupy, however, the rose diagrams of joints and linears would, of course, be identical. Where joints are arranged en echelon to the regional linear zones, however, the rose diagram maxima would differ systematically. In the third situation illustrated in Figure 68, the joint diagram would show maxima in both the direction of the regionally expressed linear and the en echelon joint set. This last situation may account for the appearance of two maxima in Figure 66a and only one in Figure 66b.

6.7.5.5 Some of the linear zones, where short en echelon linear sets abut against a single long linear within the zone, are suggestive of conjugate shear zones and associated tensional sets.

6.7.6 Field study of the prominent N20E linear set in the Catskills: The Stony Clove topographic lineament

6.7.6.1 The eastern edge of the Catskill Mountains is a notably straight steep escarpment (Figure 60) along which the Mountains rise abruptly for 800 m from the Hudson Lowlands to adjacent summits which exceed 1,000 m in height. This escarpment, long known as the "Wall of Manitou"

(Chadwick, 1944, p. 205) extends south from the latitude of Catskill for a distance of 20 km.

6.7.6.2 West of the "Wall", the Catskill Mountains are eroded to produce prominent, northwest-trending, ranges and valleys (Figure 64). Indenting these ranges at a high angle are numerous topographic lineaments which trend about N15E, and parallel the Wall of Manitou. The pervasive nature of this set, extending westward for at least 25 km, was never recognized before, and its geologic origin has only received brief mention. Chadwick (1944, p. 17) interpreted the two prominent valleys which occur 10 km west of the Wall of Manitou as being controlled by closely spaced joints along which "the internal settling known as 'keystone' faulting (Crosby, 1925)" might have occurred, although "as yet actual faulting has been demonstrated in only the easternmost of these lines, namely that which is tangent to the east end of North Lake." The fault referred to is located at the northern end of the "Wall" at the upper break in slope on Chadwick's geological map.

6.7.6.3 The Wall of Manitou and several of the parallel linears were examined and photographed from small aircraft before the leafing of deciduous trees. Figure 69 illustrates the straightness of the "Wall", and also shows traces of an orthogonal N75W set which is not well shown on the ERTS-1 imagery. Figure 70 shows a sag pond developed in the lower part of the "Wall", a feature which may indicate the trace of a "keystone" or other type fault.

6.7.6.4 A vertical aerial photograph taken by NASA at 24,000 feet altitude of an area 12 km west of the Wall of Manitou (Figure 71) provides a useful calibration device to determine how short a linear may be mapped on the ERTS-1 imagery with confidence. It can be compared with the 1:500,000 ERTS image of Figure 64 by simply identifying Clove Valley in both illustrations (avoid being confused by the slight difference in orientation of true North in the two pictures). Clove Valley is identified in the caption of Figure 71, and by a barbed dot labeled 72 in Figure 64. As can be seen in the airphoto, the relatively long N20E linears are readily confirmed, a particularly good example being Stony Clove linear itself. More impressive, however, is the fact that the two short N75E linears, spaced only 1 km apart, with the shorter one being less than 2 km long, can be discerned on the imagery; we would have been unwilling to identify such short lines on the imagery as linears without the assurance provided by the aerial photography.

6.7.6.5 Low level aerial reconnaissance of the Stony Clove linear confirms it as a well defined topographic lineament (Figure 72). A closer view of Stony Clove drainage divide shows the head of the valley to be narrow and steep-walled, carved into flat-lying shales and sandstones (Figure 73). This aerial view of the two lower sandstone beds suggests that the east side may be slightly down-dropped. Field altimetry to check this possibility was inconclusive, inasmuch as the measured elevation difference of only five meters across a valley width of 100 m in continental sediments can be explained without resort to faulting.

Of interest, however, is the fact that the valley is developed along a steeply-dipping conjugate joint system. On the west side of the valley, east-dipping joints are dominant. On the east side, westward dips predominate. The acute angle of 32° which is produced by these joint sets is bisected by the vertical plane. In some places, both joint sets can be seen in the same outcrop (Figure 74).

6.7.6.6 The orientation of the 32° acute angle is compatible with the interpretation that this sytem of conjugate joints, and the trace of the valley itself, are reflected basement structures such as might be produced by minor dip-slip reactivation along a basement fault. However, the 32° acute angle is notably less than the 50-60° angle generally associated with normal faults (Price, 1966, p. 59). This discrepancy cannot be attributed to structural anisotropy produced by bedding in the Lower and Middle Paleozoic formations involved, because the bedding surfaces are horizontal and thus at right angles to the suggested axis of principal stress. With such geometry, the bedding anisotropy would not significantly effect the development of shear surfaces (Price, 1966, p. 68). Although the small magnitude of the acute angle is not yet explained, the hypothesis of reactivated basement faulting is supported by the fact that the entire set of north-northeast trending topographic lineaments in the eastern Catskills is aligned with faults and lineaments of similar strike and spacing in the exposed basement rocks of the eastern Adirondacks (Figures 7 and 9).

6.7.6.7 Depending upon depth of overburden at the time of proposed reactivation of basement faults, Paleozoic rocks near the base of the section may have responded by monoclinal folding. According to Price (1966, p. 24) the minimum depth for such ductile behavior would range from 8000 to 10,000 feet (2400-3000 m) for compact limestone to 20,000 feet (6000 m) for arenaceous, igneous, or metamorphic rocks. The basement surface at Stony Clove is about 10,800 feet below sea level according to a basement map prepared by Rickard (1973, plate 18); the valley floor has an elevation of 1800 feet, and the relief of the Clove is 2000 feet. Above a possible zone of ductile deformation in the Paleozoic section, the response to vertical dislocation would be by fracturing (faulting), presumably with diminishing offset at increasing distance from the basement fault.

6.7.6.8 An analogous explanation may apply to the <u>plan</u> view of en echelon and conjugate linears shown in Figure 9. These could be produced by up propogated strike slip movement on reactivated basement faults, without the requirement of any substantial displacement. It has been demonstrated experimentally that a <u>system</u> of en echelon cracks propogate at only a fraction of the applied stress required to cause the development of a <u>single</u> crack of the same orientation and size (Brace and Bombolakis, 1963).

6.7.6.9 If the above conclusions are supported by future work, they may provide a means of recognizing in the Allegheny Plateau reflected basement normal faults which are manifested at the surface by a conjugate joint system, the acute angle of which is bisected by a vertical axis of maximum principal stress. Such lineaments would be distinguishable from other valleys which are controlled by vertical joint sets. This will be tested by future field work.

6.7.6.10 Another, very different method may exist for distinguishing genetic types of lineaments: those having normal background levels of radioactivity and those having on the order of 2x background. John Gabelman of the U.S. Atomic Energy Commission has made reconnaissance surveys of gamma radiation along a number of the major topographic lineaments in the Allegheny Plateau of New York and Pennsylvania, using a portable Mt. Sopris scintillometer on highway traverses (oral communication). He has found the level of radiation along such lineaments to be nearly two times the normal background count. On traverses up tributary valleys, the count returns to normal. A nearly twice-background radiation level was found along the east-northeast lineament followed by Route 7, between Binghamton and Cobleskill.

6.7.6.11 Inasmuch as our work in the Catskills has shown the existence of at least two genetic types of joint-controlled lineaments, one which parallels vertical joints and the other conjugate system of inclined joints, we plan, as a result of Gabelman's observations, to accompany future fracture analysis in the field with routine scintillometer measurements. We will do this less in the expectation of discovering highly anomalous areas (although continental sandstones such as occur in the Catskill facies <u>are</u> favorable uranium host rocks) than in the hope of finding an indirect means of discriminating between genetically different types of fracture systems. Field work to date, using a Precision Model 111B scintillometer, has not shown any significant change in gamma ray background count.

6.7.6.12 The task of relating the intricate drainage pattern in the Allegheny Plateau to joints in the field can only be achieved by continued representative sampling, analysis, extrapolation, and testing of extrapolations. Such work has only begun. If consistency appears in our test sites we may be able to turn the usual approach to joint-drainage study around -- <u>i.e.</u> to use the drainage patterns to "map" joint systems directly from ERTS imagery.

6.7.7.1 A preliminary analysis of ERTS-1 linears on a Statewide basis

6.7.7.2 Of the numerous classical studies of joint-controlled drainage which can be found in the literature, the earliest one that has direct application to our study is a 1904 paper by Hobbs. In this pioneer study, Hobbs used the best drainage map available and drew nine long linears ("hydrographic lines") in the Finger Lakes region, an area which, even then, had "long been a classical one for the perfection of its joint planes, a cut having been used by Dana in his <u>Manual of Geology</u> as the type illustration of joint structures" (Hobbs, 1904b, page 367).

6.7.7.3 The studies reported in this section parallel those of Hobbs in that they too are based on "hydrographic lines" (the drainage patterns in the various physiographic provinces of the State), and they too utilize "the best drainage map available", ERTS-imagery.

6.7.7.3 The number of ERTS-1 linears (photolinears) thus mapped in the State on 1:1,000,000 imagery is shown in Figure 9. The linears total 5066, and have

a combined length of 26,580 km or 15,950 miles. Detailed discussion of those appearing in the Adirondack and Catskill Mountains have been presented above. In the following section, rose diagrams are presented for Stage I linears in the entire Allegheny Plateau, and compared with linear data for the remainder of the State (Figures 76-78). In these diagrams, linears have been lumped into ten-degree sub-divisions of the rose diagrams. These sets were then measured for length, and the data presented in length-weighted rose diagrams. To some of the diagrams have been added an expanded scale (dashed lines) in order to make them useful at this scale of reproduction. The expansion factor is 4x. To make the original data more readily available, the full size rose diagrams have been included in this report as Appendix III.

6.7.7.4 The eleven zones outlined in Figures 76, 77 and 78 are divided along physiographic province boundaries. Zone 1 lies in the Ontario Lowland of western New York; Zone 2 includes the eastern Lowland and Tug Hill Plateau; Zone 3 comprises the westernmost portion of the Allegheny Plateau; Zones 4, 5, and 6 represent successive one degree divisions of the Allegheny Plateau of central New York; Zone 7 is the western Catskill Mountains; Zone 8 covers the Mohawk and northern Hudson Lowlands and includes portions of the Taconic Mountains; Zone 9 includes the Shawangunk Mountains, southern Hudson Lowland, Hudson Highlands, Triassic Basin, and Manhattan Prong (Figure 60); Zone 10 includes the Atlantic Coastal Plain of Staten Island and Long Island; Zone 11 comprises the Adirondack Mountains, Lake Champlain Lowlands, and St. Lawrence Lowlands.

6.7.7.5 All diagrams have equal scales, thus the size of the rose is a representation of the density of summed-length of linears in each zone. It is clear from the diagrams (also from Figure 9) that the density distribution of linears varies markedly across the State. If the density distribution shown in Figure 9 is compared with a map of glacial features, it becomes evident that the northern border of transition from high to low density linears corresponds with the location of the Kent and Valley Heads Terminal Moraines (Figure 90).

6.7.7.6 Very few linears appear in the Ontario Lowland. Here bedrock is composed of a thick sequence of shales (Salina Group), thin layers of dolostone (Lockport Group), sandstones (Medina Group), and Queenston Shale, (Fisher and others, 1971). Much of the Ontario Lowland is covered with glacial till and outwash deposits. Preglacial valleys are filled and are not distinguishable by surface mapping. The preglacial valleys, even though containing the greatest amount of ground water in the Lowlands, are not recognizable on ERTS-1 imagery. Thus it appears that density of linears may be the result of a combination of factors, including amount of glacial cover, low topographic relief, and possibly bedrock type.

6.7.7.7 An analysis was made to determine whether ERTS-1 linears provided more regional photogeological information than could be derived using the pre-ERTS technique of studying small-scale shaded relief or raised relief

maps. Figure 81 is an ERTS-1 linear analysis made from an ERTS-1 mosaic of New York and surrounding areas at 1:500,000. Figure 82 shows a similar analysis made from a shaded relief map of the same area, at the same scale. While it appears that many of the same linear directions can be observed in both data sources, it is evident that the ERTS-1 analysis gives a much clearer indication of linear spacing, density distribution, straightness, and length of segment elements.

6.7.8.1 Comparison of joint studies by Parker and by Nickelsen and Hough

6.7.8.2 The only regional synthesis of joints which applies to the C2 image area is that of Parker (1942, 1969) whose analysis is restricted to the flat-lying sedimentary rocks of the Allegheny Plateau (which includes the Catskill Mountains). Parker generally found only two or three joint sets at any one locality, and noted that the directions of these sets do not vary significantly across the area of a single 1:62,500 quadrangle. Across the entire western part of the State, however, he found a systematic clockwise rotation of the joint directions (Figure 79a).

6.7.8.3 Figure 79b is a comparison of Parker's joint data and ERTS-1 linear data for the same portion of the Allegheny Plateau. The northwest-trending maxima of Parker's western rose diagrams are not readily evident on the linear rose diagrams for Zones 5 and 6. Comparative data for the Catskills, however, shows that almost all of the joint directions mapped by Parker are represented by ERTS-1 linears (compare Figures 80a and 80b). Two linear sets seen on the imagery, however, those trending N40W and N20W, are not represented in Parker's joint diagrams. Parker divided the joint distribution into Sets I, II, and III. Set I, which is generally represented by two sets (interpreted as conjugate) averaging 19° apart at any locality, corresponds to the ERTS-1 linear sets between N-S and N20E; Set II corresponds to linear sets between N50W and N88E, and Set III corresponds to the linear sets between N45E and N67E.

6.7.8.4 The joints of Parker's Set I are generally vertical and remarkably planar. They cut all sedimentary features in the outcrop and are expressed in all types of sedimentary rock. They extend from a few centimeters to 60 m in length and are the most numerous set in any one outcrop, generally accounting for 50 to 70 percent of all joints present. Parker interprets this set to have resulted from shearing.

6.7.8.5 The joints of Parker's Set II are generally irregular, both horizontally and vertically through arcs of up to 25 degrees, and have rough surfaces. They constitute about 25 percent of all joints recorded in a given 1:62,500 quadrangle. They are interpreted by Parker as tensional fractures. Their relative lengths were not specified.

6.7.8.6 The joints of Parker's Set III are generally long, vertical and planar, although many are curved. They generally change character in passing from one stratigraphic horizon to another. They constitute about 15 percent of the total number of joints recorded in a given 1:62,500 quadrangle. Parker interprets them as tensional.

6.7.8.7 Nickelsen and Hough (1967, 1969) have presented alternate interpretations of jointing in the Allegheny Plateau of New York and Pennsylvania. They interpret the joint set pairs of Parker's Set I as an early set over-printed by a later one, rather than as a conjugate shear set. They also think that there may be as many as five distinctly different joint sets present throughout the region rather than a system of three sets which rotate clockwise across the region from west to east.

6.7.8.8 Many of the linear patterns expressed in the ERTS-1 imagery of the Catskills look surprisingly similar to joint maps of outcrops illustrated by Parker. However, the five-or-more joint set model of Nickelsen and Hough would also produce a pattern very similar to the regional linear features observed in the imagery. It seems possible that this conflict of opinions about the nature of jointing may be resolvable by field checking of the linears shown on ERTS-1 imagery.

6.7.8.9 For example, if the joints do gradually rotate across the Plateau, and, if the joint directions are expressed by linears as is the case in the Catskill Mountain part of the Plateau, a gradual rotation should be demonstratable on an ERTS-1 linear map made at a suitable scale. At the very least, the imagery has again focused attention on some basic ideas about the structural geology and the tectonic framework of New York and Pennsylvania. In addition, the regional geometry of linears provided by ERTS imagery can provide a useful framework for future structural analyses.

7. ERTS-1 CIRCULAR FEATURES IN NEW YORK STATE

7.1 As shown on Figure 9 several circular anomalies have been found in the ERTS-1 imagery: a cluster of three southeast of Rochester, one north of Oneida Lake, and three in the Adirondacks. Those in the Rochester area can be seen in Figure 84 where their upper contacts are indicated by arrows. The three additional circular features visible south and southwest of Oneida Lake in Figure 9 are not anomalous, because the one in the center was identified in U-2 aerial photography as a fortuitous arrangement of urban signatures, and those on either side correspond in large part to lithological contacts along the northern edge of the Alleghany Plateau.

7.2 The three circular features southeast of Rochester are well resolved in the U-2 aerial photograph of Figure 84. Only the central one is well defined in the U-2 photograph, and results from the combination of a scalloped drainage pattern forming the upper and lower parts of the circle, and elongate fields parallel to drumlins forming the sides. The east-west valley that extends across the photograph beneath the scalloped drainage is an ice-marginal drainage of glacial Lake Dawson. The valleys which form the circular anomaly may have a related glacial origin. The small circular anomaly north of Oneida Lake is not visible on airfoto index sheets, so remains unexplained. That located to the north-northeast across the Black River is formed in the main by a possible fortuitous arrangement of two stream courses.

7.3 The most striking of the "circular" features is the much larger one that occurs in the west-central Adirondacks, centering on Cranberry Lake, and here termed the Cranberry Lake anomaly. It is elliptical in outline, and resembles a deformed, spoked wheel. Seven of the radial valleys are arms of Cranberry Lake, at least in part. The long axis of the anomaly measures about 30 km, the short axis about 22 km. In a very general way the feature has a central domal high surrounded by a ring depression, with a lake basin at the center. The maximum topographic relief measured from lake bottom to the higher mountains within the anomaly is about 830 m. In the eastern and southern parts of the feature, a suggestion of concentric rings can be seen in the imagery (Figures 7 and 11). A recently published gravity map of the Adirondacks (Simmons and others, 1973) shows a two milligal simple Bouguer negative gravity anomaly over the Lake basin. Taken together, the above observations suggest the possibility that the Cranberry Lake anomaly may be a cryptoexplosion structure.

7.4 The relationship between the topography of the anomaly and bedrock geology may be seen by comparing Figures 85 and 86. Southwest of Cranberry Lake, the rim depression coincides with the alluvial-filled (Q) Oswegatchie River valley which is cut into hornblende-biotite granitic gneiss (hbg). The strike of foliation in the gneiss differs by 90 degrees on opposite sides of the valley. The rim valley fails to extend northward across the northeast-trending antiform of quartzofeldspathic gneisses represented by units phqs, ffg, and lgr. To the south and east, however, it

follows the Oswegatchie River (Figure 87) until it crosses Bog River Flow to follow the north-northeast-trending topographic lineament past Lake Marian, along Long Tom Mountain, and then directly north through the Grass River Valley which cuts orthogonally across a mass of resistant pyroxene syentic gneiss (ps). North of this, the rim valley merges with the broad lowland area of alluvium north of Cranberry Lake, and loses definition. West of Cranberry Lake and north of the resistant quartzofeldspathic units referred to above, the rim valley corresponds with the narrow belt of alluvium extending northeastward from Benson Mines, transecting bedrock lithology (hbg and metasedimentary rocks, mu) at right angles. The rim valley then disappears again in the same alluvial-filled lowland north of Cranberry Lake.

7.5 In summary, the rim valley parallels bedrock foliation trends along part of its course, transects it along others, and fails to develop at all across an antiform of quartzofeldspathic units in the southwest.

Aeromagnetic trends in the Cranberry Lake anomaly area (unpublished 1:250,000 map of Zietz) show no anomalous deviation from the mapped lithologic trends.

7.6 Of the major radial valleys, Sucker Brook and Sixmile Creek are eroded along a thin metasedimentary unit which defines an open fold. The remainder are probably fracture-controlled inasmuch as they cross the foliation trends of resistant gneisses. Buddington and Leonard (1962, p. 130) suggest that Dead Creek Flow is a probable fault, while noting that "the inquiring geologist cannot reach out his hand and place it on the fault surface of any one of the major faults in the district".

7.7 To date, only three days have been spent investigating the Cranberry Lake anomaly on the ground in a search for criteria indicative of cryptoexplosion structures (e.g. Short, 1968) such as shatter cones, megabreccias or injection breccia veins. Outcrop sites visited are shown on Figure 86. No shatter cones were seen, and no fracturing was observed beyond normal jointing, except in the second road cut west of Cranberry Lake village where the rock is much fractured but lacks evidence of brecciation or displacement. Rocks encountered on the traverse were all crystalline gneisses, mainly granitic.

7.8 Judging from observations at Sudbury (Bray and others, 1966) such lithologies would not be expected to yield good shatter cones, although Dietz (1968, p. 273) indicates that crude but convincing examples have been found in crystalline gneisses at several localities. Quartzite is apparently an ideal lithology for development of shatter cones (Bray and others, 1966). One remote quartzite unit (qt) located between Tomar Mountain and Bog Lake deserves scrutiny.

7.9 Outcrops of hbg exposed along shorelines and on Islands of Cranberry Lake have been examined for abnormal fracturing, with negative results; in most outcrops the granitic gneiss is only moderately jointed. The

Benson Mines open pit located along the western periphyry of the anomaly, has received limited examination, but an exhaustive search for fine-grained lithologies remains to be made.

7.10 An outcrop of diopside-rich calcsilicate rock collected from the metasedimentary rock unit (mu) at the west end of Indian Mountain contains large, kink-banded pyroxene crystals. Kink-banded pyroxene has been reported from the Holleford Crater (Short, 1968) but its presence does not prove shock metamorphism.

7.11 In conclusion, it remains possible that the Cranberry Lake anomaly is a cryptoexplosion feature, but compelling evidence, either field or petrographic, remains to be found. Additional field work and petrographic study needs to be done.

7.12 Beginning 15 km northeast of Cranberry Lake is another roughly circular feature. It measures 30 km in diameter, and is bounded by a narrow valley (Figures 11 and 12a). This feature forms the major part of an irregularly-shaped area which has a topographic and tonal signature clearly different from other parts of the Adirondacks. The area appears in the imagery as a broad depression with sparse, irregularly-scattered hills, suggestive of "broken ground" on a very large scale. The area is, in regional terms, a terrace (the Childwold Terrace of Buddington and Leonard, 1962, p. 8) with valley bottoms having elevations of 1200-1300 feet on the northwest and 1600 feet on the southeast. The scattered hills rise up to a maximum of 400 feet above the valley floor. This physiographic belt has an anomalously high percentage of sand plains and swamps, and the lowest density of bedrock outcrops of any large area in the Adirondacks (see Fisher and others, 1971). The reason for this is not know, and the feature will receive reconnaissance study for cryptoexplosion features. The area does not show any gravity anomaly on the map by Simmons and others (1972).

7.13 Figure 88 is a Stage I map of all circular lines seen on ERTS-1 imagery, independently by two of us (Fakundiny and Isachsen). It is added as an interesting "post script" to this section, without any convictions as to the geological reality or anomaly of the lines.

8. GLACIAL FEATURES OBSERVABLE IN ERTS-1 IMAGERY

8.1 Before discussing glacial features visible on ERTS-1 imagery some observations will be made with reference to winter imagery which has proved to be particularly informative in terms of glacial geology.

8.2 Although there are impressive instances where partial or even total snow cover produces topographic enhancement and advantageously reduces terrain noise (e.g. Wobber, 1972, Gregory, 1972), conventional aerial photography is rarely taken during the winter months because the combination of snow and winter sunlight generally tends to diminish tonal contrasts between different terrain features. Because of the general unavailability of aerial photography taken in the winter months, the first such products seen by the present investigators were the ERTS-1 images taken January 8 and 9, 1973 covering the C and D strips. As expected, snow-covered open fields and lakes appear white, but it was surprising to find that the extensive forests of the Adirondacks, the Tug Hill Plateau, the interfluves of the Allegheny Plateau, and scattered woodlands elsewhere, are dark grey to black in all spectral bands despite a deep ground cover of dry snow (these were the coldest days of the month, the maximum temperature reached in Albany being 7°F). This unusually low albedo characterizes not only the conifer forests of the high peaks area, where it is to be expected, but also the mixed hardwood forests at lower elevations. The effect is not due to faulty photographic processing, because all 15 shades in the grey scale are identifiable. It thus appears that, although in winter at conventional flight elevations such hardwood forests would have a high or intermediate albedo, at the lower resolution of satellite imagery the low reflectance of leafless trees, together with their long winter shadows, dominates the spectral response. The resultant imagery gives the heavily-wooded Adirondack Mountains the appearance of a carved ebony plaque having both lower reflectance levels and lower reflectance contrasts than the imagery of other seasons (compare Figures 7 and 8).

8.3 In terms of geological usefulness, the major advantage of the winter imagery observed at 1:1,000,000 is the supression of terrain noise produced by land use patterns in agricultural areas. This results in the increased detectability of small-scale topographic features. The most notable examples are individual drumlins, which can be identified directly as topographic features rather than indirectly by their control of agricultural land use patterns. These are discussed below.

8.4 Numerous previously-mapped glacial features can be seen on ERTS-1 imagery at 1:1,000,000. These include more than ten drumlin fields, drumlinoid glacial streamline forms, glacial lake sand plains and deltaic deposits, segments of glacial lake shorelines, ice-marginal drainage channels, and end moraines (Figure 89). No new glacial features have been identified. The search for mapped glacial features on ERTS imagery is greatly facilitated by using a scale-changing device such as the Bausch and Lomb Zoom Transferscope, Model ZT-4.

8.5 Several drumlin fields can be located on the summer and fall imagery due to the topographic effect of drumlin topography on land use pattern, but most are obscured. However, when snow cover obliterates land use patterns and the low sun angle of winter months highlights their relief, drumlin fields, and even individual drumlins, can readily be identified. Indeed, the stoss and lee sides of drumlins can be distinguished in some cases. Good examples can be seen south of the Mohawk River (1169-15123, 1170-15182) and in the Finger Lakes region (1243-15244). In the latter area, however, snow cover is less complete, and field patterns tend to camouflage the topography. For this reason only portions of the extensive drumlin fields of the Finger Lakes region can be identified, and of an estimated 10,000 drumlins in central New York State (Flint, 1957) only 228 could be recognized. South of the Mohawk River, 316 drumlins were counted. On the ground, the drumlins measure 2 km in length, 400 m in width and 25 m in height. It appears likely that optimum winter imagery could be "calibrated" using topographic map information, and then used to make a rapid, relatively accurate and inexpensive inventory of drumlins in any region of the State.

8.6 Numerous glacial features are visible east of Lake Ontario. On the Tug Hill Plateau, glacial streamline forms or drumlinoids with northwest axes are extensively developed. In contrast to the drumlin fields mentioned above, these are best shown on the fall imagery (1080-15180). This is understandable because the Plateau is evenly forested, rather than being camouflaged by agricultural patterns. On a topographic map, the drumlinoids average 2-4 km in length, about 80 m in width, and 15 m in height. No published data are available to indicate to what extent they are depositional landforms or erosional features in bedrock.

8.7 A small drumlin field not apparent in earlier imagery, can be seen in the winter imagery on the northwest slope of the Tug Hill Plateau (1170-15182, 1170-15175). Also visible in the winter image are several glacial lake drainage channels which roughly parallel the contours around the north slope of the Plateau. Although these could be seen to some extent in the fall imagery (1080-15180) they are enhanced in the winter imagery due to the contrast between shadowed channels (accentuated by low sun angle) and surrounding snow. On the ground they are 2-17 km long, 200-700 m wide, and 20-30 m deep.

8.8 Comparison of the imagery with existing glacial maps of the Tug Hill region (Stewart, 1958; Forster, 1971) revealed no correlation. Farther north, in the St. Lawrence Lowland, image 1080-15174 was compared with the maps of MacClintoch and Stewart (1965), and a rough correlation was noted between the extensive areas of intermediate grey density located west of Malone, and areas mapped as peat and muck (swamp). An even better correlation was found when the imagery was compared with the woodland overprint on the 1:250,000 topographic map of the USGS (N118-11, 1961) — another example of a geological signature linked to land use.

8.9 In the Central Highlands of the Adirondacks, numerous segments of eskers show up in the imagery as narrow ridges bounded by bodies of water. On the ground these are 200-400 m wide and 15-25 m high.

8.10 At the northernmost part of the State, the Covey Hill drainage channels for glacial Lake Iroquois can be recognized on image 1079-15115. On the ground, these channels are 2-4 km long, approximately 300 m wide, and 20 m deep. On the same image can be seen an area south of Plattsburg which has a distinct, uniform, tonal density. This area was found to correspond quite closely with that of a sand plain mapped by Denny (1967) as a deposit formed in glacial Lake Vermont.

8.11 Farther south, two thirds of the distance to Albany, is a tonally distinct grey area, the borders of which were found to have a fair to excellent correspondence with the boundary of stratified drift and deltaic deposits associated with glacial Lake Albany, as shown on an unpublished 1:250,000 glacial map of the area prepared by R. Dineen of the State Geological Survey.

8.12 In the southeastern part of the State, a series of moraines mapped by Connally and Sirkin (1967) in the Wallkill and Hudson Valleys were searched for on both fall (1079-15124) and winter (1205-15132) imagery. On neither image was any indication seen for these moraines.

8.13 Imagery of Long Island (1096-15074) was compared with a map of the Harbor Hill and Rankankam moraines using a direct overlay. A few short segments of these moraines were detected because of different land use on the moraine compared with surrounding areas.

8.14 Using a 1:1,000,000 enlargement of the Glacial Map of the United States east of the Rocky Mountains (Flint et al., 1959) imagery for New Jersey and Pennsylvania (1205-15135, 1170-15184, 1243-15251) was searched for end moraines and other glacial features. As shown on Figure 89 only a few short segments of moraine are visible.

8.15 For the western part of New York State the imagery (1243-15244, 1243-15251, 1244-15303, 1046-15292, 1244-15305) was compared with a compilation of moraines and beach ridges prepared by Muller, 1972. Perhaps because of land use camouflage and low relief of these ridges (10 m), only small sections of a limited number of each were seen. Moraines searched for included the Valley Heads, Olean, Almond, Arkport, Clymer, Findley Lake, Gowanda, Hamburg, Marilla, Alden, Buffalo, Niagara Falls, Batavia, Barre, Albion, Colton, Geneva, and Waterloo. Those sections seen are shown on Figure 89. Glacial lake shorelines of the following lakes were also searched for: Whittlesey, Warren, and Iroquois; only three sections of the Iroquois beach ridge were found, one south and one west of Rochester, and a longer section east of Lake Ontario.

8.16 The density distribution of linears in the State appears to be related to the positions of the Valley Heads and Kent Moraines, and to drainage divides (Figure 90). Influencing factors may be a greater thickness of glacial till and outwash deposits north of the moraines and divide, as well as lower relief.

8.17 Because one of us (Fakundiny) has a particular familiarity with the surficial geology of the western part of the State it was decided, despite the inferior quality of the best available imagery at the time of the study (images 1027-15322, 1046-15292, 1080-15180) to attempt an evaluation of tonal variations. Comparisons made with generalized soils maps at 1:1,000,000 of Arnold and others (1967) and of the Genesee/Finger Lakes Regional Planning Board (1970) show only a 10 percent correspondence of soils contacts and tonal boundaries, and that correspondence applies mainly to valley bottoms; it thus appears to be principally a correlation with topography.

9. ERTS-1 AND MAN-MADE FEATURES

No attempt was made to catalog the major works of man which can be seen on ERTS imagery. The more obvious ones, in some places confused with linears, include railroads and abandoned railroad beds, the St. Lawrence Seaway, highways, canals and transmission lines. Point data include major airports and golf courses (which have a very diagnostic high albedo in the near infrared imagery of October 10th, image number (1079-15124), as well as a number of mines and dry tailings ponds in the Adirondacks (Figure 12): the ilmenite-magnetite open pit of National Lead Industries at Tahawus is very dark grey on band 6, black on band 7 and indistinguishable on band 5; the Benson Mines open-pit magnetite mine at Star Lake appears dark grey on band 7, white on bands 4 and 5 and an indistinguishable medium-grey on band 6; in the Edwards-Balmat-Talcville area, tailings ponds appear white on bands 4 and 5 but are an indistinguishable light grey on bands 6 and 7.

10. ERTS-1 AND STORM DAMAGE ANALYSIS, LAKE ONTARIO

10.1 Introduction

10.1.1 Although outside the main objectives of this study, fascination with the extensiveness of sediment plumes along the south shore of Lake Ontario shown on ERTS-1 imagery of 23Mar73 (Figure 91), but not on earlier imagery, led us to newspaper accounts of the storm activity that was the cause, and to a brief investigation of the utility of ERTS-1 for studying storm effects on the Great Lakes. The total time involved in analysis of the imagery was only two hours.

10.1.2 On March 17, 1973 according to The Rochester Democrat Chronicle of the succeeding two days, 10 to 15 foot waves, caused by 50 to 60 mile-per-hour winds, damaged hundreds of homes along the Lake Ontario shoreline and forced evacuation of many families. Accompanying heavy rain caused lakeshore flooding along a 33-mile stretch from Webster to Hamlin, which includes Rochester. The shoreline erosion was the most severe in 20 years, and damage was estimated at more than 10 million dollars.

10.2 Dispersal Patterns of Suspended Particles Caused by the Storm

10.2.1 Two effects of the storm were analyzed in the imagery, namely, shoreline erosion and the dispersal pattern of suspended particles. The sediment plumes were studied using bands 5 and 7 of 23Mar73 (image no. 1243-15244). Band 5 was projected in red and band 7 in blue, using an SDC viewer.

10.2.2 Figure 91 illustrates the shape and magnitude of dispersed sediment. Definite longshore transport of sediment to the east can be seen clearly, and at the eastern end of the lake a curl extends some 60 km offshore. Complex currents around the mouth of the Genesee River at the left side of the photograph are evidenced by the westward hook shape of the river sediment from the point at which it enters the Lake to approximately 7 km offshore.

10.2.3 Two months after the storm, the hook shape was no longer apparent but the Genesee River plume still extended about 7 km out from the shore, (image no. 1297-15243 of 16May73). Two months later still, however, it had returned to the normal 1 km offshore (image no. 1351-15230 of 9Jul73). For unknown reasons we received only one 70 mm image, band 7, of the intermediate orbit (3June73), so cannot determine whether or not the plume had diminished to normal dimensions by that time.

10.3 Shoreline Erosion Produced by the Storm

10.3.1 The major erosional effects of the storm on the Lake Ontario shoreline were identified through multi-temporal study of band 7 for 19Aug72 (red filtered) and 23Mar73 (unfiltered), using an SDC Viewer. A comparison was also made using a Zoom Transferscope. Either instrument would have been satisfactory for the study.

10.3.2 The following effects were noted:

1. About 20 km west of the mouth of the Genesee River, the west end of an offshore bar appears to have been either eroded or inundated by storm waters, and the remainder appears to have been narrowed (compare Figures 92 and 93). Pronounced flooding of bays can also be seen in this area.

2. In the eastern third of Figures 92 and 93 (area east of Sodus Bay) several bay-mouth bars are either narrowed or no longer visible, flooding has occurred in a number of places, and a bay appears to have been created which does not appear on the 19Aug72 image.

3. In the later imagery of 9Jul73, which shows that water elevations have largely returned to the 19Aug72 levels, the western end of the pre-storm offshore bar west of the Genesee River is still not visible, indicating that it was not merely inundated, but eroded by the storm.

10.3.3 This very brief study serves to illustrate the potential of ERTS-1 imagery for analyzing erosional and transportational processes along the shorelines of major lakes.

11. ERTS-1 AND SEISMICITY IN NEW YORK STATE

11.1 One of the most intensively studied seismic areas in the world which is located entirely within a continental plate (rather than at its margin) is Blue Mountain Lake in the central Adirondacks. It can be seen in Figure 11 as an elliptical black spot, about 5 km long in an east-west direction, located approximately 15 km south of the center of the Adirondacks. It was here, during the summer of 1973, that earthquake prediction was successfully achieved (Aggarwal and others, 1973). Another reason for a continuing interest in the seismicity of this area (as well as several others within the North American plate), is its possible contribution to an understanding of the driving forces for plate motion. For these reasons, and because of the potential value of an ERTS-enhanced fracture map for relating seismicity and tectonics, it was decided to search the imagery, U-2 photography, and the epicenter area itself for relevant fracture data.

11.2 Moderate size earthquakes (up to magnitude 3.6) and many microseisms were recorded at Blue Mountain Lake during July and August 1971 by portable seismographs which were installed after two events had occurred on May 23, 1971 (Sbar and others, 1972). Quakes of similar magnitude were recorded in this area again in August 1973 by Lamont-Doherty Geological Observatory and the Geological Survey of the New York State Museum and Science Service (Aggarwal, 1973). Shallow earthquake foci (<2.0 km) were confined to a tabular zone trending

11.3 N12W and dipping 25 degrees to the east, while the deeper quakes (2-3.5 km) occurred on a surface striking N31E and dipping 59° east. First motion studies showed both focal mechanisms to be thrust faulting, in agreement with the horizontal east-west compressive stresses known to characterize the eastern United States (Sbar and others, 1973). A strong motion instrument measurement showed a surprisingly high value of 0.034g to be associated with a 2.5 magnitude (M_L) earthquake.

11.4 The deeper quakes occur along a surface which strikes parallel to the direction of the prominent northeast faulting in the eastern Adirondacks as shown on the map of linears (Figure 12) and the rose diagram of Figure 16; the tabular zone of shallower quakes on the other hand, trends in the direction of less prominent north-northwest fractures. A detailed ground search in the epicenter area disclosed only joints, but no evidence of fresh movement along their surfaces. Thirty-four joints were seen and measured. Nearly all dip more steeply than 80°. Those with strikes in the northeast quadrant show a very broad spread without any maxima. In the northwestern quadrant, however, strikes are concentrated in the sector N15-30W. Thus, for whatever it may be worth at this early stage, the strike of the steeply-dipping fault surface of the deeper quakes parallels prominent Adirondack fault trends which also dip steeply, whereas that of the shallower quakes lies near one end of the N15-40W trend of local jointing.

11.5 No linears could be found in the Blue Mountain epicenter area on either the ERTS-1 imagery (even after the computer image processing described in section 2) or in U-2 color infrared transparencies. Another confusing feature of the Blue Mountain seismicity is its occurrence west of the region of closely-spaced faults and topographic lineaments (Figure 12). A possible explanation may be that the fault surfaces in the eastern Adirondacks are steep to vertical, and hence do not provide suitably oriented shear surfaces for reactivation by the regional horizontal east-west compressive stresses in the region.

11.6 An interesting sidelight of the field study may be worth mentioning. Seven distinct earthquakes were heard emmanating from beneath a swamp which centers on the epicenter area. The sounds emitted for individual quakes were a low, resonating, "thong", "kathong", or "kong". A subsequent check of the seismic records showed that the timing of these sounds correspond to the occurrence of earthquakes of -1 intensity on the Richter scale.

11.7 Attempts to relate historical seismic events in the State as a whole to an ERTS-enhanced fracture map have been unsuccessful to date owing to the substantial radius of uncertainty in locating epicenters.

11.8 The near future holds considerable promise for such seismo-tectonic analysis, however, because of a growing interest in seismic monitoring in the northeast. This has come about both as a result of increasing scientific interest in intra-plate tectonics, and the need for a much expanded data base for evaluating safety factors associated with the siting of nuclear power plants.

12. SUMMARY AND CONCLUSIONS

12.1 ERTS-1 side-illuminated imagery, combined with known ground conditions, well displays the amazingly detailed control of topography by structure. The imagery permits mapping of most of the major faults and topographic lineaments previously known, as well as the boundaries of physiographic, geologic, and tectonic provinces. The greatest contribution of new data in New York State is in the field of regional tectonic analyses, more especially in the delineation of new linear features, many of which have been verified on the ground, and circular features which remain problematical. All ERTS-1 linears confirmed to data have been topographic features on the ground, although many of these appear on the imagery as tonal linears without relief, or as combinations of tonal and topographic features. In general, the linears extend across physiographic, geologic and tectonic province boundaries, although their photogeologic expression within a given province is quite distinctive (i.e. topographic vs. tonal expression, length, straightness or concavity, density, spacing, and cross-cutting relationships).

12.2 After experimentation with a number of photographic, optical and digital enhancement techniques, we conclude that, for the humid northeast, linear and circular features are most advantageously "mapped" using false color composite transparencies of the best fall imagery, supplemented by the best winter imagery. Almost fully as satisfactory, however, is the utilization of infrared imagery (band 7) for fall and winter.

12.3 Limited experimentation with the NASA/GSFC program for image processing (IDAM) suggest that some additional detail may be recovered on the shaded sides of mountains using the program sequence for contrast stretching, color compositing, and enlarging.

12.4 Multi-scale analysis of the same imagery may be advantageous, because what defines a topographic linear can be very much a matter of the scale at which viewed, and the geological province involved. Not only may the character of the linear elements differ, but the amount of linear information as well. For the long, relatively high-relief linears in the Adirondacks, the 1:500,000 imagery proved to be the smallest scale for deriving maximum linear information. In the Allegheny Plateau, however, with its dendritic drainage patterns and many short linears, the 1:1,000,000 imagery showed the greatest density of linears..

12.5 Shaded relief topographic maps at the same scales as ERTS-1 imagery were found to provide less definition of linear characteristics than could be seen in the imagery.

12.6 In the Adirondacks, the use of low level aerial observation and photography, coupled with ground investigation, has resulted in the elimination of about five percent of the original number of ERTS-1 linear features remaining after the exclusion of those which are either man-caused or lithologically controlled. In addition, it has led to the discovery of a system of intersecting orthogonal and oblique fractures which cut the relatively homogeneous and massive Marcy Massif metanorthosite. These, together with the previously-mapped and new ERTS-1 topographic lineaments will hopefully provide enough data, after ground study, to permit a regional basement stress analysis.

12.7 Ground study of ERTS-1 anomalies in the Adirondacks indicates that: 1) outcrops are even more rare than expected along the traces of topographic lineaments, indicating that for the detection and evaluation of some fracture systems, the representation on ERTS imagery may be the best data obtainable, short of trenching or other excavation; 2) fault breccias are found along some of the north-northeast and northwest trending lineaments, 3) chloritization and slickensiding, without brecciation, were found along one east-west lineament, and 4) closely-spaced joints and a zone of plastic shear was found along another east-west lineament.

12.8 A comparison of linears on fall and winter imagery covering southeastern New York State showed that the majority of linears are observable on the fall imagery, but some additional short linears ($\geq$4 km) are seen on the winter imagery. Tonal linears are more readily seen on the fall imagery, and many of these are expressed as topographic linears on the winter imagery.

12.9 Field work in the northern Catskills shows a fairly good correspondence between the directions of linear valleys and master joint sets. If subsequent field work confirms this relationship across the Allegheny Plateau, ERTS-1 imagery will prove to be the most economical method available for mapping major joint sets over large regions.

12.10 Field study of Stony Clove, located in one of the several north-northeast trending topographic lineaments which parallel the straight eastern terminus of the Catskill Mountains known as the Wall of Manitou, show it to be controlled by a system of conjugate joints. These strike parallel to the lineament, and dip in opposite directions to make an acute angle which is bisected by a vertical plane. The lineaments are interpreted as the traces of upward-propogated vertical movement on reactivated basement faults. This would provide the vertical maximum principal stress implied by the conjugate joints. This interpretation is supported by the fact that the entire Stony Clove set of lineaments is aligned with lineaments of similar strike and spacing in basement rocks of the eastern Aidrondacks.

12.11 Analogous conjugate fractures in plan view are suggested by the ERTS linear patterns in parts of the Allegheny Plateau. These will be investigated to test the hypothesis that they may be surface manifestations of strike slip movement in the basement.

12.12 It is suggested that many of the north-northeast faults and topographic lineaments which appear to terminate at the southern border of the Adirondacks, actually extend across the Mohawk Valley and southward beneath the Allegheny Plateau. This interpretation is supported by the fact that known fracture systems in the Adirondacks can be seen to extend as linears into other parts of New York and Pennsylvania where the basement is deeply buried. This relationship is observable on both ERTS-1 and NIMBUS-I imagery.

12.13 Based on field work to date, we believe that the majority (and perhaps the overwhelming majority) of ERTS-1 linears are real earth features, and almost all have topographic expression on the ground.

12.14 The new linear information will, in the short turn, be incorporated into a regional tectonic synthesis now in progress. In the long run, because of its shear magnitude it will doubtless occupy the attention of numerous field geologists for some time to come. It is anticipated that the ERTS-enhanced fracture map of the State now in preparation will prove to be invaluable in seismic studies now underway by Lamont-Doherty Geological Observatory and the New York State Geological Survey. At present, virtually nothing is known about the relationship between seismicity and tectonics in New York. Theoretical questions relating to seismicity within the North American Plate and to the driving mechanisms of large lithospheric plates are involved. The map will also have application to practical questions relating to nuclear power plant siting and safety design, solution mining of salt deposits, high pressure pumping of liquid wastes into deep disposal wells (both of the two preceding can trigger earthquakes), structural control of oil and gas accumulation, ground water migration, highway site selection, foundation engineering, and others.

12.15 A number of potentially anomalous circular features seen in the imagery were explained through the use of U-2 aerial photography. An elliptical anomaly with a radial system of valleys, the Cranberry Lake anomaly, however, will require additional investigation.

12.16 The variable distribution of linears across the Allegheny Plateau and the Erie-Ontario Lowlands is strongly correlated with the position of the Valley Heads and Kent Moraines and drainage divides.

12.17 Many previously mapped glacial landforms were observed on the ERTS-1 imagery, but no new ones were found.

12.18 A brief investigation of ERTS-1 imagery of Lake Ontario taken before and after a major storm showed the usefulness of the imagery in detecting shoreline changes and sediment dispersal patterns.

REFERENCES

Aggarwal, Y.P., Sykes, L.R., Armbruster, J. and Sbar, M.L. 1973. Premonitory changes in seismic velocities and prediction of earthquakes. Nature, 241: 5385:101-104.

Anderson, R.K. 1968. Picture of the month, view of snow-covered northeastern United States and a developing east coast storm. Monthly Weather Review, 96: 4:260-261.

Arnold, R.W. and eleven others. 1967. General soils map of Five-County area around City of Syracuse in New York State. Extension Publication of the New York State College of Agriculture at Cornell University, Ithaca, New York.

Boyer, R. and McQueen, J.F. 1964. Comparison of mapped rock fractures and airphoto linear features. Photogrammetric Engineering, 30:630-634.

Brace, W.F. and Bombolakis, 1963. A note on brittle crack growth in compression. J. Geophysical Research, 68:12:3709.

Bray, J.G. and others. 1966. Shatter cones at Sudbury. Jour. Geol. 74:243-245.

Broughton, J.G., Fisher, D.W., Isachsen, Y.W. and Rickard, L.V. 1966. Geology of New York, a short account. N.Y.S. Mus. and Sci. Service Map Educ. Leaflet 20. 49 pp. and colored map.

Buddington, A.F. and Leonard, B.F. 1962. Regional geology of the St. Lawrence County magnetite district northwest Adirondacks, New York. U.S. Geological Survey Prof. Paper 376, 145 pp.

Chadwick, G.H. 1944. Geology of the Catskill and Kaaterskill Quadrangles. N.Y.S. Mus. Bull. 336, 251 pp.

Cline, M.G. 1961. Soil association map of New York State. Extension Publication of the New York State College of Agriculture at Cornell University, Ithaca, New York.

Conklin, H.E. and Linton, R.E. 1969. The nature and distribution of farming in New York State. State of New York, Office of Planning Coordination.

Connally, G.G. and Sirkin, L.A. 1967. The Pleistocene Geology of the Wallkill Valley. New York State Geological Association, 39th Annual Meeting Guidebook, pp. A1-A16.

Dennis, J.G. ed. 1967. International Tectonic dictionary - English terminology. Am. Association Petroleum Geologists Mem. 7, 196 pp.

Denny, C.S. 1967. Surficial geologic map of the Dannemora Quadrangle and part of the Plattsburgh Quadrangle, New York. U.S. Geological Survey Map GQ-635.

Dietz, R.S. 1968. Shatter Cones in Cryptoexplosion Structures in Shock Metamorphism of Natural Materials, B.M. French and N.M. Short, editors. Mono Book Corporation, Baltimore, pp. 267-285.

Fakundiny, R.H. 1974. Photogeologic features of ERTS-I imagery in southeastern New York; a preliminary phase of regional tectonic analysis. Abstracts with Programs, Northeast Section Annual Meeting, Geol. Soc. Amer., p. 24-25.

Fisher, D.W., Isachsen Y.W., Rickard, L.V., Broughton, J.G. and Offield, T.W. 1961. Geologic Map of New York. New York State Mus. and Science Service Map and Chart Series No. 5.

Fisher, D.W., Isachsen, Y.W. and Rickard, L.V. 1971. Geologic Map of New York 1970, and Generalized Tectonic-Metamorphic Map of New York, 1971. New York State Mus. and Sci. Service Map and Chart Series No. 15.

Flint, R.F., Colton, R.B., Goldthwait, R.P., and Willman, H.B. 1959. Glacial map of the United States East of the Rocky Mountains. Geol. Soc. Amer.

Forster, S.W. 1971. Pleistocene Geology of the Carthage 15-minute Quadrangle. New York State: unpublished dissertation; Syracuse University, 129 pp.

Genesee/Finger Lakes Regional Planning Board. 1970. Regional soils inventory: classification and analysis. Genesee/Finger Lakes Regional Planning Board Technical Studies Series, Rept. No. 6, 39 pp.

Goetz, A.F.H., Billingsby, F.C., Elston, D., Lucchitta, I., and Schoemaker, E.M. 1973. Preliminary geologic investigations in the Colorado Plateau using enhanced ERTS images. In Symposium on significant results obtained from the Earth Resources Technology Satellite-1. NASA SP-327, p. 403-411.

Gregory, A.F. 1972. Preliminary assessment of geological applications of ERTS-I imagery for selected areas in the Canadian arctic. Symposium on significant results obtained from ERTS-I abstracts. NASA/GSFC, p. 37.

Gross, W.H. 1951. A statistical study of topographic linears and bedrock structures. Geol. Assoc. Canada Proc. 4:77-87.

Heath, R.C. 1964. Ground Water in New York State of New York Conservation Department, Water Resources Commission, Bull., GW-51, Albany, New York.

Hobbs, W.H. 1904a. Lineaments of the Atlantic border region. Geol. Soc. Amer. Bull. 15:483-506.

Hobbs, W.H. 1904b. Examples of joint-controlled drainage from Wisconsin and New York. Jour. Geol. 12:363-374.

Hoppin, R.A. 1973. Utilizing ERTS-A imagery for tectonic analysis through study of the Bighorn Mountain Region. NASA earth resources survey program weekly abstracts, U.S. Tech. Information Service, CR 131210, E10420, 15Mar73, 7 pp.

Isachsen, Y.W. and Moxham, R.L. 1968. Chemical variations in megacrysts from two vertical sections in the main Adirondack metanorthosite massif. in Y.W. Isachsen, ed., Origin of anorthosite and related rocks. N.Y.S. Mus. and Sci. Service Mem. 18, pp. 225-265.

Isachsen, Y.W. and Fisher, D.W. 1970. Geologic Map of New York, Adirondack Sheet. N.Y.S. Mus. and Sci. Service Map and Chart Series No. 15.

Isachsen, Y.W. 1973a. Geological features and spectral anomalies in satellite imagery of the Adirondack Mountain region. Abstracts with Program, Northeast Section Annual Meeting, Geol. Soc. Amer., p. 180-181.

Isachsen, Y.W. 1973b. Spectral geological content of ERTS-I imagery over a variety of geological terranes in New York State. in Anson, A., ed., Symposium proceedings, management and utilization of remote sensing data. Amer. Soc. Photogrammetry, p. 342-363.

Isachsen, Y.W., Fakundiny, R.H. and Forster, S.W. 1973. Evaluation of ERTS-I imagery for geological sensing over the diverse geological terranes of New York State, in Symposium on significant results obtained from the Earth Resources Technology Satellite-1. NASA SP-327, p. 223-230.

Isachsen, Y.W., Fakundiny, R.H. and Forster, S.W. 1974a. Evaluation of ERTS imagery for spectral geological mapping in diverse terranes of New York State. NASA, in press.

Isachsen, Y.W., Fakundiny, R.H. and Forster, S.W. 1974b. Analysis of ERTS-I linear features in New York State. U.S. Technical Information Service E74-10264, 63 pp.

Isachsen, Y.W. 1974. Utilization of ERTS-I imagery in a tectonic synthesis of New York State. Abstracts with Program, Northeast Section Annual Meeting. Geol. Soc. Amer. p. 40.

Lattman, L.H. 1958. Techniques of mapping geologic fracture traces and lineaments on aerial photographs. Photogrammetric Engineering, 24:568-572.

Lattman, L.H. and Nickelsen, R.P. 1958. Photogeologic fracture trace mapping in Appalachian Plateau. Amer. Assoc. Petroleum Geologists. 42:2238-2245.

MacClintock, P. and Stewart, D. 1965. Pleistocene geology of the St. Lawrence Lowland, N.Y.S. Mus. and Sci. Service Bull. 394, 152 pp.

MacDonald, H.C., Kirk, T.N., Dellwig, L.F. and Lewis, A.J. 1969. The influence of radar look-direction on the detection of selected geological features. Proceedings of the 6th International Symposium on Remote Sensing of the Environment. Univ. of Mich., pp. 603-615.

Muller, E.H. 1972. Moraines of Western New York. unpublished map.

Nickelsen, R.P. and Hough, V.D. 1967. Jointing in the Appalachian Plateau of Pennsylvania. Geol. Soc. Amer. Bull. v. 78, p. 609-629.

Nickelsen, R.P. and Hough, V.D. 1969. Jointing in south-central New York: Reply, Geol. Soc. Amer. Bull. 80:923-926.

Page, R.A., Molnar, P.H. and Oliver, J. 1968. Seismicity in the vicinity of the Ramapo Fault, New Jersey-New York. Bull. Seism. Soc. Amer. 58:681-687.

Parker, J.M. 1942. Regional systematic jointing in slightly deformed sedimentary rocks. Geol. Soc. Amer. Bull., v. 53, p. 381-408.

Parker, J.M., III. 1969. Jointing in south-central New York: Discussion, Geol. Soc. Amer. Bull. 80:919-922.

Powell, C.W., Copeland, C.W. and Drahovzal, J.A. 1970. Delineation of linear features and application to reservoir engineering using Apollo multispectral photography. Univ. of Alabama Information Series 41, Univ. Alabama, 37 pp.

Price, N.J. 1966. Fault and joint development in brittle and semi-brittle rocks. Oxford, Pergamon.

Rickard, L.V. 1973. Stratigraphy and structure of the subsurface Cambrian and Ordovician Carbonates of New York. New York State Mus. and Science Service Map and Chart Series no. 13, 25 pp. and 19 plates.

Sbar, M.L., Armbruster, J., and Aggarwal, Y.P. 1972. The Adirondack New York, earthquake swarm of 1971 and tectonic implications. Bull. Seismol. Soc. Amer. 62:5:1303-1317.

Schmitt, H.A. 1966. The porphyry cooper deposits in their regional setting. in S.R. Titley and C.L. Hicks, eds., Geology of the porphyry cooper deposits, southwestern North America, Univ. of Arizona, p. 17-33.

Schultz, P.H. and Ingerson, F.E. 1973. Martian lineaments from Mariner 6 and 7 images. J. Geophys. Res. 78:35:8415-8427.

Short, N. and Bunch, T.E. 1968. A Worldwide Inventory of Features Characteristic of Rocks Associated with presumed Meteorite Impact Structures. in Shock Metamorphism of Natural Materials, B.M. French and N.M. Short, editors. Mono Book Corporation, Baltimore, pp. 267-285.

Short, N. 1973. View from 570 miles, Geotimes, May 1973, pp. 16-20.

Simmons, G. and Diment, W.H. 1972. Simple Bouguer anomaly map of northern New York. N.Y.S. Mus. and Sci. Service Map and Chart Series No. 17A.

Stewart, D.P. 1958. Pleistocene Geology of the Watertown and Sackets Harbor Quadrangles, New York. N.Y.S. Mus. and Sci. Service Bull., 369, 79 pp.

Stout, N. 1958. Atlas of forestry in New York. State University College of Forestry at Syracuse University. Bull. 41.

Suter, H.M. 1904. Forest fires in the Adirondacks in 1903. U.S. Agriculture Department, Bureau of Forestry, Circular no. 26, 15 pp.

Taggart, C.I. 1965. Interpretation of geological features on a satellite photograph. Nature v. 207, no. 4996, pp. 513-514.

Vincent, R.K. 1973. Ratio maps of iron ore deposits, Atlantic City District, Wyoming. in Symposium on significant results obtained from Earth Resources Technology Satellite-1 NASA SP-327, p. 379-386.

Wise, D.V. 1969. Pseudo-radar topographic shadowing for detection of sub-continental sized fracture systems. Proceedings of the 6th International Symposium on Remote Sensing of the Environment, Univ. of Mich., pp. 603-615.

Wobber, F.J. 1972. Geological exploitation of satellite imagery using snow enhancement techniques XXIV. Int. Geol. Congress, Section 9, p. 6.

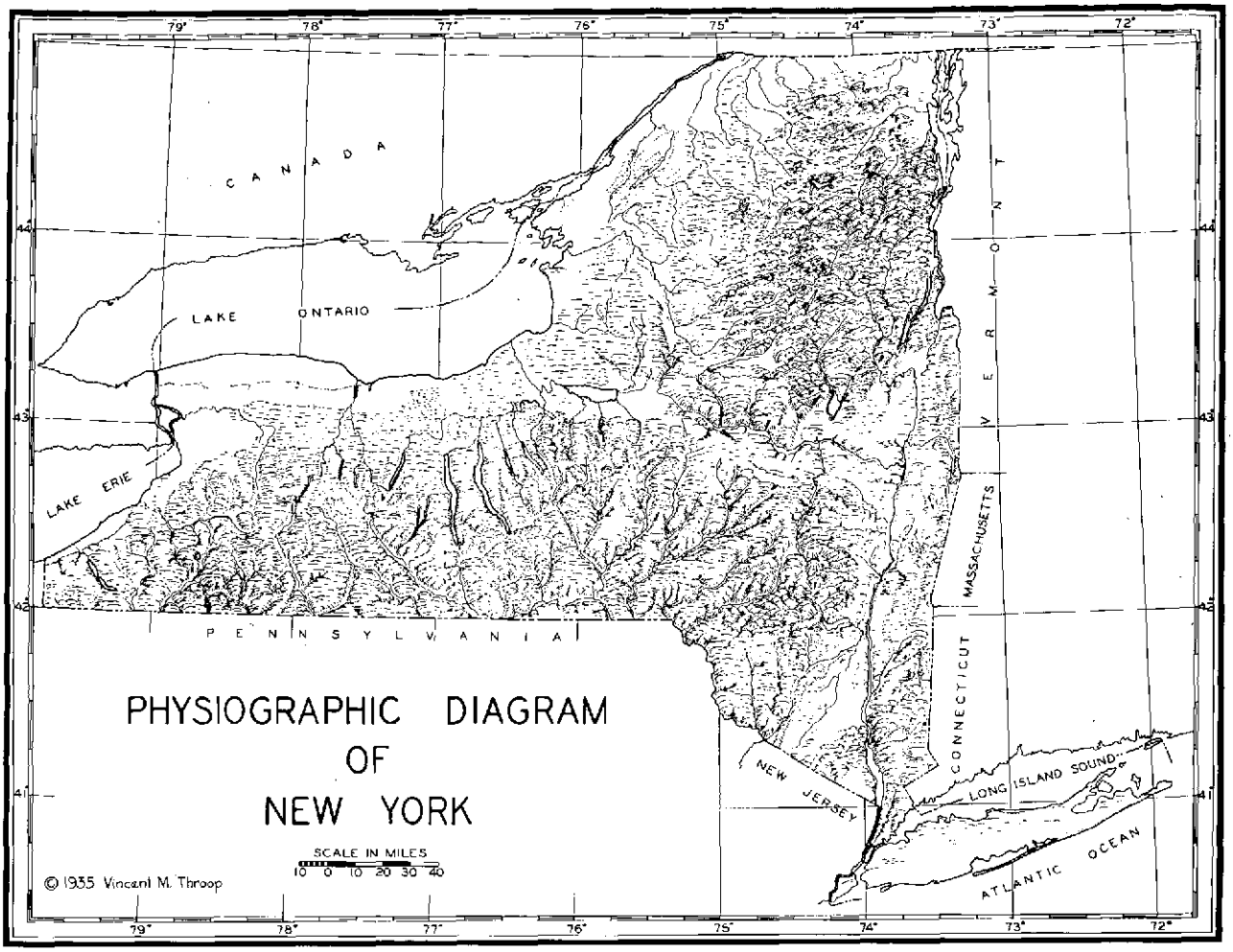

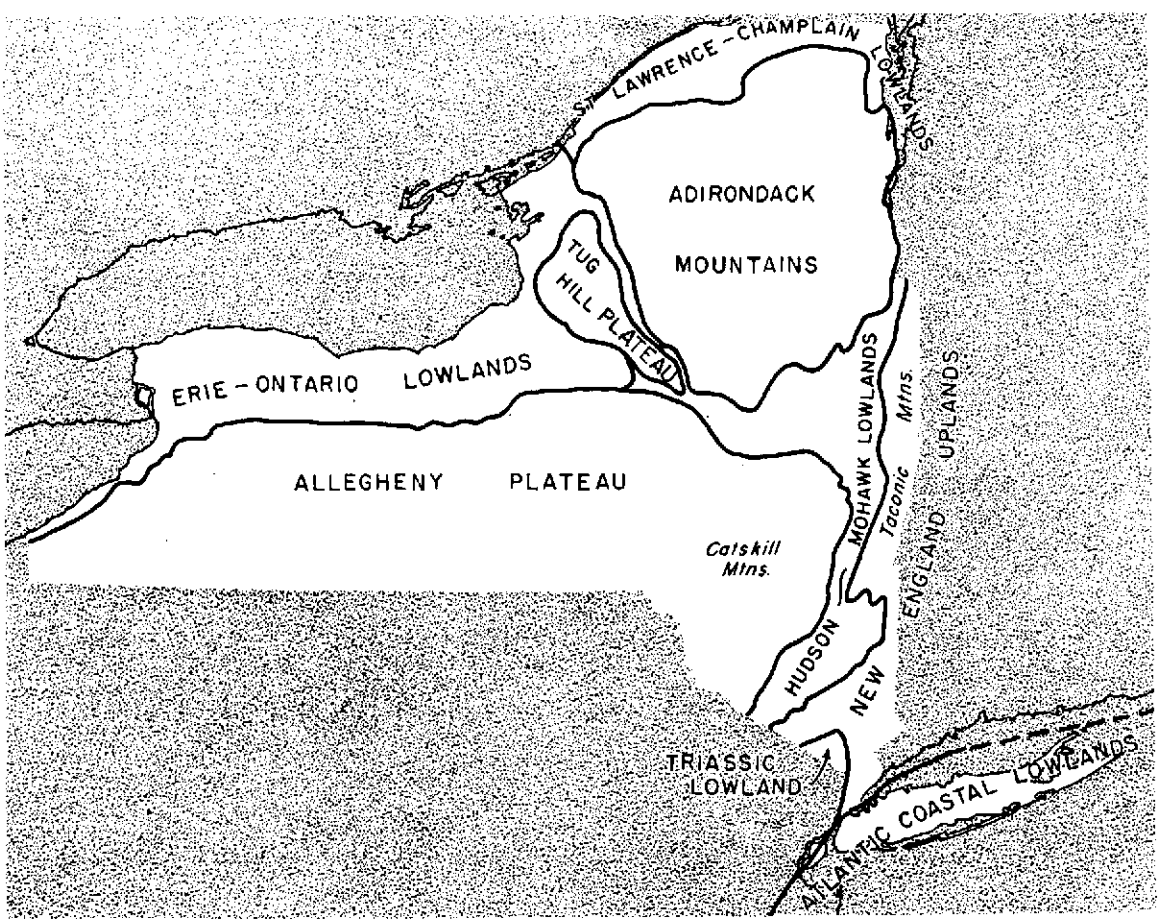

Figure 1. Physiographic subdivisions of New York State. Lower diagram after Broughton and others, 1966.

gure 2.

GENERALIZED BEDROCK GEOLOGY OF NEW YORK STATE

COMPILED BY
GEOLOGICAL SURVEY
OF THE
NEW YORK STATE MUSEUM AND SCIENCE SERVICE
1972

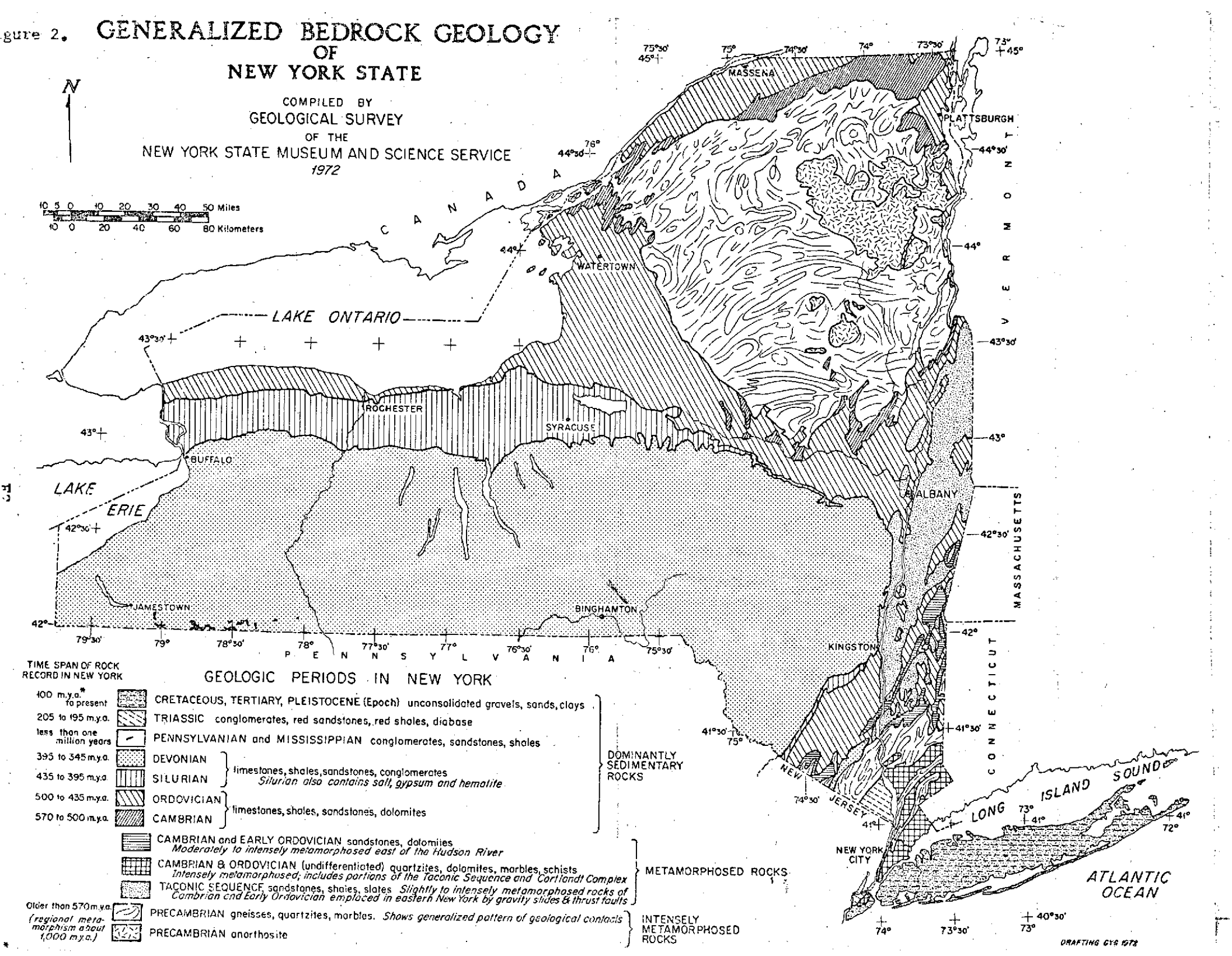

TIME SPAN OF ROCK RECORD IN NEW YORK

GEOLOGIC PERIODS IN NEW YORK

- 100 m.y.a.* to present — CRETACEOUS, TERTIARY, PLEISTOCENE (Epoch) unconsolidated gravels, sands, clays
- 205 to 195 m.y.a. — TRIASSIC conglomerates, red sandstones, red shales, diabase
- less than one million years — PENNSYLVANIAN and MISSISSIPPIAN conglomerates, sandstones, shales
- 395 to 345 m.y.a. — DEVONIAN
- 435 to 395 m.y.a. — SILURIAN
  - limestones, shales, sandstones, conglomerates. *Silurian also contains salt, gypsum and hematite*
- 500 to 435 m.y.a. — ORDOVICIAN
- 570 to 500 m.y.a. — CAMBRIAN
  - limestones, shales, sandstones, dolomites

DOMINANTLY SEDIMENTARY ROCKS

METAMORPHOSED ROCKS

- CAMBRIAN and EARLY ORDOVICIAN sandstones, dolomites. *Moderately to intensely metamorphosed east of the Hudson River*
- CAMBRIAN & ORDOVICIAN (undifferentiated) quartzites, dolomites, marbles, schists. *Intensely metamorphosed; includes portions of the Taconic Sequence and Cortlandt Complex*
- TACONIC SEQUENCE sandstones, shales, slates. *Slightly to intensely metamorphosed rocks of Cambrian and Early Ordovician emplaced in eastern New York by gravity slides & thrust faults*

INTENSELY METAMORPHOSED ROCKS

- Older than 570 m.y.a. (*regional metamorphism about 1,000 m.y.a.*) — PRECAMBRIAN gneisses, quartzites, marbles. *Shows generalized pattern of geological contacts*
- PRECAMBRIAN anorthosite

DRAFTING GYS 1978

Figure 3.

GENERALIZED TECTONIC - METAMORPHIC MAP

of

NEW YORK

COMPILED BY

Donald W. Fisher
Yngvar W. Isachsen
Lawrence V. Rickard

NEW YORK STATE MUSEUM AND SCIENCE SERVICE
MAP AND CHART SERIES NO. 15
1971

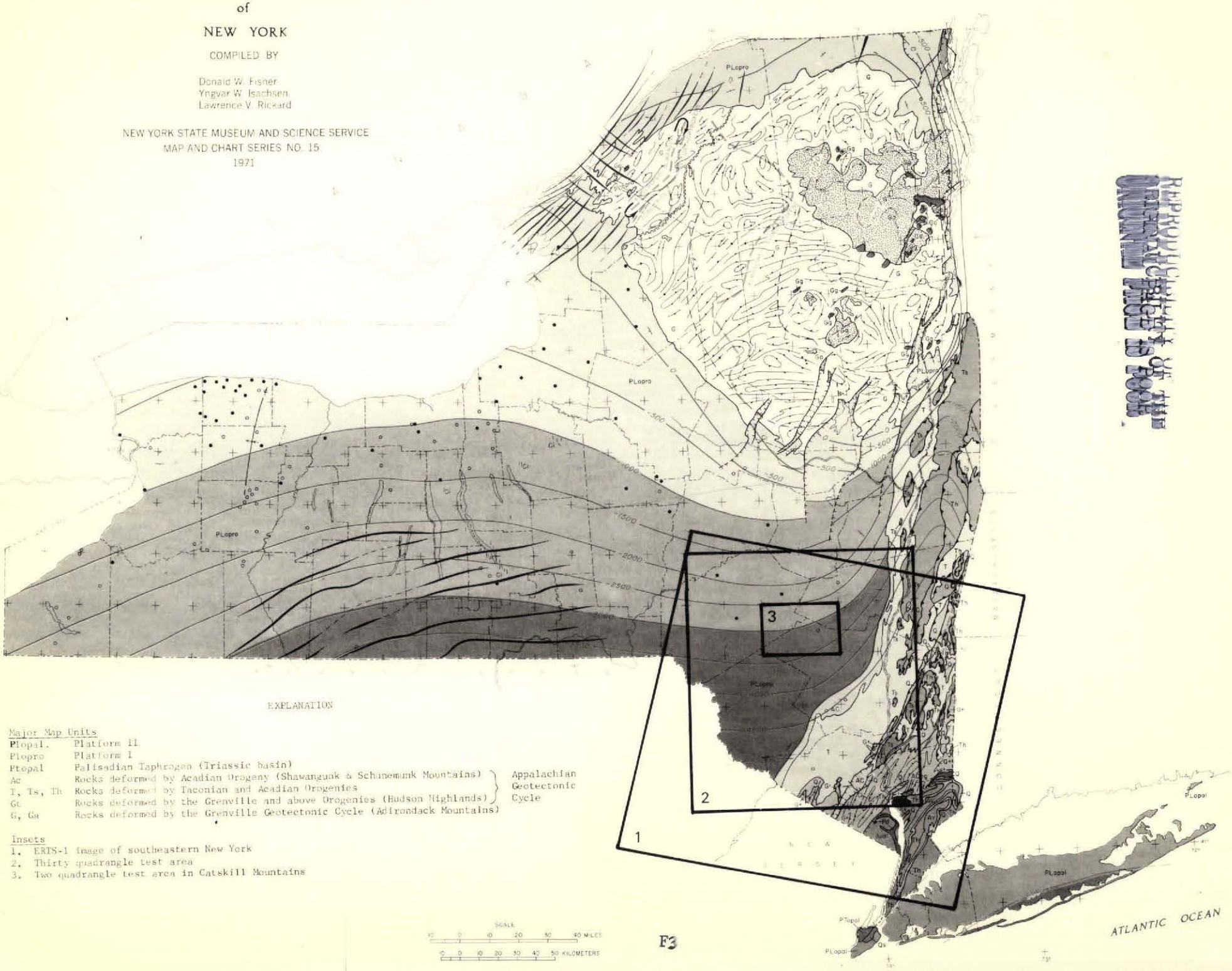

EXPLANATION

Major Map Units

Plopal.	Platform II	
Plopro	Platform I	
Ptopal	Palisadian Taphrogen (Triassic basin)	
Ac	Rocks deformed by Acadian Orogeny (Shawangunk & Schunemunk Mountains)	Appalachian Geotectonic Cycle
T, Ts, Th	Rocks deformed by Taconian and Acadian Orogenies	
Gt	Rocks deformed by the Grenville and above Orogenies (Hudson Highlands)	
G, Gs	Rocks deformed by the Grenville Geotectonic Cycle (Adirondack Mountains)	

Insets

1. ERTS-1 image of southeastern New York
2. Thirty quadrangle test area
3. Two quadrangle test area in Catskill Mountains

SCALE

10 0 10 20 30 40 MILES

0 0 10 20 30 40 50 KILOMETERS

F3

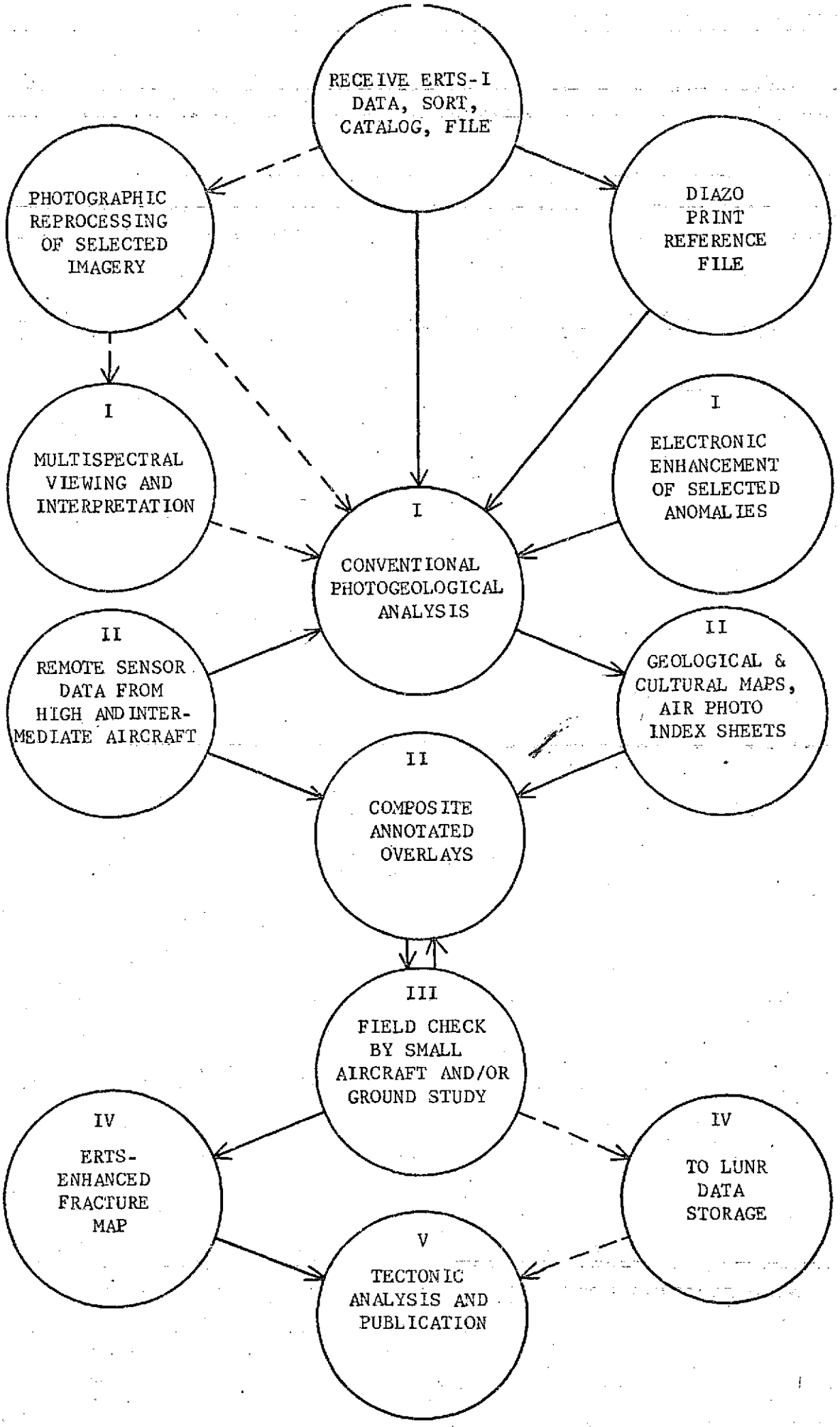

Figure 4. Flow chart of data handling and imagery analysis for ERTS-1.

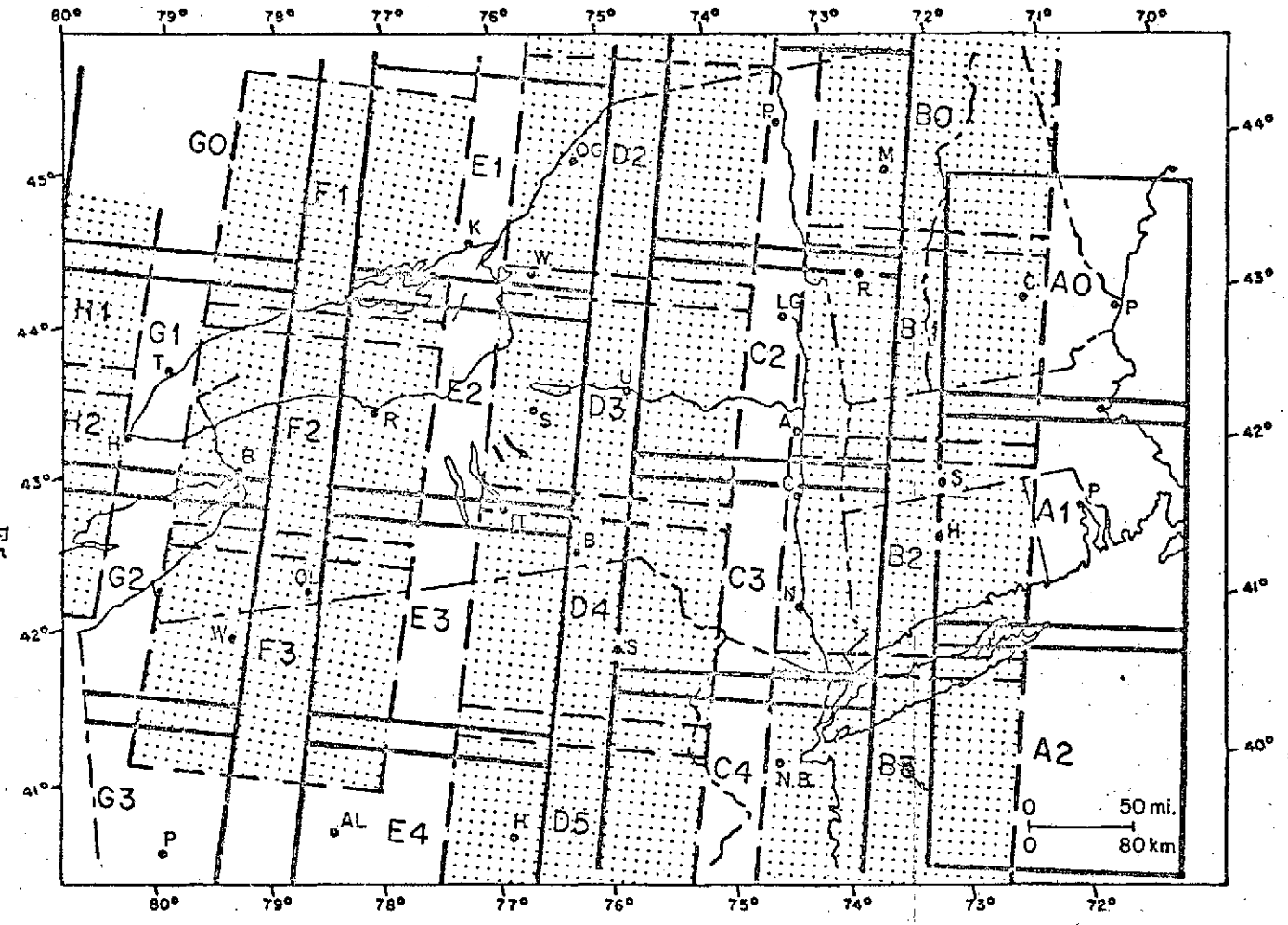

N.Y.S. GEOLOGICAL SURVEY SYMBOL	LOCALITY DESIGNATION
A0	New Hampshire-Maine
A1	Rhode Island
A2	Long Island
B0	No. Vermont-New Hampshire
B1	So. Vermont-New Hampshire
B2	Connecticut
B3	New York-Long Island
C0	Montreal East
C1	Lake Champlain
C2	Hudson-Mohawk
C3	Catskill-Hudson Highlands
C4	Philadelphia
D1	Montreal West
D2	Adirondacks
D3	Utica-Binghamton
D4	Scranton
D5	Harrisburg
E0	Ottawa
E1	Kingston
E2	Finger Lakes
E3	Elmira
E4	South Mountain-Alleghany Plateau
F0	Pembroke
F1	Rochester
F2	Genesee River
F3	Alleghany River
G1	Toronto
G2	Lake Erie East
G3	Pittsburgh-Youngstown
H1	Lake Ontario-Lake Huron
H2	Lake Huron-Lake Simcoe

Figure 5. Scene designations for ERTS-1 imagery covering New York State and adjoining areas which is on file at the New York State Geological Survey.

Bands red'd*	Orbit	Date flown / rec'd	Product I.D.	% Imagery usable	Location of usable areas (1 2 3 / 4 5 6 / 7 8 9)	Browse file	photo-reprocessed	1:1,000,000 color prints**	1:1,000,000 color transp.**	1:500,000 B & W prints***	1:250,000 B & W prints***	1:500,000 color prints**	1:250,000 color prints**	Img. dscrptrs	SDC photos	NYS Strip # E_3
9 P N / 4 4 4 / 5 7 2	124	1Aug72 / 11Oct72	1009-15235	45	2,3,5,6 8,9	x								x		
9PN / 4-7	375	19Aug72 / 25Oct72	1027-15240	70	1-6	x	x							x		
9PN / 4-7	626	6Sep72 / 24Oct72	1045-15240-	75	2-9	x				5 7				x		
9PN / 4-7	1379	30Oct72 / 22Nov72	1099-15243	<10	-	0								x		
9PN / 4-7	1630	17Nov72 / 8Jan73	1117-15244	20	2,3	0								x		
9PN / 4-7	2132	23Dec72 / 2Feb73	1153-15244	25	1,2,4	0								x		
9PN / 4-7	2383	10Jan73 / 22Feb73	1171-15243	70	all	x								x		
9PN / 4-7	3387	23Mar73 / 1May73	1243-15251	100	all	x		x	x	5 7				x		
9NP / 4-7	4140	16May73 / 27Jun73	1297-15245	90	all	x		x	x	5 7				x		
9PN / 4-7	5897	19Sep73 / 5Nov73	1423-15231	75	all									x		
9PN / 4-7	6399	25Oct73 / 3Dec73	1459-15221	95	all			0	0					x		
9PN / 4-7	6901	30Nov73 / 23Jan74	1495-15220	80	2,5-9			0						x		

*9 = 9" positive
P = 70 mm positive
N = 70 mm negative

**o = on order
X = received

***o = on order
5 = band 5 received
7 = band 7 received

Figure 6. Sample page of log book for ERTS-1 data products on file at the New York State Geological Survey.

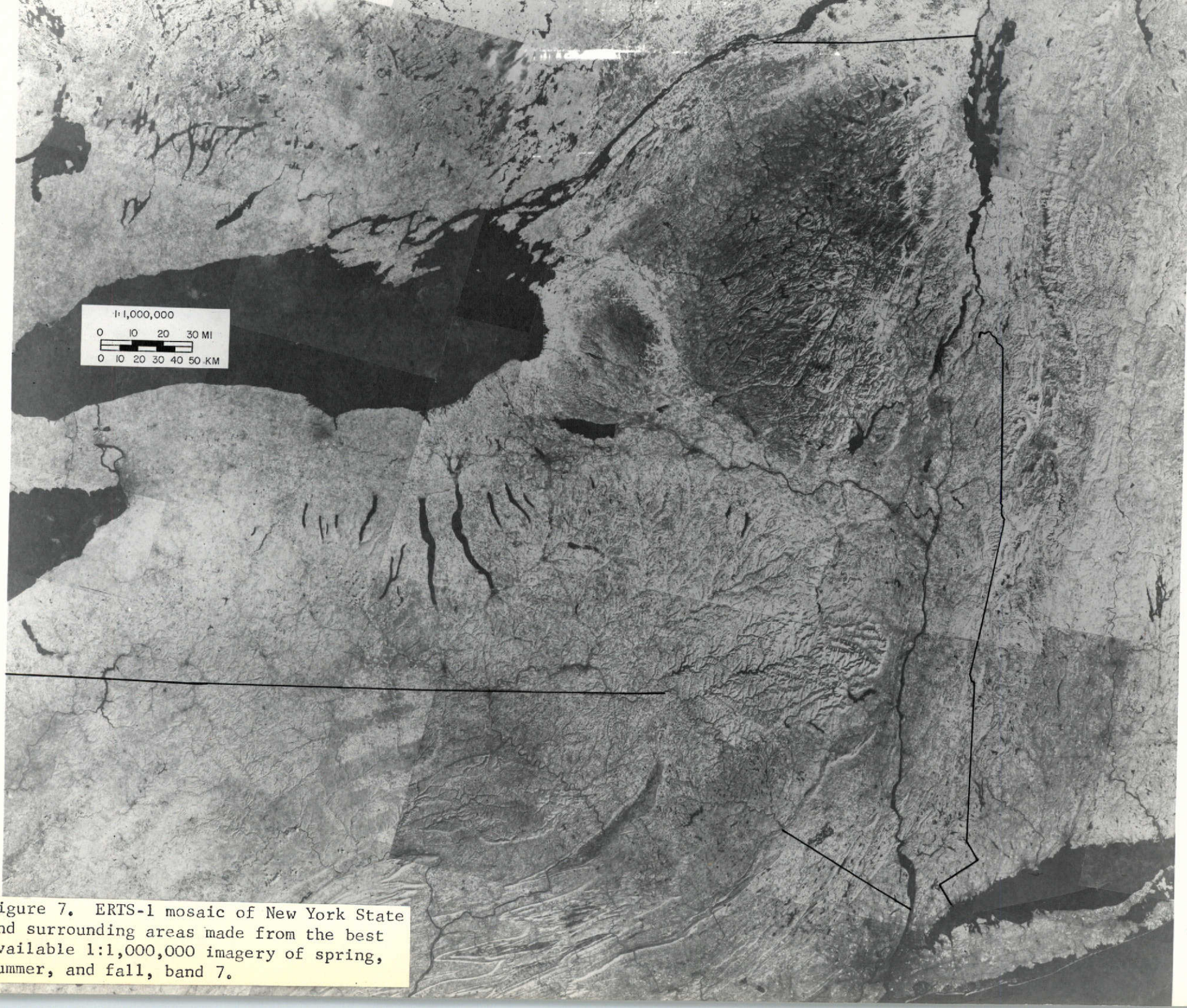

Figure 7. ERTS-1 mosaic of New York State and surrounding areas made from the best available 1:1,000,000 imagery of spring, summer, and fall, band 7.

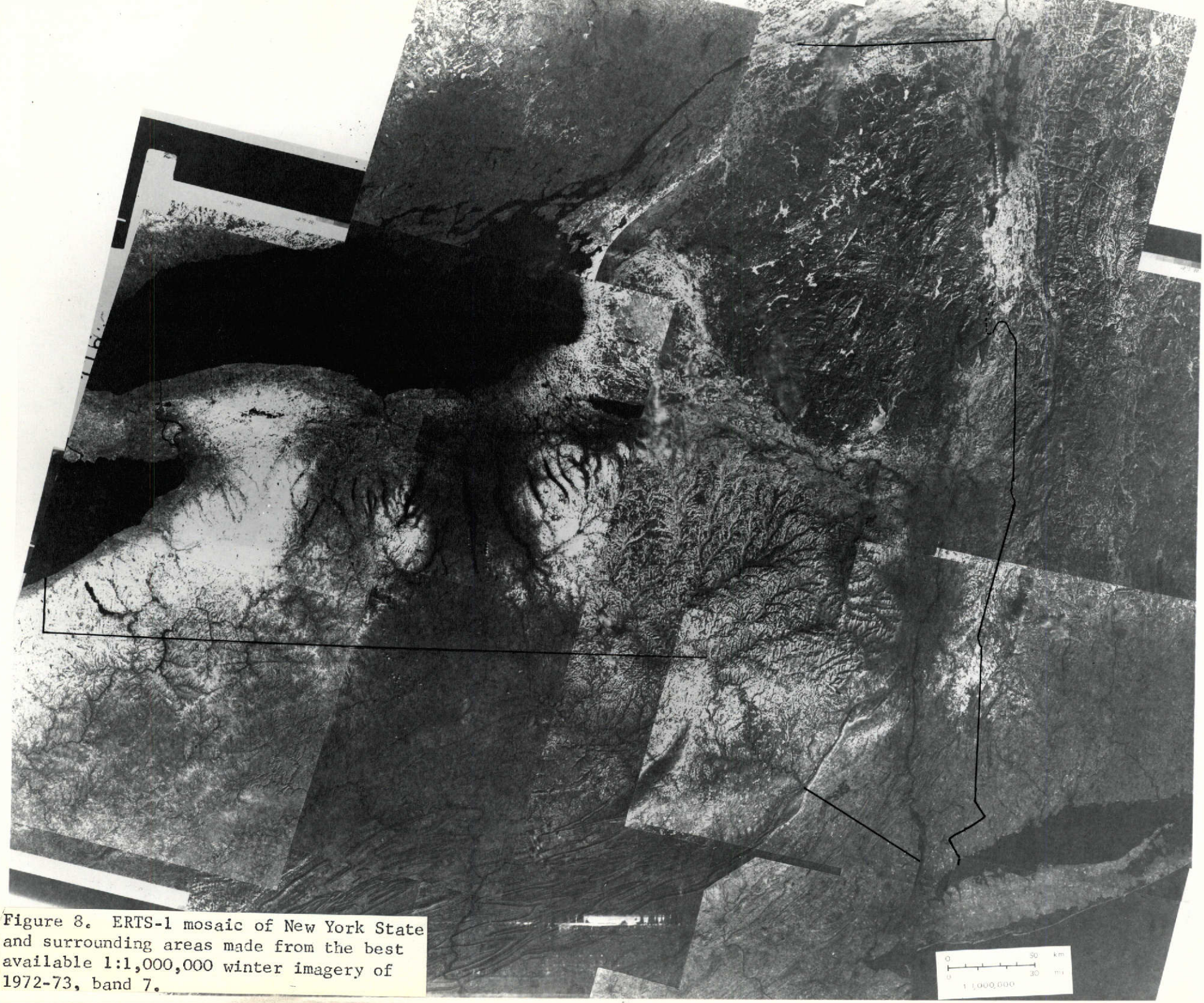

Figure 8. ERTS-1 mosaic of New York State and surrounding areas made from the best available 1:1,000,000 winter imagery of 1972-73, band 7.

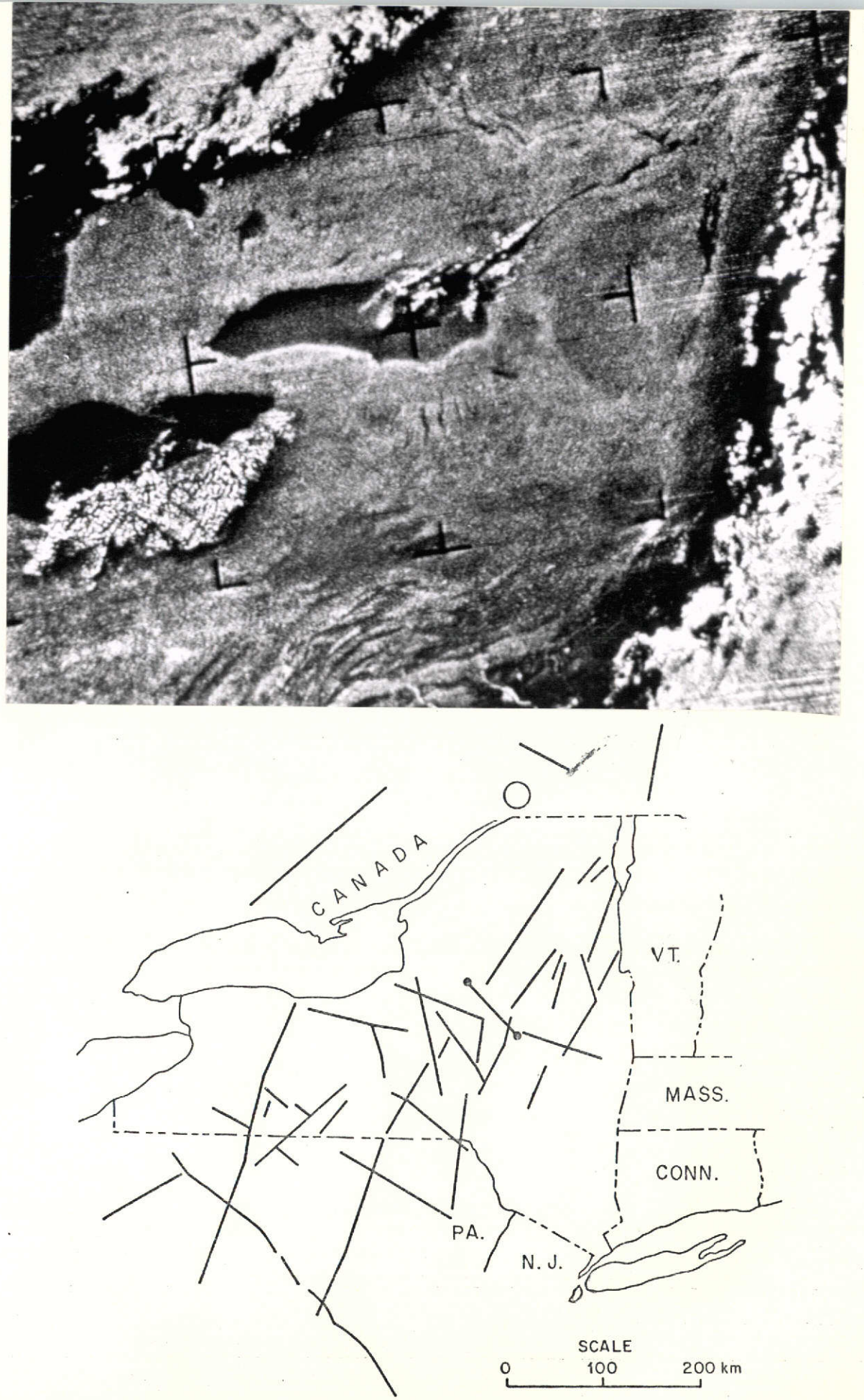

Figure 10. Linear and circular features seen on NIMBUS-I image, orbit 254.

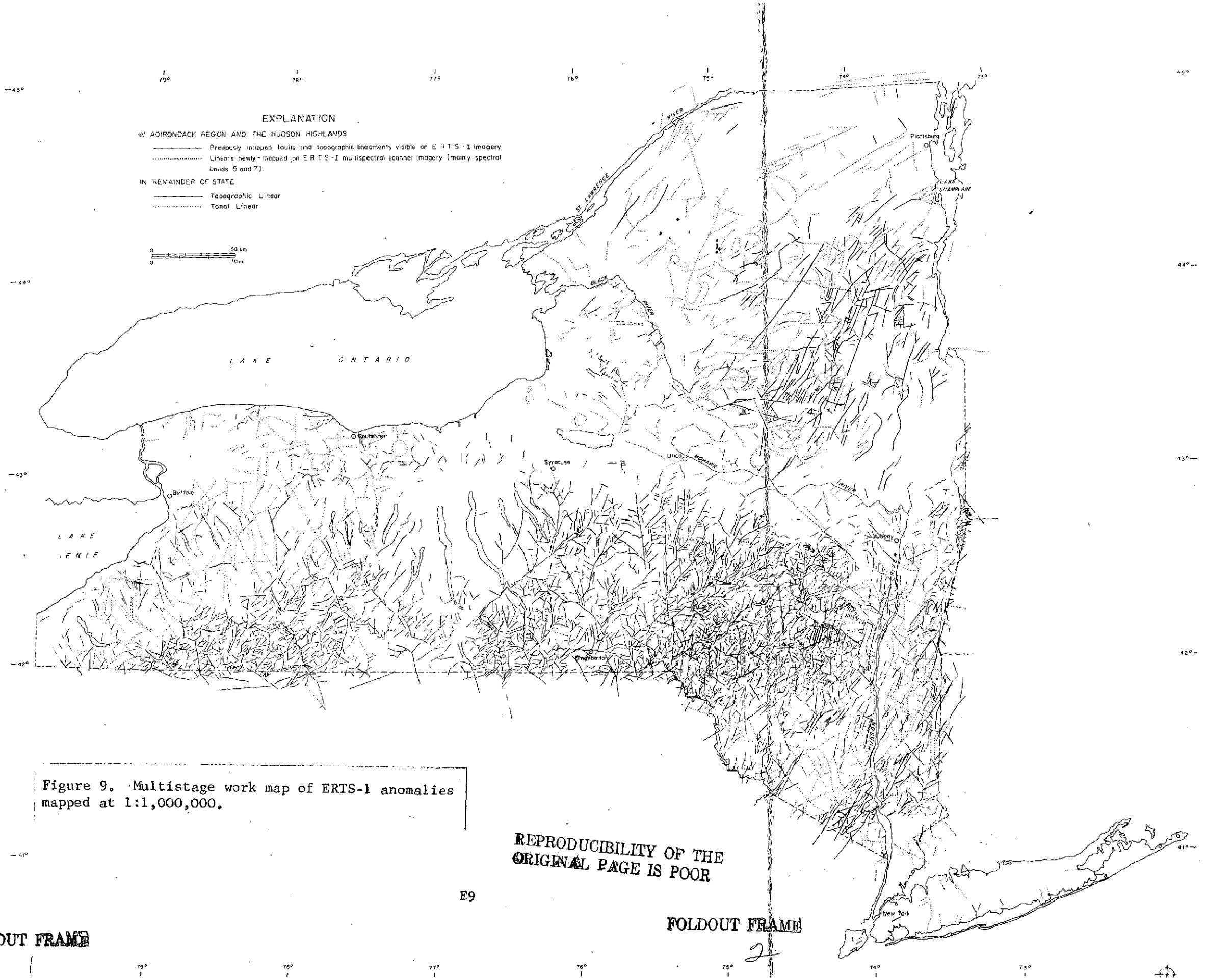

Figure 9. Multistage work map of ERTS-1 anomalies mapped at 1:1,000,000.

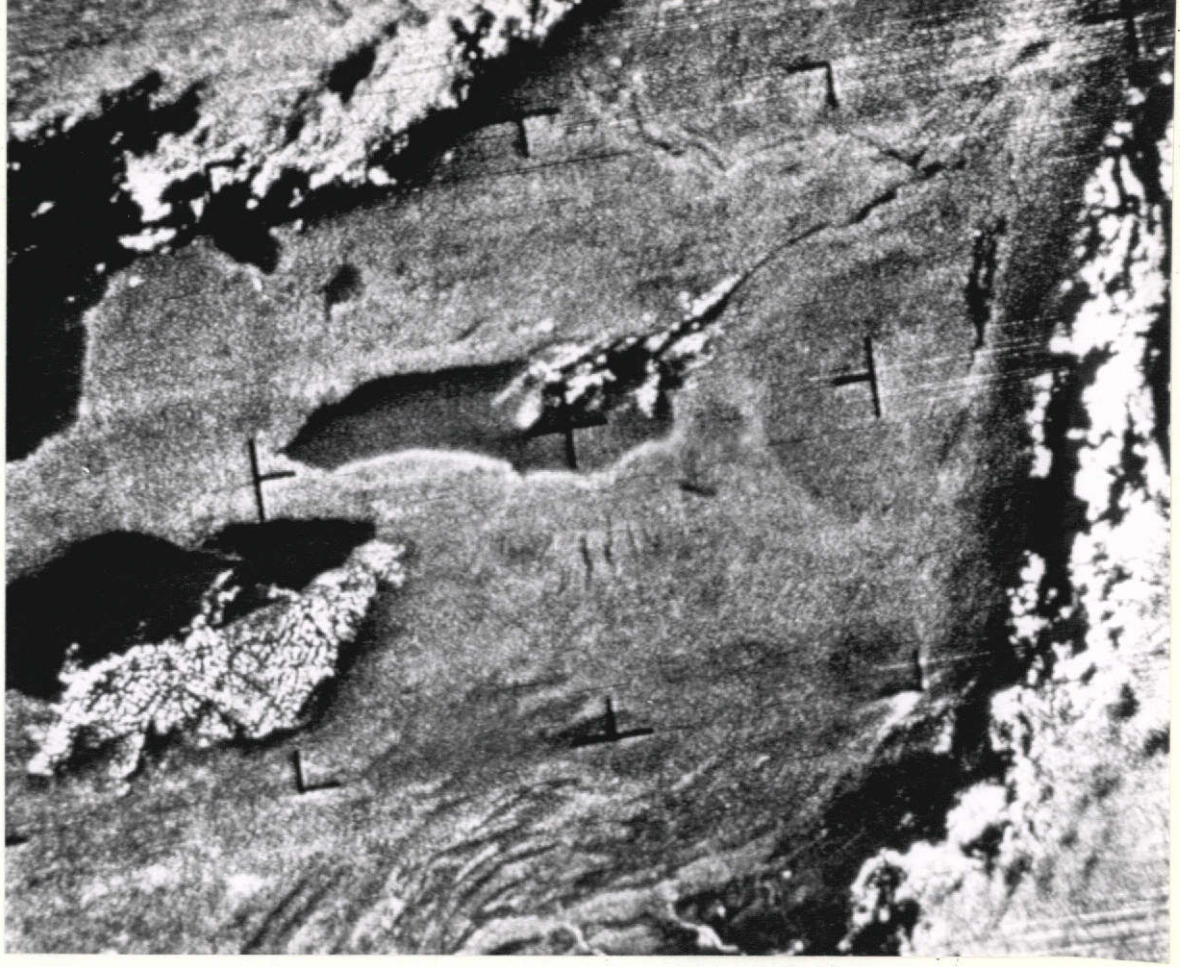

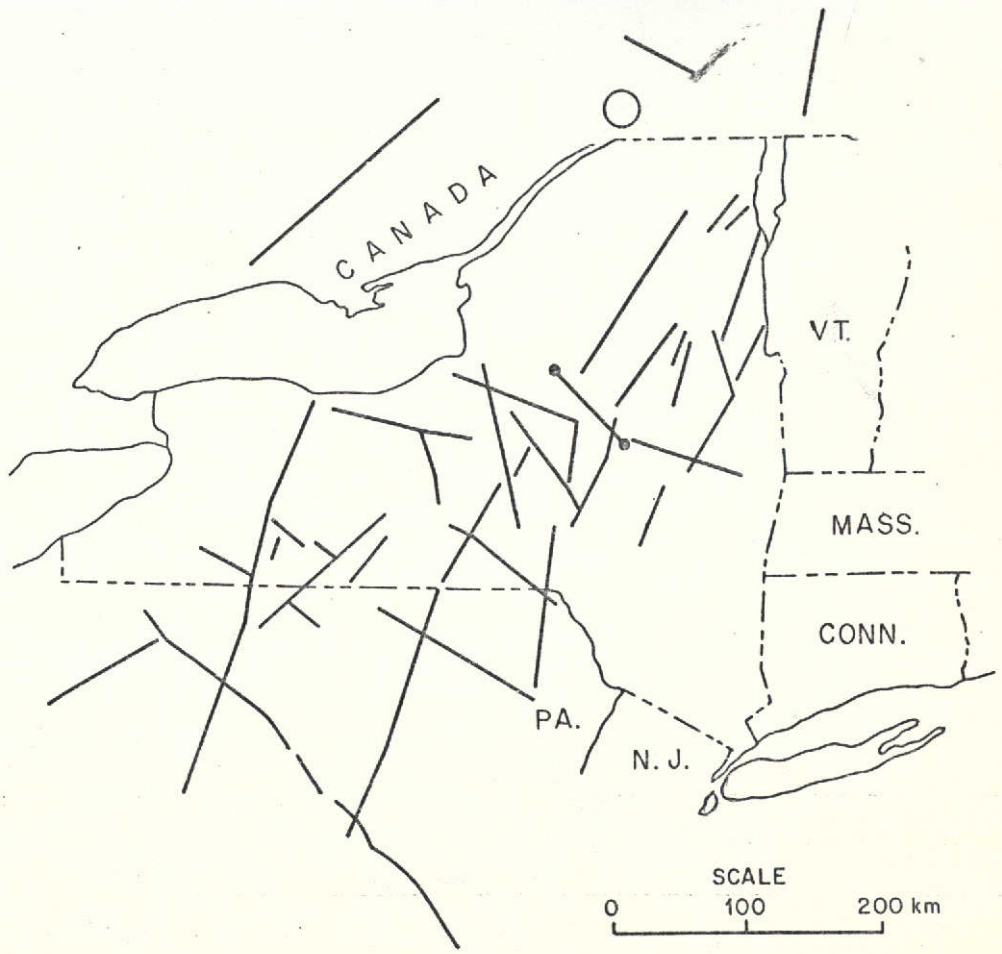

Figure 10. Linear and circular features seen on NIMBUS-I image, orbit 254.

Figure 11. ERTS-1 mosaic of the Adirondack region, band 7, images 1079-15115, 1079-15122, 1080-15174, 1080-15180. Scale, 1 mm = 1 km.

Figure 12a. Stage I linear and circular features seen on ERTS-1 imagery at 1:1,000,000 (image nos. 1079-15115, 1079-15122, 1080-15174, 1080-15180). Dotted lines represent new Stage II and Stage III features, pale solid lines indicate previously mapped faults and topographic lineaments seen on the imagery, and heavy solid lines show previously mapped faults and topographic lineaments not shown on the imagery. Large dots and short thick line represent open pit mines dry tailings ponds. Scale: 1 mm = 1 km.

Figure 12b. Stage I and Stage II linear and circular features seen on ERTS-1 imagery at 1:500,000 and 1:250,000 (here photoreduced), using images 1079-15115, 1079-15122, 1080-15174, and 1080-15180. Solid lines represent topographic linears, dotted lines signify tonal linears.

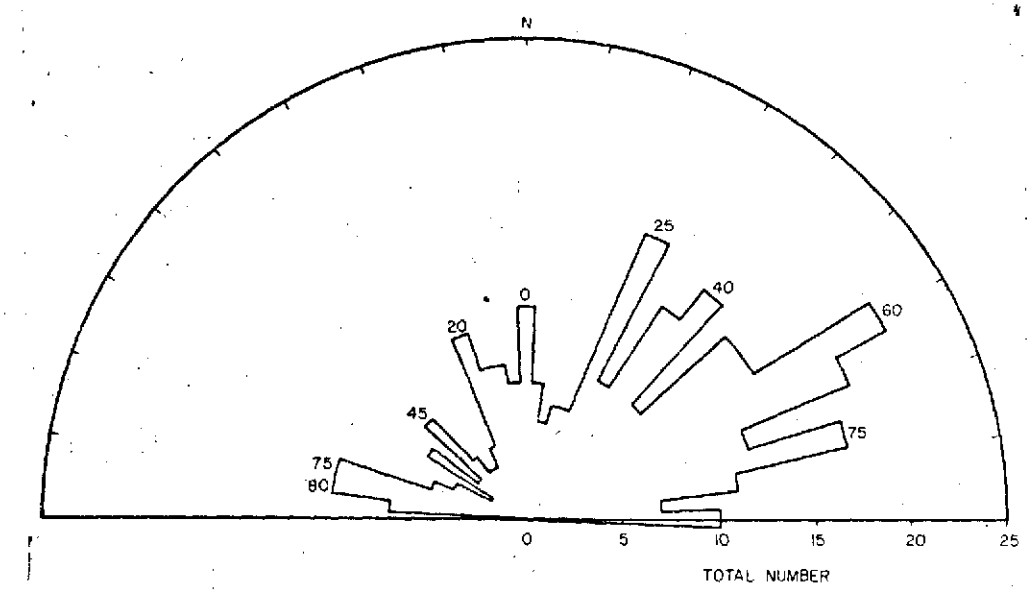

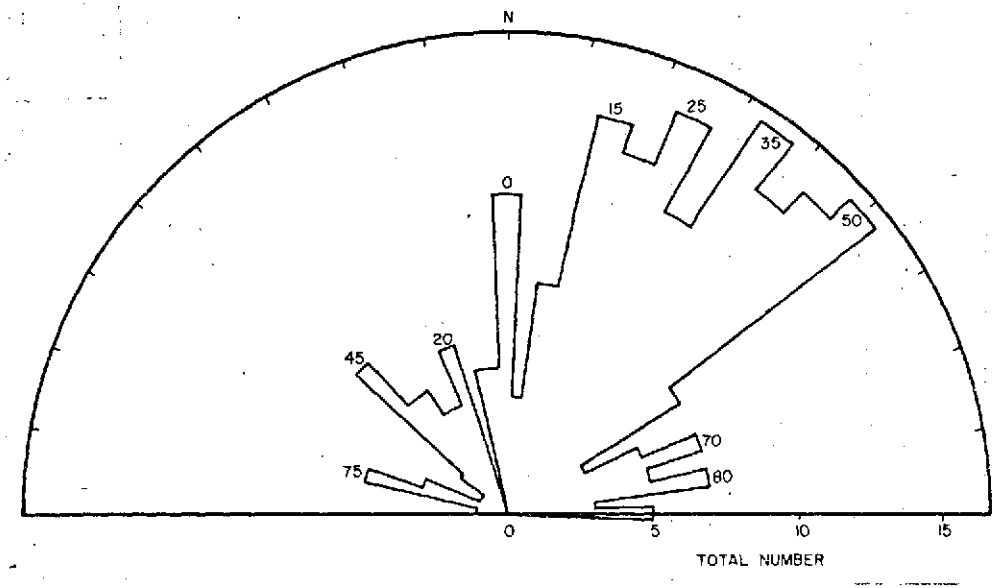

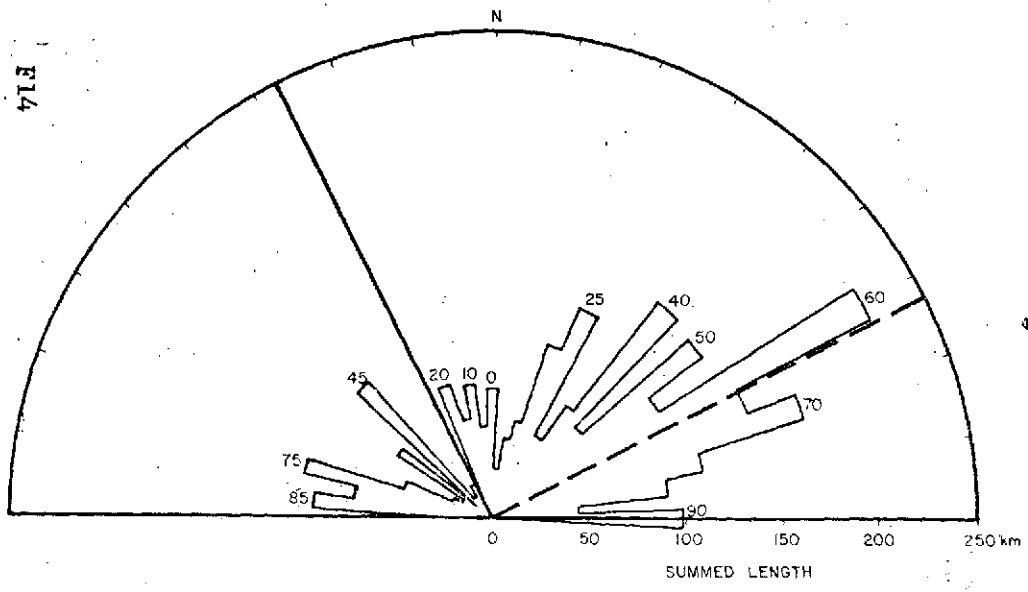

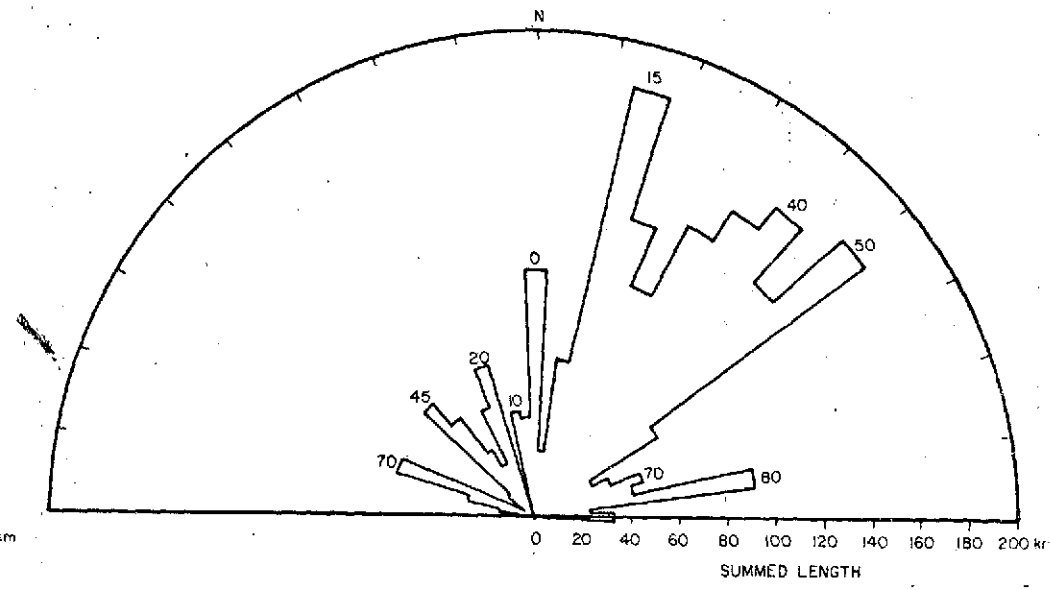

Figure 13a. Rose diagrams of ERTS-1 linear features in the Adirondack region, which have survived Stage II analysis, with data lumped into 5 degree intervals. Upper diagram is a plot of total number of linears (319), whereas lower diagram sums total lengths. Heavy solid line shows azimuth of solar illumination (elevation = 34°); long-dash line is perpendicular to it.

Figure 13b. Rose diagram of previously mapped faults and topographic lineaments in the Adirondack region, with data lumped into 5 degree intervals. Upper diagram is a plot of total number of linear features (235), whereas lower diagram sums total lengths.

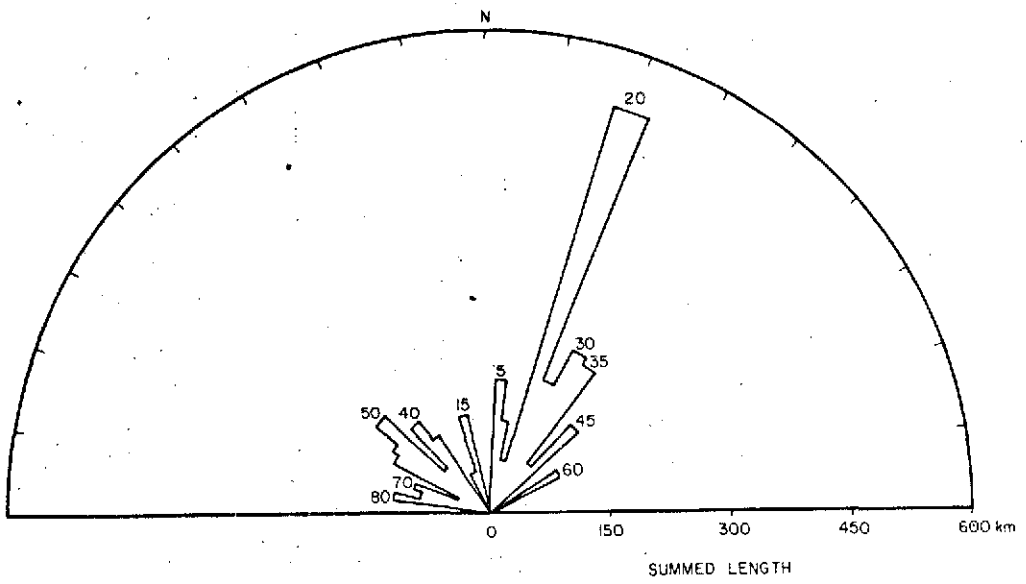

Figure 14. Rose diagram of summed lengths of NIMBUS-I linears for New York State and northern Pennsylvania shown in Figure 10.

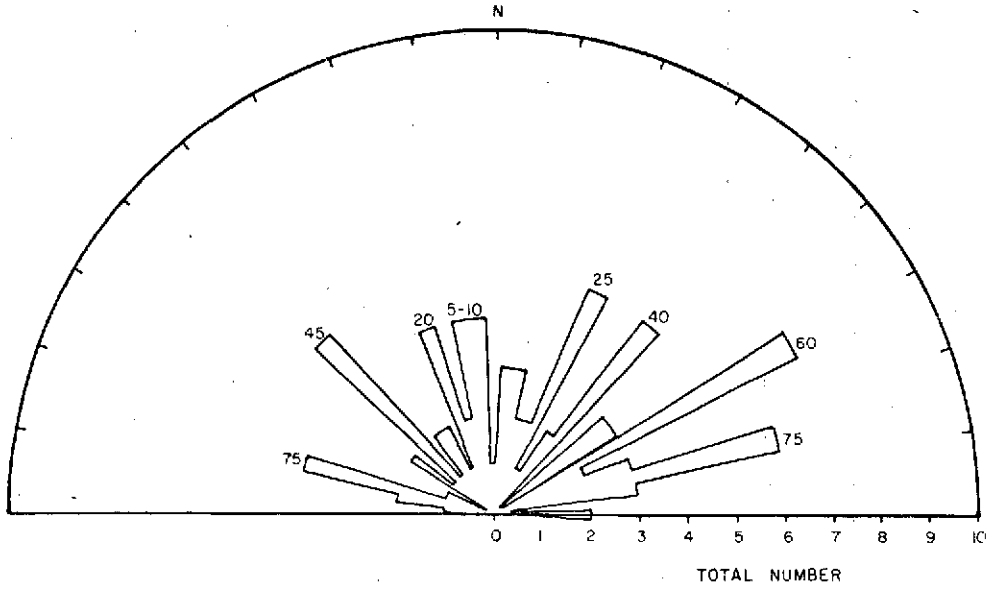

Figure 16a. Rose diagram of total number of ERTS-1 linears in the NTL category discussed in text.

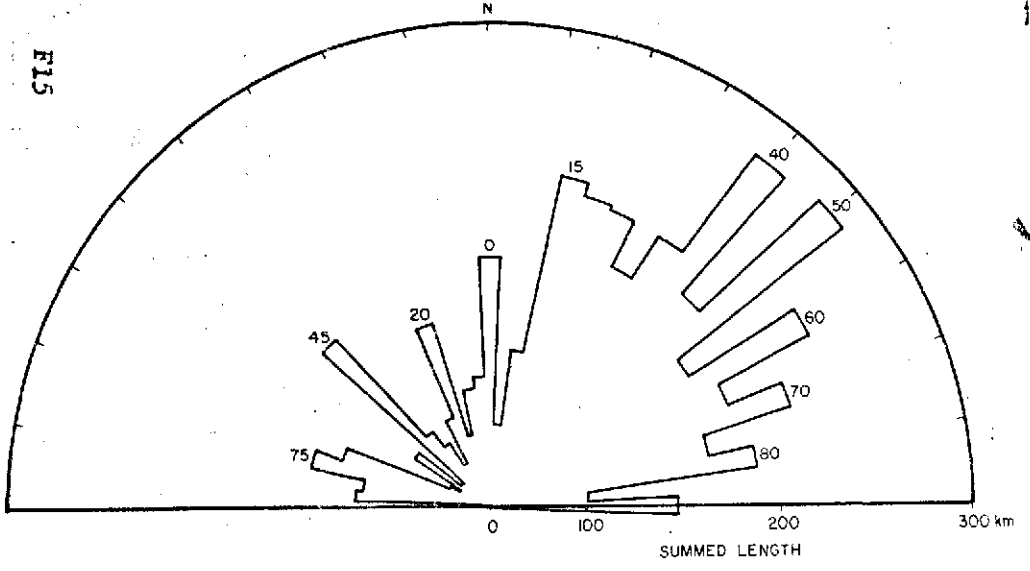

Figure 15. Rose diagram of previously mapped faults and topographic lineaments together with new Stage II and Stage III ERTS linears.

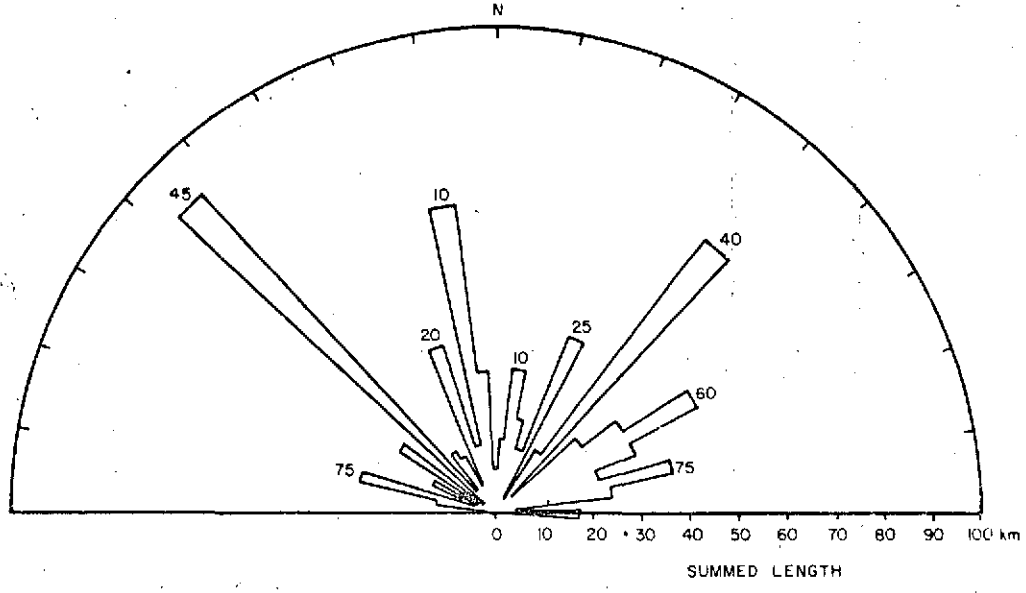

Figure 16b. Rose diagram of summed lengths of ERTS-1 linears in the NTL category discussed in text.

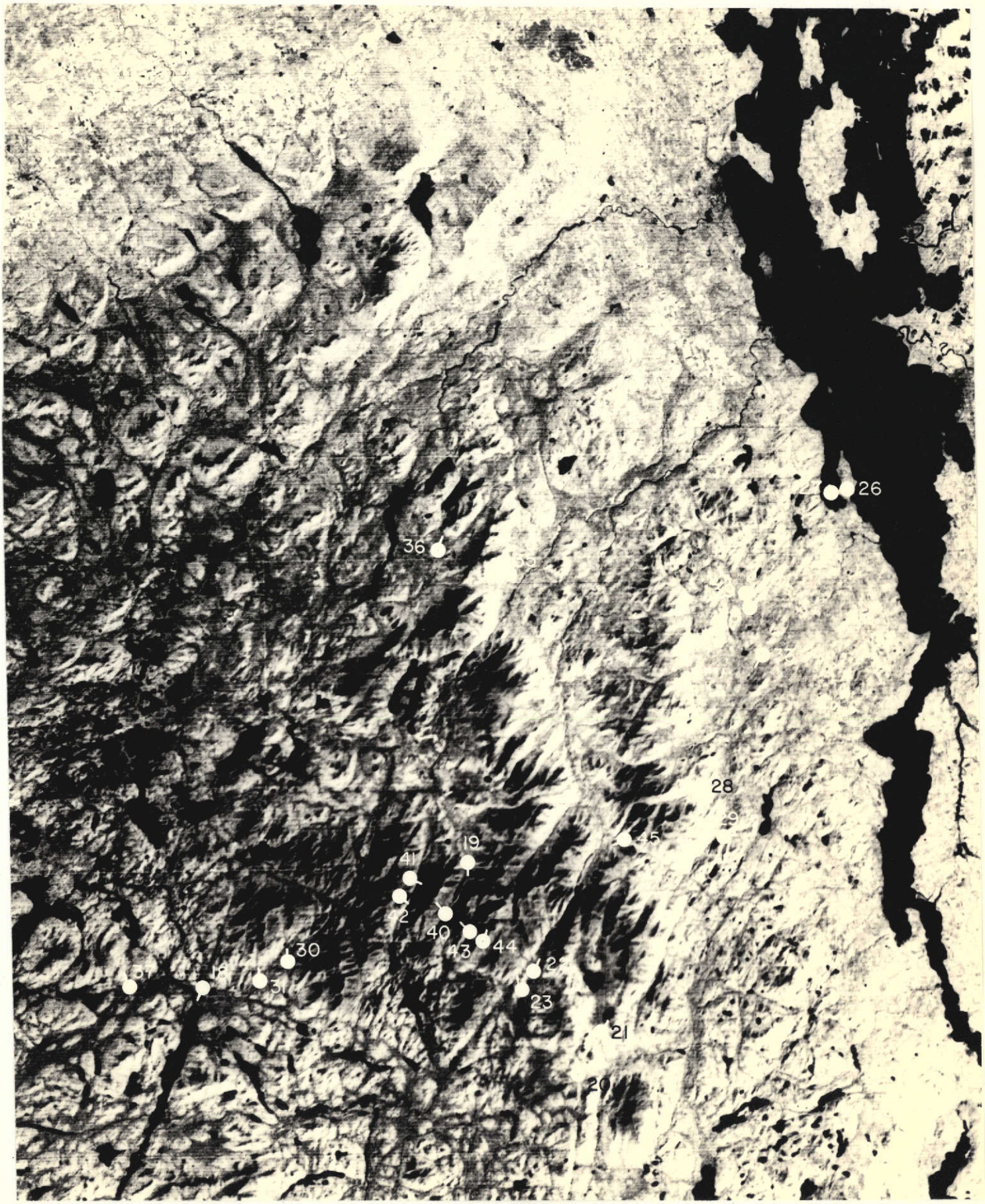

Figure 17. ERTS-1 image of northeastern Adirondacks showing sites from which photographic illustrations were taken. Barbs on the dots indicate view directions, and the accompanying numbers refer to figures in the text. Band 7 of 100ct72 (no. 1079-15115). Scale, 1:500,000

Figure 18. Aerial view south-southwest along the longest (115 km) clearly-defined topographic lineament in the Adirondack Mountains. About 30 km of the lineament are visible in the photograph.

Figure 19. View looking southwest along the previously-mapped Avalanche Lake lineament which borders Mt. Colden. The topographic lineaments crossing Mt. Colden orthogonally cannot be distinquished on the imagery. The most deeply incised of these is eroded along the Mt. Colden meta-gabbro dike.

Figure 20. ERTS-1 linear 291, shown here to be a topographic lineament. It strikes N43E and extends in both directions across Clear Pond in the foreground. View is northerly. The mountain peaks west of the linear are McComb (with slide), Hough (sharp peak), Dix, the valley of Hunters Pass, and Dial. Hunters Pass is part of a topographic lineament 25 km in length which extends across Elk Lake in the middleground. All bedrock in clear view is metamorphosed anorthosite.

Figure 21. Central and upper portion of linear shown in Figure 20. Topographic expression is slightly enhanced by the contrast between deciduous trees in the valley and conifers plus rock outcrop along

Figure 22. View looking NNE along Ausable Lake topographic lineament, a previously mapped feature parallel to and west of the as yet unexplained ERTS-1 linear no. 289; located entirely within Marcy Massif metanorthosite; slides on Gothics discernible at 1:500,000; Mt. Marcy 15' quadrangle.

Figure 23. ERTS-1 linear no. 287, extending N52W from White Lily Pond; entirely within Marcy Massif metanorthosite; Mt. Marcy and Santanoni 15' quadrangles.

Figure 24. View of Cranberry Lake from the southwest showing radial arms of the Lake as well as two new topographic lineaments visible on the ERTS-1 imagery, which converge at the southern end of the Lake. Bedrock is mainly granitic gneiss.

Figure 25. View looking northeast up linear 175 which forms the west-southwestern arm of Cranberry Lake. Bedrock is mainly granitic gneiss.

Figure 26. View of the west shore of Lake Champlain showing two topographic lineaments (343a on left and 343 on right) converging toward the camera; aerial reconnaissance along the shoreline cliffs shows a break in outcrop at both sites (see figure below). A narrow belt of mixed gneisses parallels the shore, beyond which the bedrock is gabbroic metanorthosite gneiss.

Figure 27. Closer view of lineament 343 showing shoreline expression, namely, cove indentation, discontinuity in shoreline cliffs, and inclined fracture traces in cliffs near the lineament.

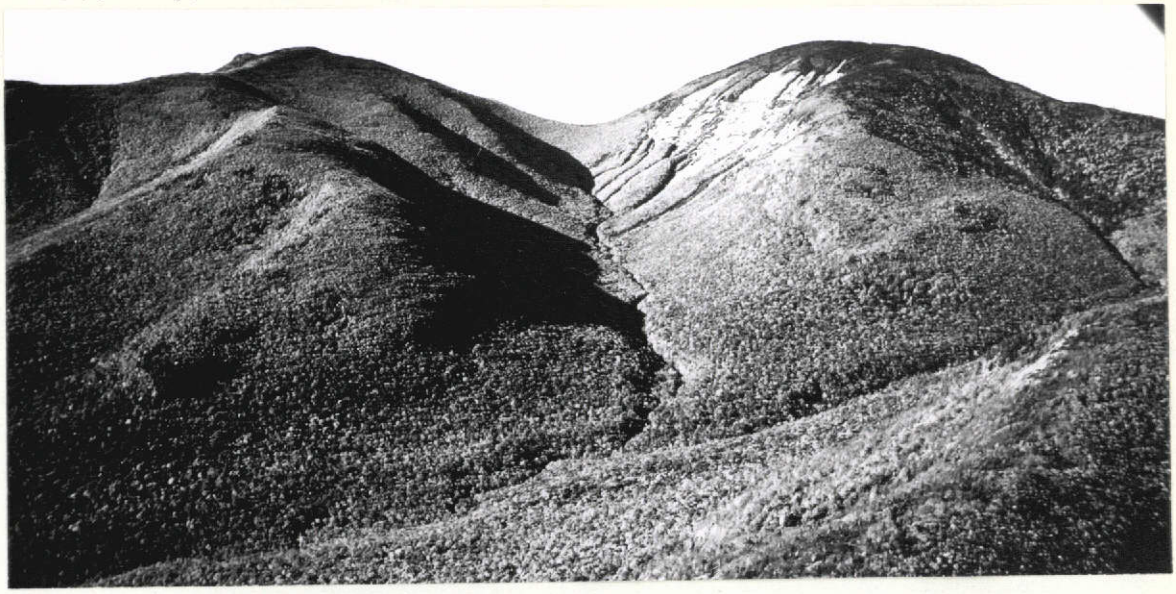

Figure 28. View westward up topographic lineament 354, entirely in metanorthosite, which continues to the west beyond the divide. Orthogonal valley in foreground roughly follows contact between the metanorthosite and an olivine metagabbro body.

Figure 29. Looking eastward toward Lincoln Pond along topographic lineament 356.

Figure 30. View north-northeast along lineament 215 in the Seward Mountains, entirely within metanorthosite. The valley immediately to the left is linear 216, and that adjacent to the right a previously mapped topographic lineament which is better shown in Figure 31.

Figure 31. Looking north-northeast along previously mapped topographic lineament which separates the Seward Mountains on the left from Mt. Seymour on the right, entirely within metanorthosite.

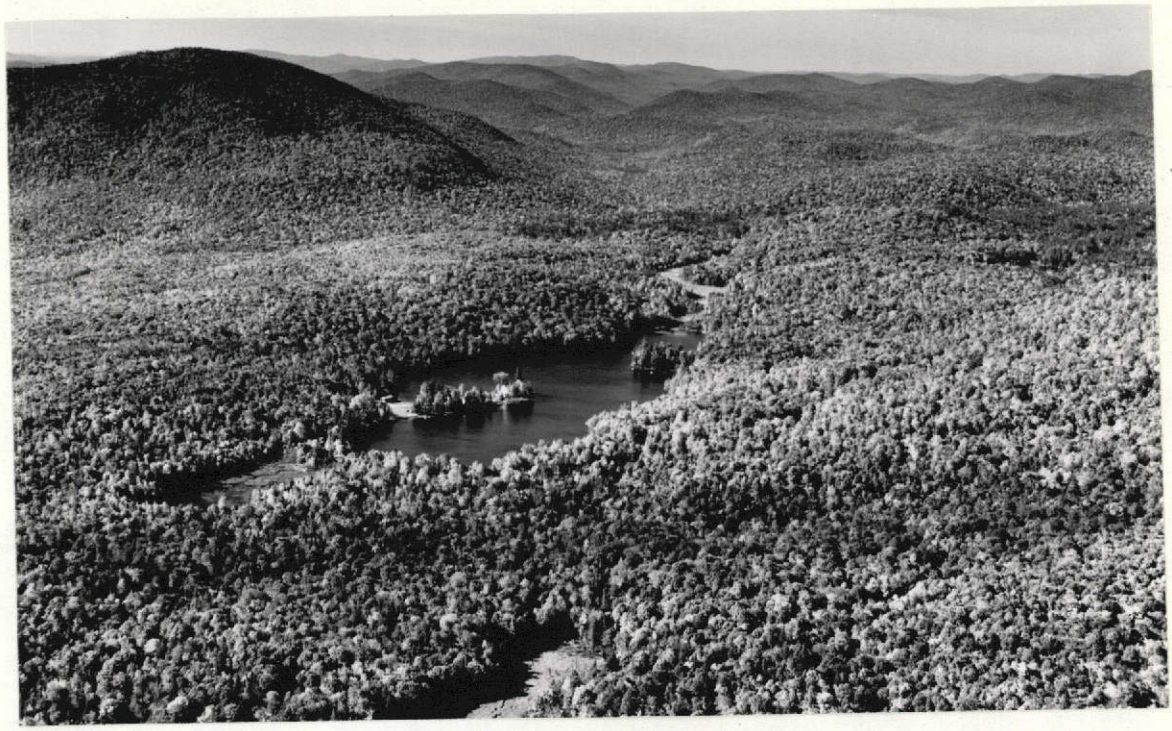

Figure 32. Topographic lineament 309 looking southwest from Chatiemac Lake.

Figure 33. Looking southwest along linear 350 which borders the hill in the middleground; seen from the best vantage point.

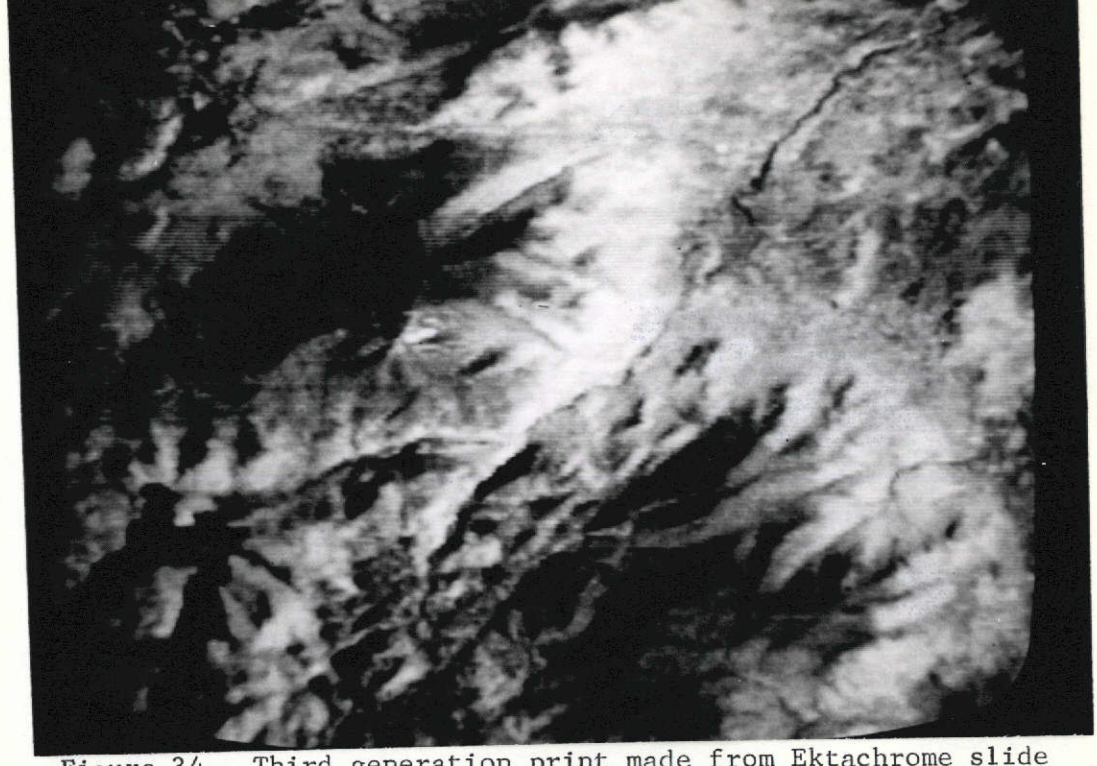

Figure 34. Third generation print made from Ektachrome slide of 4X computer-generated color composite of Mt. Whiteface. The photograph is unconventionally oriented to facilitate comparison with figure below. Note bare summit and landslide scars on shadowed side of Mountain.

Figure 35. Mt. Whiteface, looking southwest up linear valley of White Brook. Note four fresh landslide scars of 1971. Mt. Whiteface is dominantly metanorthosite.

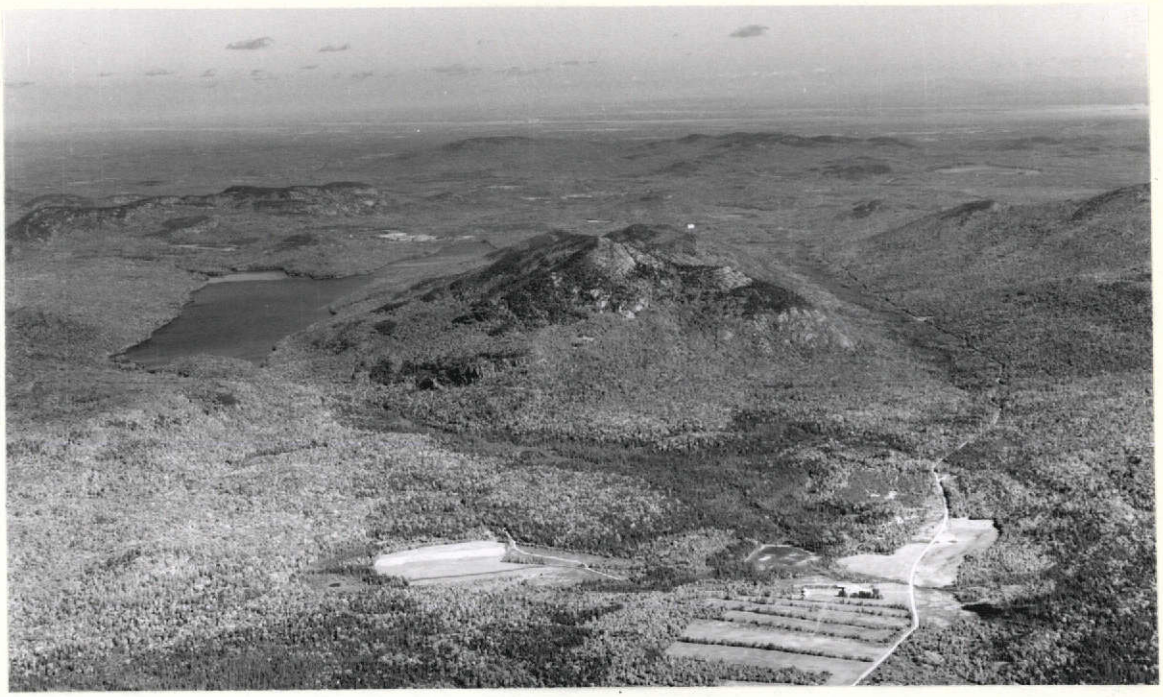

Figure 36. View northeast toward Catamount Mountain which is banded on the east by lineament 264 and on the west by Taylor Pond, the shorelines of which parallel this lineament.

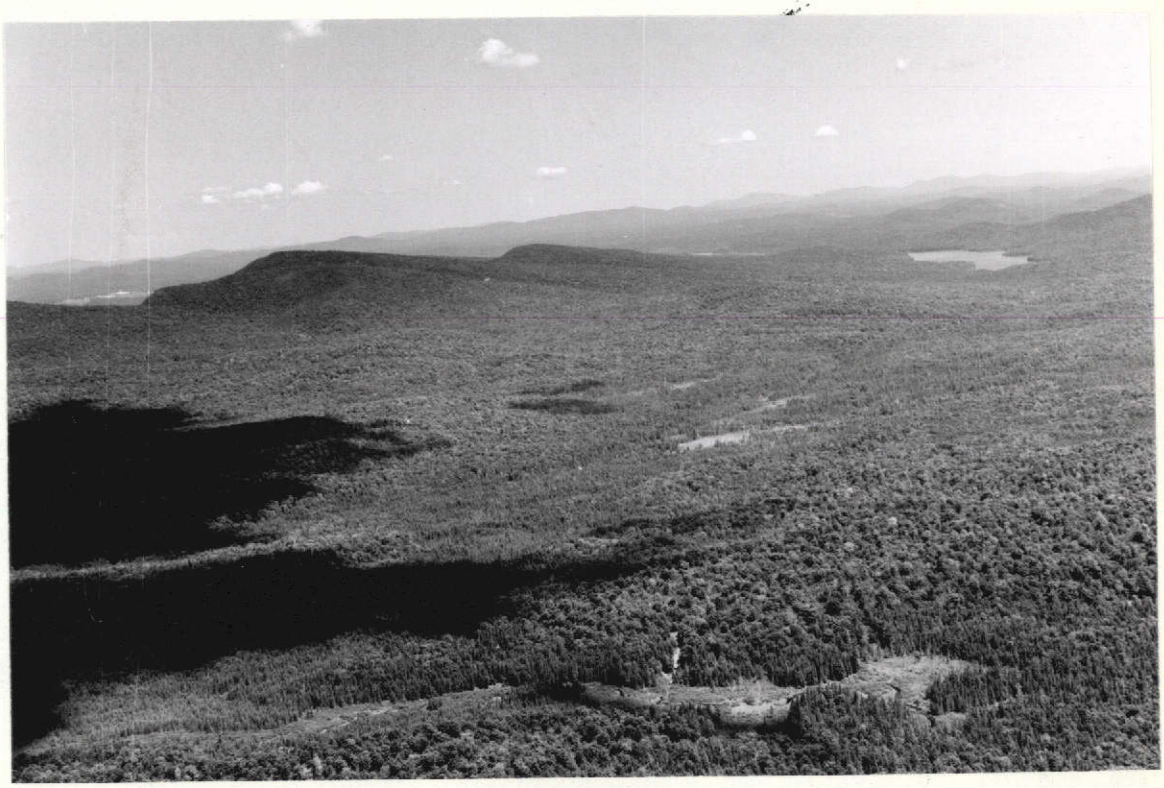

Figure 37. View looking north toward Follensby Pond. Linear valley 219 crosses photograph diagonally from lower left corner to beyond the Pond, and cuts orthogonally across metasediments, charnockite, and metanorthosite.

Figure 38. Linear valley 348 extending northeastward from lower left corner to middle of picture. Although well displayed on ERTS-1 imagery, the valley is only faintly visible in this view under midday solar illumination.

Figure 39. Looking northeastward along linear 349 which is located parallel to and immediately north of topographic lineament 348. It is seen to be a ridge-line demarcation between conifers on the south and mixed hardwoods on the north; it was declassified as a linear.

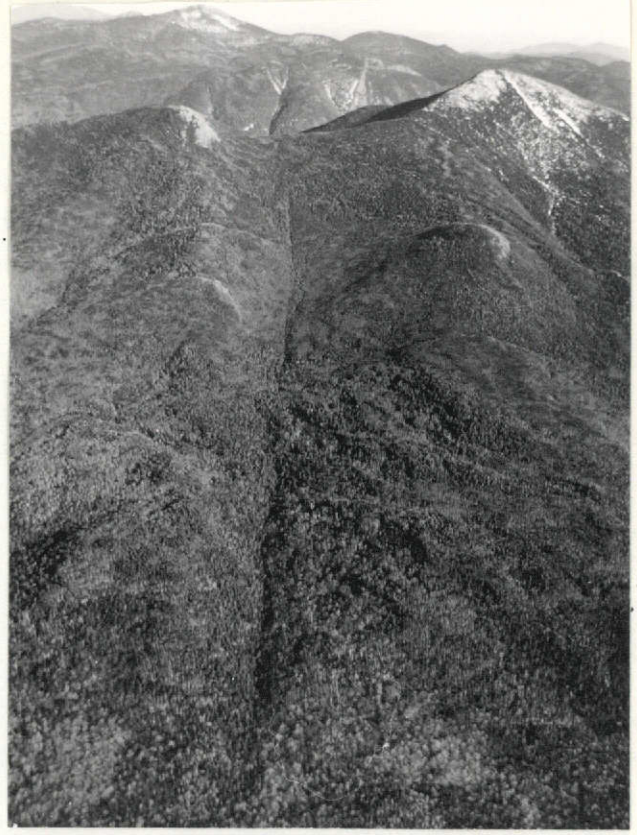

Figure 40. Linear valley in MacIntyre Range trending N35W between Wright and Algonquin Peaks. Entire area is within the Marcy metanorthosite massif. Mt. Marcy, highest peak in the Adirondacks, is visible in the middleground.

Figure 41. View of MacIntyre Range looking southeast, with Algonquin, Boundary, and Iroquois Peaks from north to south. The numerous linears shown are discussed in the text.

Figure 42. Aerial view taken over the lip of Wallface, looking southeast, showing blocky nature of the MacIntyre Range produced by intersecting topographic lineaments; photograph taken south along the Range from the preceding figure. The vertical lineament shown in the left middleground crosses Cliff Mountain (see below).

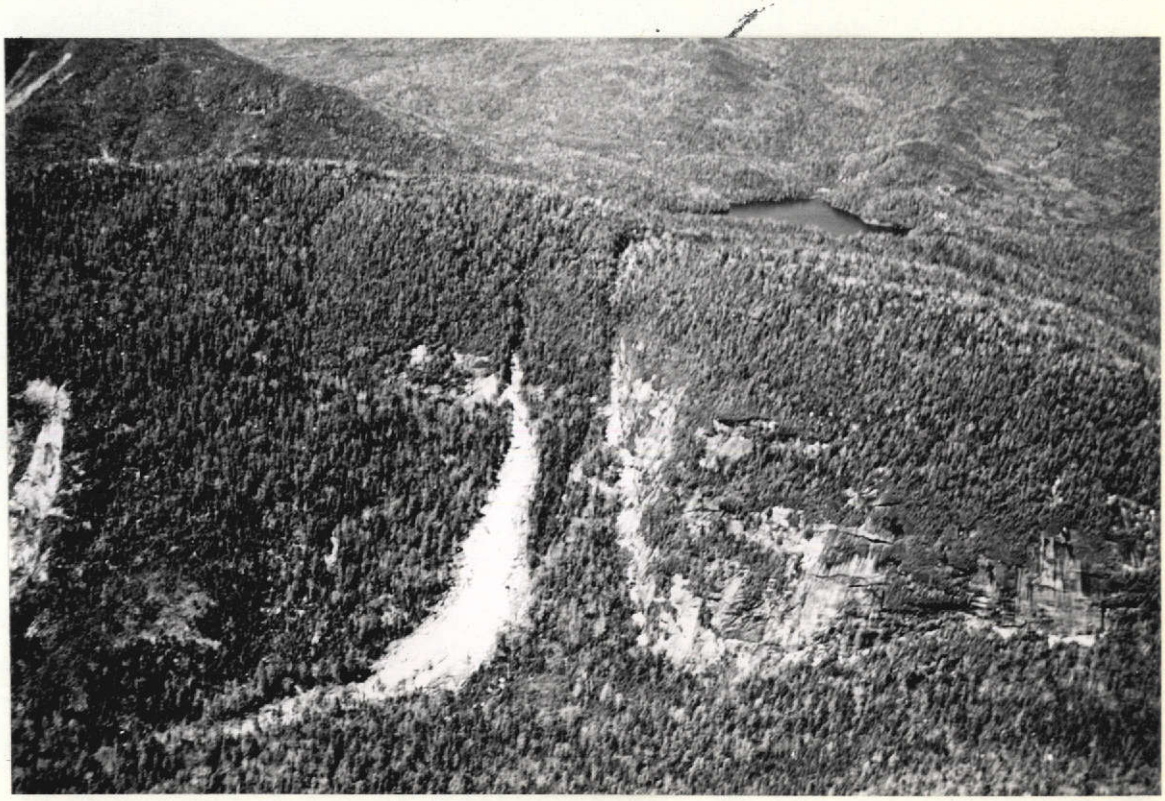

Figure 43. Looking westward at recent landslide bounding topographic lineament that crosses Cliff Mountain. This linear is marginally visible in ERTS-1 imagery but could not be drawn with confidence. Scene is entirely within metanorthosite.

Figure 44. View of Mt. Marcy (metanorthosite) looking northeasterly. The northerly-trending topographic lineaments on the Mountain, here enhanced by snow, are beyond the resolution of ERTS-1 imagery.

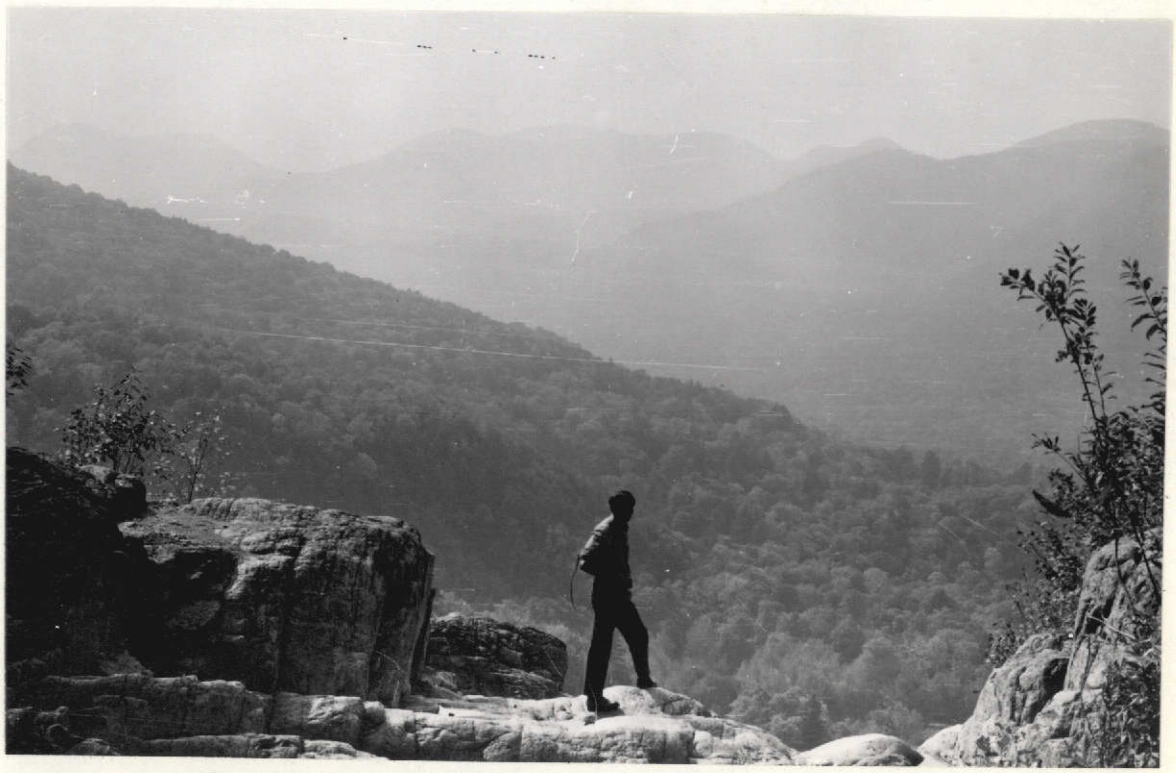

Figure 45. Looking westward across the lip of Roaring Brook Falls showing the closely spaced joints which control the stream bed trend.

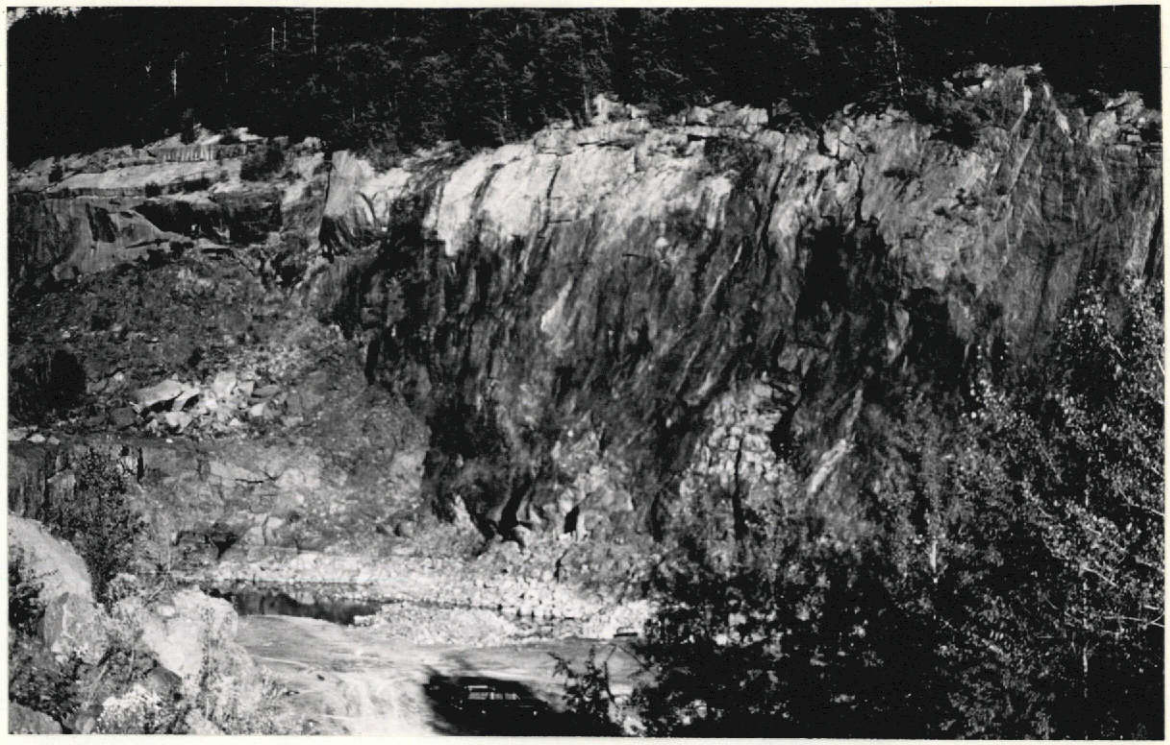

Figure 46. Excavated fault surface at Barton Garnet Mine in the southeastern Adirondacks. The fault marks the contact between the garnetiferous olivine metagabbro ore in the pit and charnockite to the right.

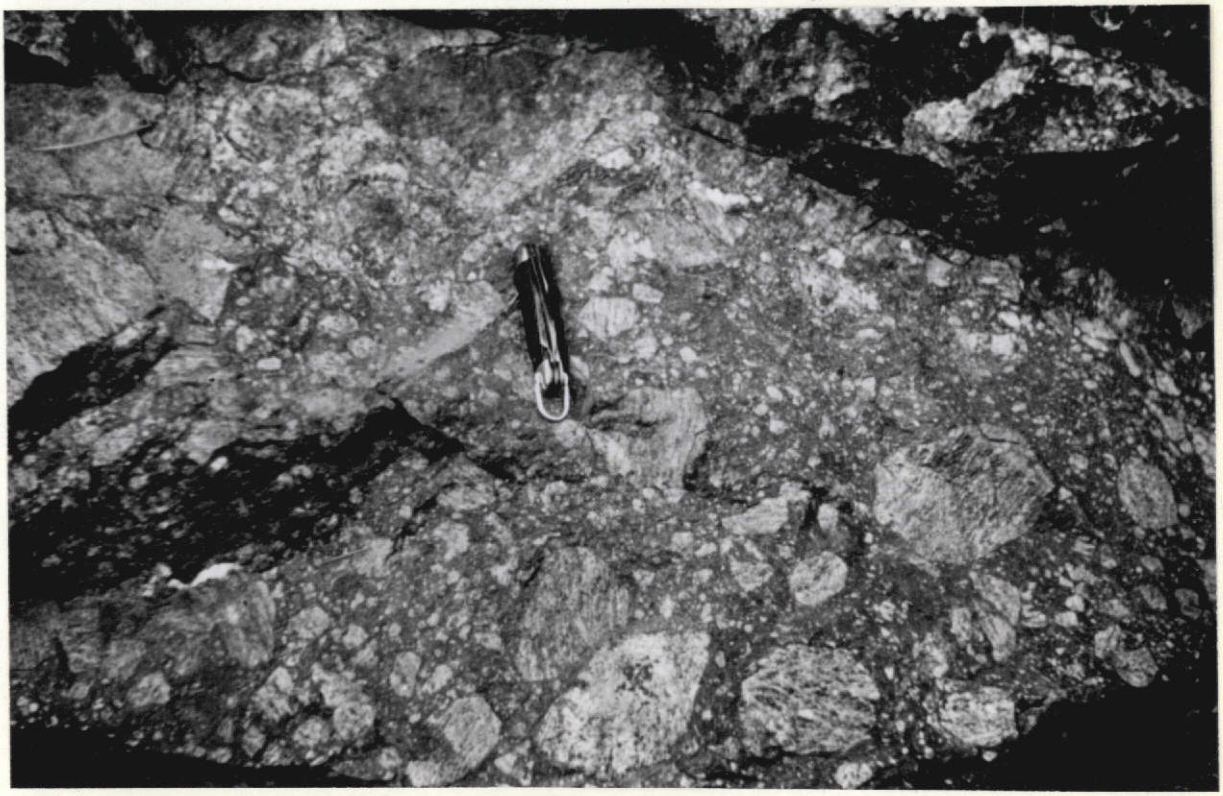

Figure 47. Chloritized fault breccia developed along a N25W fault which forms the valley occupied by Route 9 between Lake George Village and Warrensburg, southeastern Adirondacks.

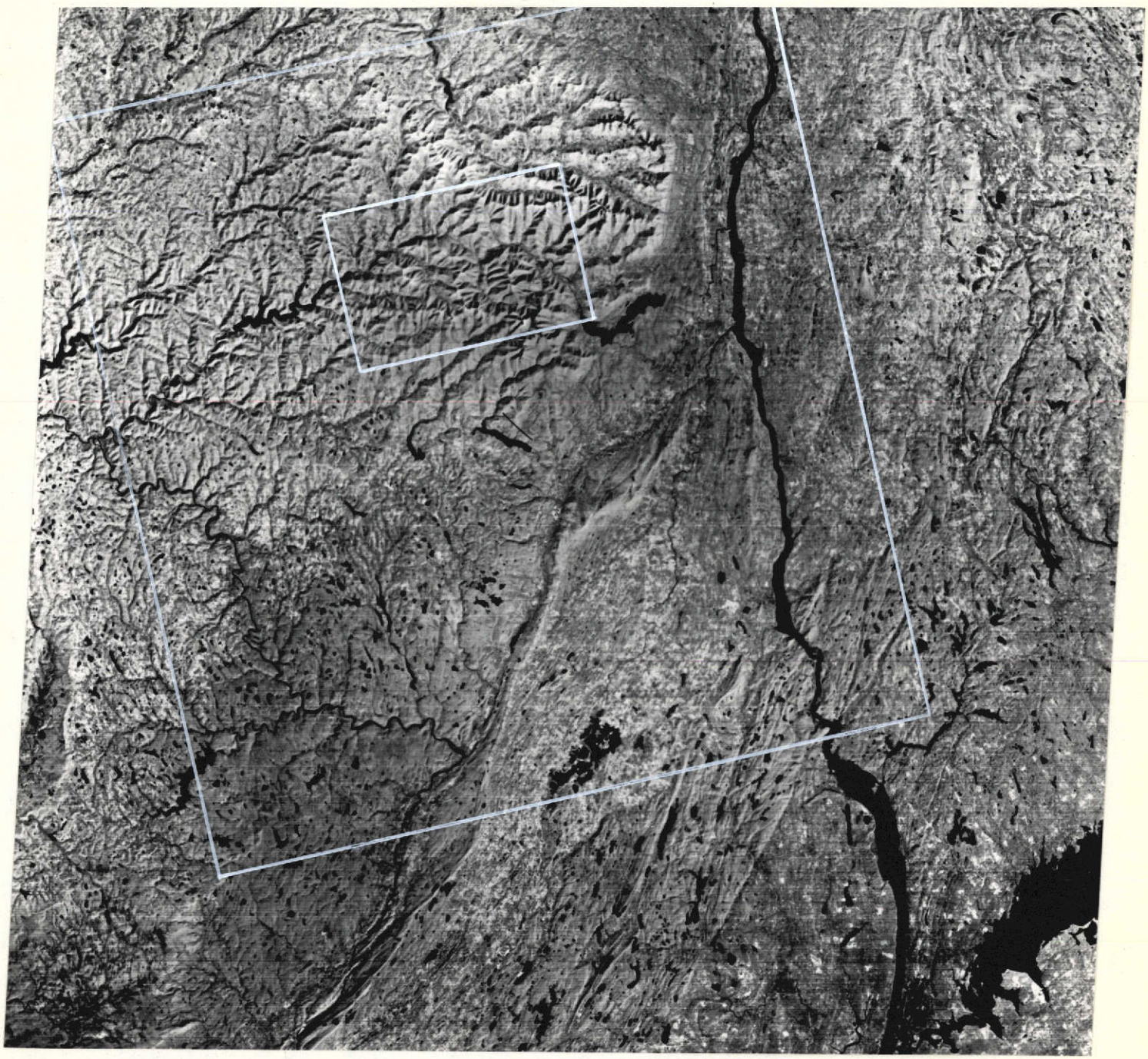

Figure 48. Black and white print made from color composite of 100ct72 image (no. 1079-15124) of southeastern New York from which fall analysis was made. Scale, 1mm = 1 km. Large square outlines the 30 quadrangle field study area. Small box indicates Margarettville and Phoenicia 15 minute quadrangles.

Figure 49. Black and white print made from color composite of 13Feb73 (no. 1205-15132) of southeastern New York from which winter analysis was made. Scale, 1 mm = 1 km.

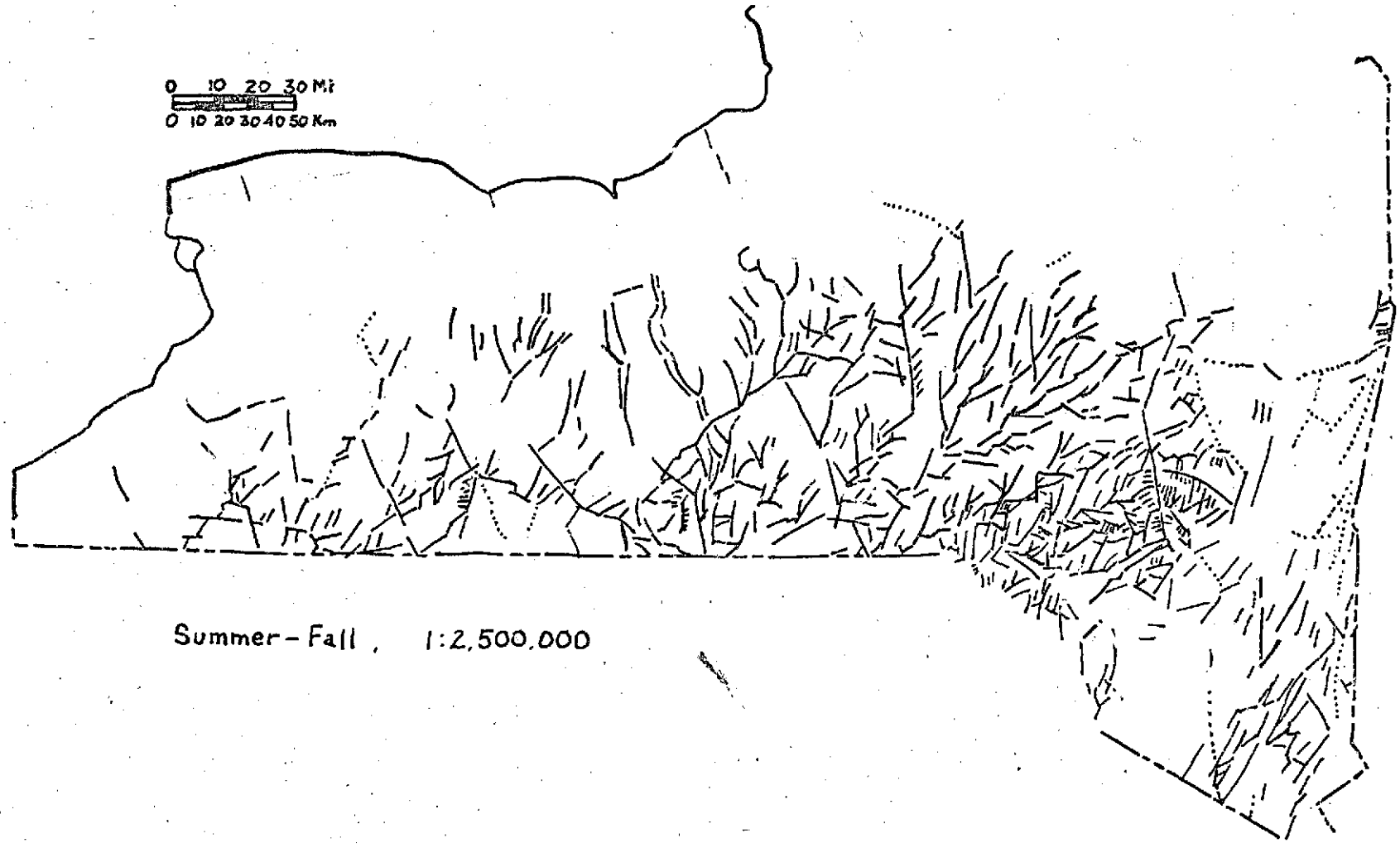

Figure 50. Linears observed on ERTS-1 mosaic of New York and surrounding region made from 1:1,000,000 late summer and early fall imagery of 1972, band 7 (Figure 7); analyzed at 1:2,500,000 scale.

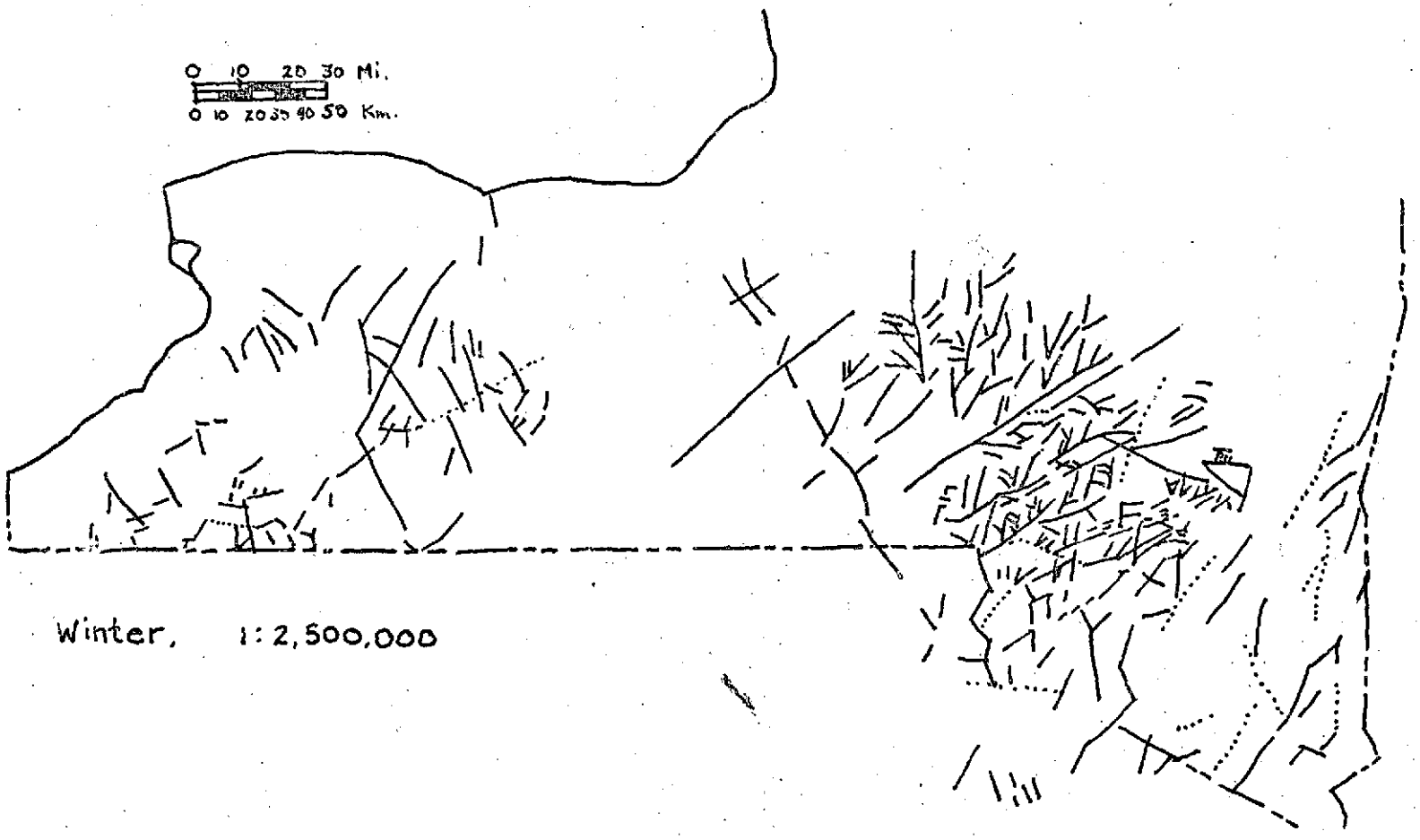

Figure 51. Linears observed on ERTS-1 mosaic of New York and surrounding region made from 1:1,000,000 winter imagery of 1972-73, band 7 (Figure 8); analyzed at 1:2,500,000 scale.

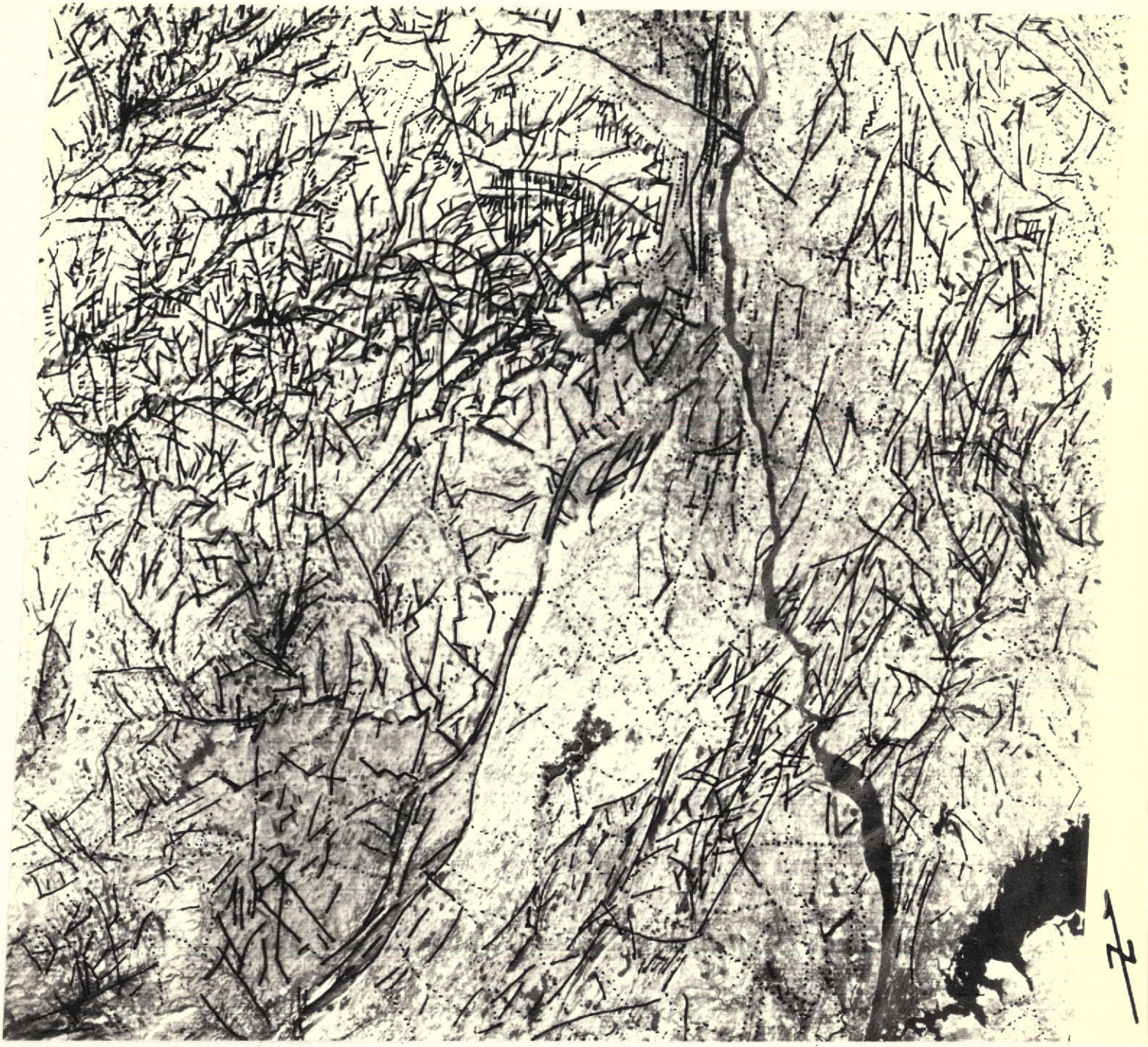

Figure 52a. Linears observed on fall imagery of 100ct72 (no. 1079-15124) of southeastern New York superimposed on ERTS-1 imagery. Scale, 1 mm = 1 km. Solid lines are topographic linears; dotted lines are tonal linears.

Figure 52b. Linears observed on fall imagery of 10Oct72, southeastern New York.

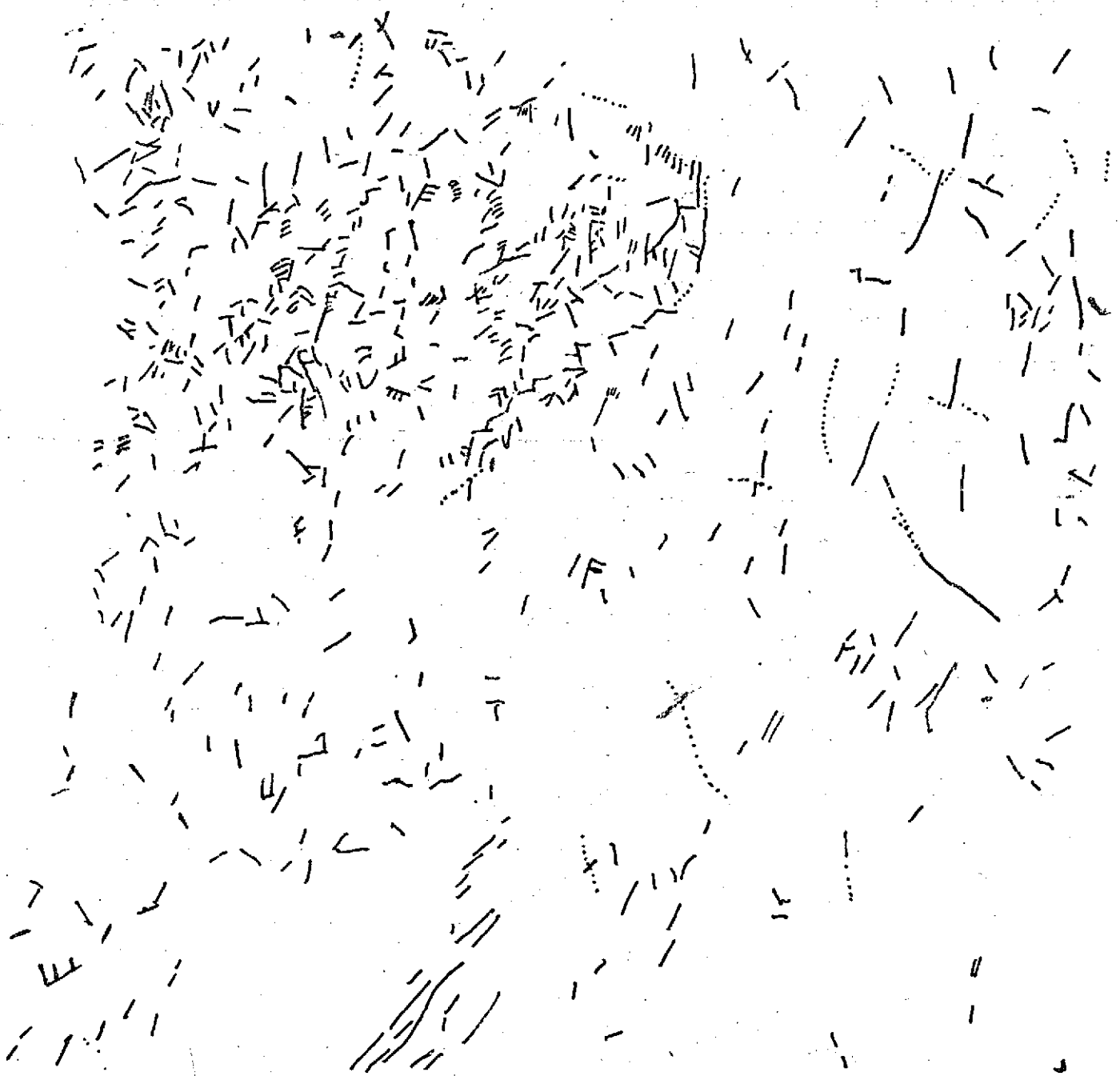

Figure 53. Linears observed on winter imagery of 13Feb73 (no. 1205-15132) of southeastern New York that were not seen on the fall image. Scale, 1 mm = 1 km. Solid lines are topographic linears; dotted lines are tonal linears.

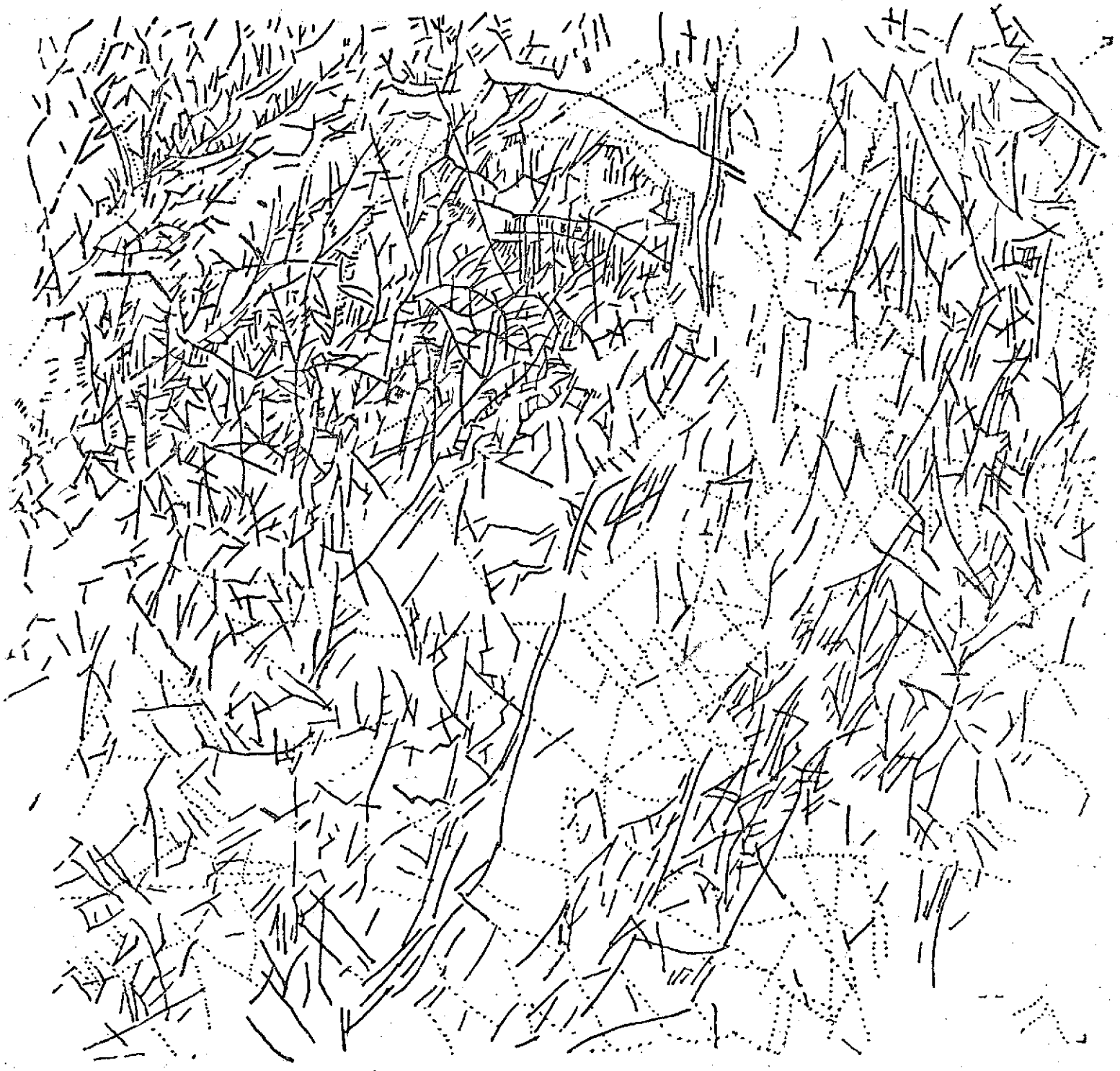

Figure 54. Linears observed on all imagery for fall 1972 and winter 1973 (nos. 1205-15132 and 1079-15124) of southeastern New York. Scale, 1 mm = 1 km. Solid lines indicate topographic linears on at least one of the images; dotted lines represent tonal linears on all images.

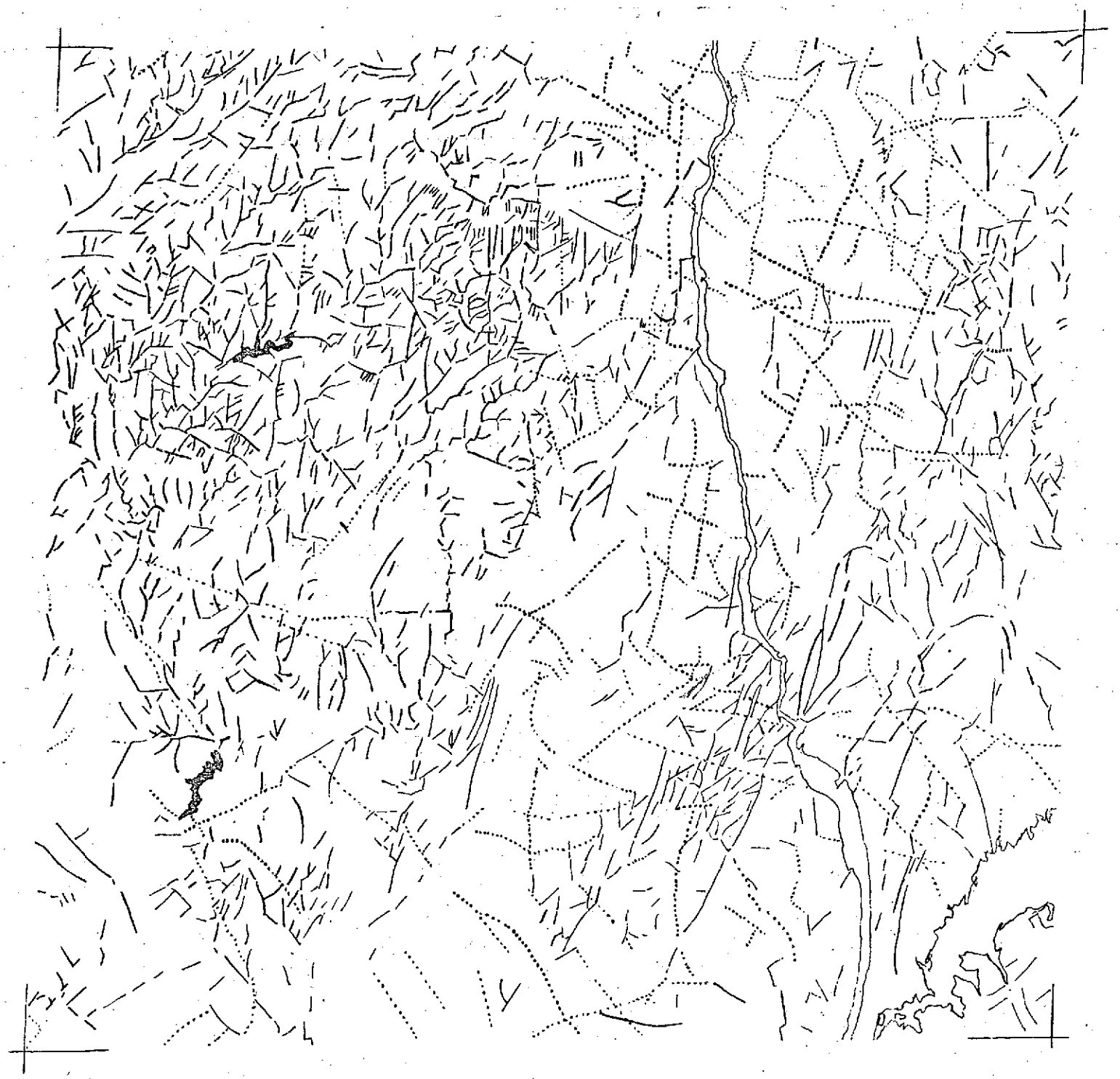

Figure 55. Linears observed at 1:500,000 on black and white print of 100ct72 (image no. 1079-15124-7) of southeastern New York. This Figure is the 1:500,000 analysis on acetate reduced back to a scale of 1:1,000,000.

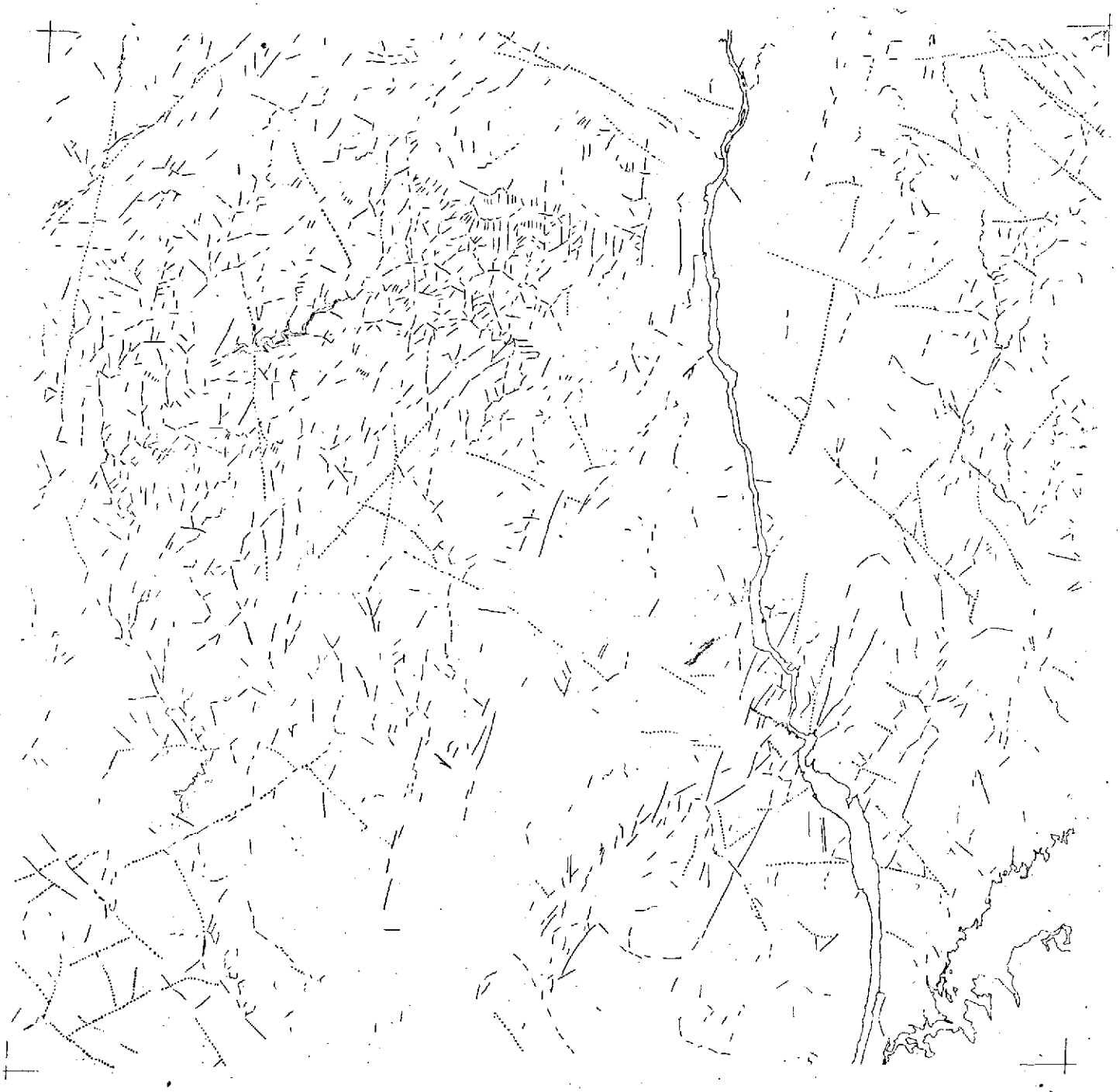

Figure 56. Linears observed on black and white print of 100ct72 image (no. 1079-15124-7) of southeastern New York enlarged to 1:250,000 scale. This Figure is the 1:250,000 analysis on acetate reduced back to a scale of 1:1,000,000.

Figure 57. Map of straight valleys observed on 1:62,500 topographic quadrangle maps of Margaretville (left) and Phoenicia (right); see Figure 48 for location. Original analysis at 1:62,500 is here reduced to approximately 1:150,000 scale.

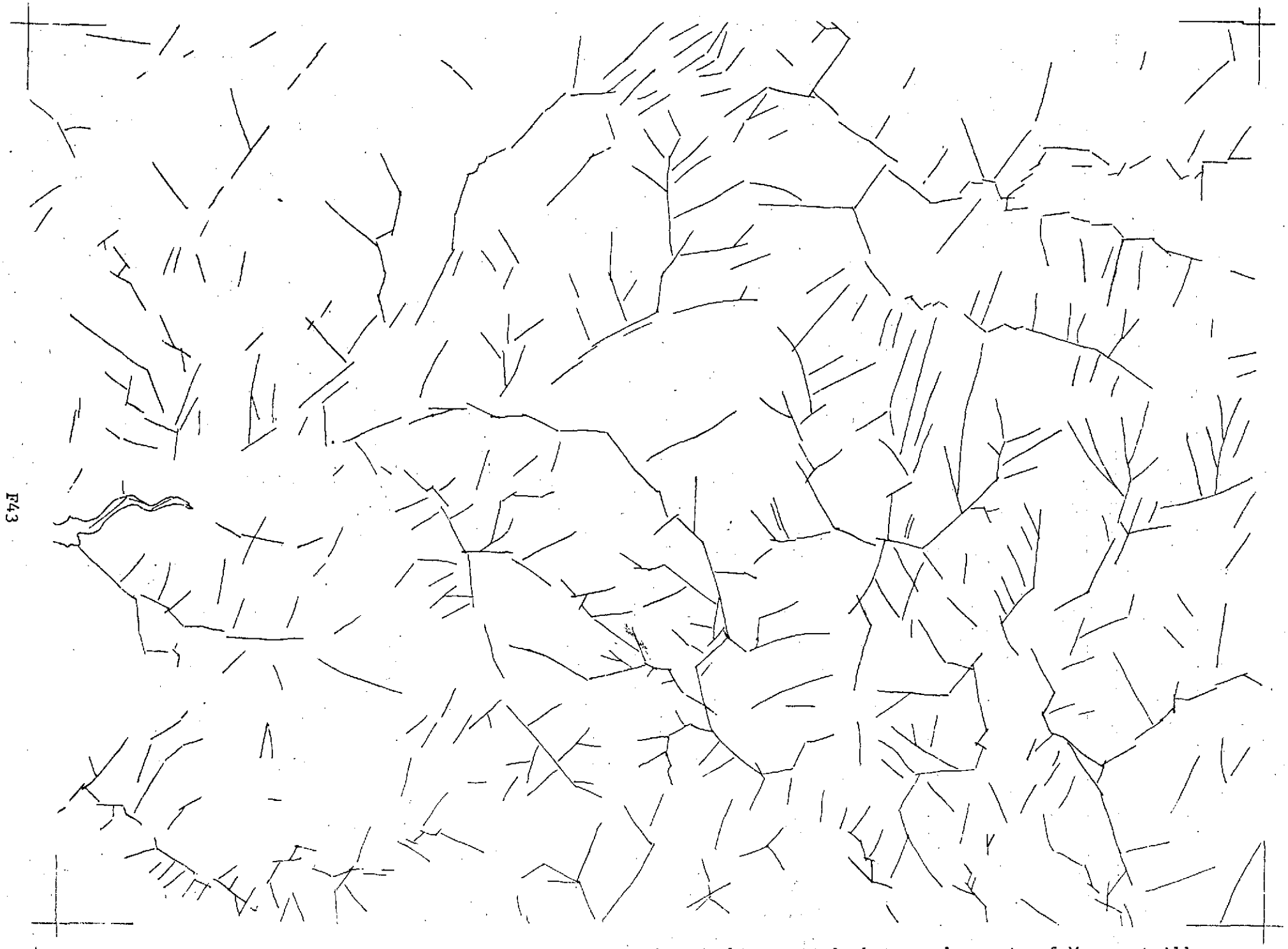

Figure 58. Straight valleys observed on 1:62,500 scale black and white aerial photograph mosaic of Margaretville (left) and Phoenicia (right) quadrangles (see Figure 48 for location). Original analysis at 1:62,500 is here reduced to approximately 1:150,000.

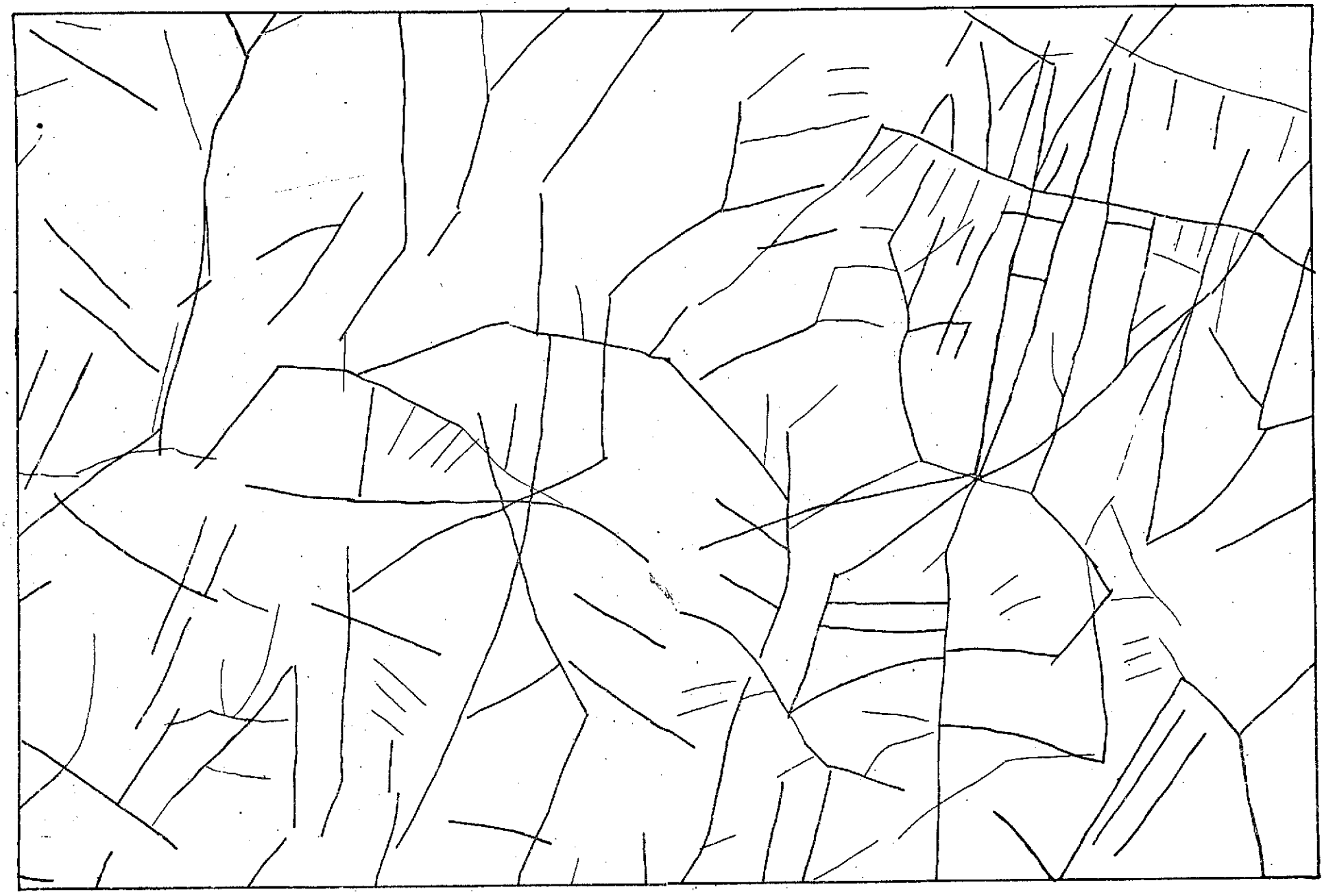

Figure 59. ERTS-1 linears in area of Margaretville and Phoenicia quadrangles, as observed at 1:1,000,000, enlarged to approximately 1:150,000.

Figure 60. Geologic provinces of southeastern New York, shown on ERTS-1 image no. 1079-15124, band 7.

Figure 61. ERTS-1 image showing location of the 30 15 minute quadrangles of field study area in the Catskill Mountains, Hudson Lowlands and Hudson Highlands.

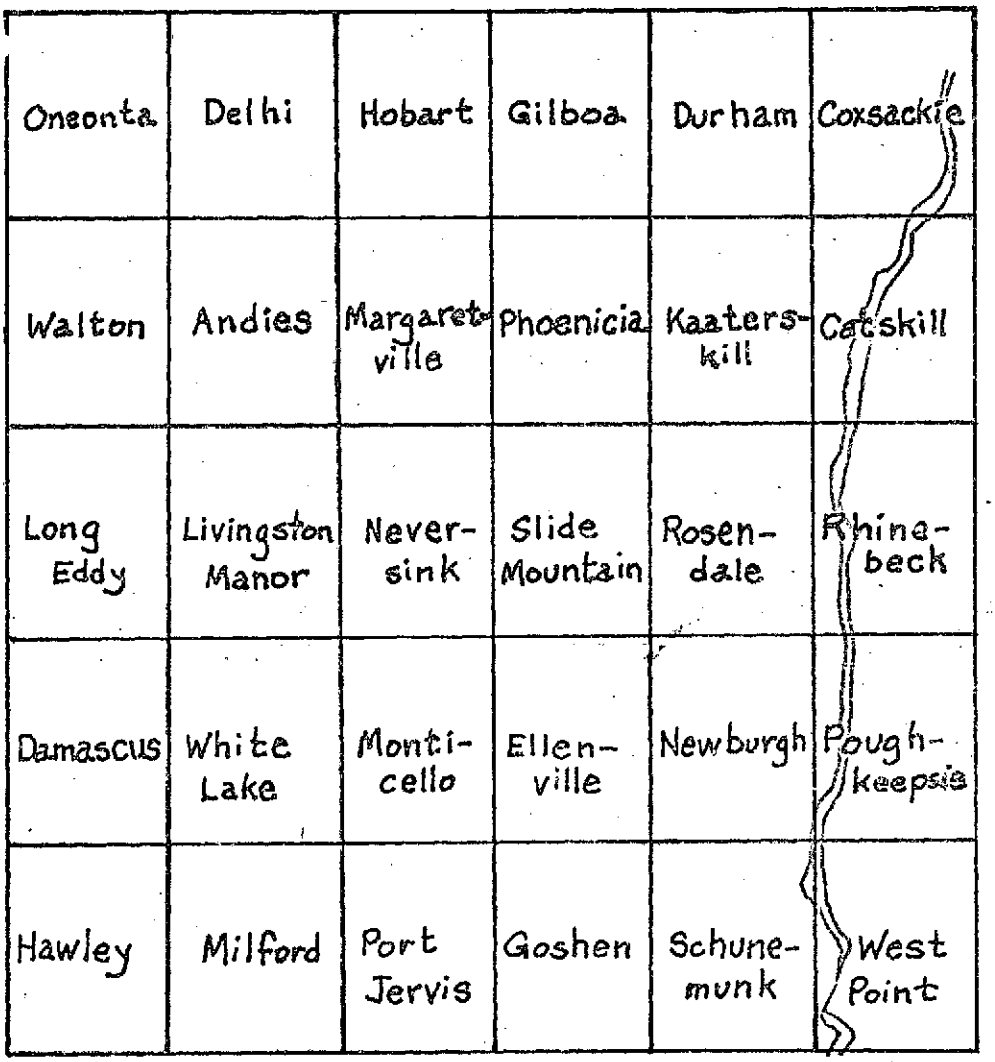

Figure 62. Index map identifying the 30 15 minute quadrangle maps of the field study area in southeastern New York.

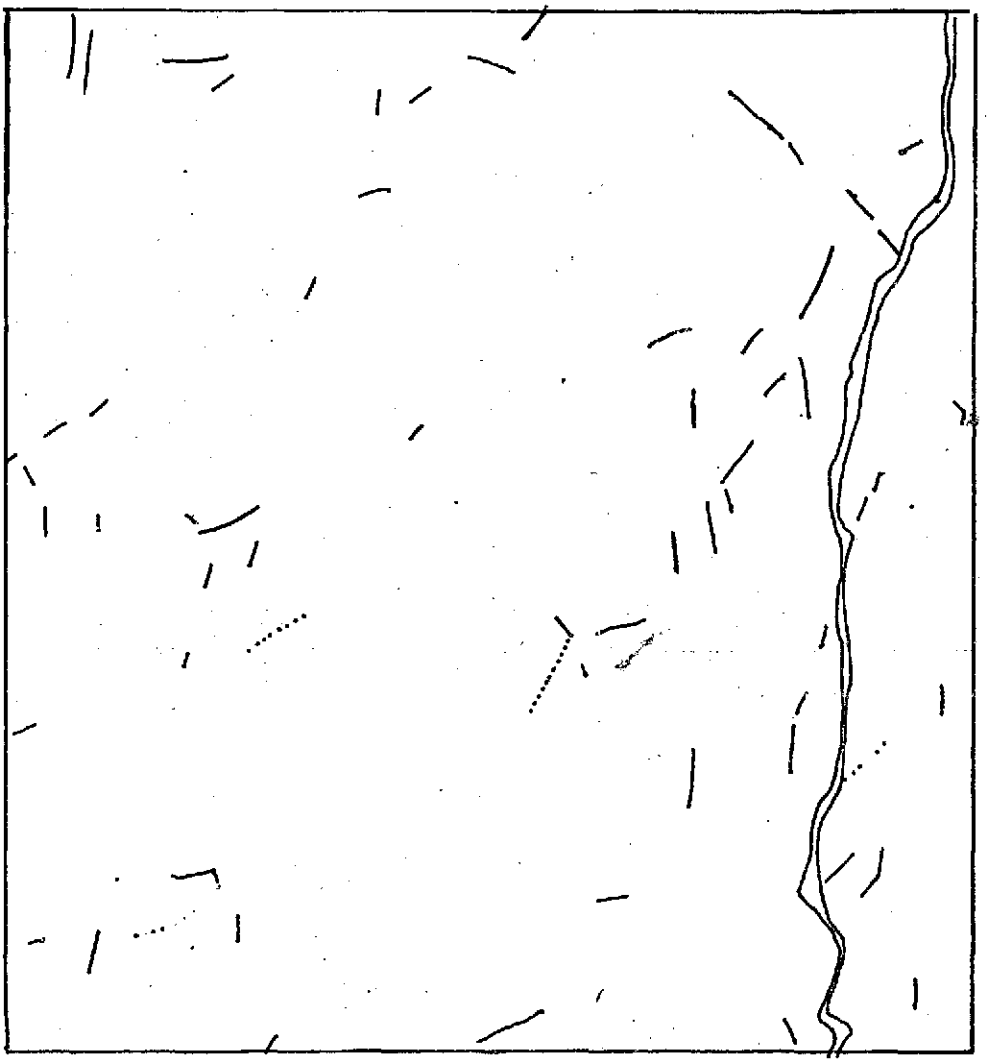

Figure 63. ERTS-1 linears in field study area which have different signatures on the fall and winter imagery. Linears which have tonal signatures on the fall image, and topographic signatures on the winter image, are shown by solid line. Dotted lines signify the reverse.

Figure 64. ERTS-1 image showing field localities listed in table 3 (dots) and sites from which photographic illustrations were taken (barbs on the dots indicate view directions, and the accompanying numbers refer to figures in text). Scale: 2mm = 1km.

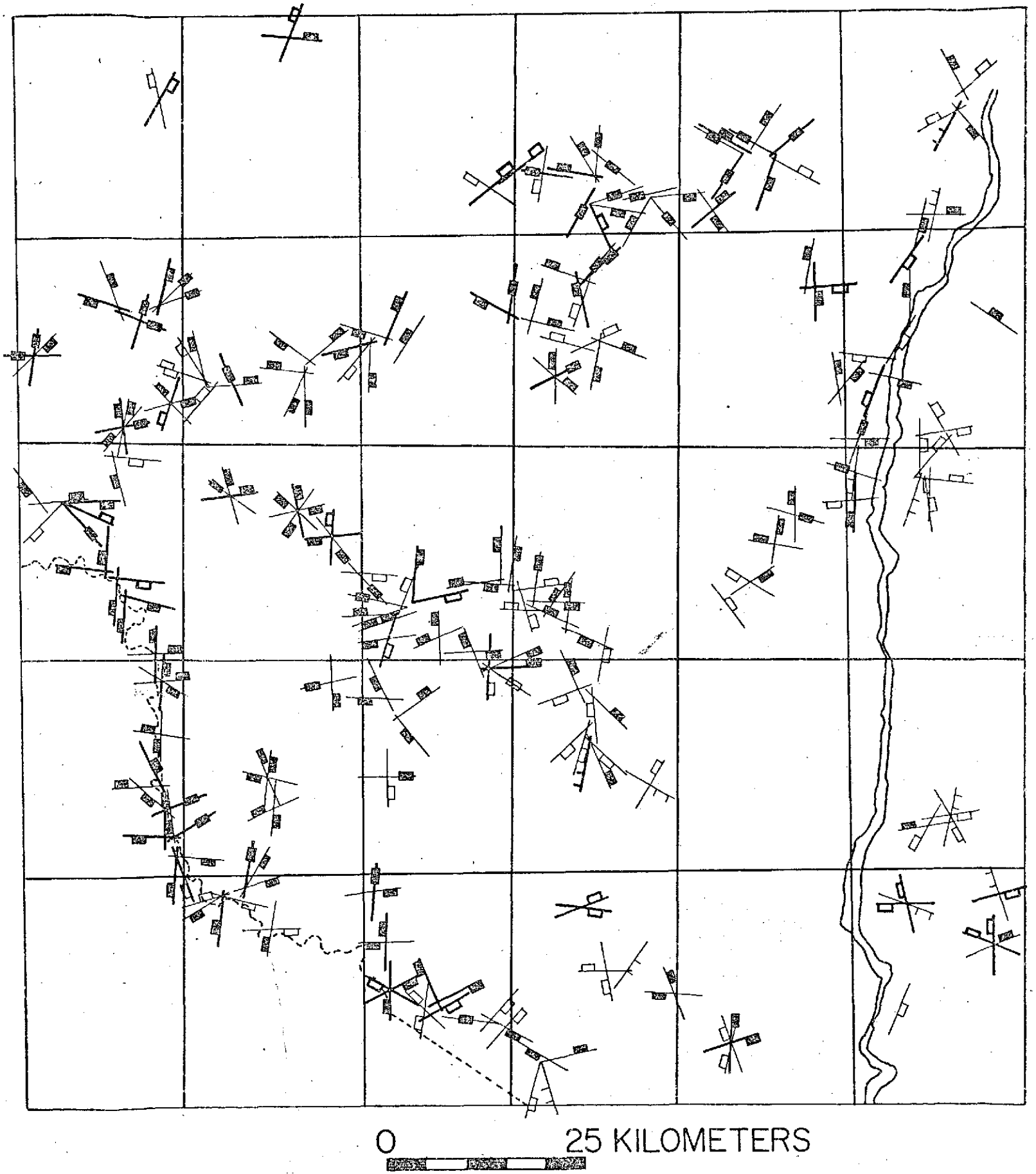

Figure 65. Map of joint data from 30 quadrangle field study area. Thick symbols are master joint sets, thin symbols are weak joint sets. Solid boxes indicate dips greater than 60 degrees, open boxes signify dips between 30 and 60 degrees, and double barbs indicate dips less than 30 degrees.

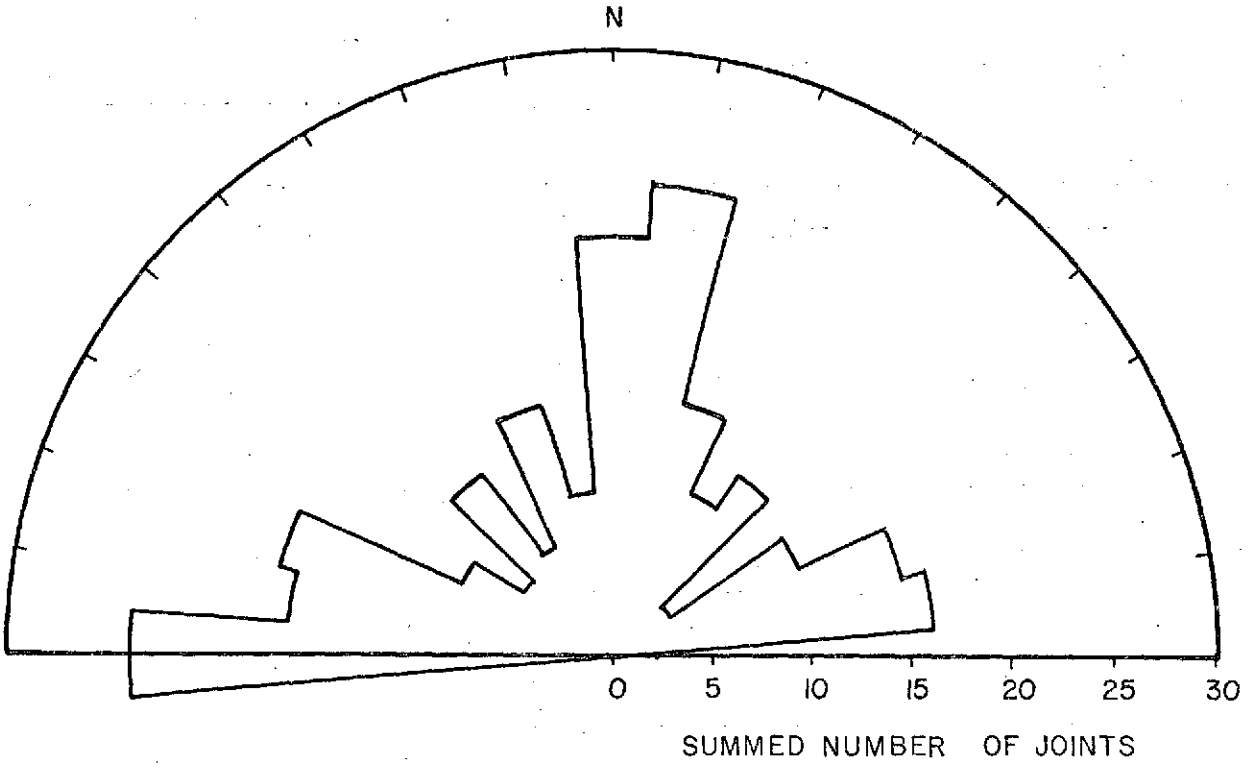

Figure 66a. Rose diagram of 230 joint measurements in 30 quadrangle field study area. Only joints with dips greater than 60 degrees are included.

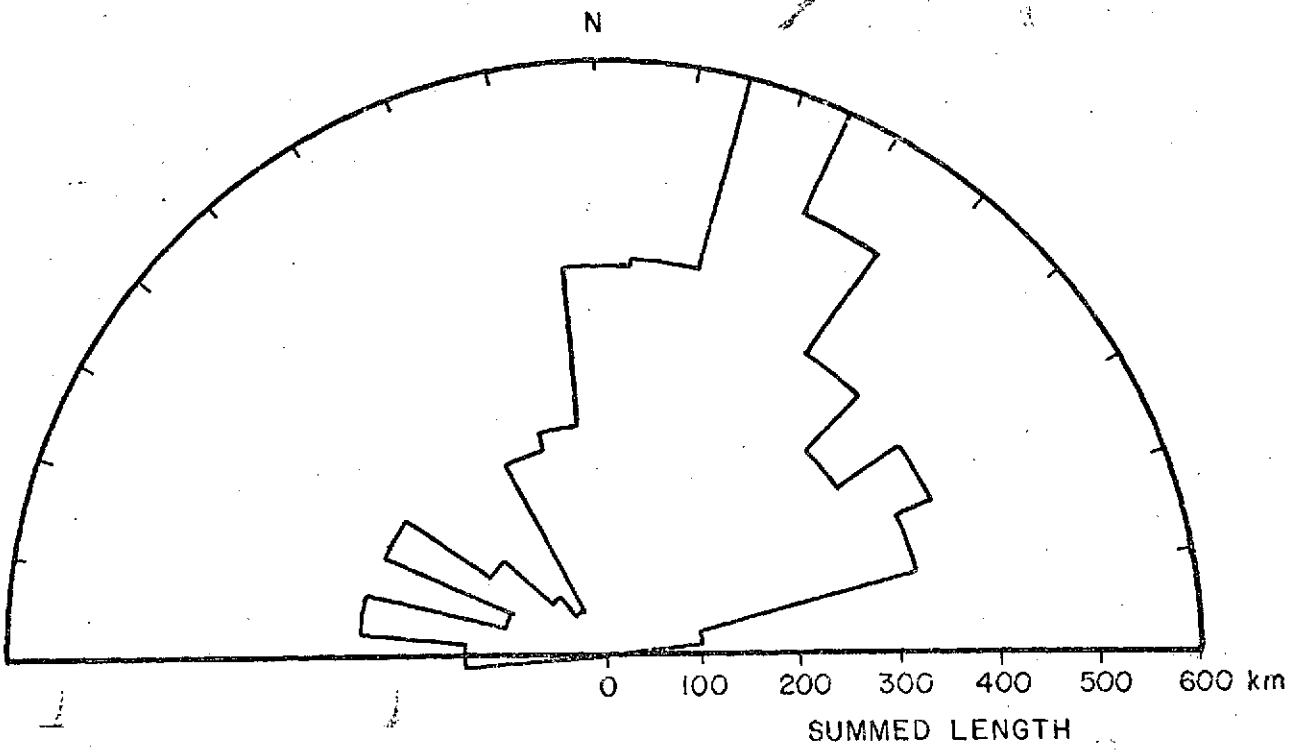

Figure 66b. Rose diagram of linears in Zone 7. Zone 7 includes much of the 30 quadrangle field study area.

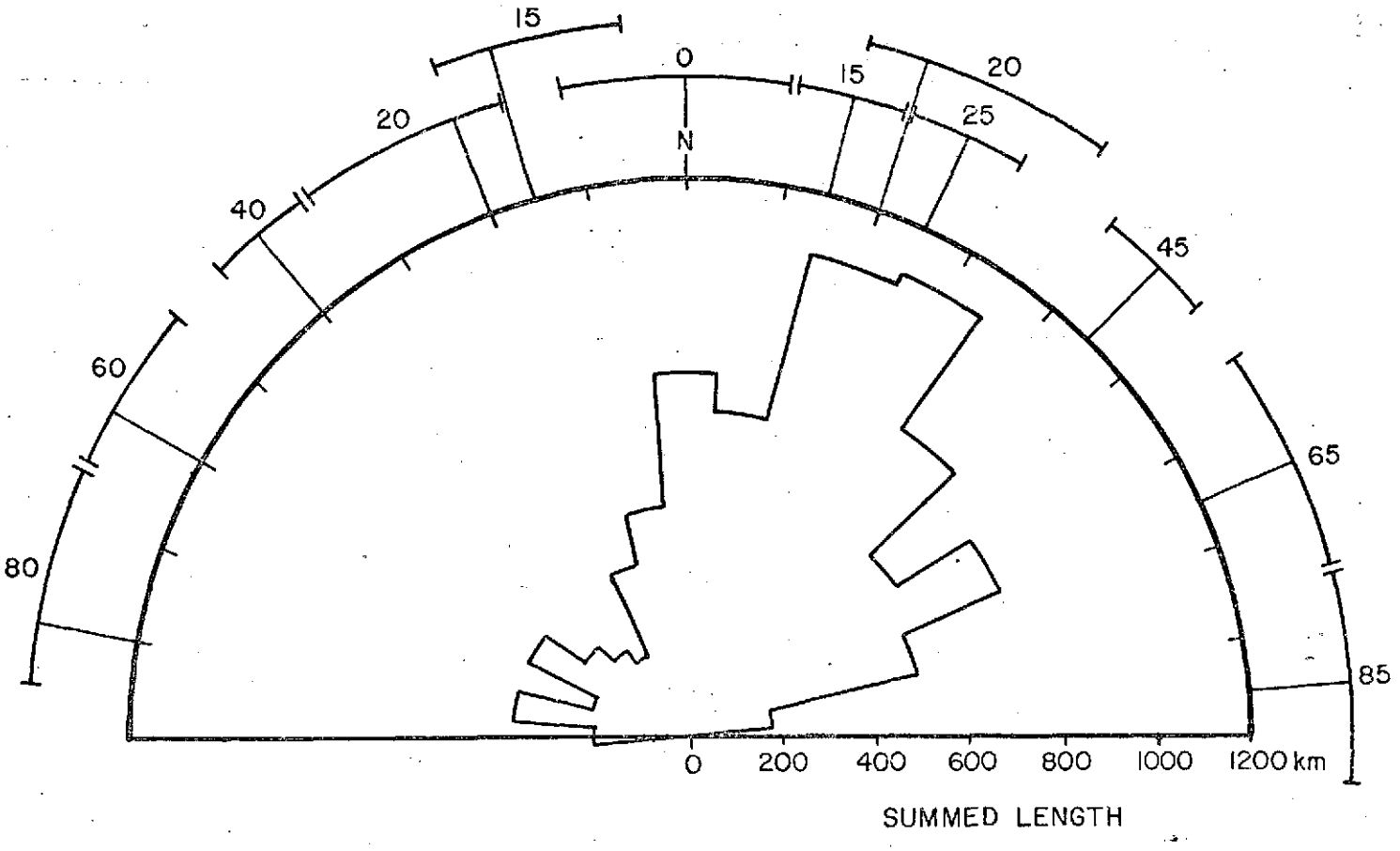

Figure 67. Rose diagram of summed lengths of linears of southeastern New York. Outer arcs represents range of azimuth variation for the linear sets described in table 2. Average azimuths of these linears are lettered along the arcs.

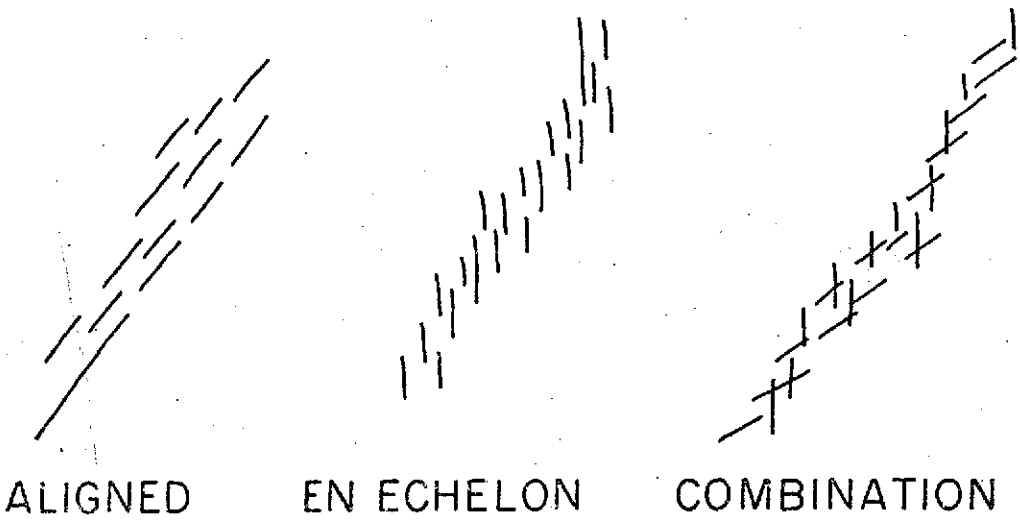

Figure 68. Variations in linear zone geometry.

Figure 69. Aerial oblique view of small segment of "Wall of Manitou" showing its straightness. Note also, perpendicular to the Wall, at least four parallel linears: two tonal and two tonal-topographic. The bedrock consists of interbedded red and green shales and cross-bedded sandstones of the Catskill facies. From color-infrared photo.

Figure 70. Aerial oblique view of suspected sag pond located on the Wall of Manitou. The apparent inclination of the horizontal strata is a photographic illusion. From color-infrared photo.

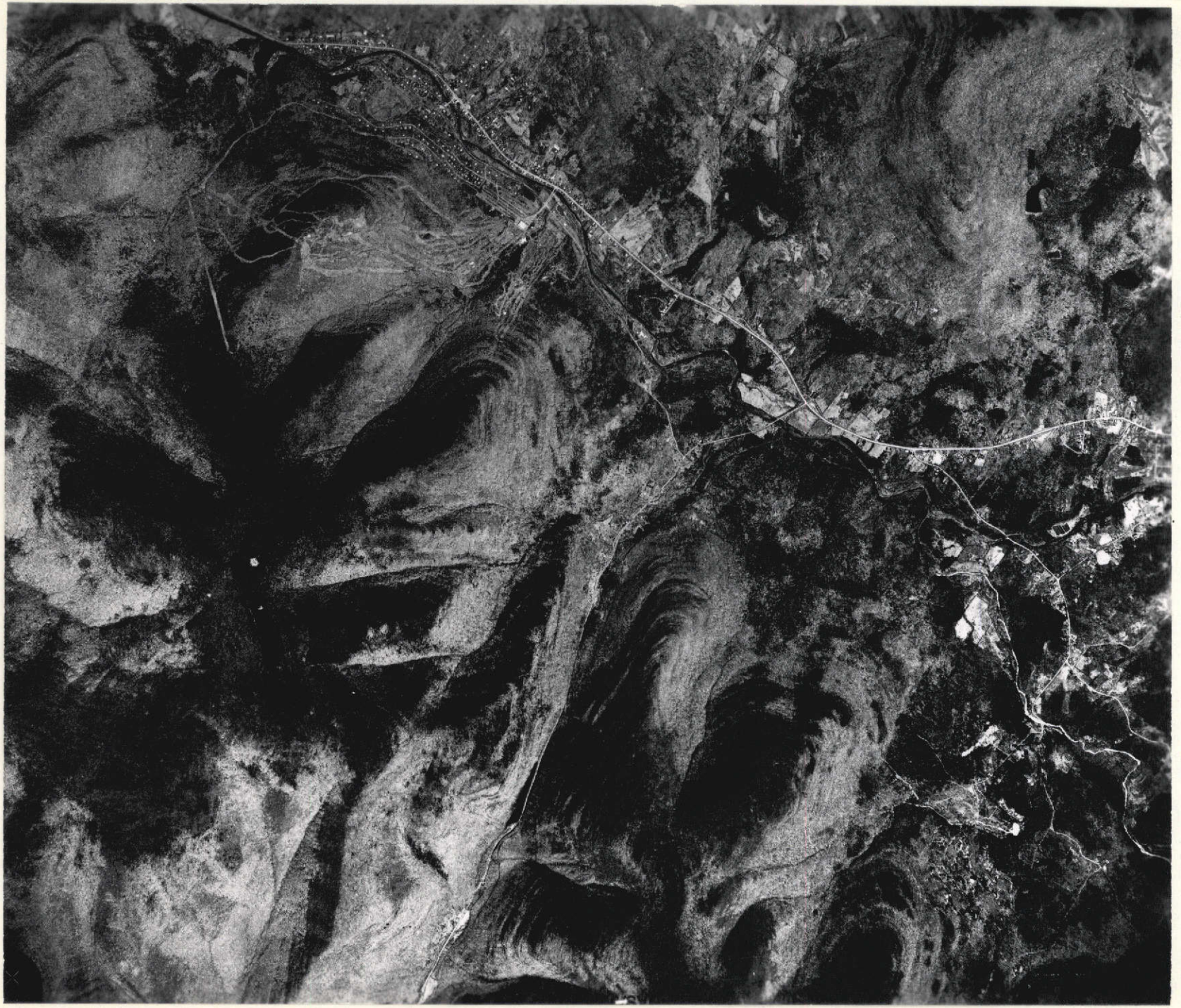

Figure 71. Print from color infrared aerial photograph transparency over the eastern Catskill Mountains. North is toward the top of the photograph. Clove Valley linear extends about N15E from the south center of the photo; Hunter Mountain ski area is near the north edge of the photo. Note the pair of N75E topographic linears. Photo by NASA, 30Apr73. Scale: 4 cm = 1 km.

Figure 72. Stony Clove topographic lineament, looking N15E over Edgewood (hidden behind hill in foreground) with drainage divide at Clove in middleground; Hunter 7½' quadrangle. From color-infrared photo.

Figure 73. Stony Clove drainage divide of Figure 72. Outcrop along lower sandstone member on east side of valley is shown in Figure 75. Print was made from color infra-red transparency.

Figure 74. Lowermost cross-bedded sandstone cliff along east wall of Stony Clove, looking north. Note dominance of westward dipping joint set (which parallels valley) and conjugate joints at east side of outcrop; dips are 75°E and 73°W making an acute angle of 32°.

Figure 75. Looking west-southwest at the Wall of Manitou and along linear no. 75 which runs up the center of the picture. On ERTS-I imagery it appears as a tonal linear (Figure 64), but here it can be identified as a topographic lineament. Note at least three other examples which do not show on ERTS imagery.

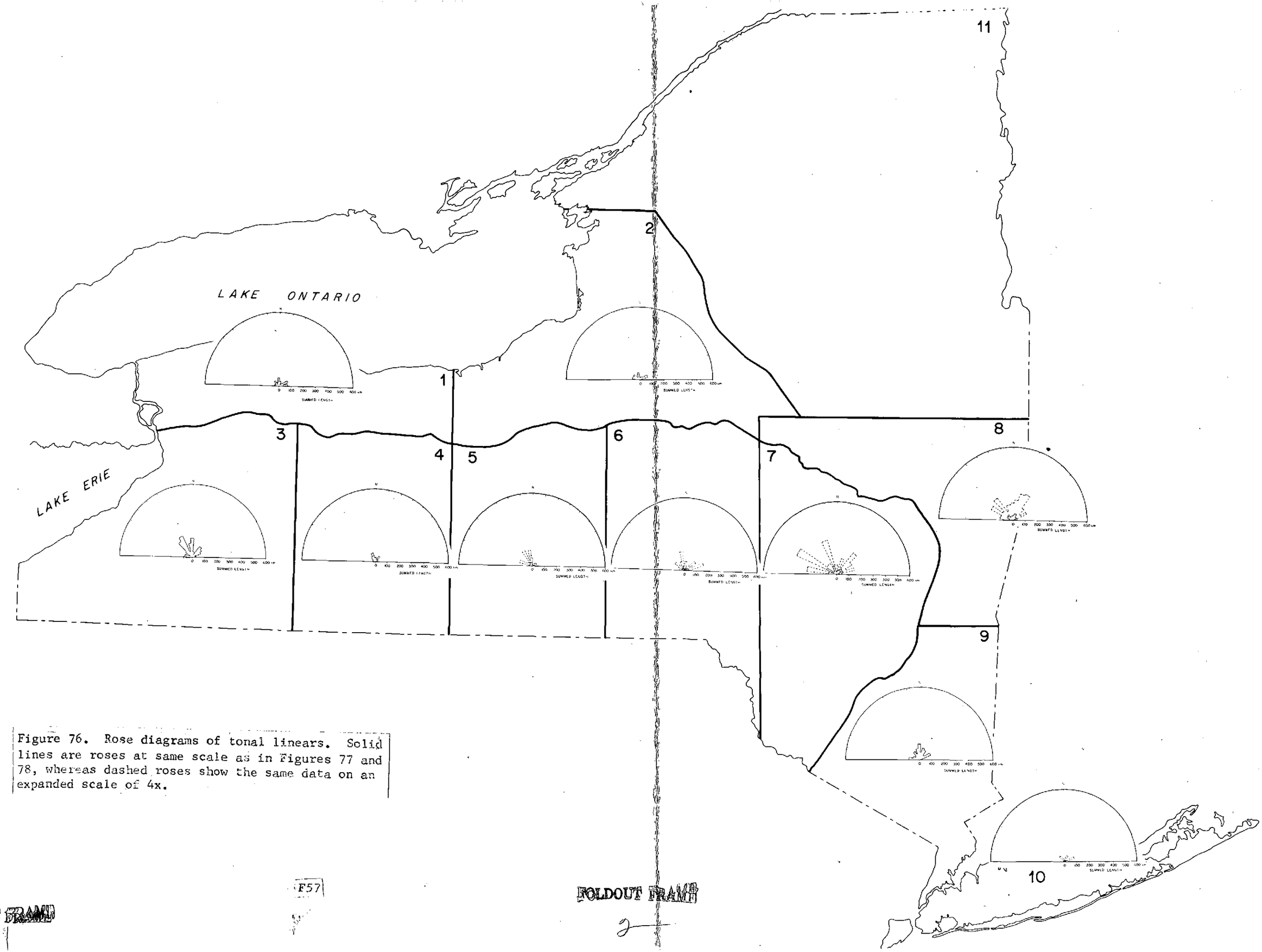

Figure 76. Rose diagrams of tonal linears. Solid lines are roses at same scale as in Figures 77 and 78, whereas dashed roses show the same data on an expanded scale of 4x.

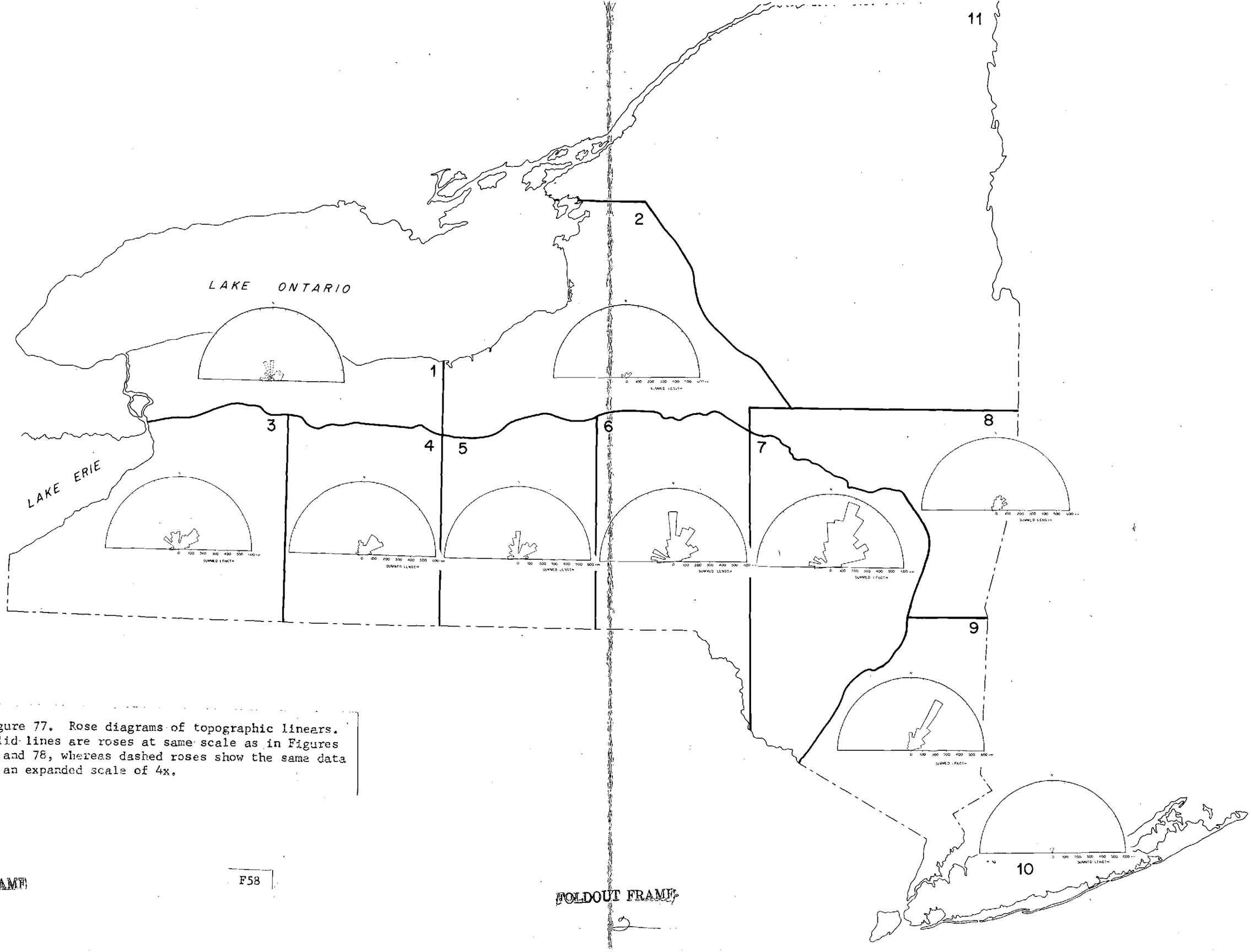

Figure 77. Rose diagrams of topographic linears. Solid lines are roses at same scale as in Figures 76 and 78, whereas dashed roses show the same data on an expanded scale of 4x.

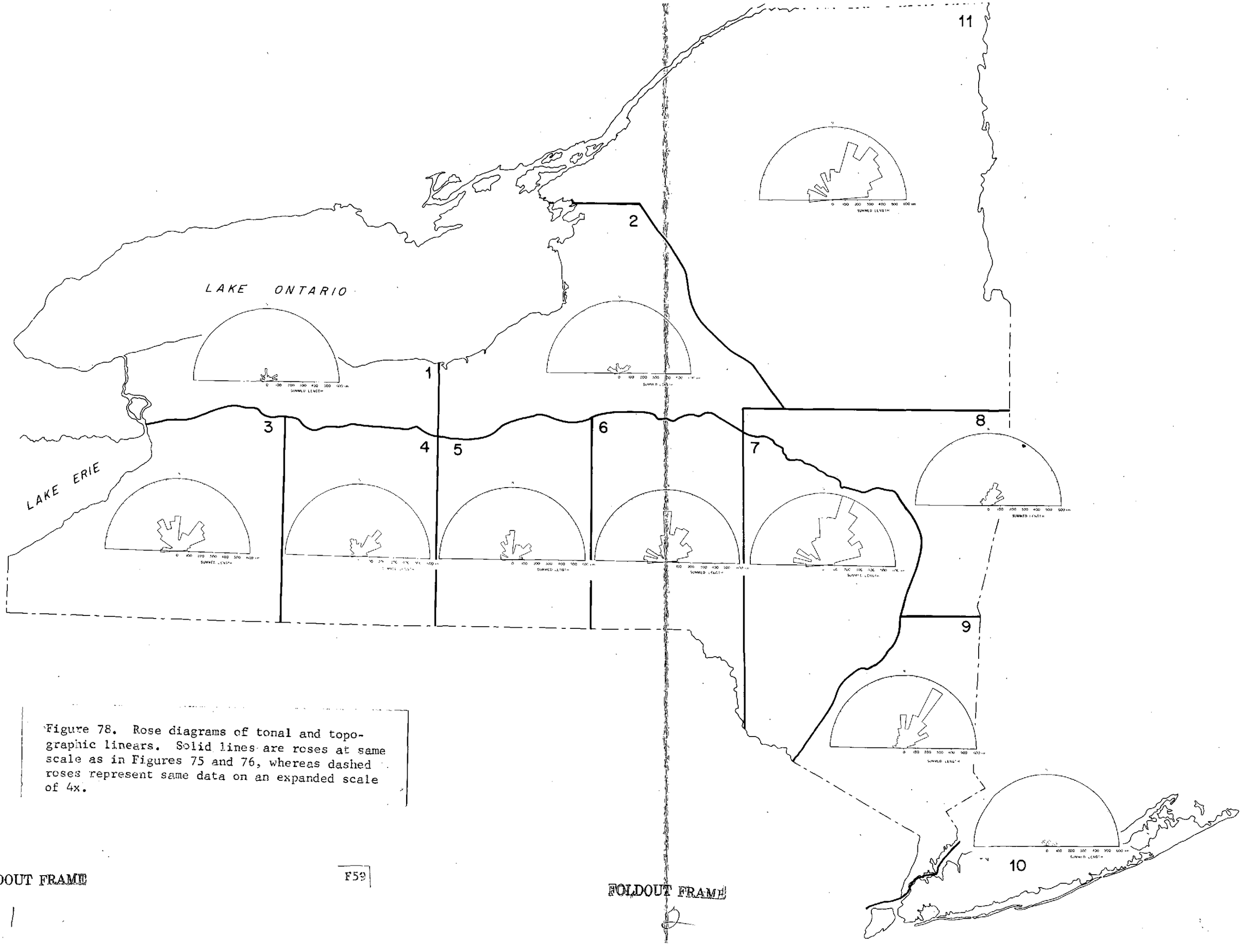

Figure 78. Rose diagrams of tonal and topographic linears. Solid lines are roses at same scale as in Figures 75 and 76, whereas dashed roses represent same data on an expanded scale of 4x.

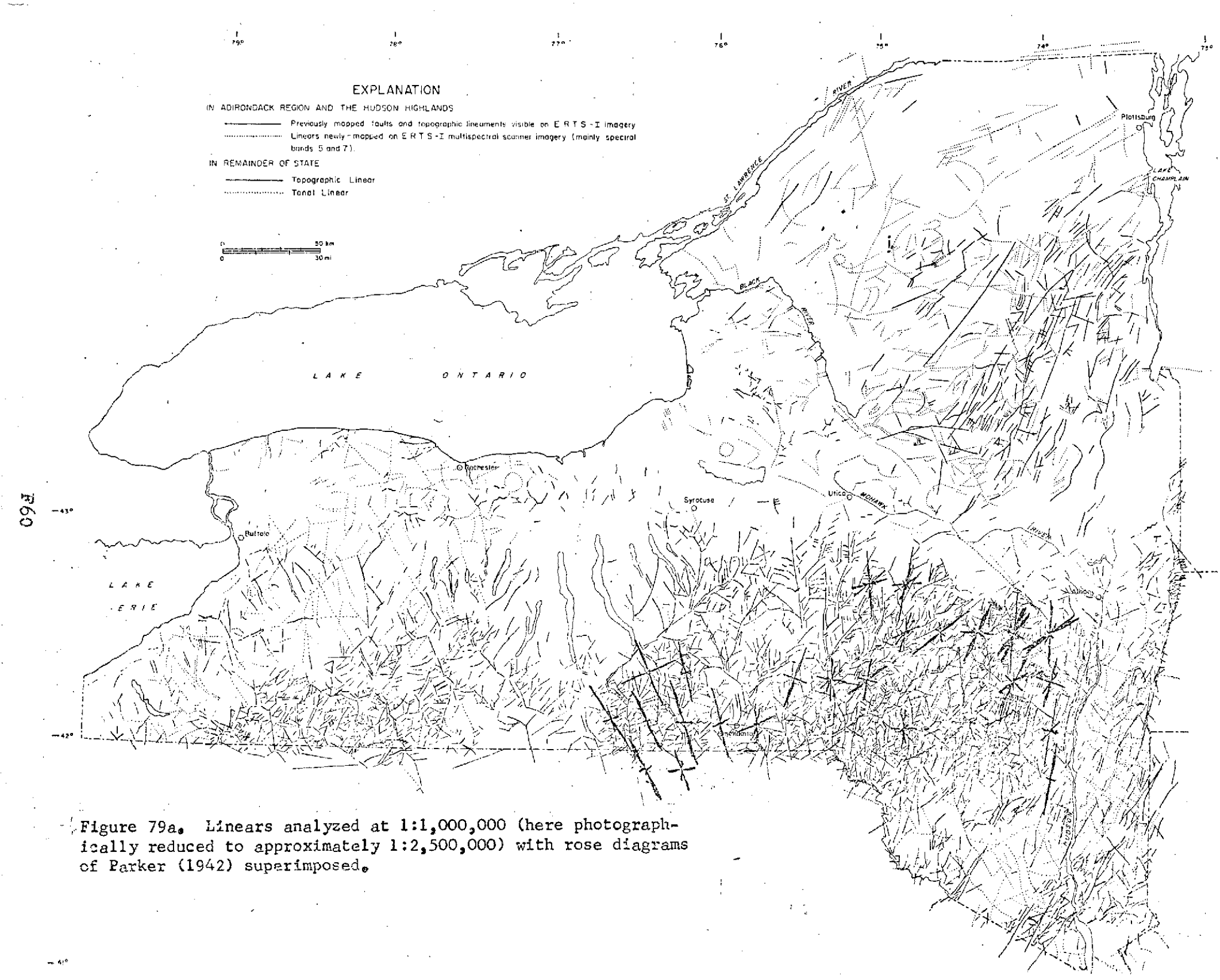

Figure 79a. Linears analyzed at 1:1,000,000 (here photographically reduced to approximately 1:2,500,000) with rose diagrams of Parker (1942) superimposed.

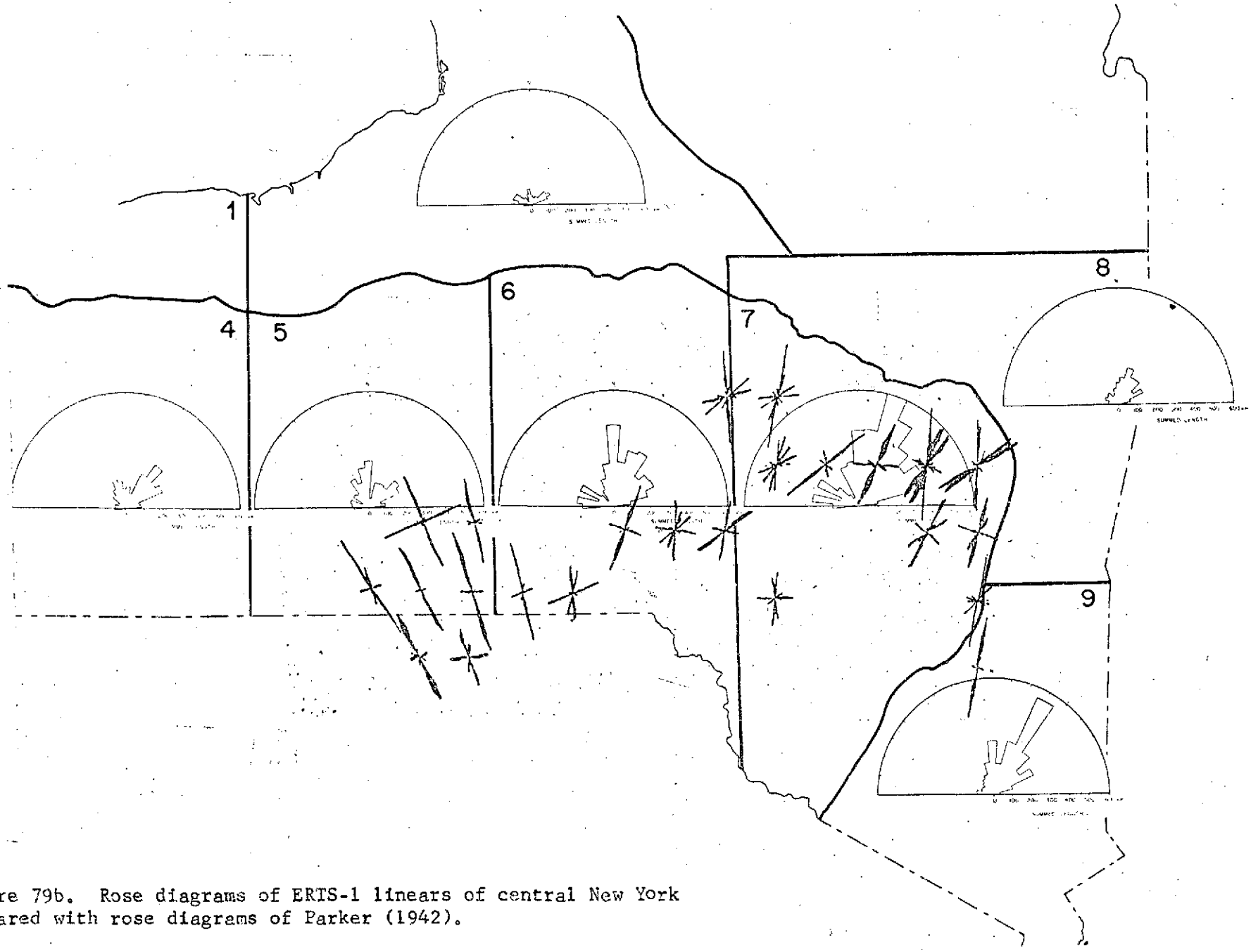

F61

Figure 79b. Rose diagrams of ERTS-1 linears of central New York compared with rose diagrams of Parker (1942).

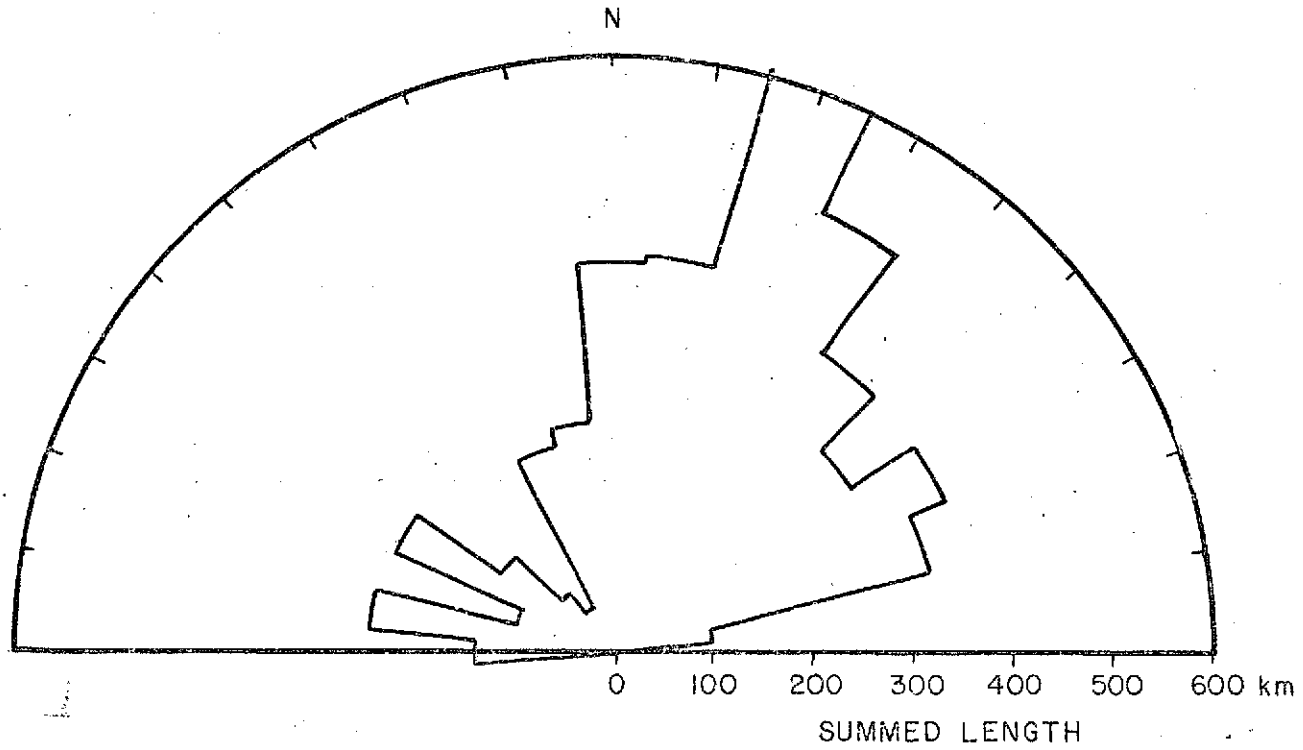

Figure 80a. Rose diagram of ERTS-1 linears in eastern Catskill Mountains, Zone 7.

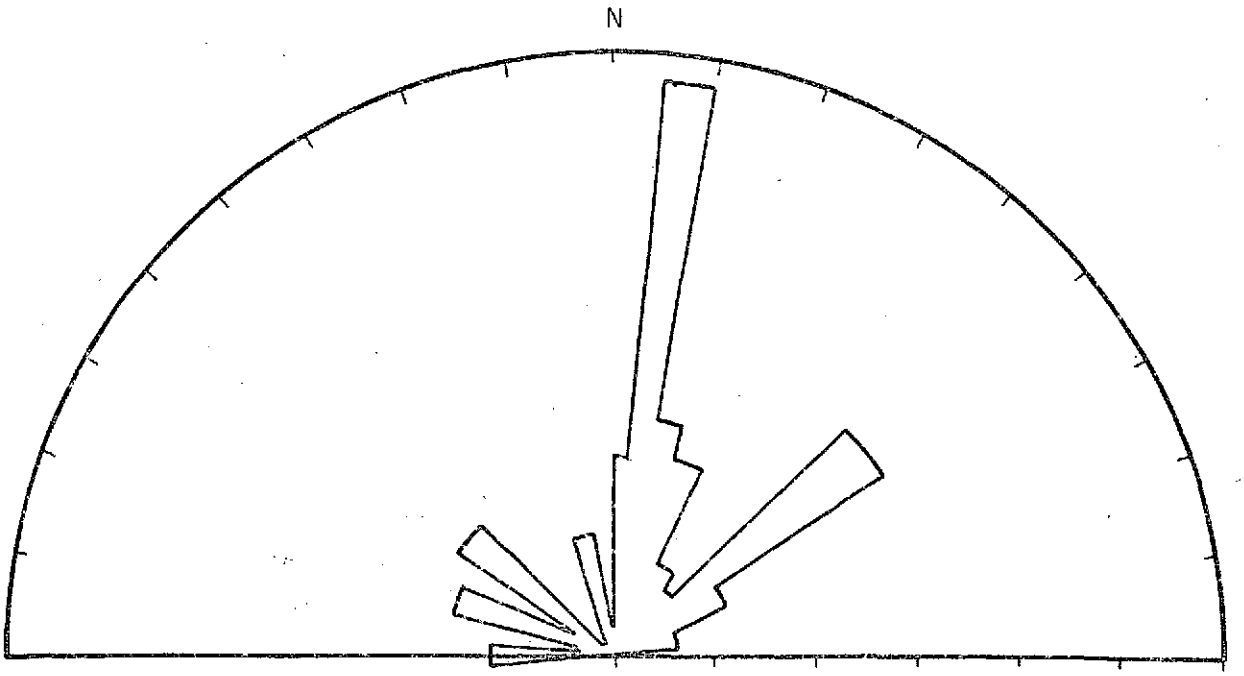

Figure 80b. Rose diagram of joint direction data from Zone 7, derived from Parker's (1942) data.

Figure 81. ERTS-1 linears of New York State and adjacent areas analyzed at 1:500,000, and here reproduced at approximately 1:2,500,000.

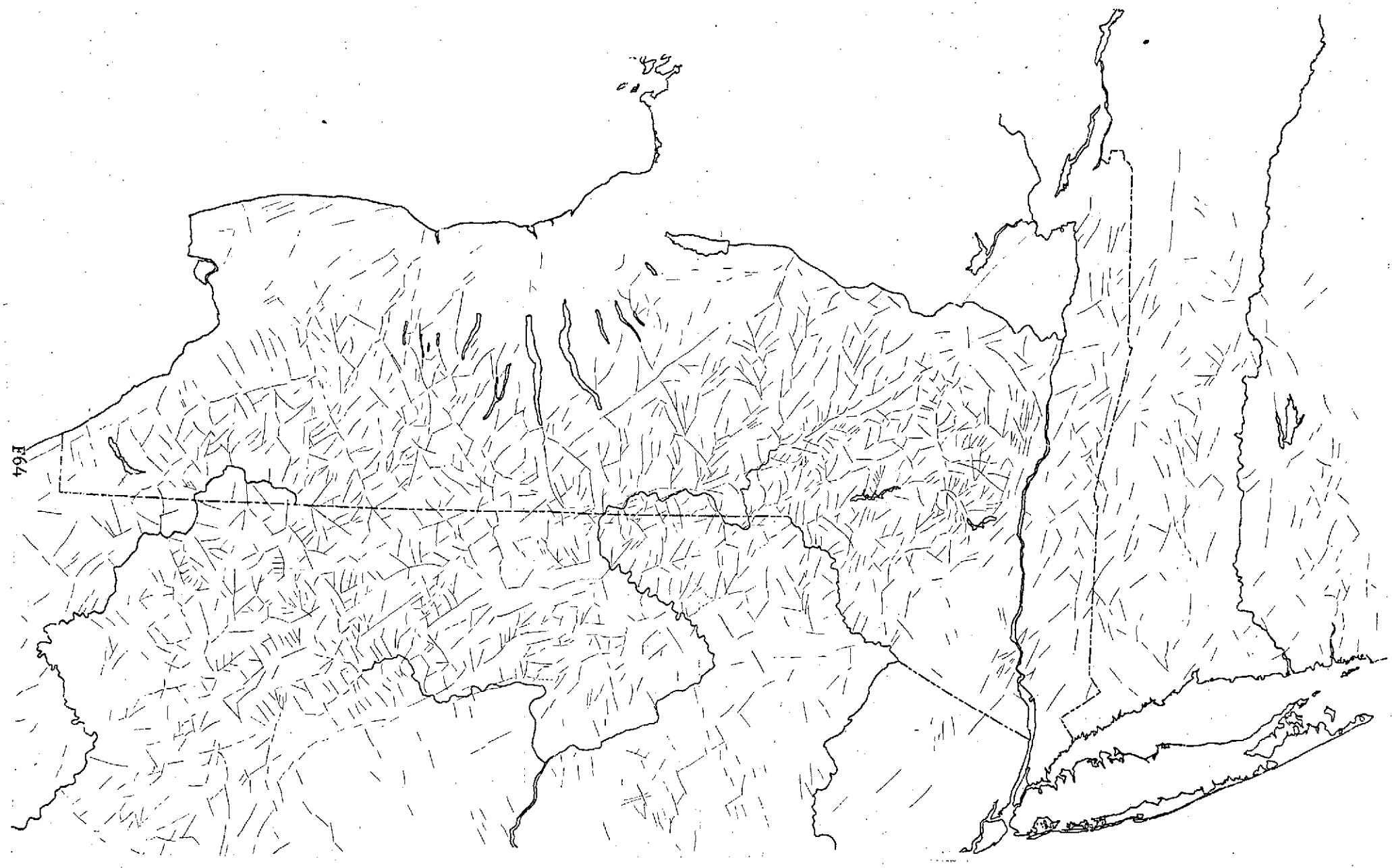

Figure 82. Straight valleys observed on shaded relief map of New York State and adjacent areas at 1:500,000, and here reduced to approximately 1:2,500,000.

Figure 83. Southern portion of scene E2 (image no. 1027-15233), band 5, showing circular features by arrows; dashed arrow indicates sun azimuth and angle. Scale: 1 mm = 1 km.

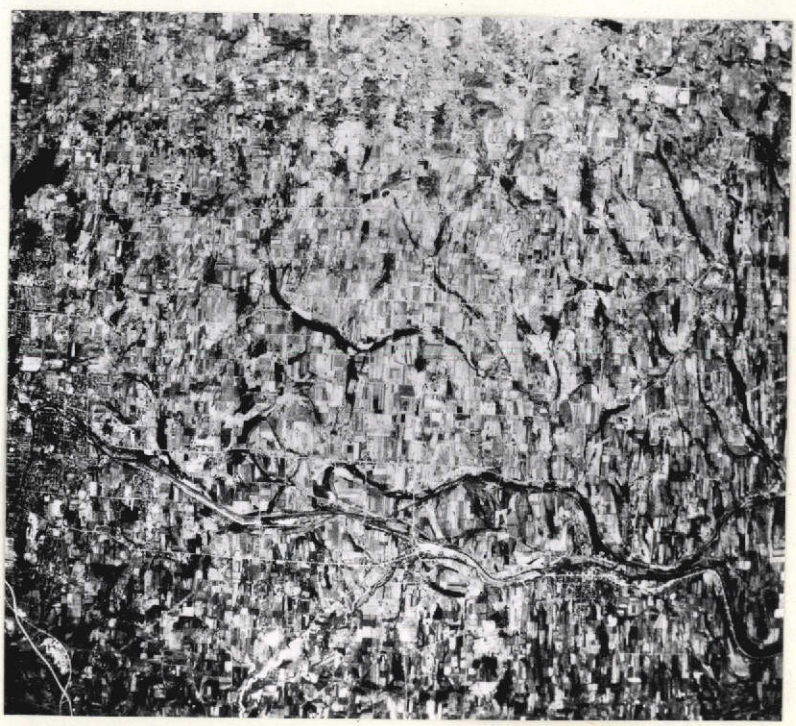

Figure 84. Print of high altitude (U2) color infrared aerial photograph showing circular feature southeast of Rochester. The east-west topographic low which forms the southern boundary of the feature is an ice-marginal drainage channel. Photo by NASA, 27Apr72. Scale: 1 cm = 2.3 km.

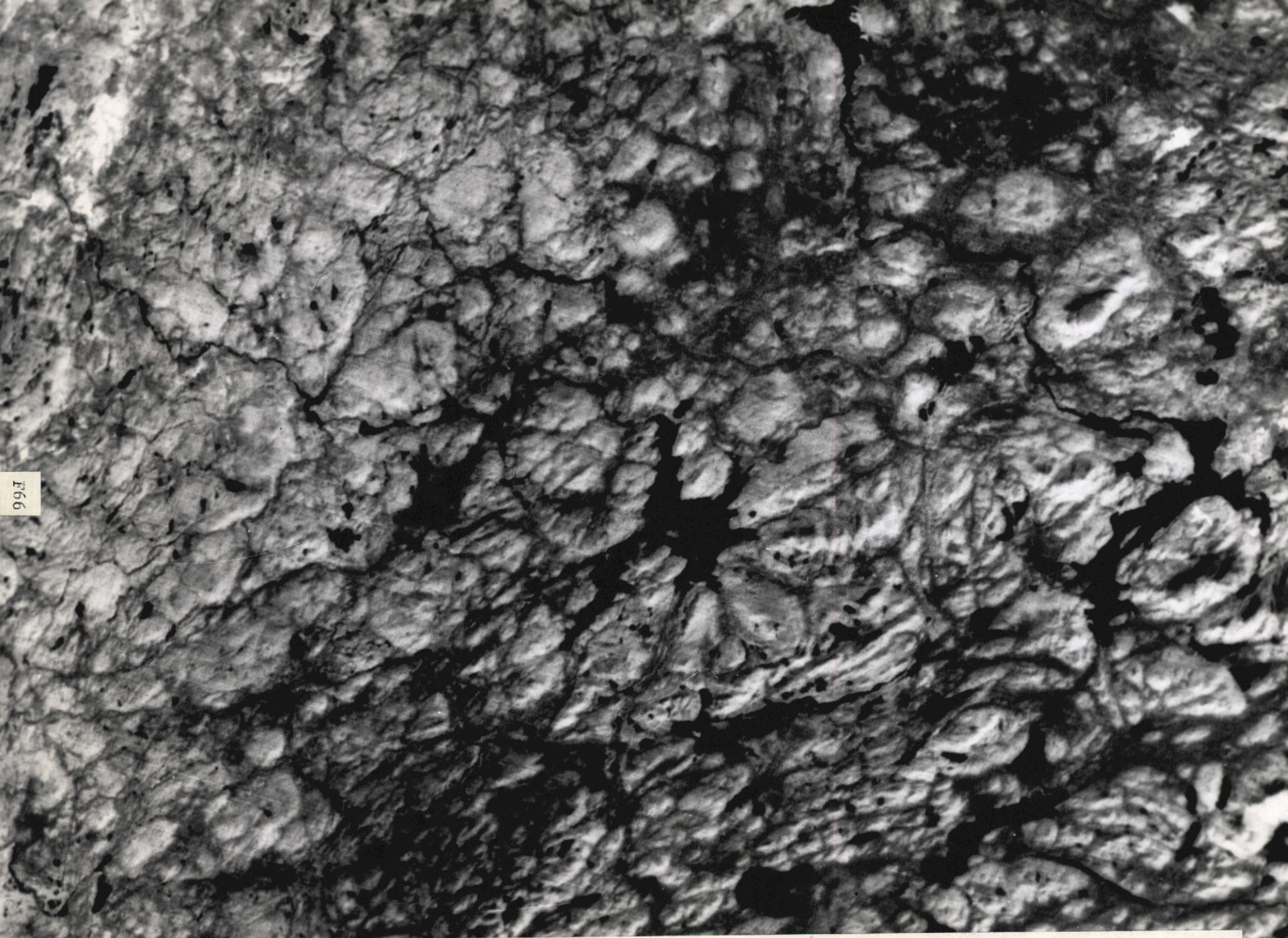

F66

Figure 85. ERTS-1 image at 1:250,000 of Cranberry Lake anomaly, west-central Adirondacks; band 7 of scene 1080-15174.

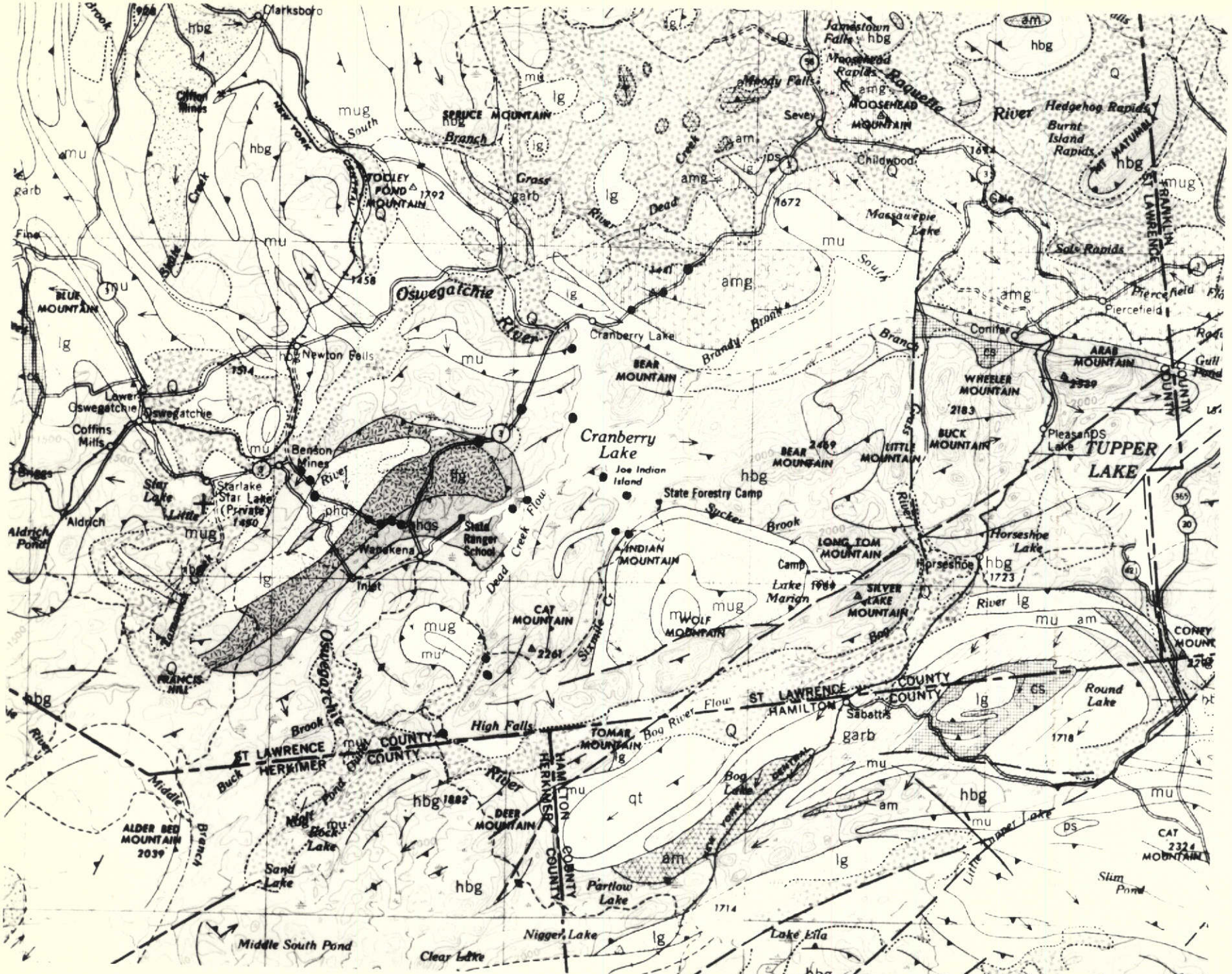

Figure 86. Geologic map of same area shown in Figure 85. Dots indicate sites studied for fracture data. (Geology from Isachsen and Fisher, 1971).

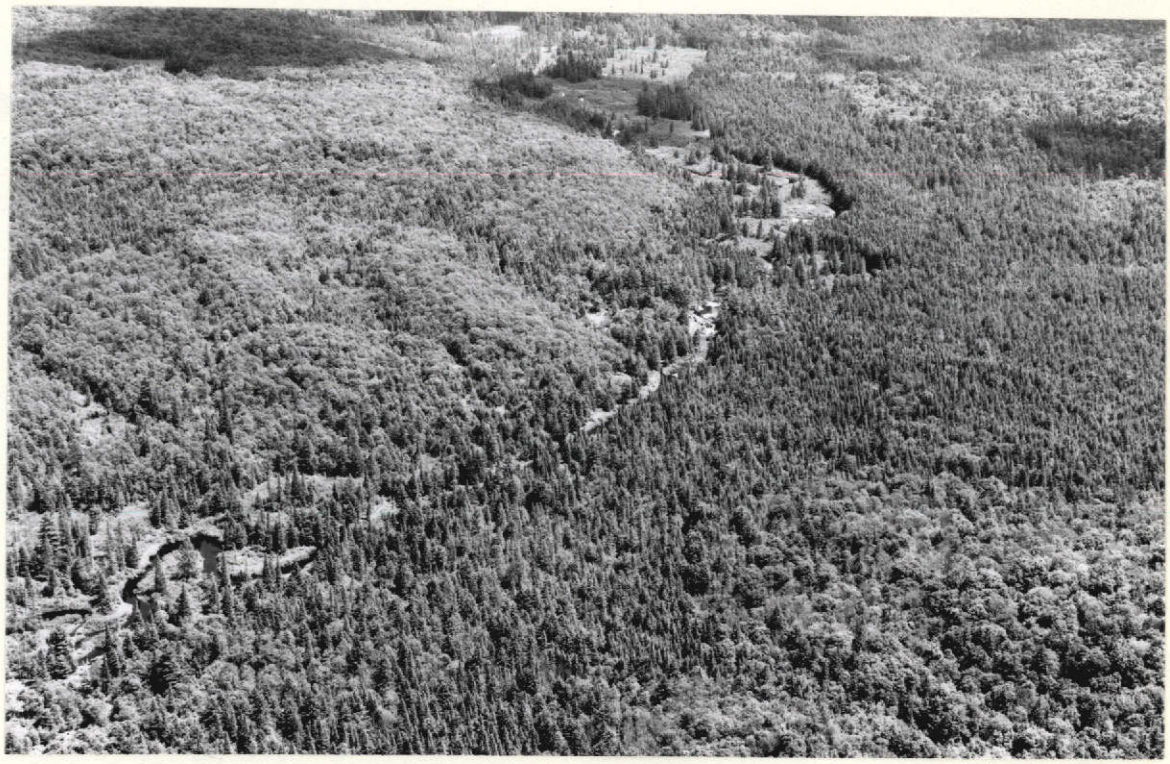

Figure 87. Aerial view showing the southern portion of the Cranberry Lake elliptical anomaly -- here the Oswegatchie River up to High Falls, and Bog River Flow beyond.

Figure 88. Map of all circular features seen on ERTS-1 imagery.

EXPLANATION

- Drumlin field showing drumlin axes
- Stratified drift and Lake Albany deltaic deposits
- Lake Vermont sand plain
- Glacial streamline forms east of Lake Ontario
- End moraine
- Lake Iroquois shoreline
- Ice-marginal drainage channel
- Esker

0 50 km
0 30 mi

LAKE ONTARIO
LAKE ERIE
ST. LAWRENCE RIVER
BLACK RIVER
GENESEE RIVER
MOHAWK RIVER
DELAWARE RIVER
HUDSON RIVER
LAKE CHAMPLAIN

Buffalo
Syracuse
Utica
Albany
Binghamton
Plattsburgh
New York

Figure 89. Map of glacial features observed in ERTS-1 imagery.

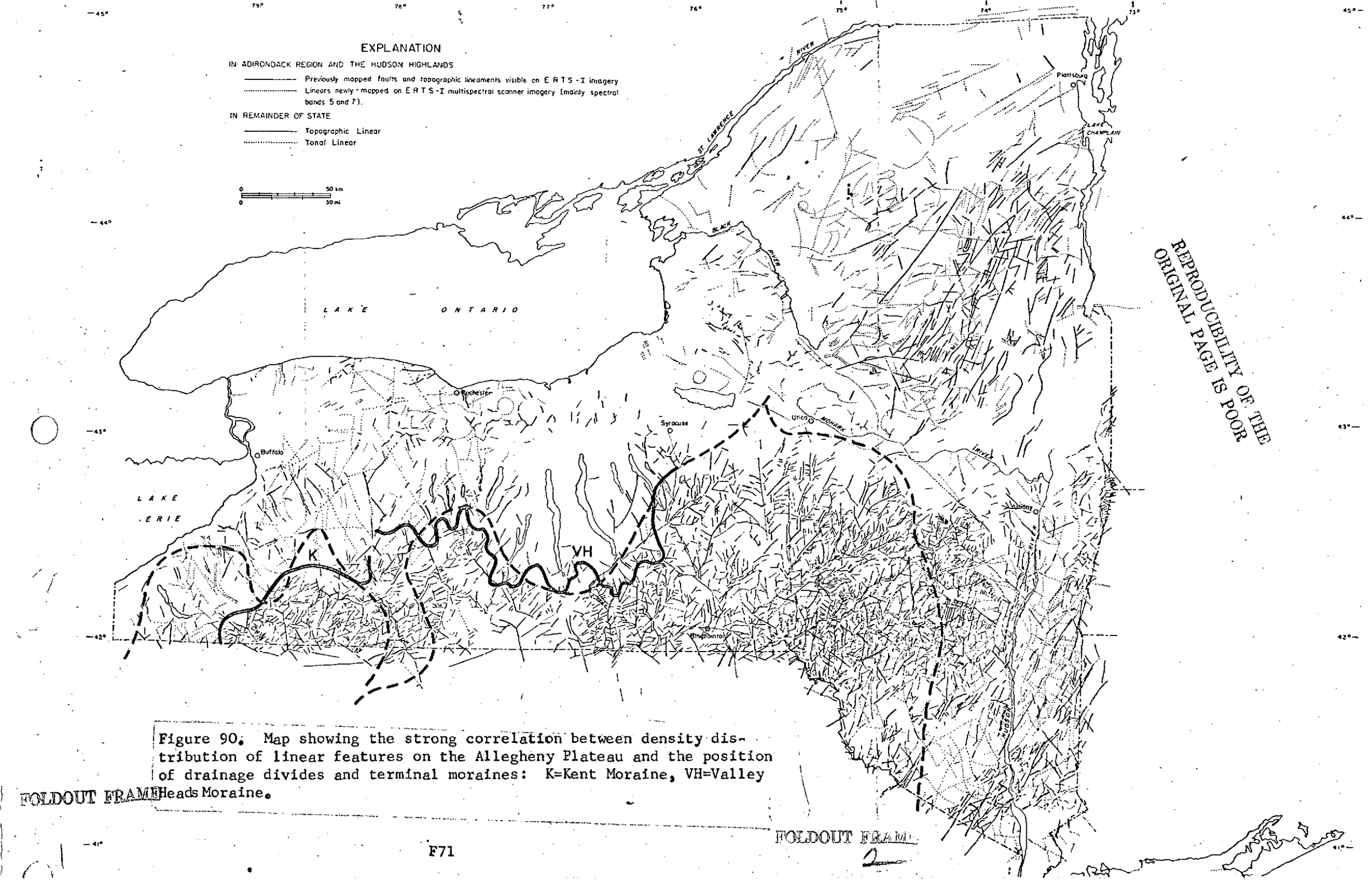

Figure 90. Map showing the strong correlation between density distribution of linear features on the Allegheny Plateau and the position of drainage divides and terminal moraines: K=Kent Moraine, VH=Valley Heads Moraine.

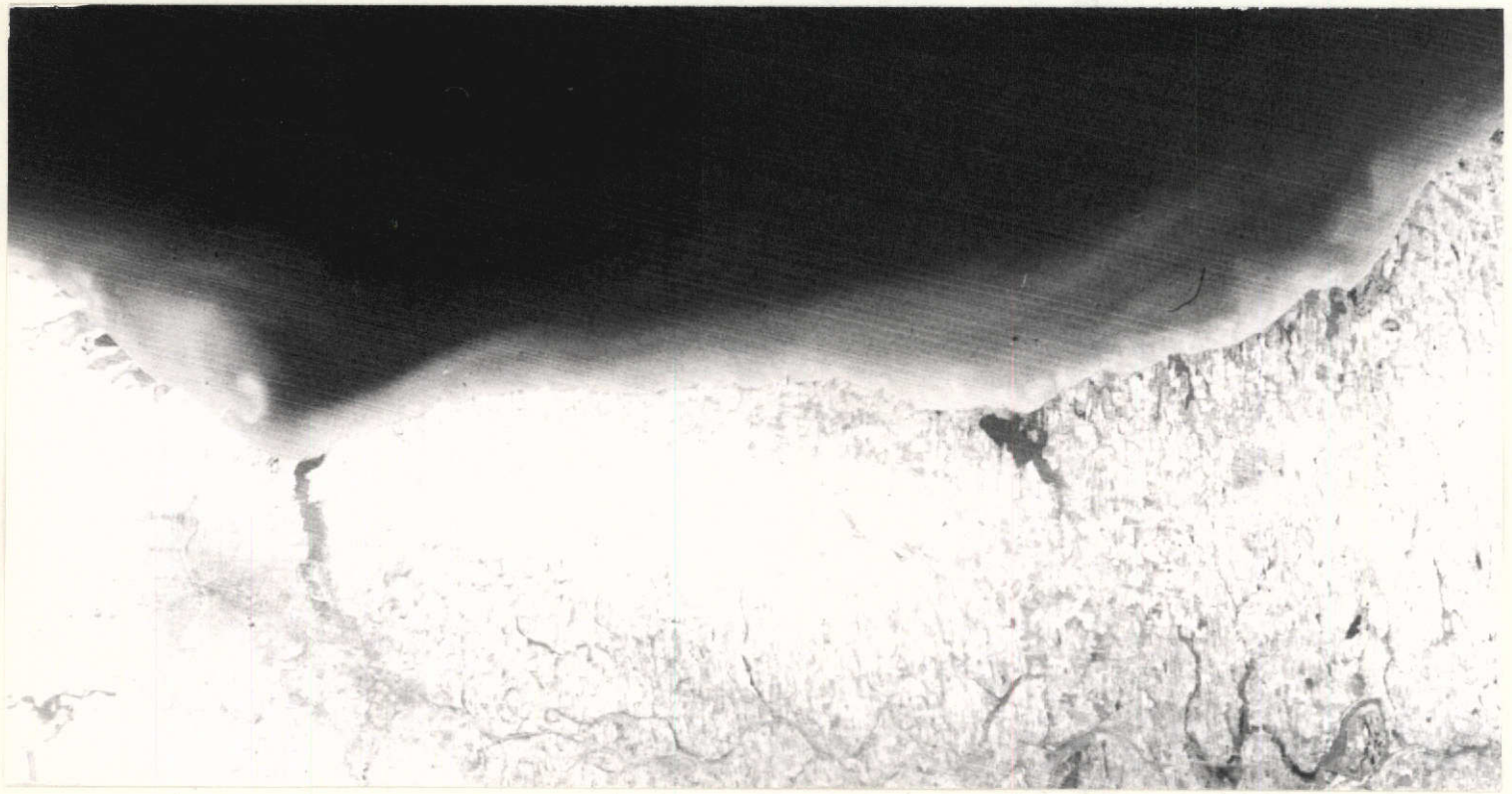

Figure 91. South shore of Lake Ontario showing patterns of suspended sediment following severe storm which occurred five days previously. Band 5, image no. 1243-15244, of 23Mar73.

Figure 92. South shore of Lake Ontario prior to storm of 17Mar73. Band 7, image no. 1027-15233, of 19Aug72.

Figure 93. South shore of Lake Ontario five days after storm of 17Mar73. Band 5, image no. 1243-15244, of 23Mar73.

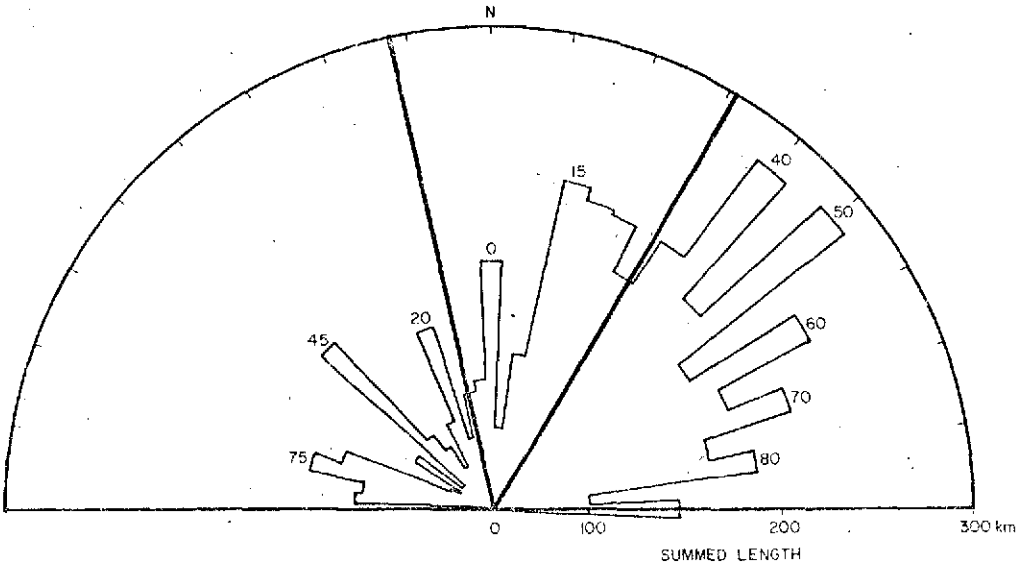

Figure 94. Fault plane solutions of Sbar and others (1972) of seismic events at Blue Mountain Lake, plotted on rose diagrams of previously mapped faults and topographic lineaments together with Stage II and Stage III ERTS linears.

APPENDIX I

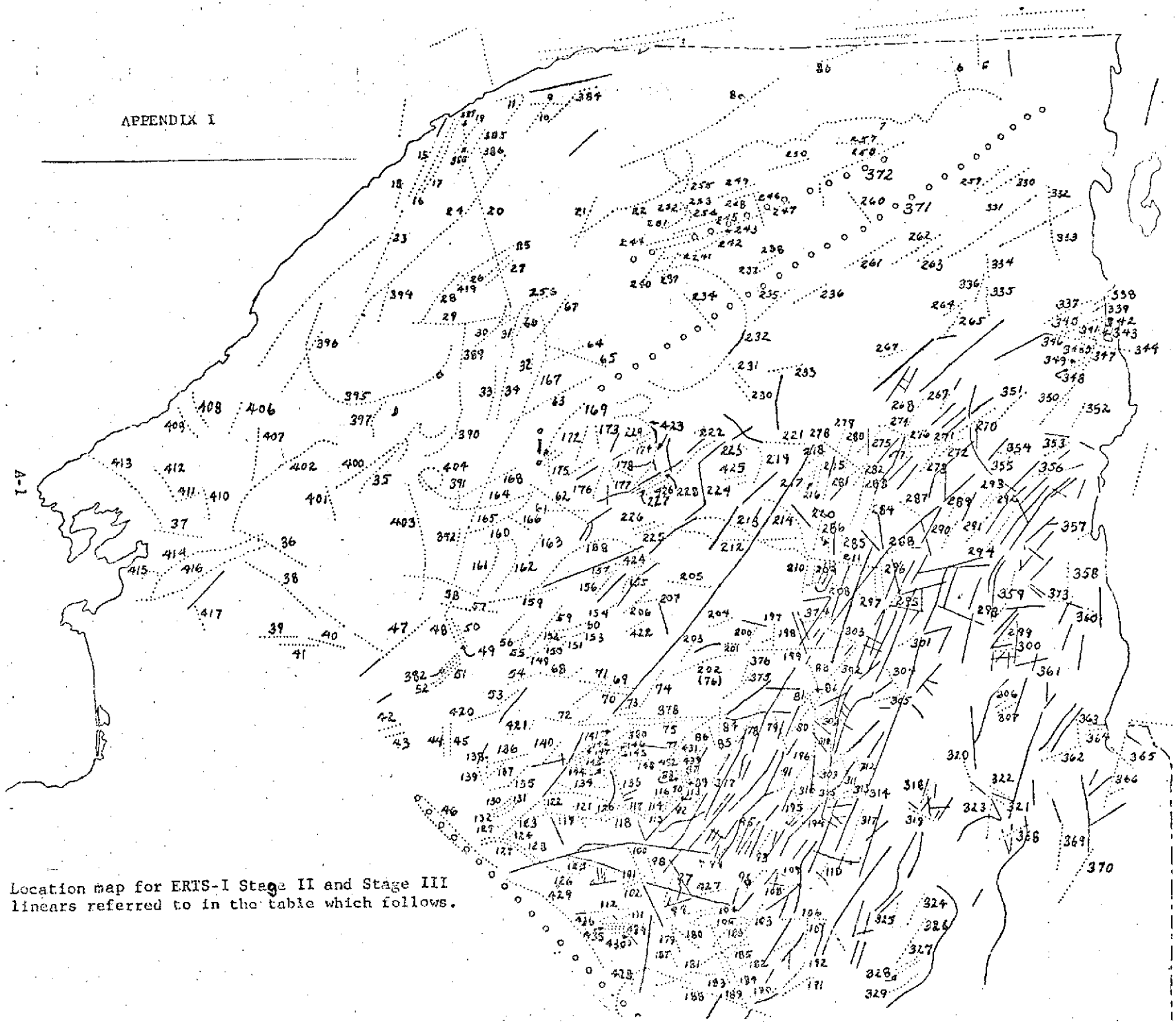

Location map for ERTS-I Stage II and Stage III linears referred to in the table which follows.

STAGE II AND III LINEAR ANOMALIES IN THE ADIRONDACK REGION

Ident. No.*	Air-foto Index Sheet	Strike	Length in km	Airfoto Index Identification	Field Identification and Remarks CTL=clearly a topographic lineament on imagery and on ground TL=topographic lineament on ground but not obviously so on imagery NTL=not a topographic linear feature on imagery or ground	Photo No.
5	96	N2W	8	Allen Brook (straight stream)	CTL	
6	96	N17W	7	dark vegetation strip	NTL	
15	53	N25E	9	southern half is several forest areas aligned and a stream section	NTL	
16	53	N24E	13	linear wooded area and stream	NTL	
17	53	N26E	6	road at southern end; rest is unexplained	NTL	
18	53	N20E	6	unexplained	NTL	
19	65	N41E	8	border of dark vegetation and stream	NTL	
20	66	N12W	35	unexplained	NTL	
24	53	N42E	38	southern 1/3 is Beaver Creek; road and fields are mid 1/3; northern 1/3 is the Grass River	NTL	
25	66	N60E	14	lithology and road and unexplained	NTL	
28	54, 66, 67	N40E	14	southern ½ parallels lithology; northern ½ is probably a stream	NTL	

29	54, 67	N80E	8	road segment in center, possible woodland boundary	NTL
31	67	N62E	1	stream valley	NTL
32	67	N5E	4	unexplained	NTL
33	67	N12E	12	unexplained	NTL
36	43, 56	N67W	14	northwest ½ is a road, southeast ½ is unexplained	NTL
39	56	N89E	9	unexplained; possible vegetation border	NTL
40	56	N75W	8	tree-lined stream valley	TL
41	56	N89W	8	unexplained	NTL
42	57	N77E	6	winding stream	NTL
43	57	N74E	5	unexplained	NTL
44	57	N1W	9	parallels lithology; also short section of river	CTL
45	70	N2E	7	appears to parallel lithology and stream segment	CTL
46	71, 58	N47W	17	southern ½ is road and stream northern ½ is an elongate woodland	NTL
48	69	N21W	7	southern 2/3 parallels lithology; northern 1/3 is unexplained	CTL
49	69	N19W	7	southern 2/3 parallels lithology; northern 1/3 is unexplained	CTL

50	69	N19W	5	southern 2/3 parallels lithology; northern 1/3 is unexplained	CTL
55	69	N2OE	6	unexplained	CTL
57	69	N86W	13	straight stream valley	CTL
58	69	N28E	5	straight stream valley	CTL
61	68	N9OE	9	southwest ½ is stream, northeast ½ is unexplained	CTL
62	68	N55W	14	southeast 2/3 is a straight stream; rest is probable stream	CTL
63	67	N61E	18	northeast 4/5 is straight stream; southwest 1/5 is unexplained	CTL
64	67	N67E	8	straight stream valley	CTL
65	67	N7OW	15	mid 1/3 is unexplained; remainder is winding stream	CTL
66	67	N27E	8	straight valley	CTL
68	70	N77W	5	unexplained	NTL
69	70, 85	N82W	9	mid section is lake shore; rest is unexplained	CTL
70	70, 85	N8OW	8	valley and lake shore	CTL
71	70	N53E	7	southern 2/3 is stream; northern 1/3 is apparent dry valley	CTL

72	70	N82W	15	straight stream valley	CTL
73	85	N84E	4	straight stream valley	CTL
74	85	N48E	17	stream valley	CTL
76	85	N74E	16	edge of topographically high area	CTL
77	85	N46E	21	stream valley	CTL
78	85	N35E	31	southern 3/4 is stream valley; northern ¼ is unexplained	CTL
79	85	N21W	8	Indian Lake and unexplained	CTL
81	85	N11W	5	sub-parallel to stream valley	CTL
82	85	N40E	6	straight valley	CTL
83	85	N17W	6	edge of topographically high area	CTL
84	85	N5E	6	stream valley	CTL
85	85	N19W	5	stream valley	CTL
86	85	N31E	6	apparent dry valley	CTL
91	85	N19W	4	straight valley	CTL
92	86	N41E	7	straight valley	CTL
93	86	N38E	6	possible vegetation border	NTL
94	86	N48E	5	stream valley	CTL
96	86	N43E	7	small valley	TL
97	86	N24E	7	straight valley	CTL
98	86	N18W	6	lake and stream	CTL

100	86	N19W	10	unexplained	NTL
103	86	N32E	7	straight valley	CTL; breccia on Gloversville quadrangle (J.M.**); no information on Lake Pleasant quadrangle.
105	86	N87W	15	stream valley	CTL
106	86	N56W	7	highway and stream	CTL
107	86, 87	N4E	3	northern part is stream; rest is unexplained	CTL; lithologic contact in southern part (J.M.)
108	86	N67E	5	valleys with drak vegetation	CTL
110	86	N31E	4	straight valley	CTL
111	86	N64E	5	straight valley	CTL
112	71, 86	N85E	10	straight valley	CTL
113	86	N53E	6	straight stream valley	CTL
114	86	N68E	6	stream + unexplained	CTL
117	71, 86	N73W	26	stream valley	CTL
119	71	N79W	19	½ length is stream valley; rest is unexplained	CTL
120	71	N61E	7	straight river valley	CTL
121	71	N30W	6	mid 1/3 is stream; rest is unexplained	CTL
122	71	N9W	4	straight stream valley	CTL
123	71	N48E	12	straight stream valley	CTL
124	71	N44E	3	straight stream valley	CTL
125	71	N75W	10	straight stream valley	CTL
126	71	N76W	7	unexplained	CTL
129	71	N67E	6	stream valley	TL
133	70, 71	N18W	11	straight stream valley	CTL

135	70	N60E	13	winding stream	CTL
136	70	N76E	9	straight valley + unexplained	CTL
137	70	N52E	7	straight stream valley	CTL
138	70	N1W	5	small stream valley	CTL
139	70	N28W	4	lake and dark vegetation	NTL
141	70	N58E	7	northern ¼ is stream; southern 3/4 is a road	CTL
148	70, 85	N82E	8	stream valley	CTL
149	69	N65E	3	stream valley	CTL
150	69	N46E	2	stream valley	CTL
151	69	N42E	3	border of dark vegetation area (also edge of topographic high)	CTL
152	69	N60E	7	stream valley	CTL
153	69	N75E	3	lake shoreline	NTL
154	69	N69E	4	unexplained	NTL
155	69, 84	N49E	8	stream valley	CTL
156	69	N42E	7	stream valley	CTL
157	69	N70E	5	straight valley	CTL
159	69	N76E	16	lake shoreline and boundary between topographic high and low areas	CTL

160	69	N84E	6	several aligned stream valleys + lake	CTL	
163	69	N32E	6	stream and lake	CTL	
164	68	N80E	21	winding stream	CTL	
165	68	N52E	12	stream and road	CTL	
166	68	N68W	4	½ is stream; rest is unexplained	NTL	
167	67, 68, 69	N19E	67	long linear composed of several stream, lakes and roads	CTL	
169a	68	N68E	6	stream valley	CTL	II-3-4
169b	68	N45E	5	lake arm + stream	CTL	II-3-4
170	68	N55E	5	lake	CTL	
171	68	N57E	4	unexplained	NTL	
172	68	N21E	8	stream and unexplained low area	CTL	
173	68	N6W	6	Cranberry Lake shoreline	NTL	
174	68, 63	N63E	8	stream valley	CTL	
175	68	N60E	7	narrow WSW arm of Cranberry Lake	CTL	II-3-5
176a	68	N44E	4	stream valley + lake arm	CTL	II-3
176b	68	N44E	10	stream valley + lake arm	CTL	II-3
177	68	N17W	3	portions of two lakes and topographically low area	CTL	
179	87	N12W	2	lake + dark vegetation patches	TL No information (JM**)	
180	87	N55W	8	stream + lake + unexplained	TL No information (JM**)	
182	87	N88W	9	stream + lake shore + dark vegetation area	CTL	

183	87	N22W	9	road and dark vegetation area + small valley	NTL; fault, metagabbro against charnockite (J.M.)
184	87	N25W	7	road + lake + low areas	TL; No information (JM**)
185	87	N55E	20	stream + unexplained	CTL; fracturing along stream and also to north beyond linear on imagery (J.M.)
186	87	N43E	5	lake + unexplained + stream	CTL
187	87	N24W	4	unexplained	NTL; in glacial deposits (J.M.)
188	87	N73W	21	stream + road + unexplained	CTL; SE ½ is glacial except central knob which is lithologic contact; W ½ is close to fold axes and crosses lithologic contact (J.M.)
189	87	N44W	4	unexplained	NTL; in glacial deposits
190	87	N79W	5	unexplained	NTL; fault between Precambrian and Paleozoic (J.M.)
191	87	N61E	6	stream + dark vegetation	NTL; in Paleozoic rocks
193	87	N68E	7	unexplained + short stream segment	TL; E ½ is lithologic contact, remainder not mapped (J.M.)
194	86	N57W	4	straight valley	CTL
195	86	N42E	3	straight valley	CTL
197	84	N5E	5	straight valley	CTL
198	84	N69E	2	straight valley	CTL
199	84	N89E	23	stream + boundary of topographically high area	CTL
200	84	N33E	5	straight valley	CTL
201	84	N86W	3	unexplained	NTL
202	70	N45E	4	edge of topographic high	CTL
203	84	N40E	5	straight valley with dark vegetation	CTL

204	84	N71E	6	stream valley	CTL	
205	84	N80W	10	stream + low areas with darker vegetation	CTL	
206	84	N51E	8	stream valley	CTL	
207	84	N82E	6	stream valley	CTL	
208	84	N88W	6	stream + lake + stream	CTL	
209	84	N7E	4	stream valley + unexplained	CTL	
210	84	N12E	6	dark vegetation strip	NTL	
211	84, 100	N81W	12	valley + lake + road	CTL	
212	83	N85W	31	stream + small lake	CTL	
215	83	N11E	9	straight valley	CTL; a Seward Mountain lineament	II-3-10
216	83	N11E	5	straight valley + unexplained	CTL; a Seward Mountain lineament	II-3-10
217	83	N39E	5	unexplained	NTL	
218	83	N60E	6	unexplained	NTL	
219	83	N11E	9	stream valley + lake shoreline	CTL	
220	83	N14E	8	lake shoreline + edge of topographic high	CTL	
221	83	N85W	10	straight stream valleys	CTL	
223	83	N52W	3	lake shore + unexplained	NTL	
224	83	N75E	2	stream valley	CTL	
229	83	N63E	5	straight stream valley	CTL	
230	82	N35W	6	unexplained	NTL	

231	82	N40W	6	stream + unexplained + stream	NTL
234	82	N40W	11	stream valley + unexplained location only approximate	TL
235	82	N49E	11	unexplained	NTL
236	82, 97	N61E	8	valley + unexplained	NTL
237	81	N60E	5	ridge	CTL
238	81	N73E	4	ridge	CTL
239	81	N33E	5	stream valley	CTL
240	81	N37E	9	stream + unexplained + stream	CTL
241	81	N81E	6	stream valley	CTL
242	81	N62E	9	stream valley	CTL
243	81	N73E	8	stream + unexplained + stream	CTL
244	81	N80E	12	unexplained	NTL
245	81	N73E	11	unexplained	NTL
246	81	N16W	8	stream valleys	CTL
248	81	N73E	5	stream valley	TL
249	81	N73E	9	stream valley + unexplained	TL
250	81	N76E	9	dark vegetation patches + unexplained	CTL
252	81	N67W	2	stream valley	TL

253	81	N42W	1	stream valley	TL	
254	81	N2W	5	stream valley	TL	
256	67	N62E	11	stream + transmission line	CTL	
257	96	N88W	10	several stream valleys	CTL	
260	97	N36W	4	straight stream valley	CTL	
261	97	N60E	12	stream + unexplained + stream	CTL	
262	97	N60E	8	stream valley	CTL	
263	97	N58E	6	straight stream	NTL	
264	98	N57E	6	stream valley	CTL	
265a	98	N65E	4	straight valley	CTL; Mt. Whiteface	II-3-15
267	98	N77E	7	dark vegetation strip	NTL	
268	98	N37E	7	southern 3/4 is stream; northern ¼ is unexplained	CTL	
269	98	N37E	5	straight valley	CTL	
270	99	N60E	10	two aligned valleys	CTL	
271	99	N83E	12	unexplained + straight valley	CTL	
272	99	N48E	4	straight valley	CTL	
274	99	N70W	9	small valley	TL	
275	99	N53E	7	straight valley	CTL	
276	99	N11W	5	stream valley	TL	
278	99	N54W	13	stream + unexplained	CTL	

279	99	N24E	6	stream + unexplained	CTL	
280	99	N15E	9	two small stream valleys	CTL	
281	99	N54E	5	stream valley	CTL	
282	99	N36E	4	stream valley	CTL	
283	99	N15E	14	unexplained + stream	CTL	
284	99	N24E	6	stream + lakes	CTL	
285	99	N6E	4	straight stream valley	CTL	
286	99	N1E	4	stream valley	CTL	
287	99	N52W	4	stream + unexplained	CTL	II-2-21
288	99	N76E	5	stream + lake	CTL	unnumbered
290	99	N38E	9	stream + unexplained ridge	TL	II-2-18
291	99	N42E	9	straight valley	CTL	unnumbered
294	99, 116	N38E	10	sharp valley with dark vegetation	TL	
295	100	N35E	6	wide stream valley with dark vegetation	TL	
296	100	NOE	9	unexplained	NTL	
297	100	N2W	8	stream valley	CTL	
298	100	N38E	5	stream + unexplained	TL	
299	100, 117	N74E	6	stream valley	TL	
301	100	N56E	6	stream valley	TL	
302	100, 101	N41E	11	stream valley	CTL	

303	100	N64W	8	stream + unexplained	TL	
305	101	N75E	4	stream + unexplained	TL	
306	101	N58E	4	two straight valley with dark vegetation	CTL	
307	101	N61E	5	dark vegetation areas around stream	CTL	
309	101	N48E	20	stream + unexplained	CTL; North Creek - Schroon Lake Village topographic lineament connects two previously-mapped segments, and extends one for a total length of 50 km.	II-3-12
310	101	NOE	5	stream valley with dark vegetation	CTL	
311	101	N14W	6	stream valley	CTL	
312	101	N18W	4	stream + valley with dark vegetation	CTL	
313	102	N25E	5	straight stream valley with dark vegetation	CTL	
314	102	N81E	8	stream valley	CTL	
315	102	N6W	3	stream valley	CTL	
316	102	N7W	4	stream valley	TL	
317	102	N57E	3	straight stream valley	CTL	
318	102	N26E	7	straight stream valley	TL	
319	102	N64W	7	stream + unexplained	TL; fault, chlorite, slickensides (J.M.)	
320	101, 102	N13W	7	stream	NTL	
321	102	N56W	5	dark vegetation strip	NTL	
322	102	N55W	6	small valley with dark vegetation strip	CTL	
323	102	N11E	10	small valley with dark vegetation strip	CTL	

324	102	N29E	8	stream valley	CTL; possible stratigraphic offset (J.M.), west through Bachellorville pegmatites (J.M.)	
325	102	N12E	6	straight valley with dark vegetation	TL; no information, but breccia through Bachellorville pegmatite deposits	
326	103	N39E	12	stream + unexplained	TL	
330	114	N63E	11	irregular dark vegetation strip	NTL	
331	97, 114	N54E	11	dark vegetation + unexplained + dark vegetation	NTL; clear line on imagery but unclear in field	
332	114	N4W	16	dark vegetation strip	NTL	
333	114	N64E	20	stream + unexplained + stream	NTL	
334	114	N5W	6	stream valley	CTL	
335	114, 116	N4W	8	stream valley	CTL	
336	114, 115	N20E	8	unexplained	NTL	
337	115	N66E	12	unexplained + lake	TL	
338	115	N63E	4	valley with small relief	TL	
339	115	N64E	4	valley with small relief	TL	
340	115	N50E	7	unexplained	NTL	
341	115	N69E	9	stream + unexplained	NTL	
342	115	N26E	4	unexplained	NTL	
343	115	N13W	2	unexplained	CTL; unnamed creek to Willsboro Bay	II-3-6
343a	115	N74E	2.5	stream valley	CTL; Rattlesnake Mt. lineament	II-3-6
346	115	N78W	7	unexplained	NTL	
347	115	N27E	7	stream + dark vegetation border	NTL	

350	115	N43E	13	unexplained + stream + unexplained	CTL; Elizabethtown - Burpee Brook	II-3-13
351	115, 116	N34E	11	unexplained + stream	CTL	
352	115, 116	N32E	8	two stream valleys	TL	
353	116	N61E	6	unexplained	NTL	
354	116	N82W	6	stream valley	CTL; Roaring Brook; continues beyond divide	II-3-8
355	116	N36E	7	two stream valleys	CTL	
356	116	N82E	7	stream valley	CTL; fault in mangerite at western end	II-3-9
357	116	N65E	5	short straight stream valley	TL	
358	117	N5E	6	lake + stream	NTL	
359	117	N6E	2	lake + stream + dark vegetation area	CTL	
360	117	N69W	4	stream + unexplained	TL	
361	118	N74E	5	unexplained	NTL	
362	118	N70E	9	unexplained + lake + unexplained	NTL	
363	118	N7W	4	stream + unexplained	NTL	
364	118	N80E	4	unexplained	NTL	
365	118	N45W	8	stream + dark vegetation area	NTL	
366	118	N19E	4	winding stream + canal	CTL	
368	119	N69E	7	stream + unexplained	CTL	
369	119	N13E	11	unexplained	NTL	
370	119	N33E	3	canal + unexplained	NTL	

371	67, 81, 82, 97, 113	N58E	75	stream + unexplained + dark vegetation areas	CTL
372	81, 97	N69E	61	edge of topographic high + lake	CTL
373	117	N88E	3	road + lake	CTL
374	100	N84E	8	broad stream valley	CTL
375	85	N48E	11	stream valley	CTL
376	85	N17E	5	stream valley	CTL
377	85	N28E	2	dark vegetation strip	NTL
378	85	N89E	19	stream valley	CTL
384	65	N54E	16	combination of stream and vegetation borders	NTL
385	65, 66	N35E	12	dark vegetation border	NTL
386	65	N19W	8	dark vegetation border	NTL
387	65	N13W	3	dark vegetation border	NTL
388	65	N7W	3	dark vegetation border	NTL
391	68	N9W	7	dark vegetation area + stream valley	CTL
392	69	N10E	3	parallels lithology + dark vegetation area	CTL
393	69, 56	N74W	18	Beaver River	NTL
394	54	N17E	9	stream	NTL
400	55	N56E	18	stream + parallels lithology	CTL
402	55	N74W	5	railroad + stream	NTL
403	55, 56	N10W	21	river + dark vegetation area	NTL

405	56	N54W	18	unexplained	NTL
407	43	N8E	12	stream + unexplained	NTL
409	42, 43	N30W	9	unexplained + vegetation border	NTL
410	43	N12W	5	stream + road	NTL
412	43	N33W	9	unexplained	NTL
413	43	N46W	25	unexplained	NTL
414	43, 44	N69E	26	railroad + dark vegetation strip	CTL
415	44	N66W	4	stream + dark vegetation strip	TL
416	44	N86E	35	stream + unexplained	CTL
417	44	N21W	9	stream + unexplained	NTL
418	53, 54	N49E	26	railroad + black lake	CTL
419	66	N49E	4	unexplained	NTL
420	70	N72E	8	stream valley	CTL
421	70	N66E	9	stream + unexplained	CTL
422	84	N62E	6	stream valley with dark vegetation strip	CTL
424	69	N83W	6	stream with surrounding irregular dark vegetation strip	TL
425	83	N80E	5	unexplained + stream + dark vegetation strip	CTL

426	83	N63E	6	lake + stream	CTL
427	86	N77E	7	small stream valley	CTL; cuts diagonally across stratigraphy (J.M.)
429	71	N46W	35	stream + lake	NTL
431	85	N46E	7	stream	TL
432	85	N7E	5	dark vegetation strip	NTL
433	85	N53E	4	straight valley	CTL
437	97	N35E	7.5	valley + lake shore + ridge	CTL

*Numbers not shown in table represent linears that were declassified as a result of field study, because they are caused by man or because they are lithologically controlled.

**Oral communication from James McLelland

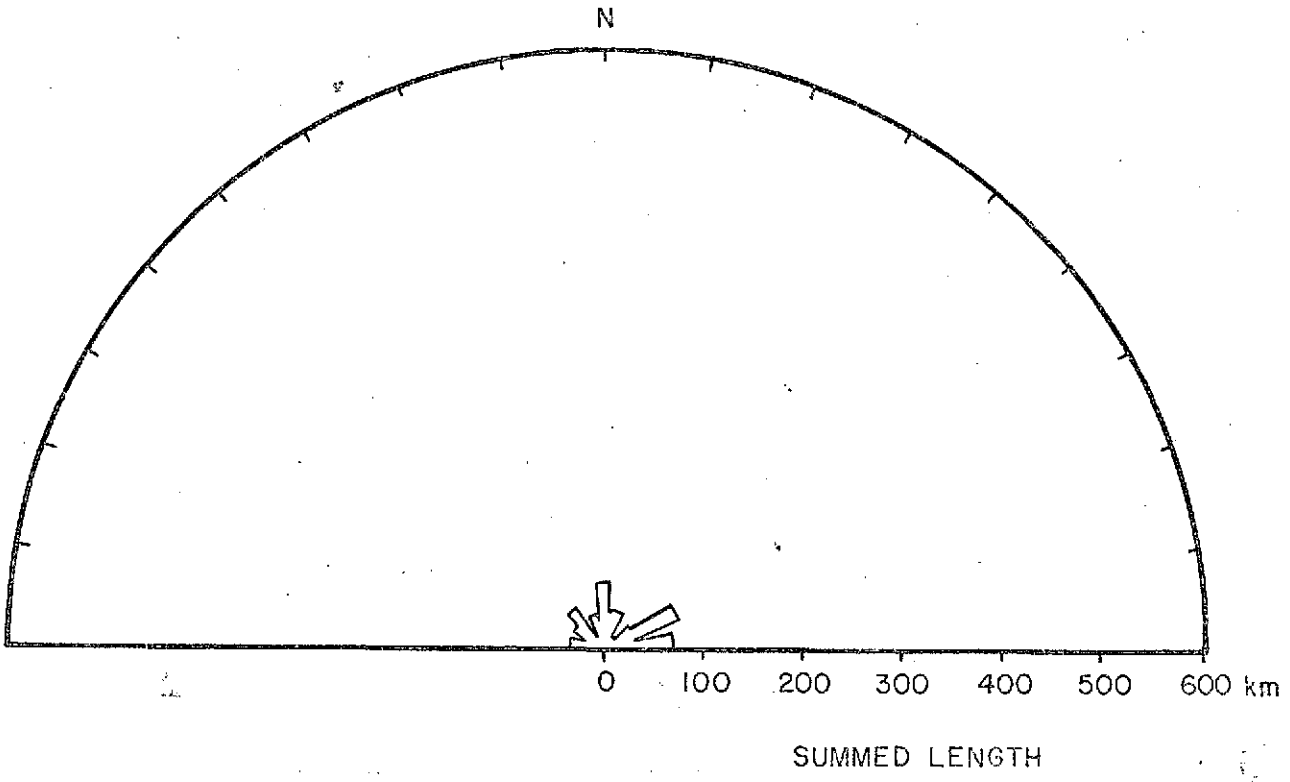

Appendix III-1. Rose diagram of tonal linears in Zone 1 (Figure 76).

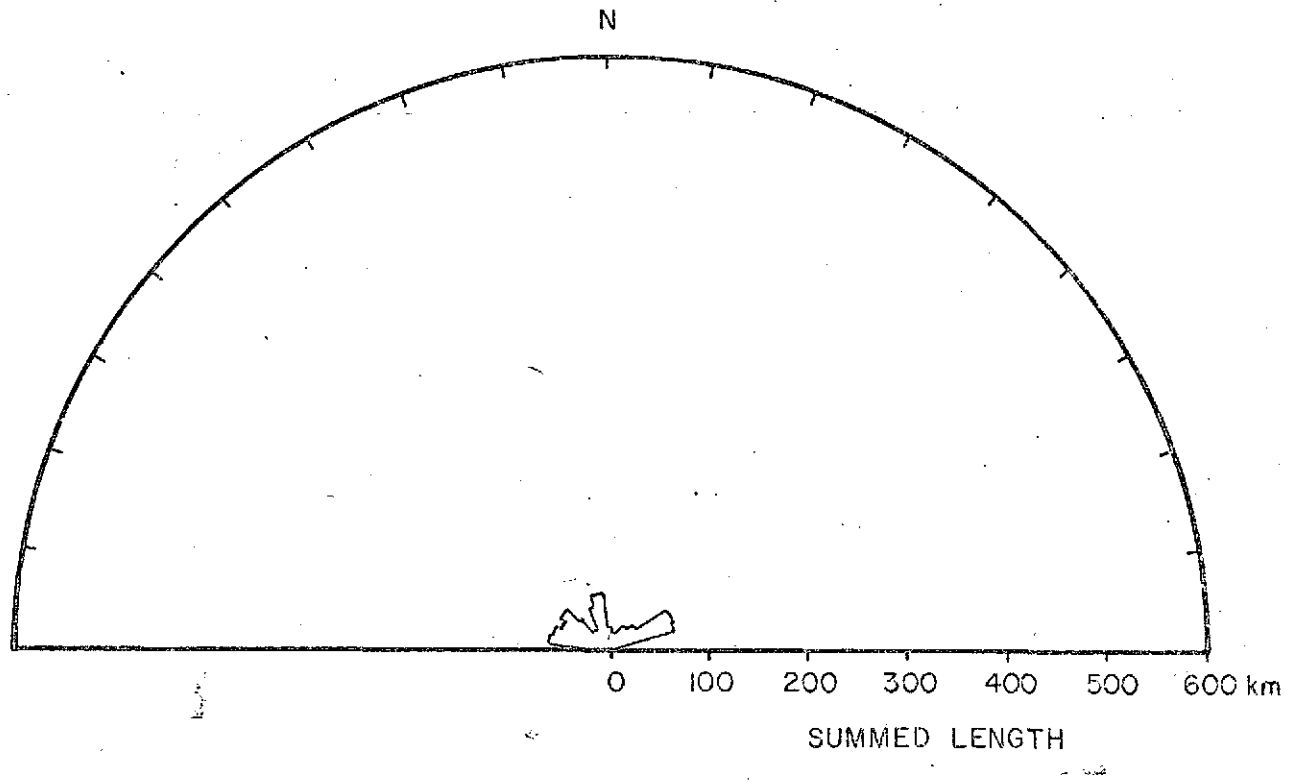

Appendix III-2. Rose diagram of tonal linears in Zone 2 (Figure 76).

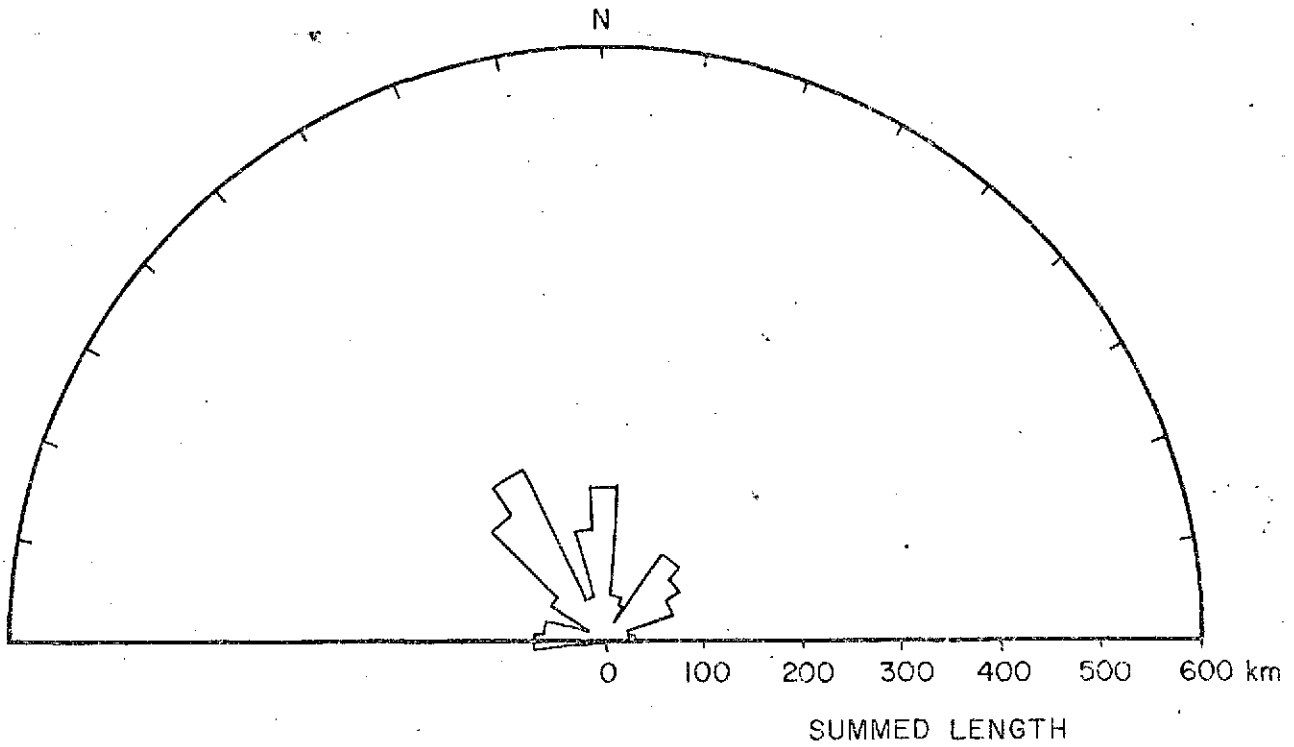

Appendix III-3. Rose diagram of tonal linears in Zone 3 (Figure 76).

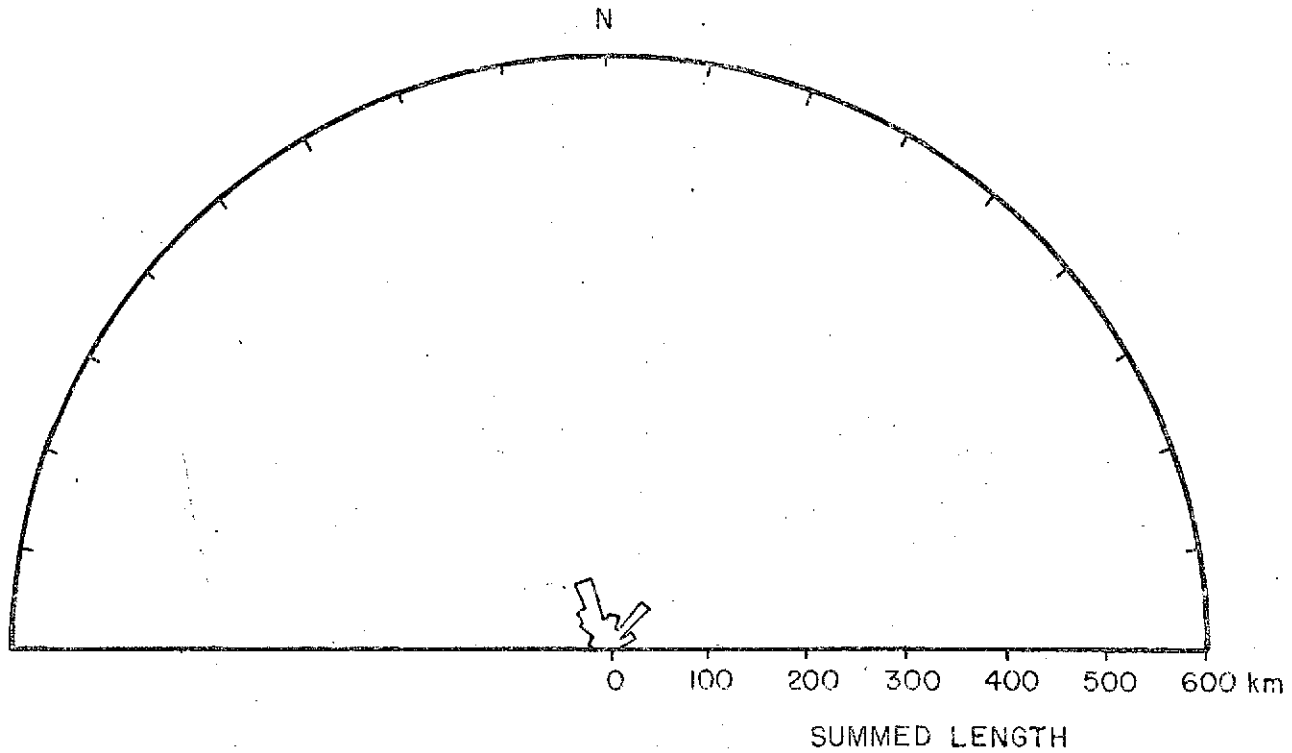

Appendix III-4. Rose diagram of tonal linears in Zone 4 (Figure 76).

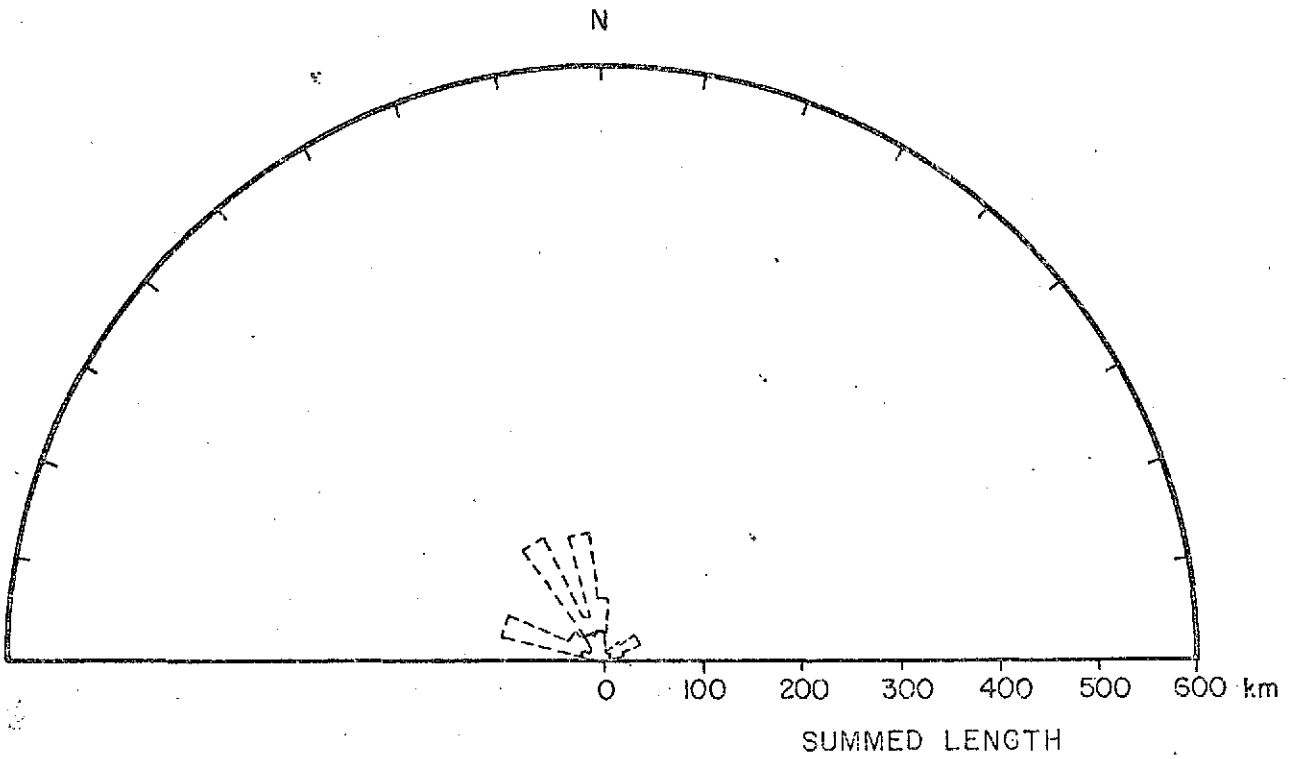

Appendix III-5. Rose diagram of tonal linears in Zone 5 (Figure 76). Dashed lines show same data on an expanded scale where each division represents summed lengths of 25 kilometers (x4).

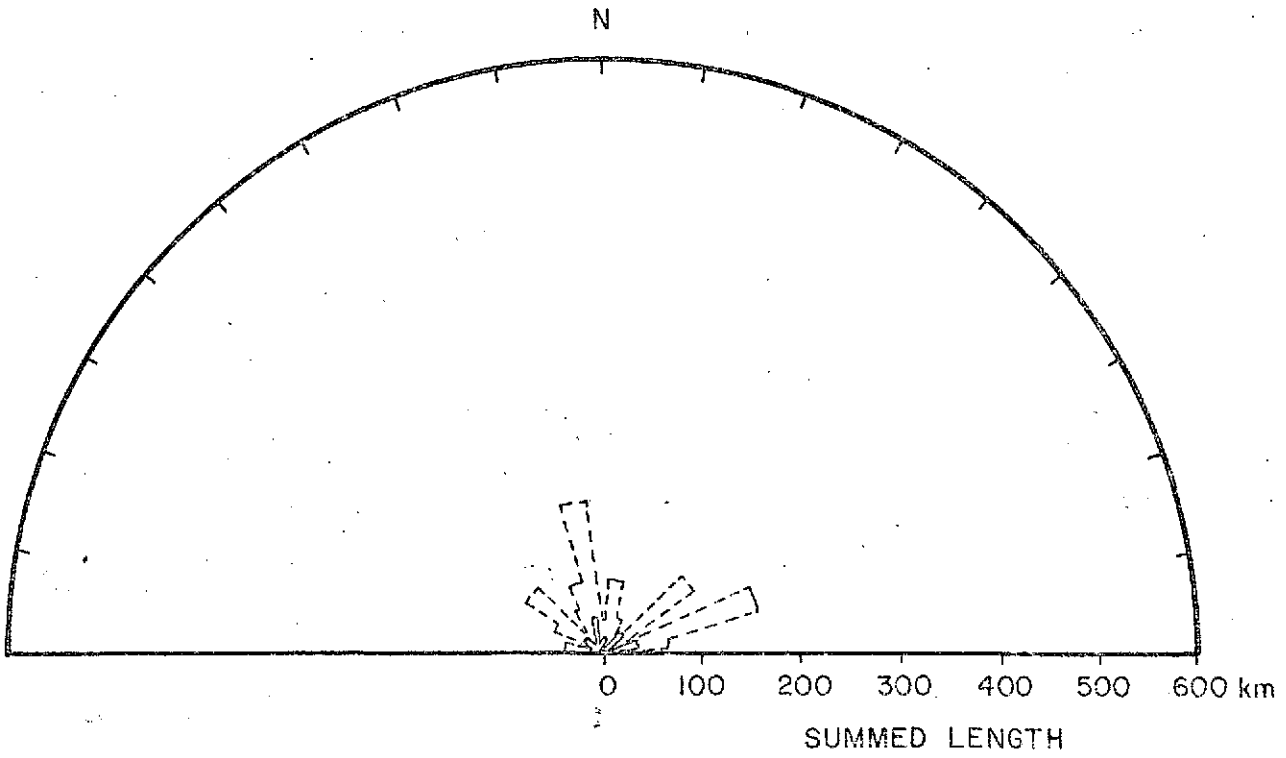

Appendix III-6. Rose diagram of tonal linears in Zone 6 (Figure 76). Dahsed lines show same data on an expanded scale (x4).

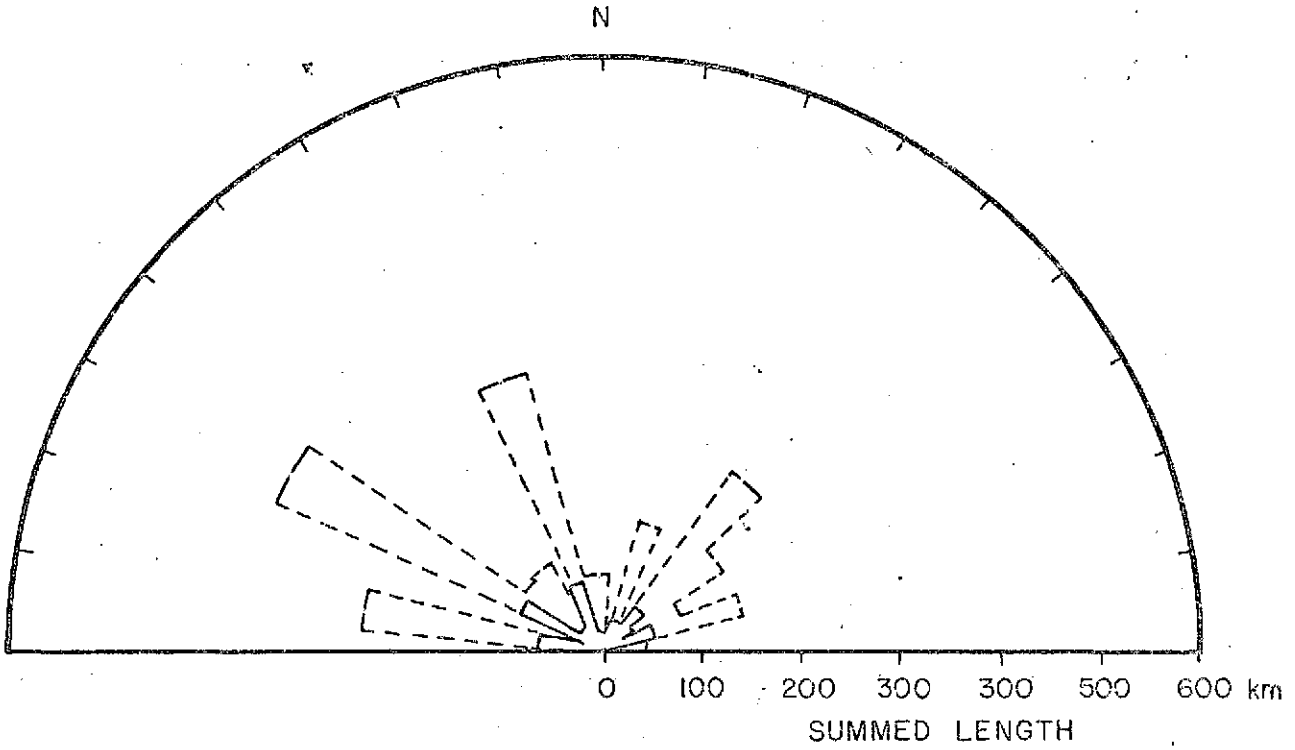

Appendix III-7. Rose diagram of tonal linears in Zone 7 (Figure 76). Dashed lines show same data on an expanded scale (x4).

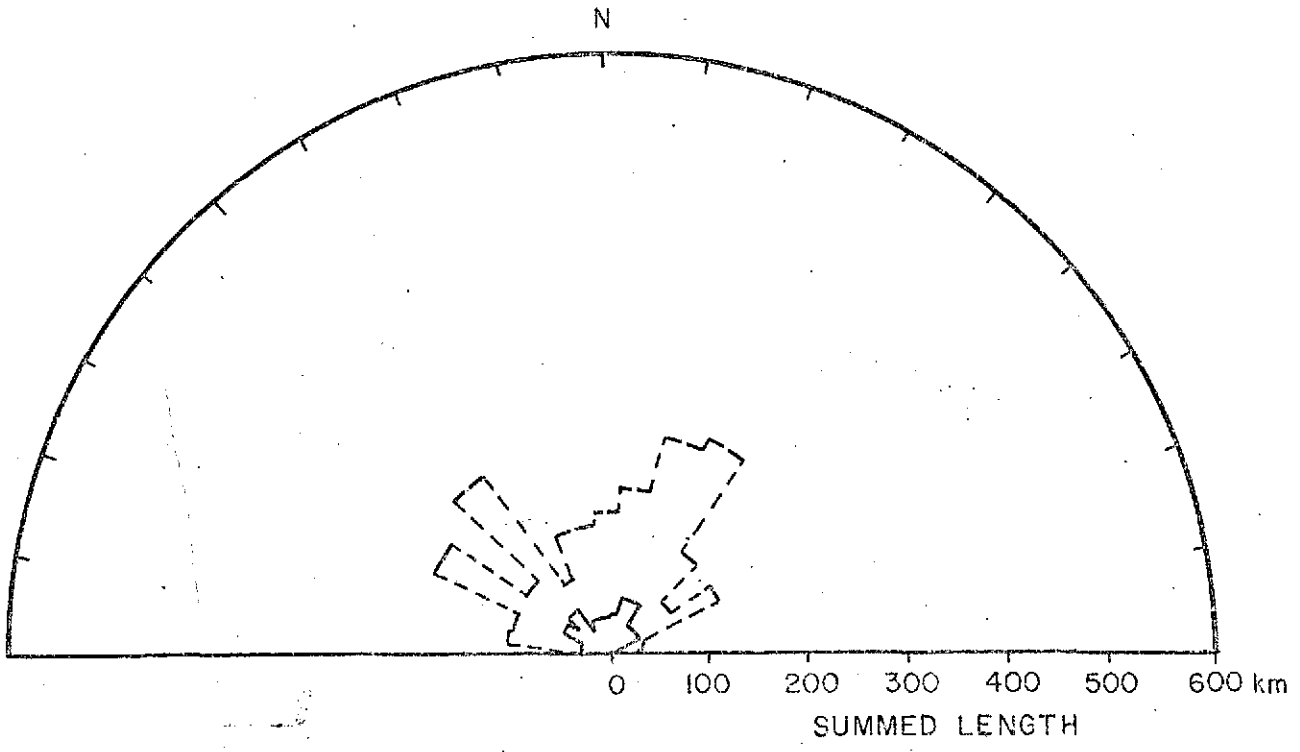

Appendix III-8. Rose diagram of tonal linears in Zone 8 (Figure 76). Dahsed lines show same data on an expanded scale (x4).

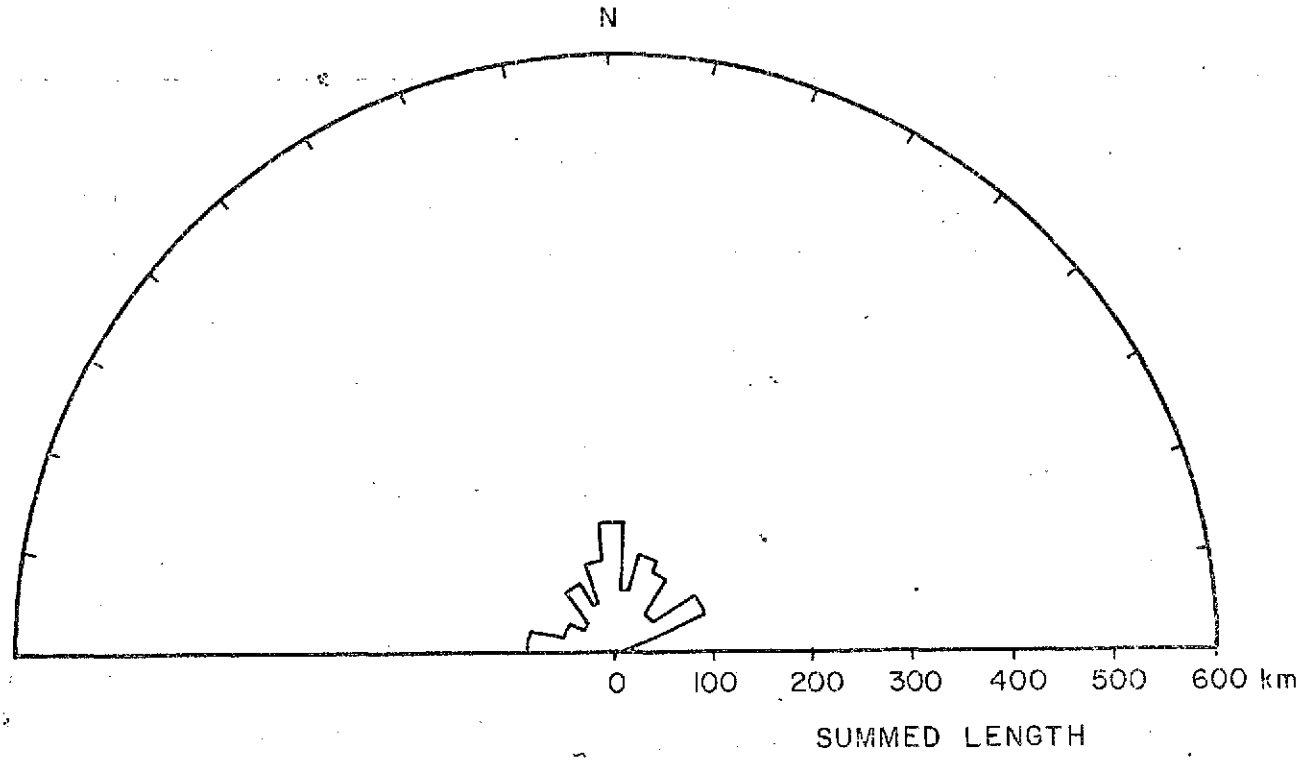

Appendix III-9. Rose diagram of tonal linears in Zone 9 (Figure 76).

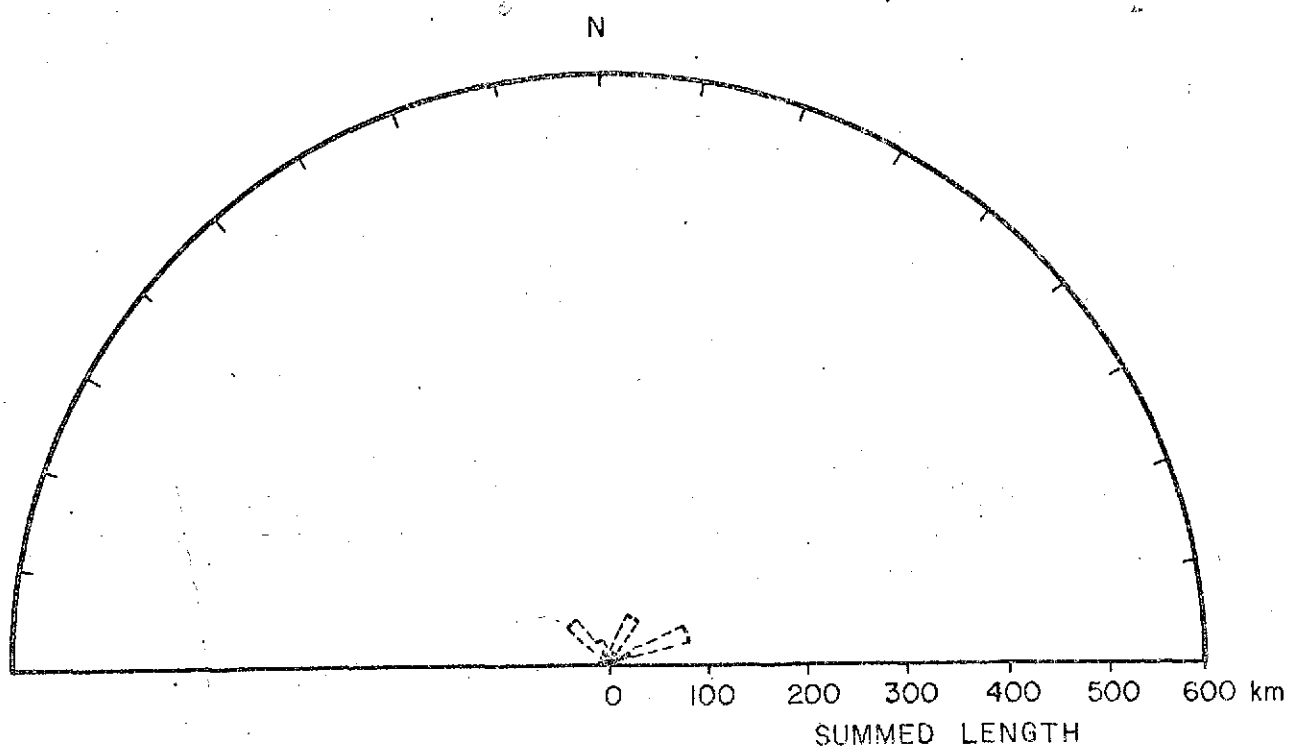

Appendix III-10. Rose diagram of tonal linears in Zone 10 (Figure 76). Dashed lines show same data on an expanded scale (x4).

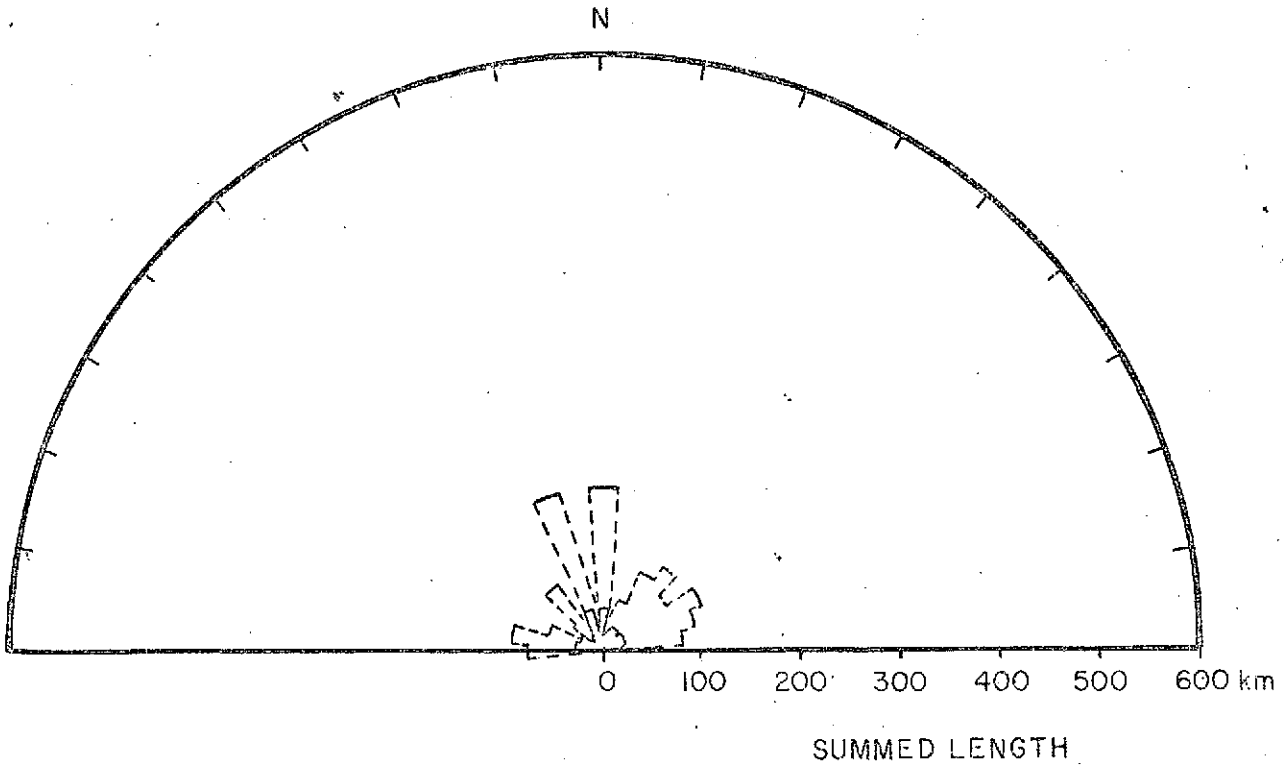

Appendix III-11. Rose diagram of topographic linears in Zone 1 (Figure 77). Each division along the base of the diagram represents 100 kilometers of summed lengths. Dashed lines show same data with the base scale expanded to summed lengths of 25 kilometers.

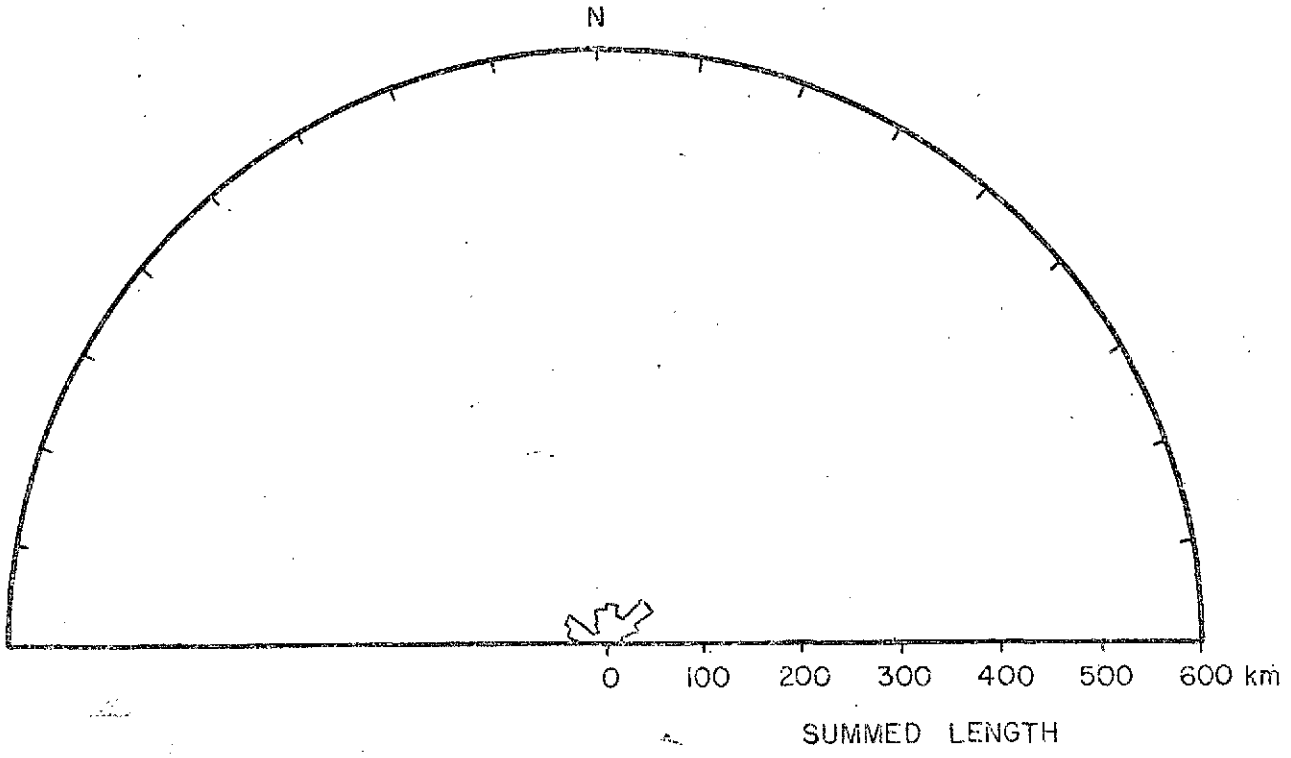

Appendix III-12. Rose diagram of topographic linears in Zone 2 (Figure 77).

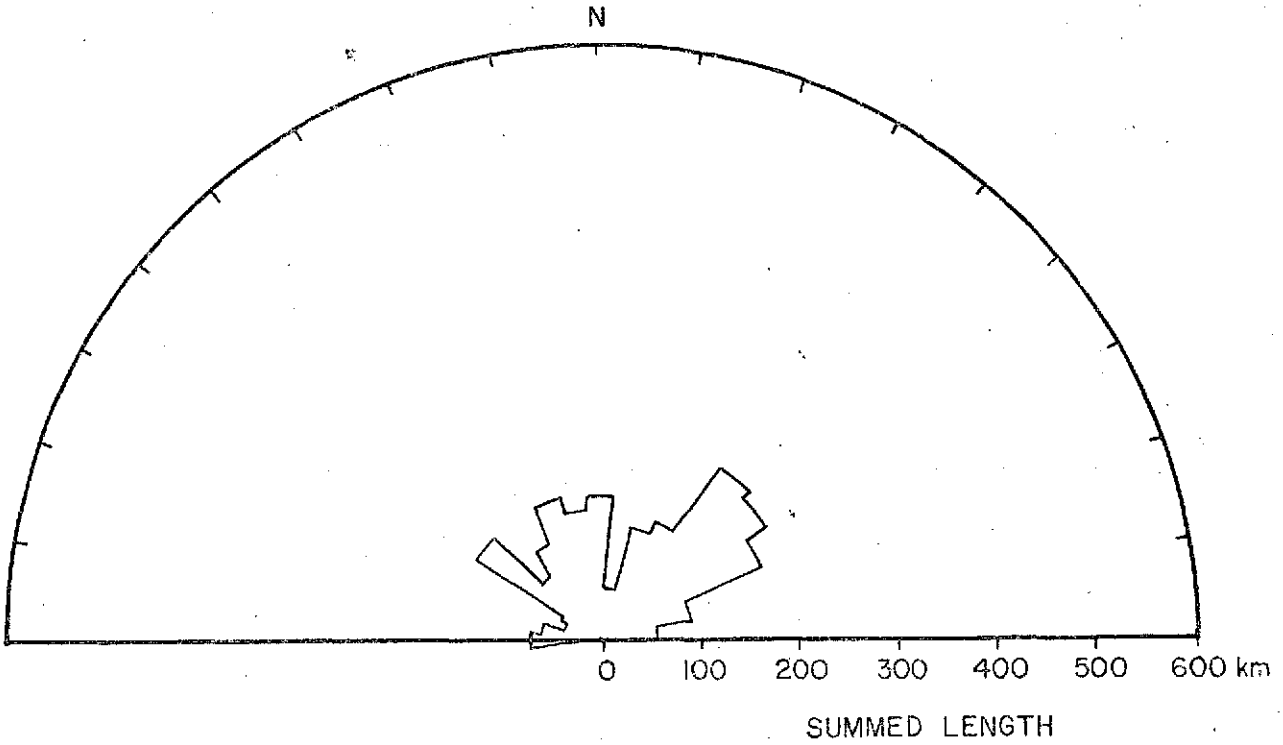

Appendix III-13. Rose diagram of topographic linears in Zone 3 (Figure 77).

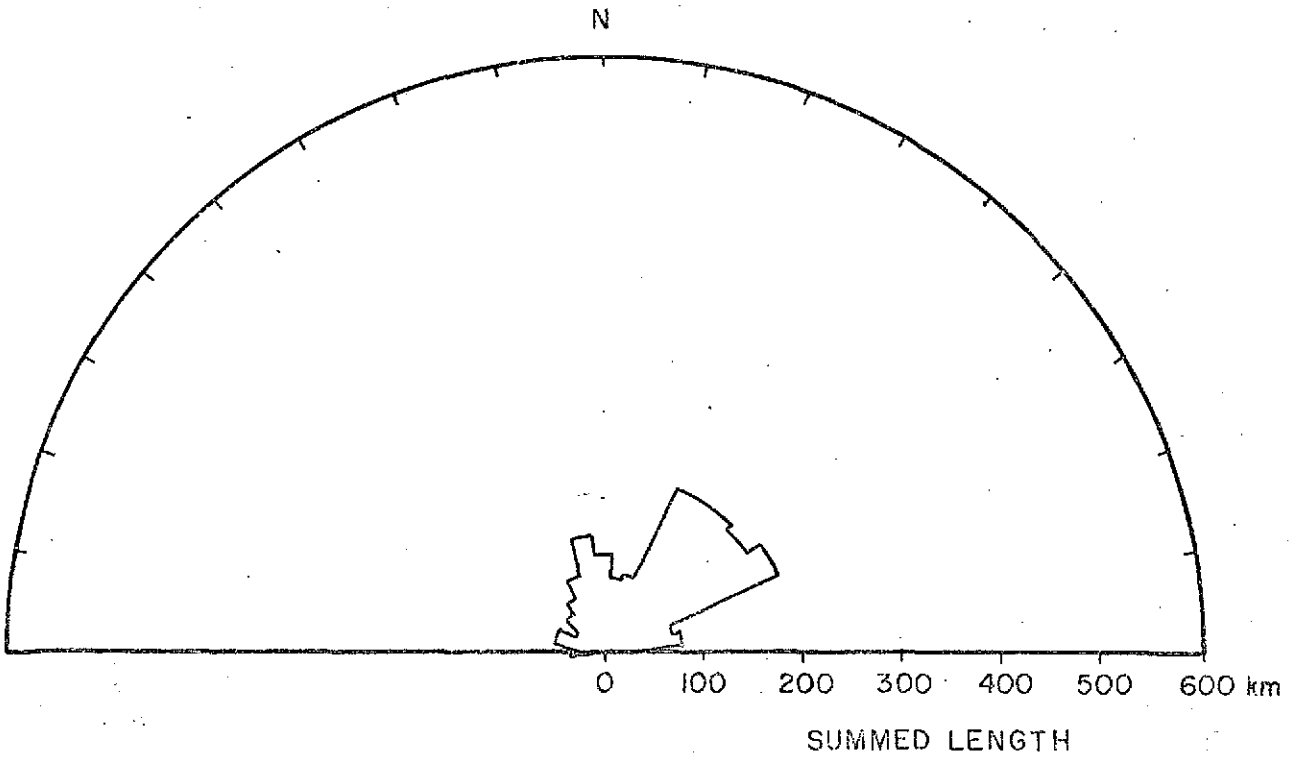

Appendix III-14. Rose diagram of topographic linears in Zone 4 (Figure 77).

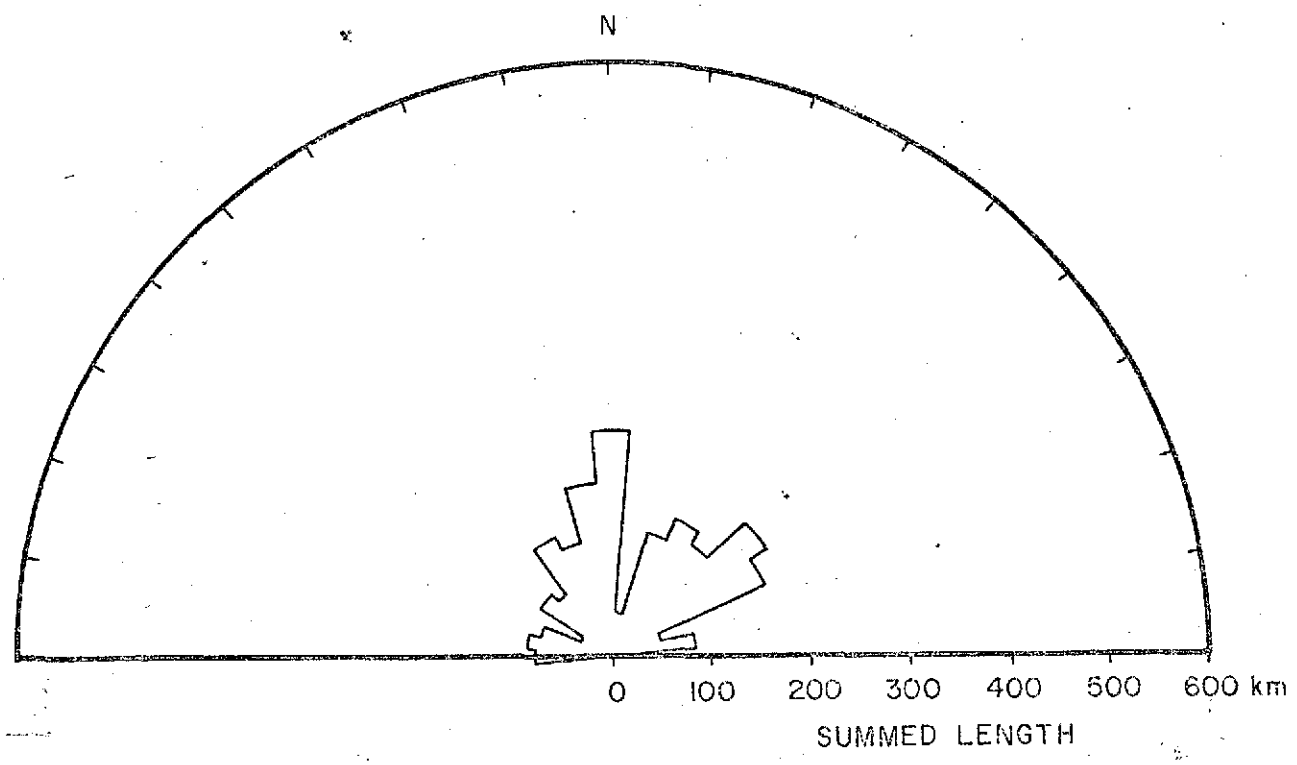

Appendix III-15. Rose diagram of topographic linears in Zone 5 (Figure 77).

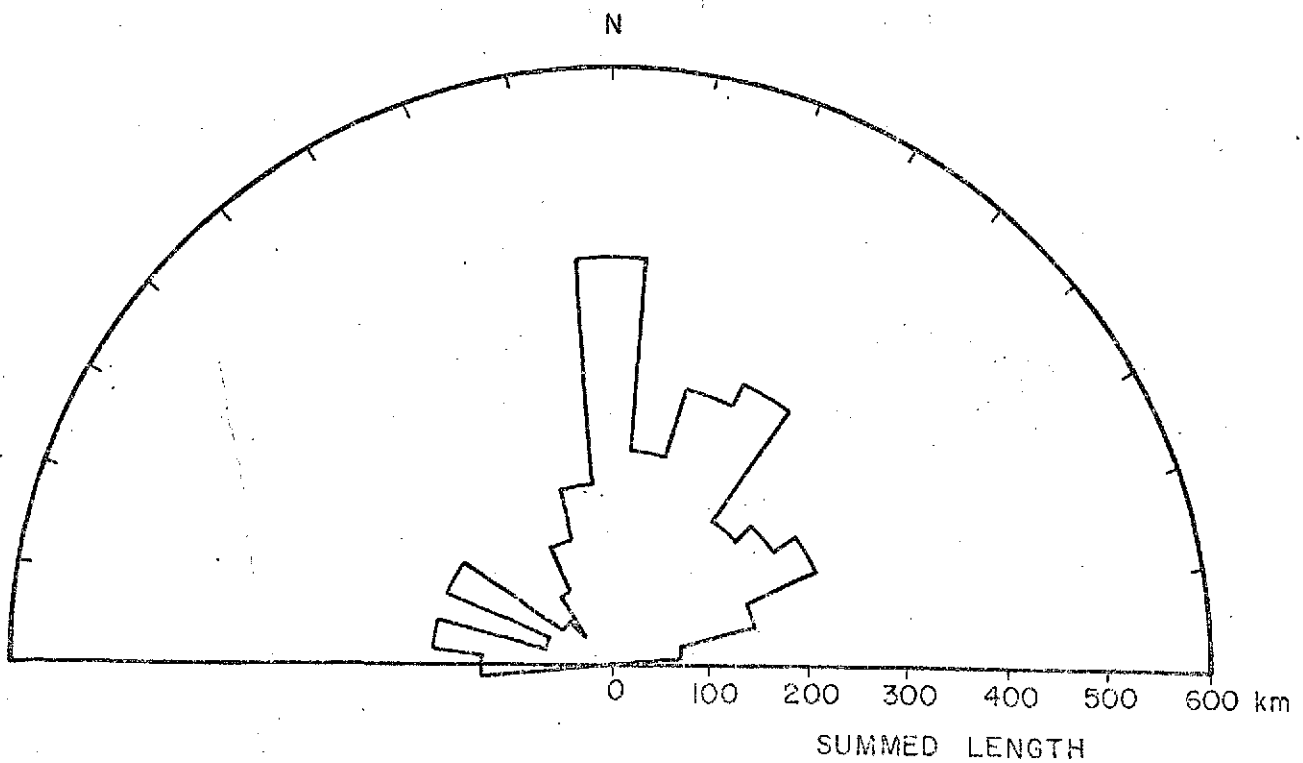

Appendix III-16. Rose diagram of topographic linears in Zone 6 (Figure 77).

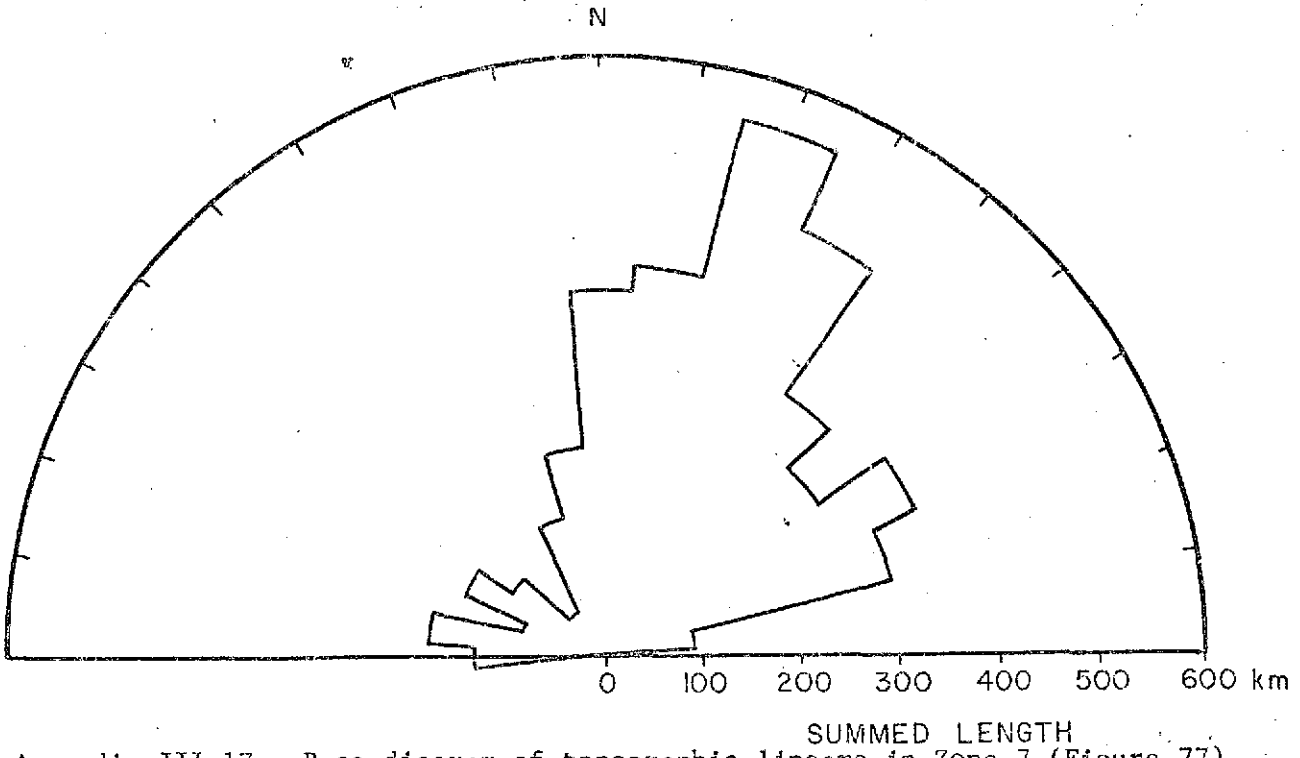

Appendix III-17. Rose diagram of topographic linears in Zone 7 (Figure 77).

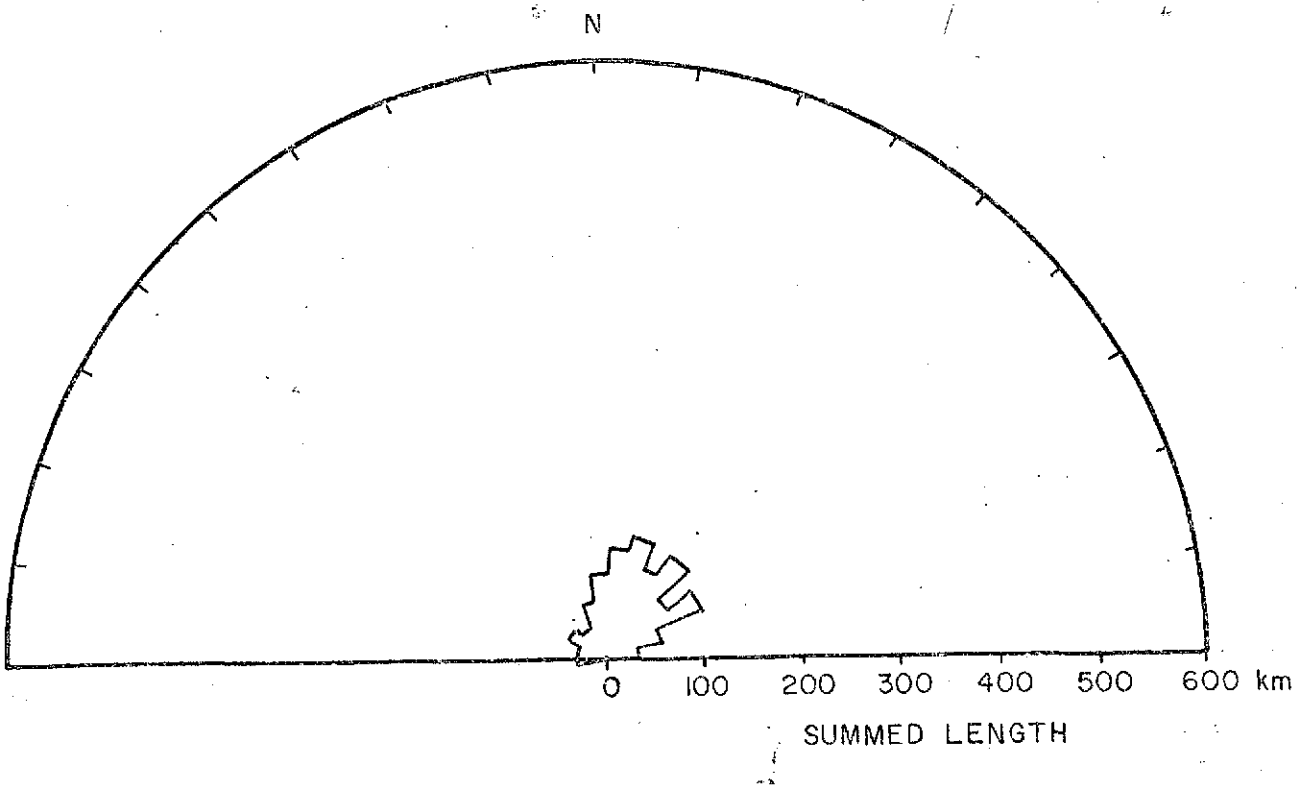

Appendix III-18. Rose diagram of topographic linears in Zone 8 (Figure 77).

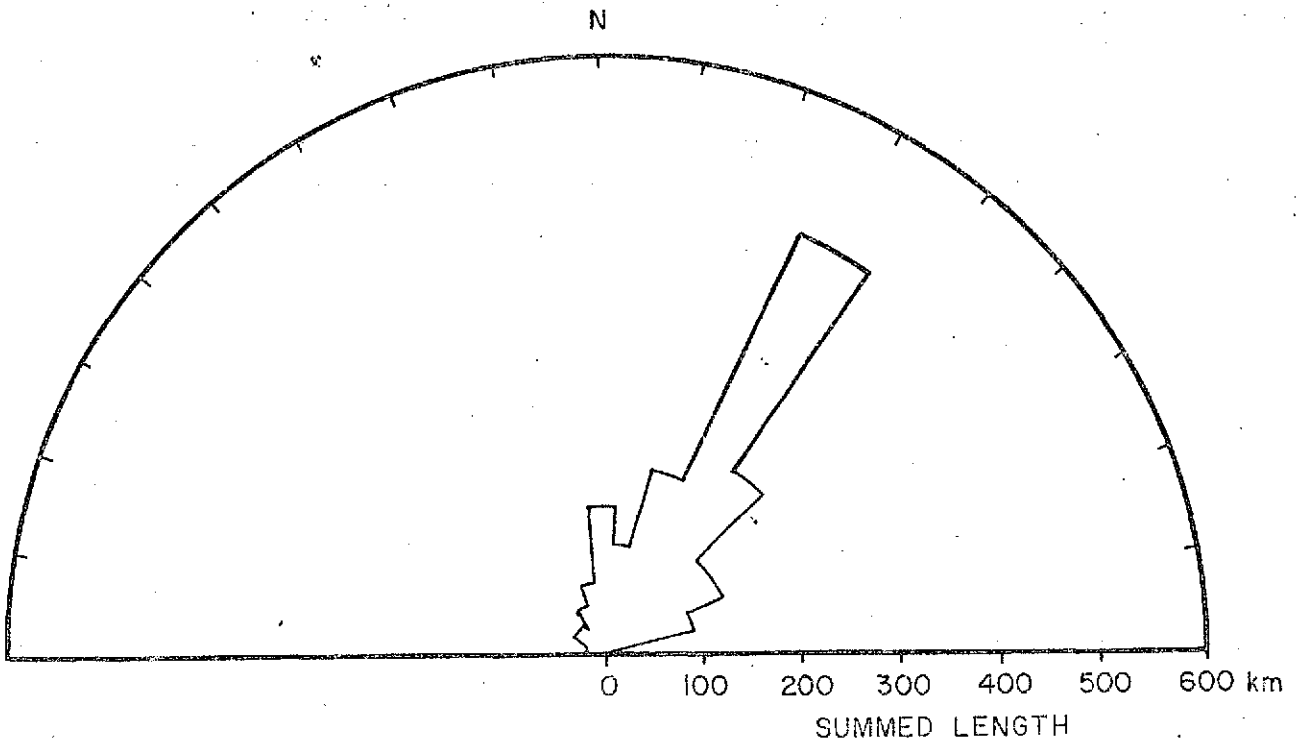

Appendix III-19. Rose diagram of topographic linears in Zone 9 (Figure 77).

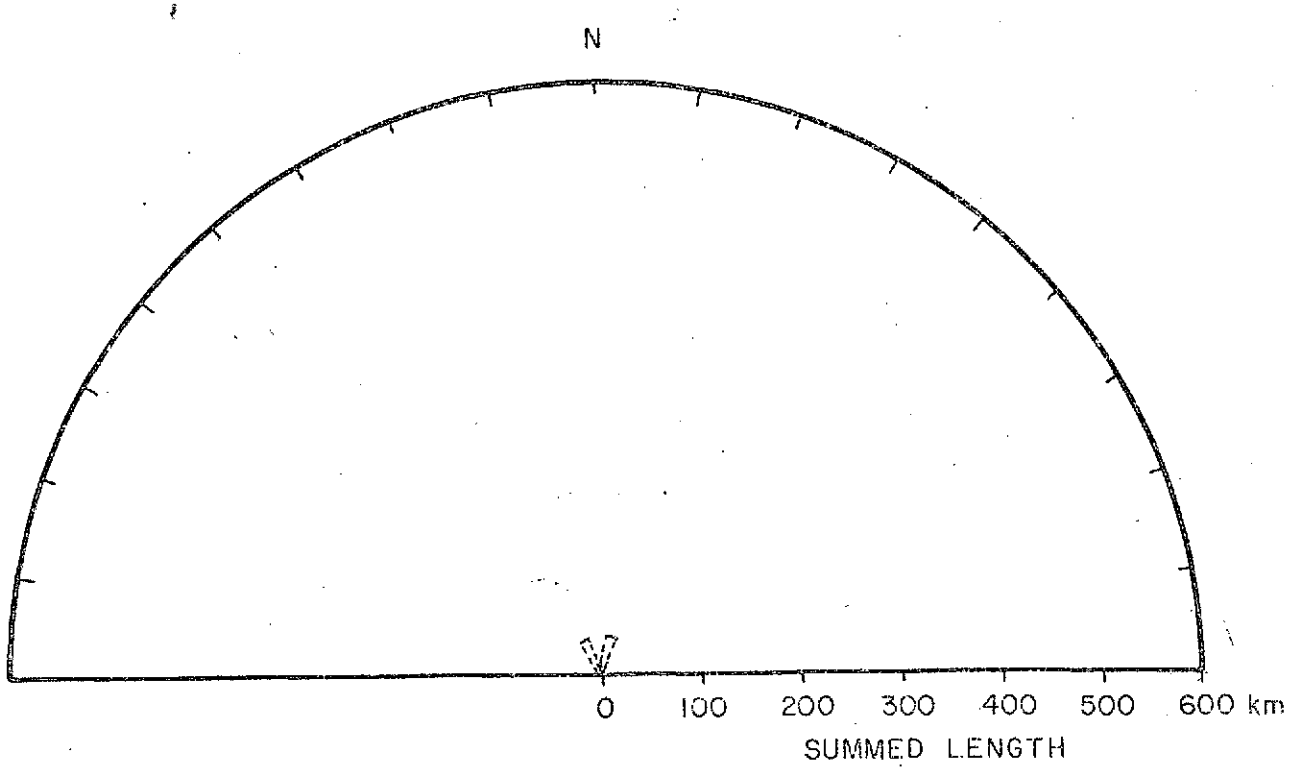

Appendix III-20. Rose diagram of topographic linears in Zone 10 (Figure 77). Dashed lines show same data on an expanded scale (x4).

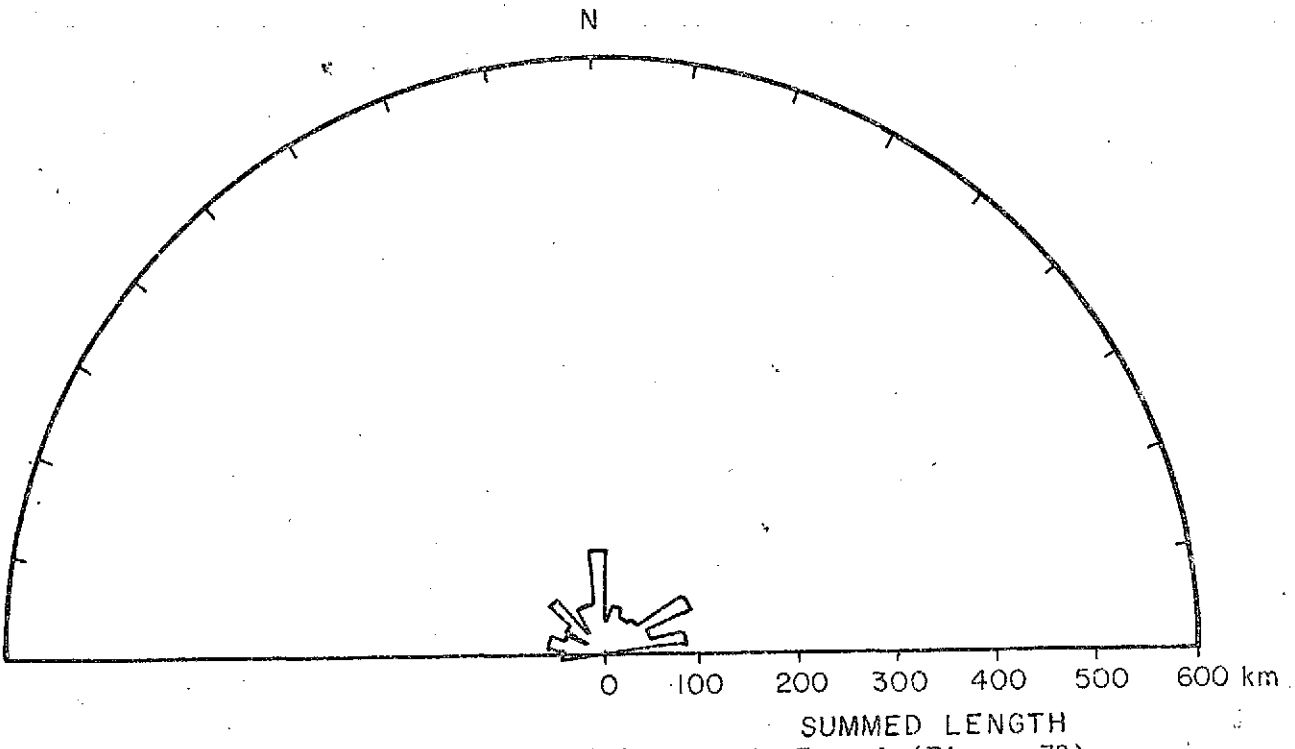

Appendix III-21. Rose diagram of all linears in Zone 1 (Figure 78).

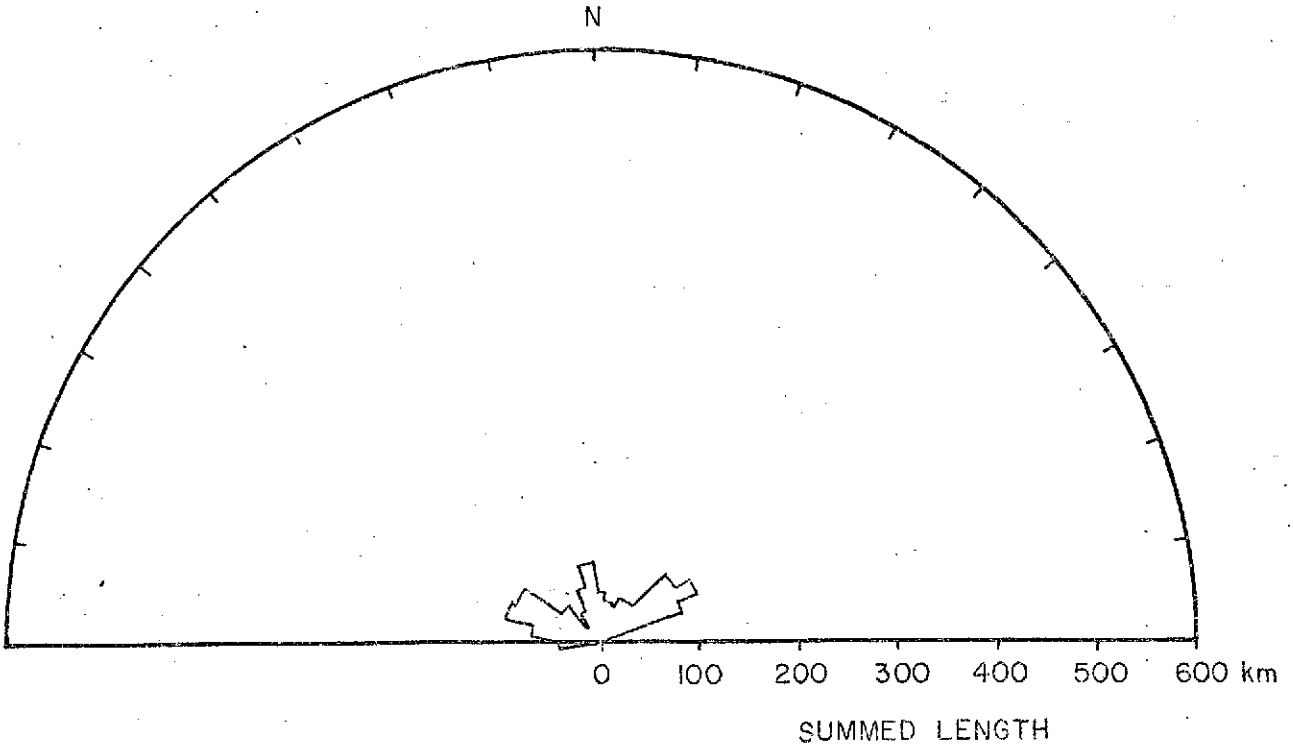

Appendix III-22. Rose diagram of all linears in Zone 2 (Figure 78).

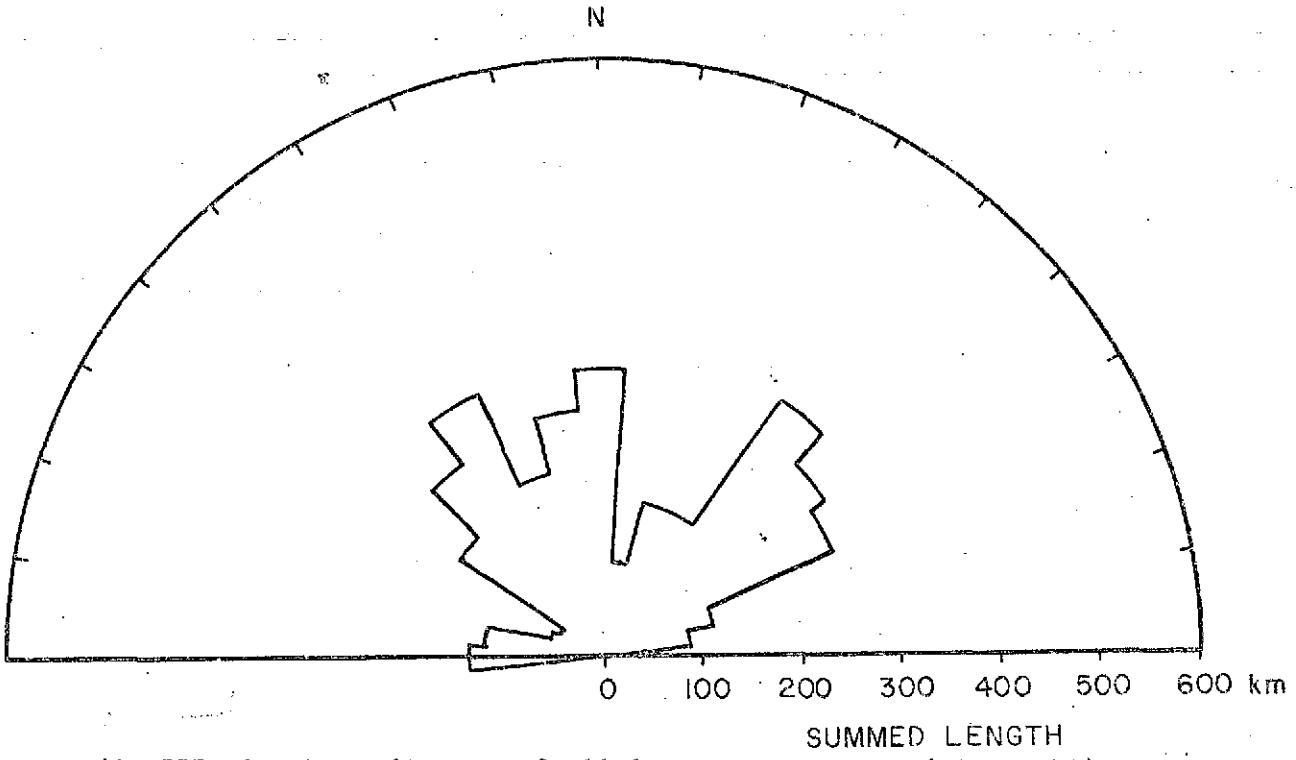

Appendix III-23. Rose diagram of all linears in Zone 3 (Figure 78).

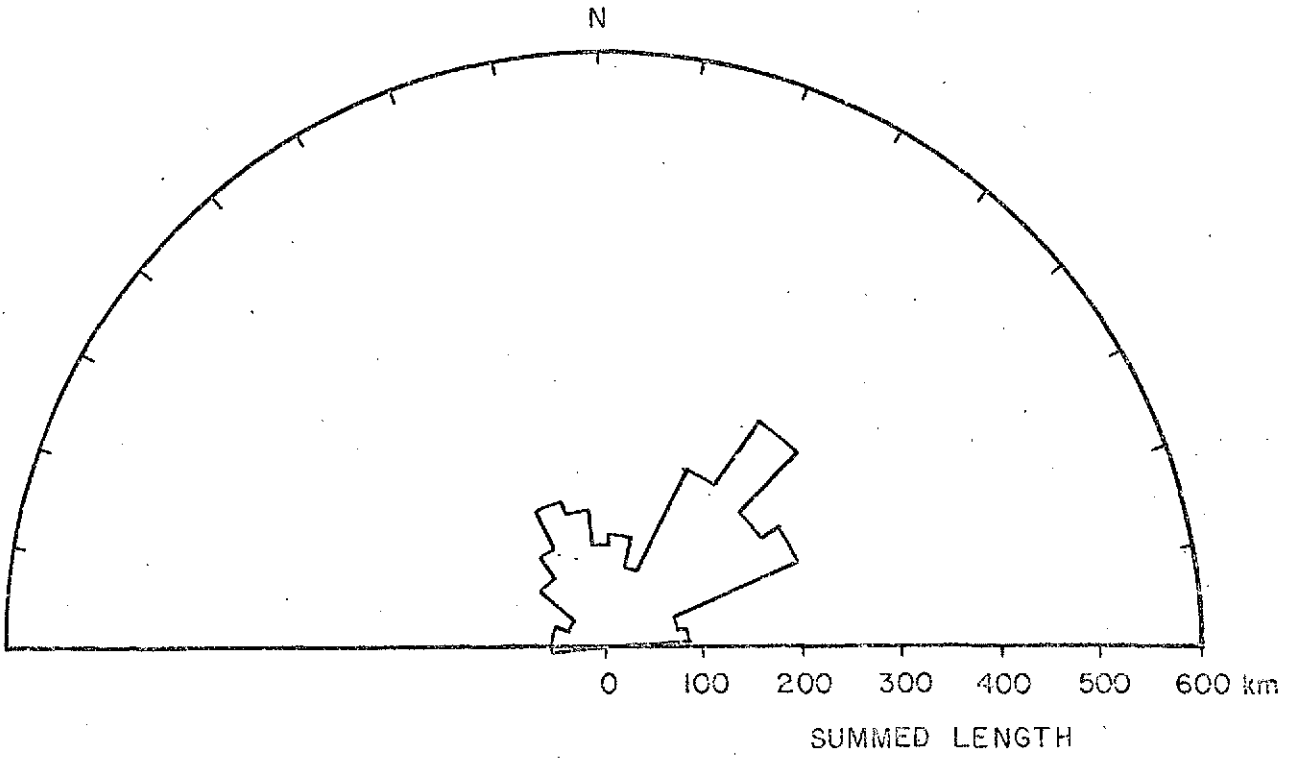

Appendix III-24. Rose diagram of all linears in Zone 4 (Figure 78).

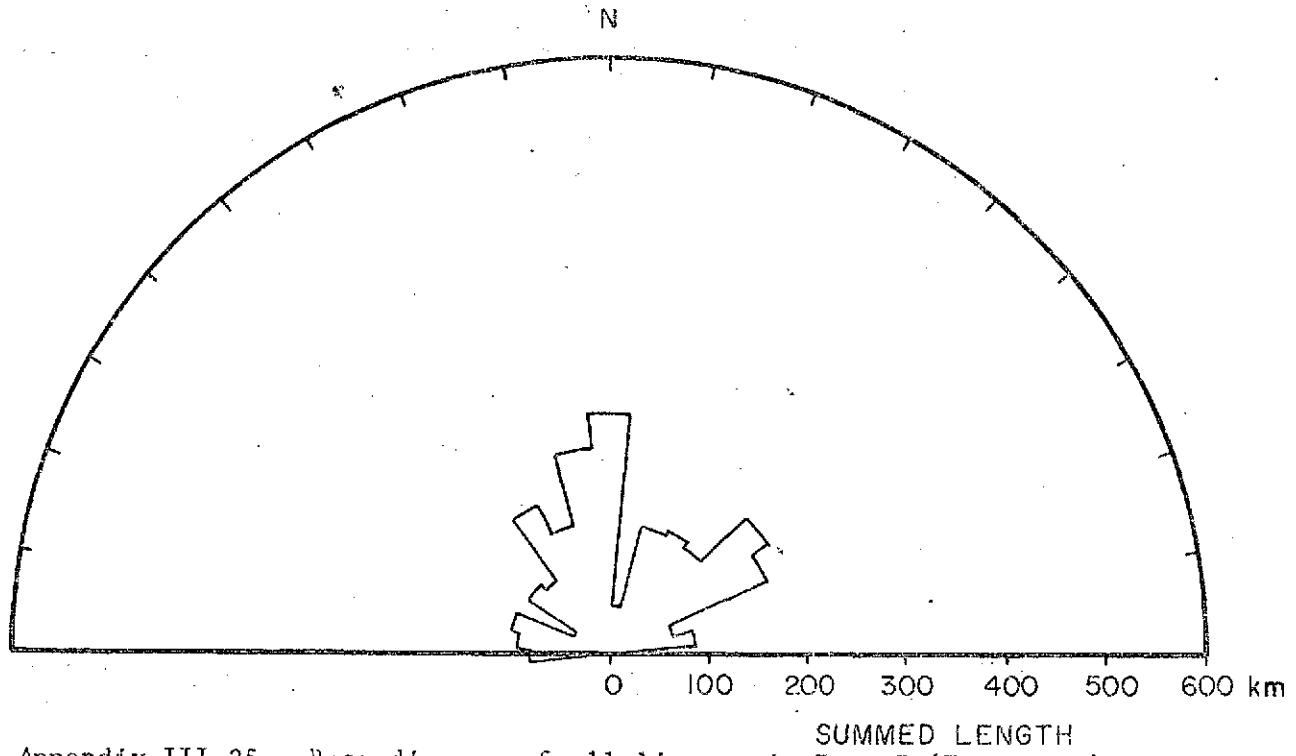

Appendix III-25. Rose diagram of all linears in Zone 5 (Figure 78).

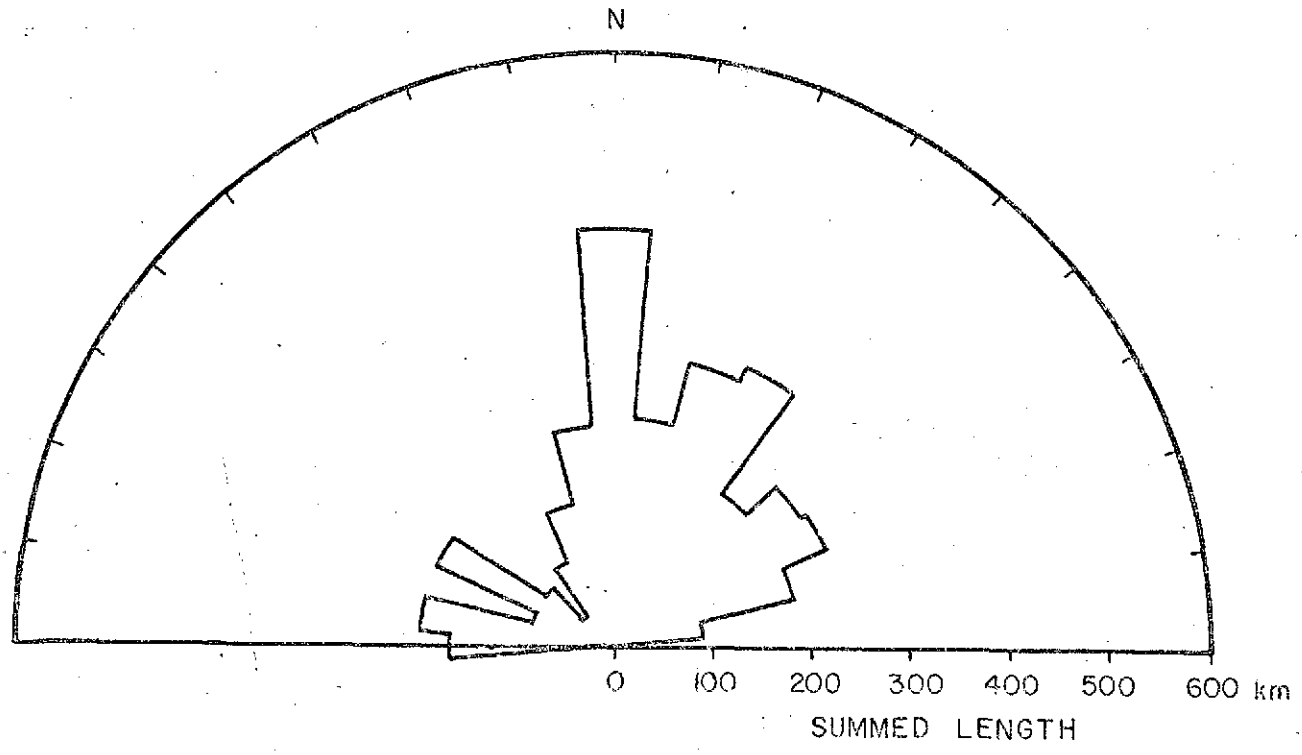

Appendix III-26. Rose diagram of all linears in Zone 6 (Figure 78).

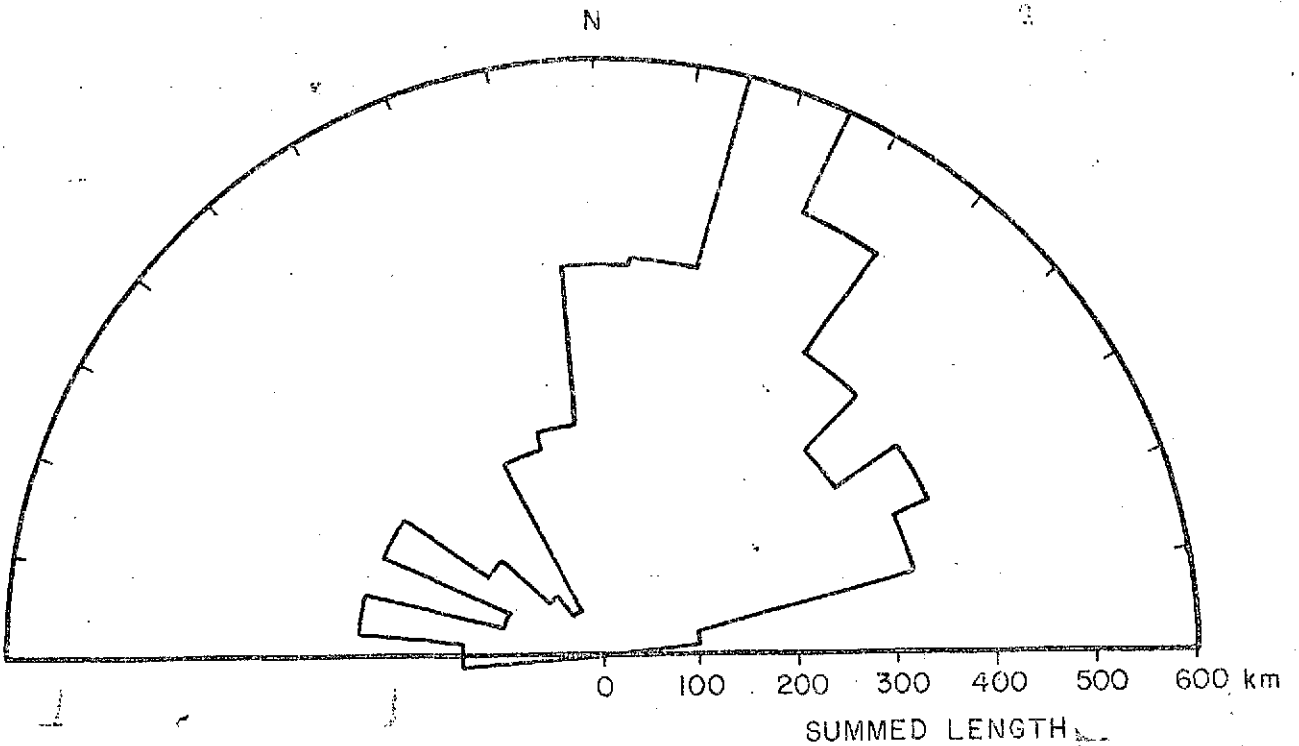

Appendix III-27. Rose diagram of all linears in Zone 7 (Figure 78).

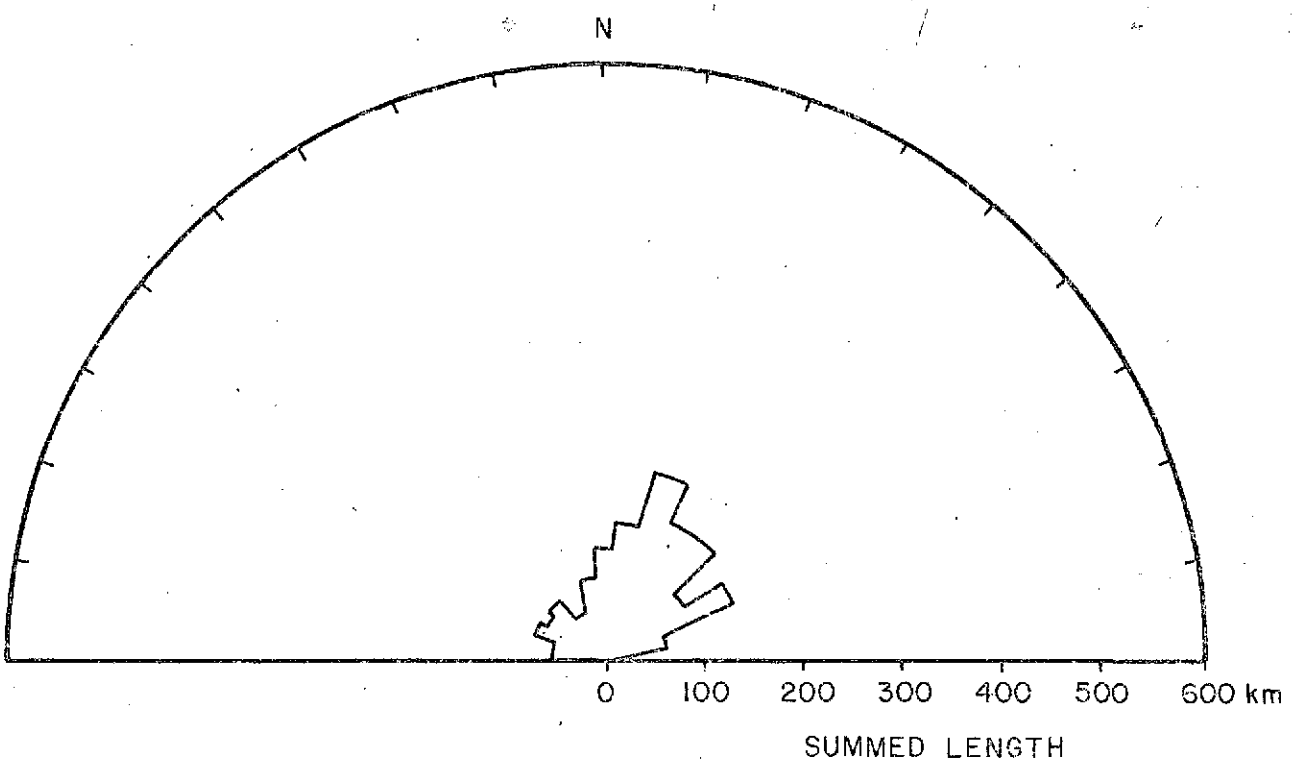

Appendix III-28. Rose diagram of all linears in Zone 8 (Figure 78).

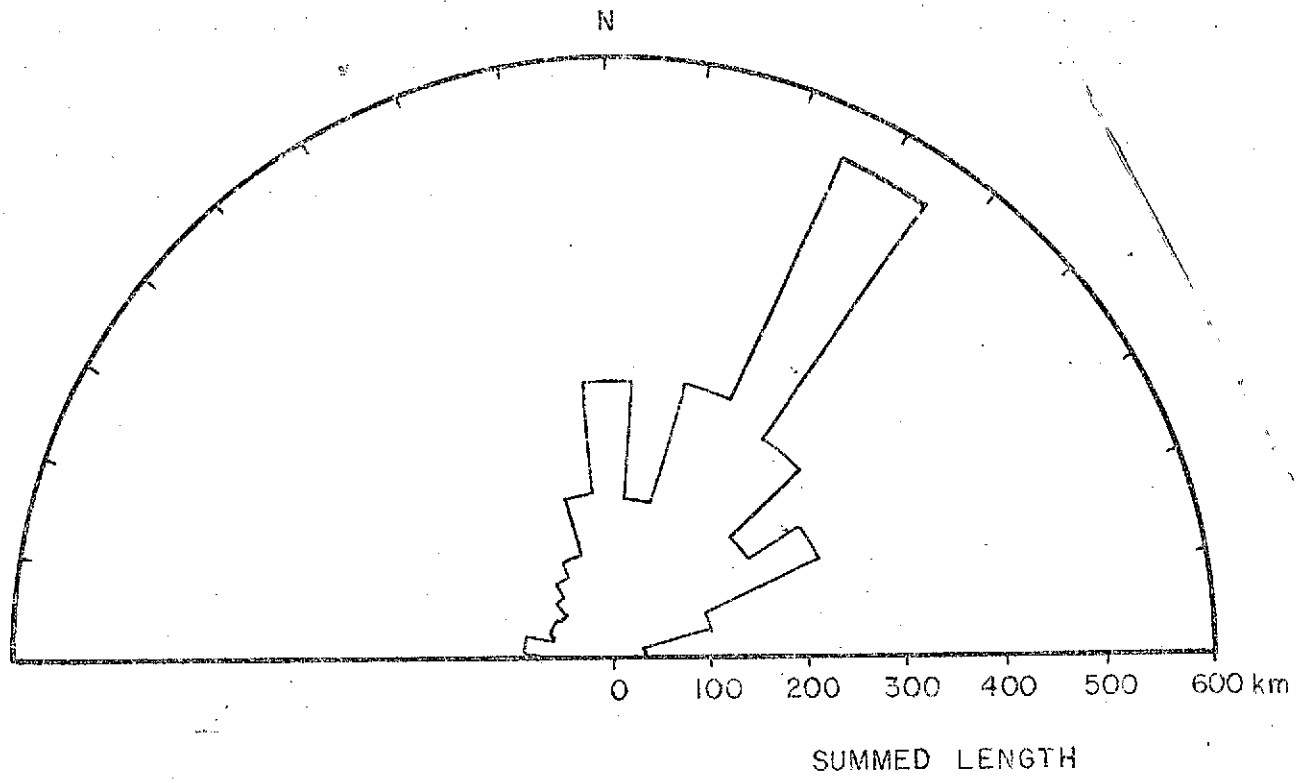

Appendix III-29. Rose diagram of all linears in Zone 9 (Figure 78).

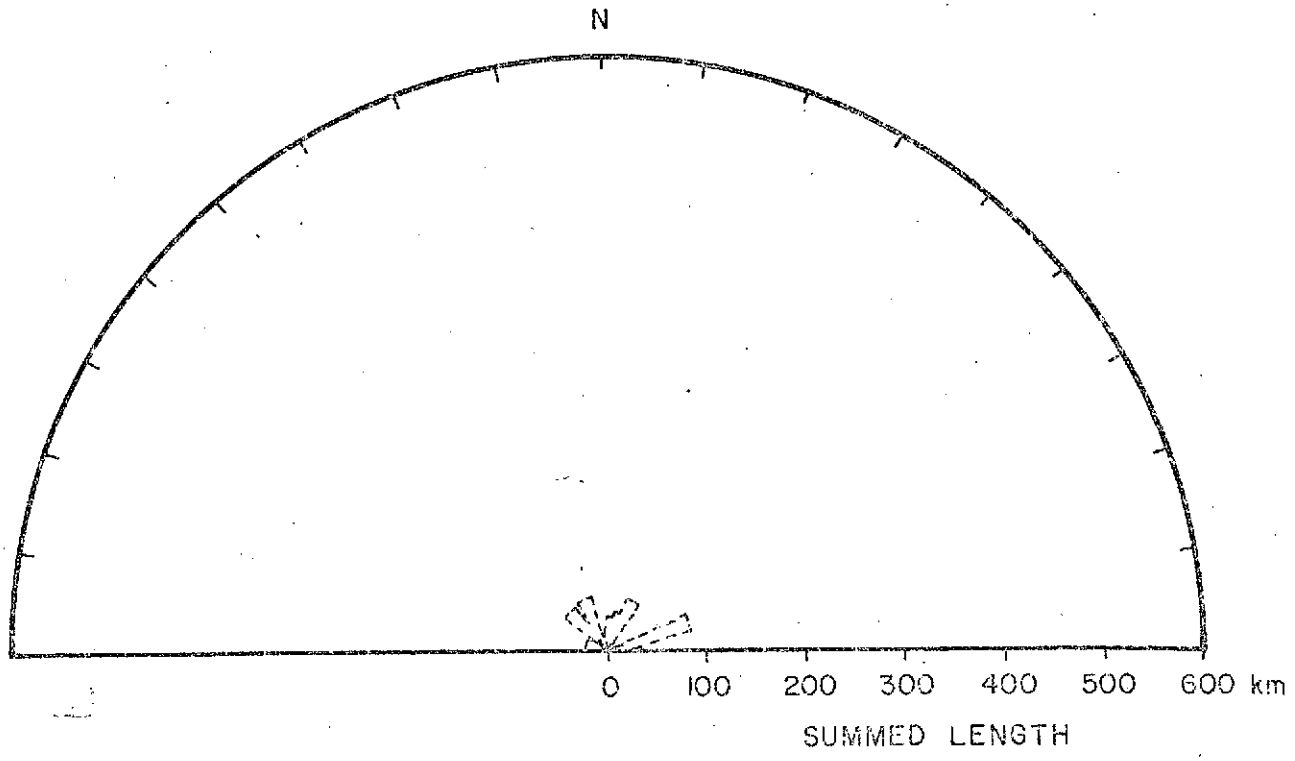

Appendix III-30. Rose diagram of all linears in Zone 10 (Figure 78).

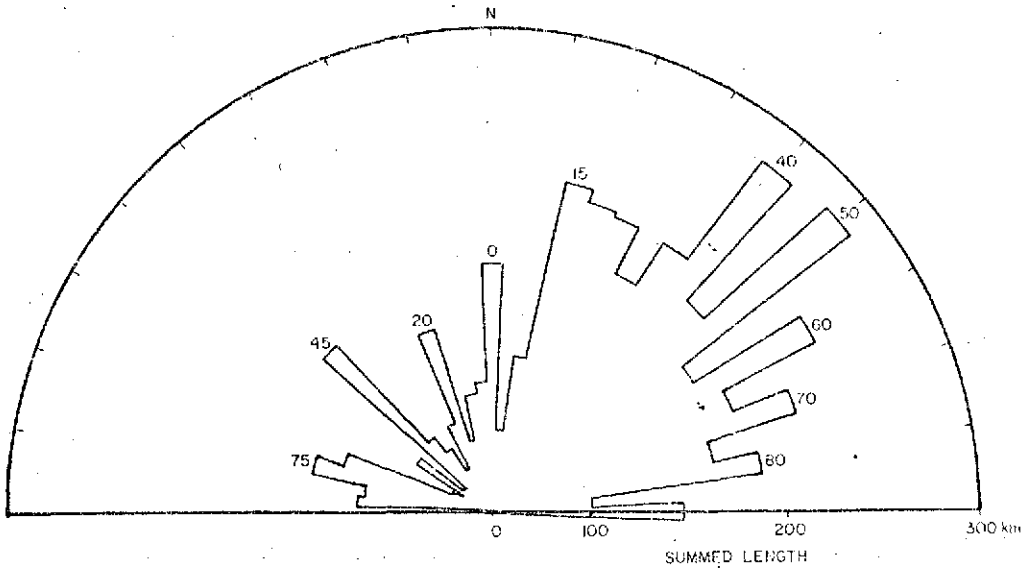

Appendix III-31. Rose diagram of all linears in Zone 11 (Figure 78).